HUGHES TOOL COMPANY

HOUSTON, TEXAS

418 760

XEROX

HUGHES TOOL COMPANY

Final Technical Report on

Preliminary Feasibility Study of

Drilling A Hole On the Moon

Performed for
Jet Propulsion Laboratory
Pasadena
California

under

JPL Contract No. N-33553
(Subcontract under NASA Contract No. NASw-6)

September 23, 1960

Hughes Tool Company Houston, Texas

Summary

and

Recommendations for Future Work

1. <u>Feasibility Study</u>

The preliminary feasibility study has shown that of every known proven drilling method and many untried methods, percussion drilling will be the most suitable for Lunar drilling, where the weight and space requirements are limited for the first drill-equipped Lunar craft. While diamond drilling shows some unreliability in tests to date, some future work with diamond drilling should be done before a final choice is made. The choice might be made on the basis of:

(a) the drilling mission,

(b) reliability of the drilling system,

(c) development time and expense,

(d) value of information to be obtained by the probe.

Regarding the drilling mission, the desired end result might be:

(a) to produce a given diameter and depth of hole,

(b) to accumulate sample cuttings for analysis, or

(c) to drill a relatively large diameter hole into which geological instruments could be inserted.

This study indicates that the mechanical simplicity of the rotary system should give it a reliability advantage for small diameter (1/2 inch) holes which are less than 5 feet deep. Conversely, deeper holes and holes of 3/4" to 4" diameter can best be made by a percussor. For heavier space craft of the future where deep holes larger than 4" diameter are desirable, it is almost certain that rotary drilling with rolling cutter bits will have many advantages.

2. Recommendations for Additional Work

The next logical step is a study to obtain more exact and detailed information for a final system design. It should be emphasized that this second phase of the study will be planned to obtain design information under conditions which simulate those of the expected environment and mode of operation. For example, the following steps would be included in the study of the percussor:

(a) Dependable values of rock properties would be determined for use in optimizing the percussor design, and for predicting the total energy requirements for a given hole. This would require hammer drop tests and/or actual percussion tool test in a vacuum.

(b) Experimental apparatus would be built to simulate the expected percussor blow energy and cyclic rate, in order to determine gas requirements for chip scavenging.

(c) Concurrently, the problem of seals, bearings and lubricants for use in the expected environment would be investigated.

(d) Finally, the information resulting from steps (a), (b), and (c) would be used to size the overall system.

(e) A working model of the system would be built.

A comparable procedure would be followed for the rotary diamond bit system.

It should be noted that the actual design and construction of a functional prototype or prototypes would not be undertaken until after completion and evaluation of this second phase study.

The course of the new study depends upon which of the following two possible interpretations of the preliminary study results, is adopted;

(a) The preliminary conclusions regarding the relative performance, reliability and weight of the two methods are correct.

(b) The preliminary study serves merely to determine the feasibility of two of many drilling methods. The comparison of these two systems is based on certain well founded assumptions which need further investigation.

If the first interpretation is made, then one of the two feasible methods would be chosen for further study on the basis of project objectives or drilling mission. If, however, the second interpretation is preferred, both methods would be further explored to permit the choice of the optimum system for a given mission. It is recommended that the latter course be pursued.

Table of Contents

SYMBOL DEFINITIONS FOR SECTIONS I, II, AND III

Symbol	Definition
D_B	Bit diameter, (in).
D_M	Inside diameter of core bit, (in).
E_b	Energy per blow, (in-lb).
E_o	Energy input, (in-lb).
F_o	Reaction force, (lbs).
h	Hole depth, (in).
K_{hp}	Horsepower constant.
K_{pr}	Penetration rate constant.
MA	Mechanical drill advance.
ME	Mechanical extension of telescoping shaft.
M_h	Hammer mass, (lb-sec^2/in).
N	Cyclic rate, (blows/sec). - Percussor.
N	Shaft speed, (rpm). - Rotary Drill.
P	Axial load on bit, (lb).
PA	Pneumatic drill advance.
PE	Pneumatic extension of telescoping shaft.
P_r	Rate of penetration, (ft/hr).
P_{rc}	Rate of penetration, core bit.
P_{rs}	Rate of penetration, solid bit.
W_b	Battery weight, (lbs), (on earth).
W_s	Weight of gas system, (lbs), (on earth).
β	Diameter ratio.
ΔD_B	Difference between outside & inside diameters of core bit, (in).
η_i	Overall energy conversion efficiency of the impact tool.
σ_c	Specific energy, (lb/in^2).

Section 1

Methods of Making a Hole on the Moon

1. Introduction

The Hughes Tool Company has been requested to prepare a study of the feasibility of drilling a hole on the moon. The study should provide an estimate of the weight and volume requirements of the drilling mechanism.

The following parameters are to be evaluated in the study, and used wherever possible to choose the optimum system:

1. Depth of penetration.
2. Diameter of hole.
3. Penetration rate in various materials for a given load.
4. Amount, type and rate of expenditure of energy.
5. Size of equipment package.
6. Weight of equipment as a function of hole diameter and depth.
7. Degree of complexity of equipment.
8. Information obtainable from each technique (penetration rate, load, torque, etc.)
9. Growth potential.
10. Vibration resulting from drilling.

2. Methods of Drilling the Hole

Many techniques have been used or suggested for making holes in rock. Several of these are presented in Table I, together with available performance data. Examination of these methods – and elimination of those with high power requirements, low drill rates, low state of development, complex and bulky equipment and poor growth potential – leaves two apparently feasible techniques:

(a) diamond rotary bit,

(b) percussion tool.

These two methods will be examined in more detail in Sections II and III of this report.

Table I

Methods Of Drilling Rock

Group	Type	Typical Performance	Remarks
Rotary	Roller Bit (Microbit)	Grey Granite (1) 1 1/4" Diameter 50 Pound Load 570 rpm Air Cleaning Penetration Rate 0.065 ft/hr	The very low rate of penetration under light bit loads and the high rate of tooth wear, make this method unsuitable. Note: The numbers in parentheses in the Typical Performance column key to the references at the bottom of the table.
	Diamond Bit	Grey Granite (2) Coring Bit 1 3/16" O.D., 1" I.D. 70 Pound Load 920 rpm 0.105 hp Air Cleaning Penetration Rate 0.62 ft/hr	The data indicate an energy requirement of .047 hp-hr per cubic inch of rock fractured. For a hole 5 feet deep and 1 inch in diameter, the total energy requirement would be about 2.2 hp-hr. From the data available this system appears to be feasible. The primary disadvantage is the long operating time required for drilling a given depth of hole.
	Drag Bit	No data	Generally used in relatively soft, gummy, and unconsolidated formations. This system is not suitable for drilling rock.
Shock	Electric Shock Wave Drill	Rock (type not specified) (3) 10" dia. hole 200 kw Liquid Clearing Penetration Rate 30 ft/hr	Requires fluid for shock wave propagation. The power requirements are reasonable - about 0.011 hp-hr/ in^3. The general lack of knowledge of this system and the extensive development program necessary rule it out for consideration.
	Shaped Charge	Rock (type not specified) (4) Tapered Hole 1" dia. at bottom 8" dia. at top, about 10 ft deep 50 lb charge	For holes of this size into which instruments can be inserted, this method appears very good. For a longer hole for which a number of holes must be fired, it is necessary to ream the hole between shots. A secondary mass, the so-called "carrot", follows the initial hole-making jet of liquid metal and effectively plugs up the hole. Techniques for getting around this are possible but add considerable weight. Therefore, on the grounds of poor growth capabilities, extensive development work required, and also because information on rock hardness and drillability is not readily acquired, this method is ruled out.
Thermal	Flame Drill (or rocket	Taconite (3) 6 1/2" dia hole Gaseous Oxygen	For a 5 ft long, 1 inch diameter hole (47 in^3), assuming linear relations, the fluid requirements are: gaseous oxygen 78 ft^3

Thermal	Flame Drill (or rocket exhaust drill)	Taconite (3) 6 1/2" dia hole Gaseous Oxygen - 10,000 ft^3/hr Kerosene - 40 gal/hr Water - 1000 gal/hr	For a 5 ft long, 1 inch diameter hole (47 in^3), assuming linear relations, the fluid requirements are: gaseous oxygen 78 ft^3 kerosene 0.31 gal water 7.8 gal Even for this scaled-down size of hole, the mass of fluids required is too large. Moreover, these estimates would undoubtedly be exceeded. Therefore, this method is discarded.
	Electric Arc	Rock (type not specified) (3) 3000 volts d.c. 100 amp.	Data are too sketchy to draw any conclusions as to energy requirements. The state of development of this tool has not advanced beyond the laboratory curiosity stage and for this reason it is ruled out.
Impact	Pellet impact	No data (3)	This system requires a large amount of working fluid and for this reason it is not suitable for the task.
	Rotary-percussive	No data (3)	This system is a combination of the rotary roller-bit and the jack-hammer. Since it will, therefore, be twice as complicated as either, and no great improvement in performance is anticipated, it is ruled out of consideration.
	Jack-hammer	Harris Granite (5) 1" chisel bit 30-35 lb load 2000 blows/min Air flow rate 17.1 SCFM Air Cleaning Penetration Rate 9.4 ft/hr	Specific gas requirements are 0.1 lb_m per inch of depth; for a 5 foot hole, 6.0 lb_m of air are required. This will give a total system weight of about 60 lb_m which is reasonable. An advantage is the high penetration rate. A possible disadvantage is excessive vibration from the drill. All in all, this is one of the most promising systems.

<u>References</u>

(1) Hughes Tool Company Laboratory Report L.J. 17530-2. "Study of Drilling Performance of 1 7/8" Core and Full-Hole Type Diamond Bits in Berea Sandstone, Rush Springs Sandstone, and Grey Granite". August 24, 1960

(2) Foster-Miller Associates' test result.

(3) Ledgerwood, L.W. Jr. "Needed Now: A Better Understanding of the Basics of Earth Boring". <u>Oil and Gas Journal</u>, vol. 58, no. 19, May 9, 1960. PP 127-41.

(4) Personal communication from Professor F.A. McClintock of M.I.T.

(5) Hughes Tool Company Laboratory Report L.J. 17530-2. "Jackhammer Tests on Harris Granite, Rush Springs Sandstone and Berea Sandstone". August 25, 1960.

2

Section II

Diamond Bit Rotary Drilling Mechanisms

1. Introduction

As indicated in Section I, only two of the many possible drilling methods appear feasible for the moon drilling project, namely, rotary diamond bit and percussive. This section is devoted to the diamond bit rig and its discussion includes: (a) the several tasks which a diamond bit rig must perform and various methods of accomplishing them; (b) a description of a few mechanisms which appear to be promising; (c) the approximate weight of these mechanisms as a function of hole depth and diameter; and (d) the approximate weight of the overall drilling system which includes the energy source, chip scavenging means and the mechanism.

2. Principal Tasks of the Diamond Rotary Bit

The principal tasks or operations necessary for drilling a hole on the moon with a diamond bit are shown in block diagram form by Figure 1. It is seen they are:

a) Loading the bit
b) Rotating the shaft
c) Advancing the shaft
d) Removing the chips
e) Providing cooling for the bit

The general requirements of these operations will now be considered. The specific mechanical design requirements and systems are presented in Section 3 which follows.

2.1 Loading the Bit

There are several methods for providing bit thrust. These are: (a) the weight of the package; (b) reaction thrust produced by expanding a high energy gas through a nozzle; and (c) some means of anchoring the package to the moon's surface, e.g., an explosive imbedment anchor.

Until more complete knowledge of the composition of the moon's surface is available, the anchoring method is ruled out. The amount of propellant required to produce reaction thrust is prohibitive; hence this method is also ruled out.

Thus, the only feasible means of providing thrust is

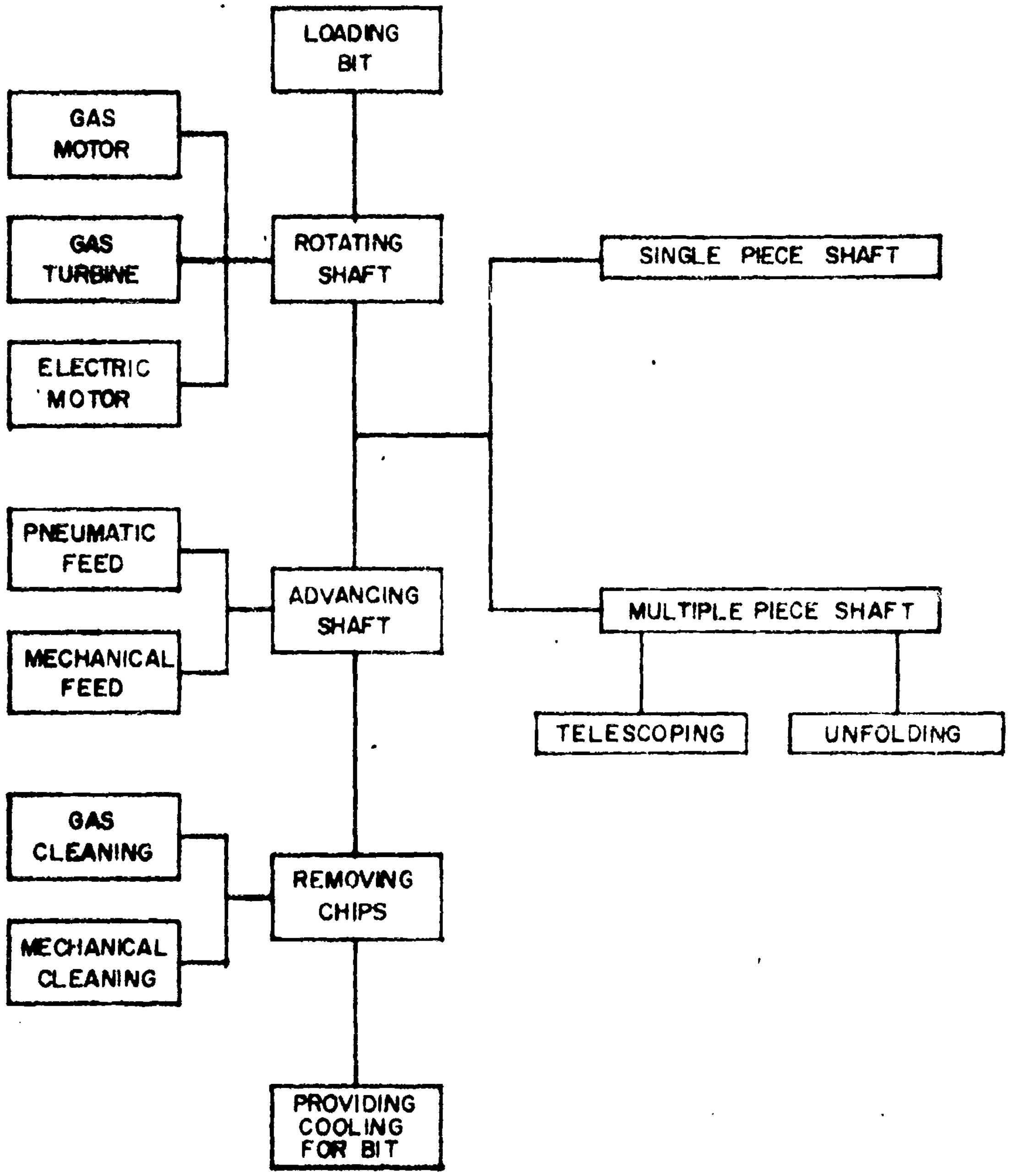

REQUIRED OPERATIONS FOR DRILLING A HOLE ON THE MOON

FIGURE 1

to "push" against the package. If the package weighs 100 pounds on the moon, the available thrust may be assumed to be fifty pounds for purposes of estimating drill performance.

Methods (a) and (b) are examined in detail in Appendix A.

2.2. Rotating the Shaft

2.2.1. Rotary Drive Power Requirements

An analysis of the operation of a diamond bit, (Appendix E) indicates that the rate of penetration and the horsepower required for rotation are given by the following equations for drilling in grey granite:

(a) Solid Bit

$$P_r = 1.5 \times 10^{-6} \; \frac{PN}{D_B} \quad \text{ft/hr} \tag{1}$$

$$hp = 1.0 \times 10^{-6} \; PND_B \quad \text{hp} \tag{2}$$

(b) Core Bit

$$P_r = 1.5 \times 10^{-6} \; \frac{PN}{\Delta D_B} \quad \text{ft/hr} \tag{3}$$

$$hp = 2.0 \times 10^{-6} \; PND_M \quad \text{hp} \tag{4}$$ *

where

P = Axial load on bit, lb

N = Shaft speed, rpm

D_B = Diameter of solid bit, in

D_M = I.D. of core bit, in

ΔD_B = Difference between O.D. and I.D. of core bit, in

The constants in the above equations were determined from a limited series of tests run by Foster-Miller Associates using a coring bit having the dimensions 1-3/16 inch O.D. and 1 inch I.D. (D_M = 1" and ΔD_B = 3/16"). The range of loads covered was 70 to 90 pounds and the range of speeds 560 to 920 rpm. These constants were compared with the more extensive results presented in a Phillips Petroleum memorandum.**

* Strictly true only when $\Delta D_B/D_M \ll 1$.

** Phillips Petroleum, Drilling Engineering Div., Houston, Texas. Memorandum: Project No. 4. "Application and Performance of Diamond and Chert Bits", by R.S. Hock, Feb. 23, 1954.

(See Appendix E.) The constant in the power equations checked very well; however, the constant in the penetration rate equations obtained by Phillips was several times larger than that presented here. Hence, it is felt that these equations are adequately conservative and, if anything, too pessimistic regarding penetration rate.

Equations (1) to (4) were used to plot the curves in Figures 2 through 6, which present the anticipated performance of various size diamond bits in grey granite. It should be noted that Figures 5 and 6 are plotted by combining the expressions for power and penetration rate. The results are independent of bit load and speed.

2.2.2. Rotary Drives

As shown in Figure 1, three rotary drives were investigated: (a) a gas turbine; (b) a gas motor; and (c) an electric motor.

The gas systems, either motor or turbine, consist of the engine; a source of gas (hot or cold); and accessories such as pressure regulators, relief valves, starters, gear boxes, etc. The gas source, which consists of a container and charge, is the main contributor to system weight for long times of operation; the engine and accessories totaling about 5 or 6 pounds (earth weight) in either case. Appendix D, Section III presents a detailed analysis of the gas systems and it is concluded that a liquid monopropellant is the lightest and most reliable gas source.

The electrical system consists of an electric motor and gear train plus an energy storage or conversion device. The latter may be a storage battery, fuel cell, thermoelectric generator, solar cell, or even a ~~thermonuclear device~~ such as a SNAP-type unit. For comparison purposes, the storage battery (using silver-zinc cells) is considered as typical of this type of energy source. Furthermore, batteries require no extensive development work and are commonly used in missile work.

System weights for each of the three methods of providing rotational power to the drill bit are presented in Figures 7, 8 and 9 as a function of the operating time and at several power levels. These data are consolidated as Figure 10 to permit easy comparison of the systems.

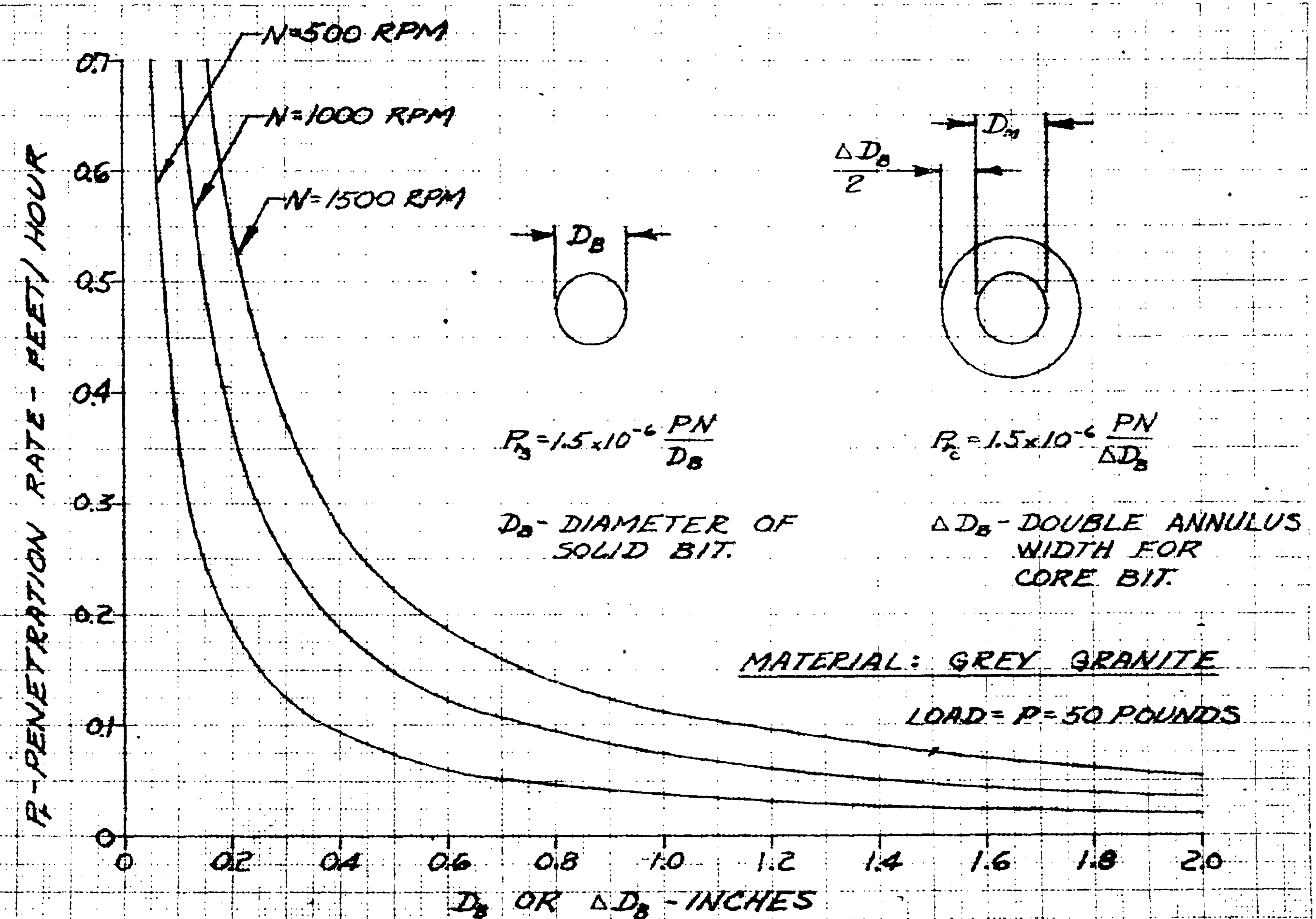

PENETRATION RATE vs. BIT SIZE FOR SOLID & CORE DRILLS

FIGURE 2

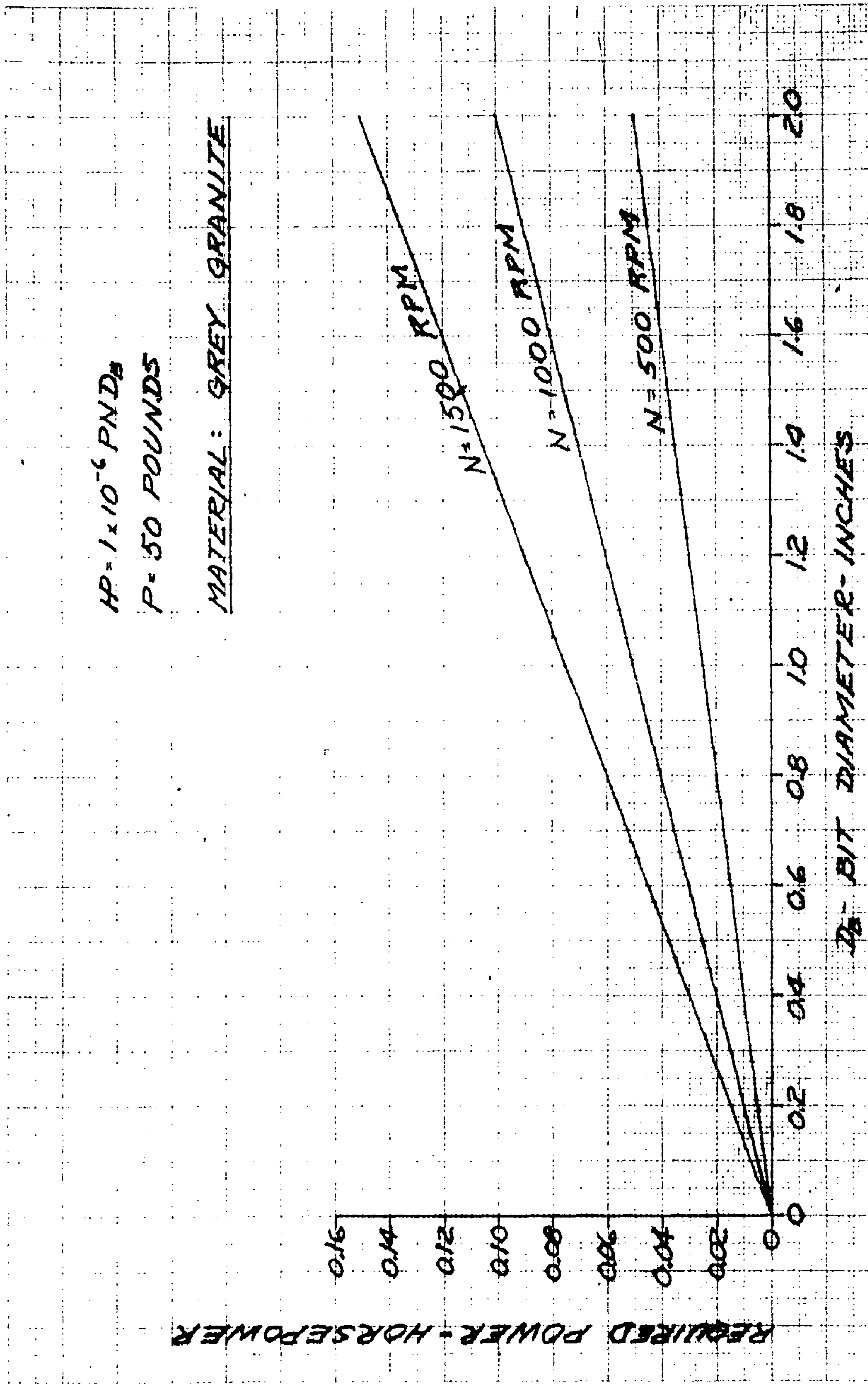

POWER REQUIRED vs. BIT SIZE FOR SOLID BIT

FIGURE 3

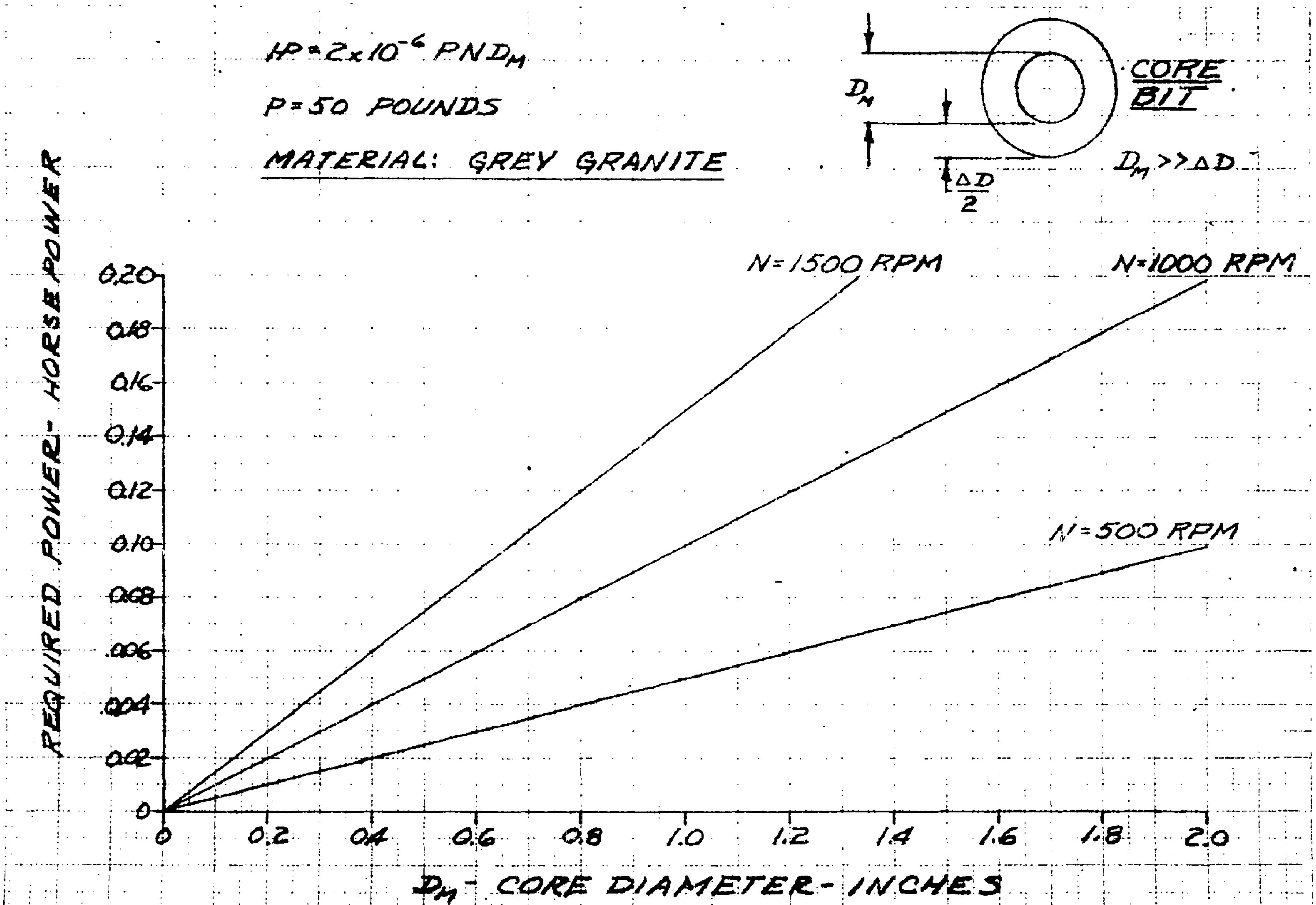

POWER REQUIRED vs. BIT SIZE FOR CORE BIT

FIGURE 4

$$HP = \frac{K_{HP}}{K_R}(D_B)^2 \cdot R_r = .667(D_B)^2 \cdot R_r$$

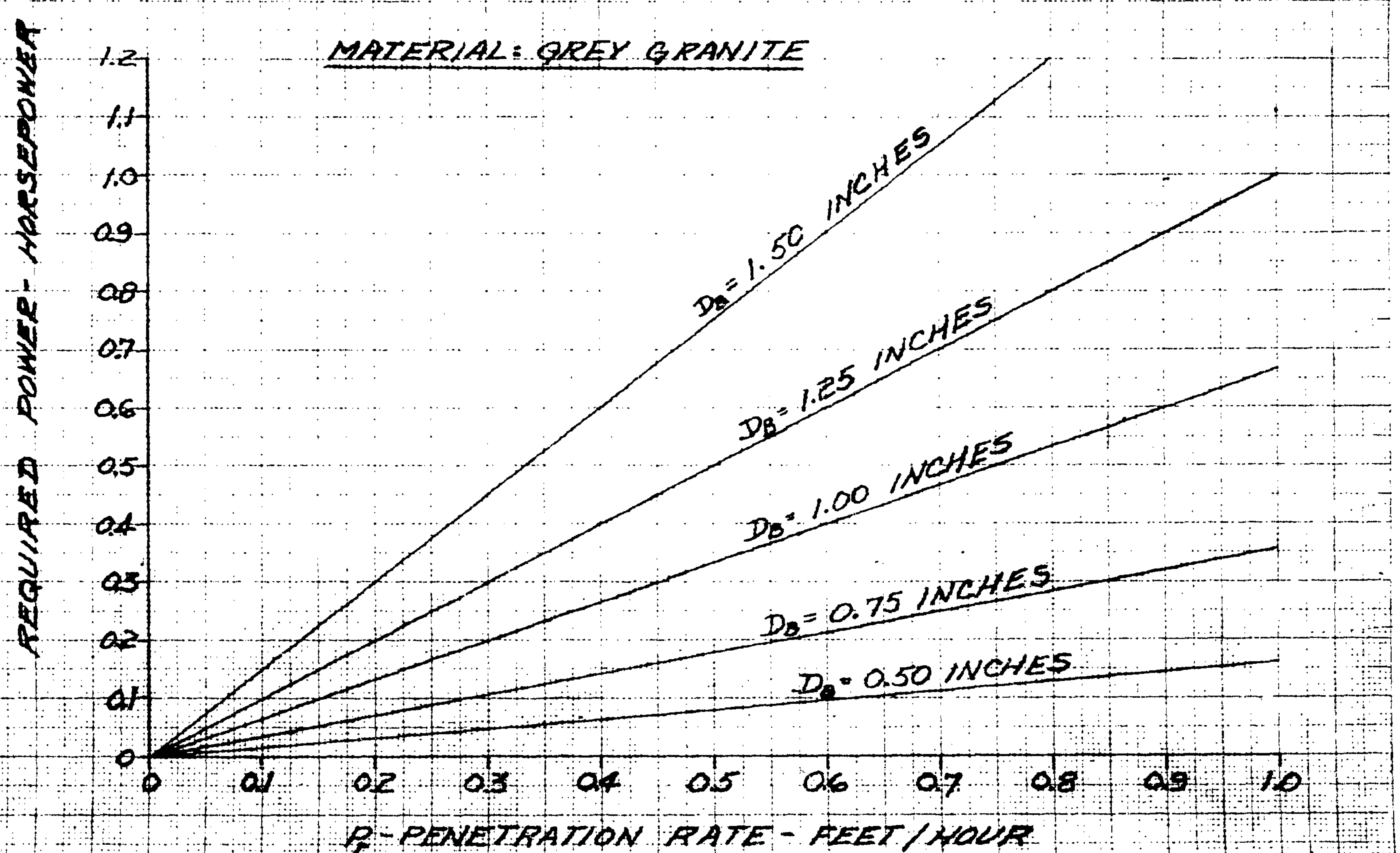

POWER REQUIRED vs. PENETRATION RATE FOR SOLID BIT

FIGURE 5

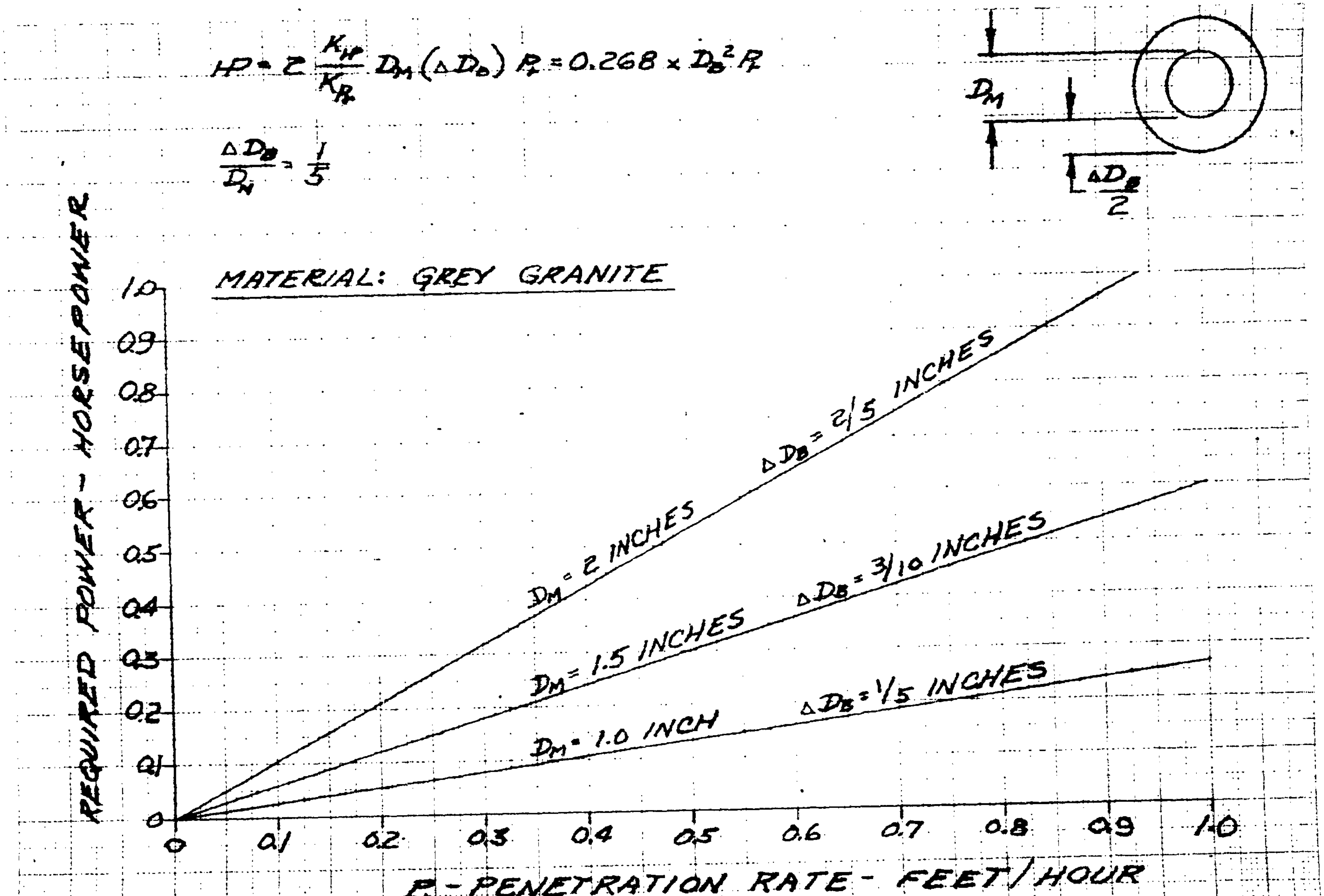

POWER REQUIRED vs PENETRATION RATE FOR CORE BIT

FIGURE 6

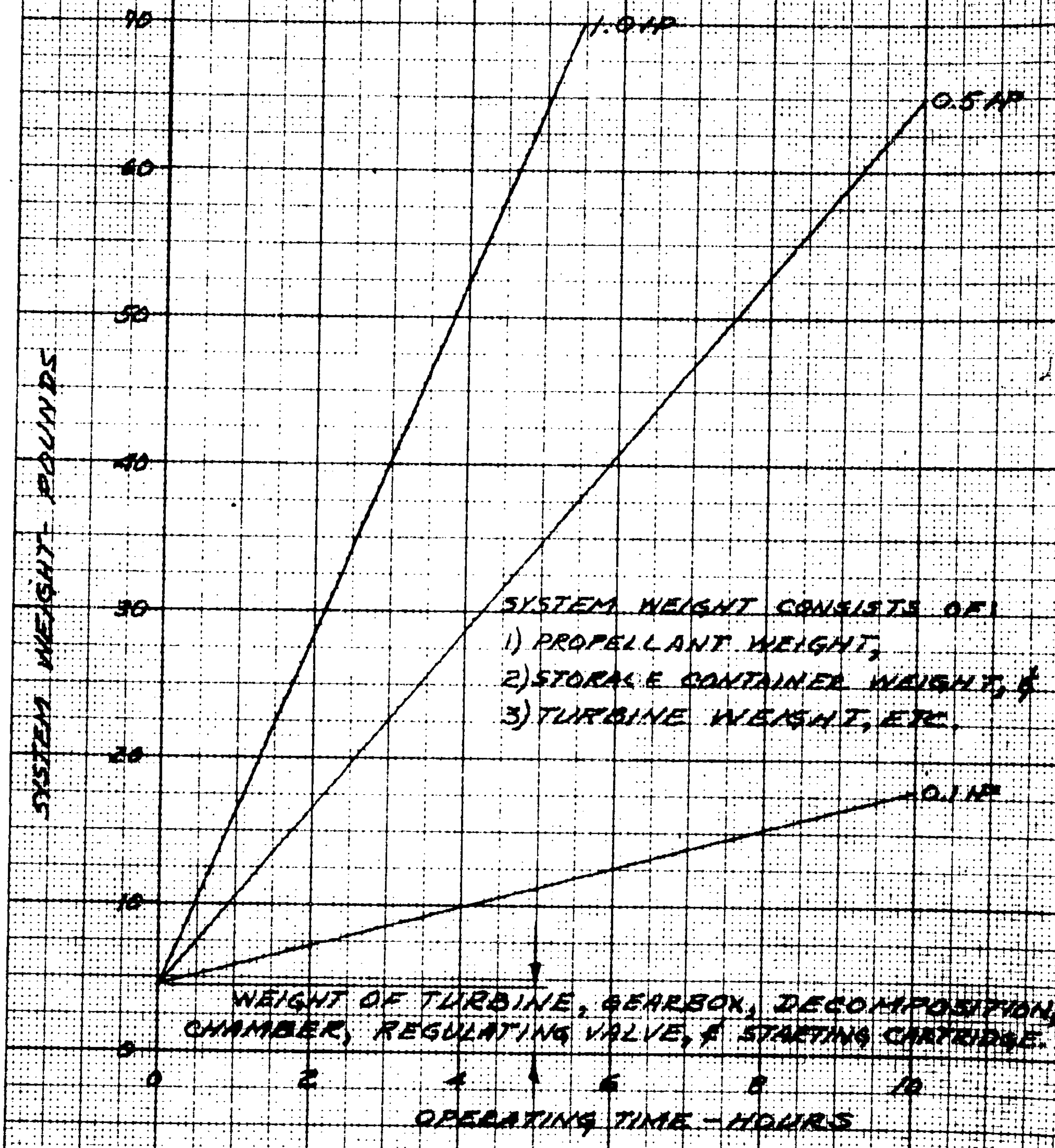

HOT GAS PARTIAL ADMISSION TURBINE SYSTEM WEIGHT

FIGURE 7

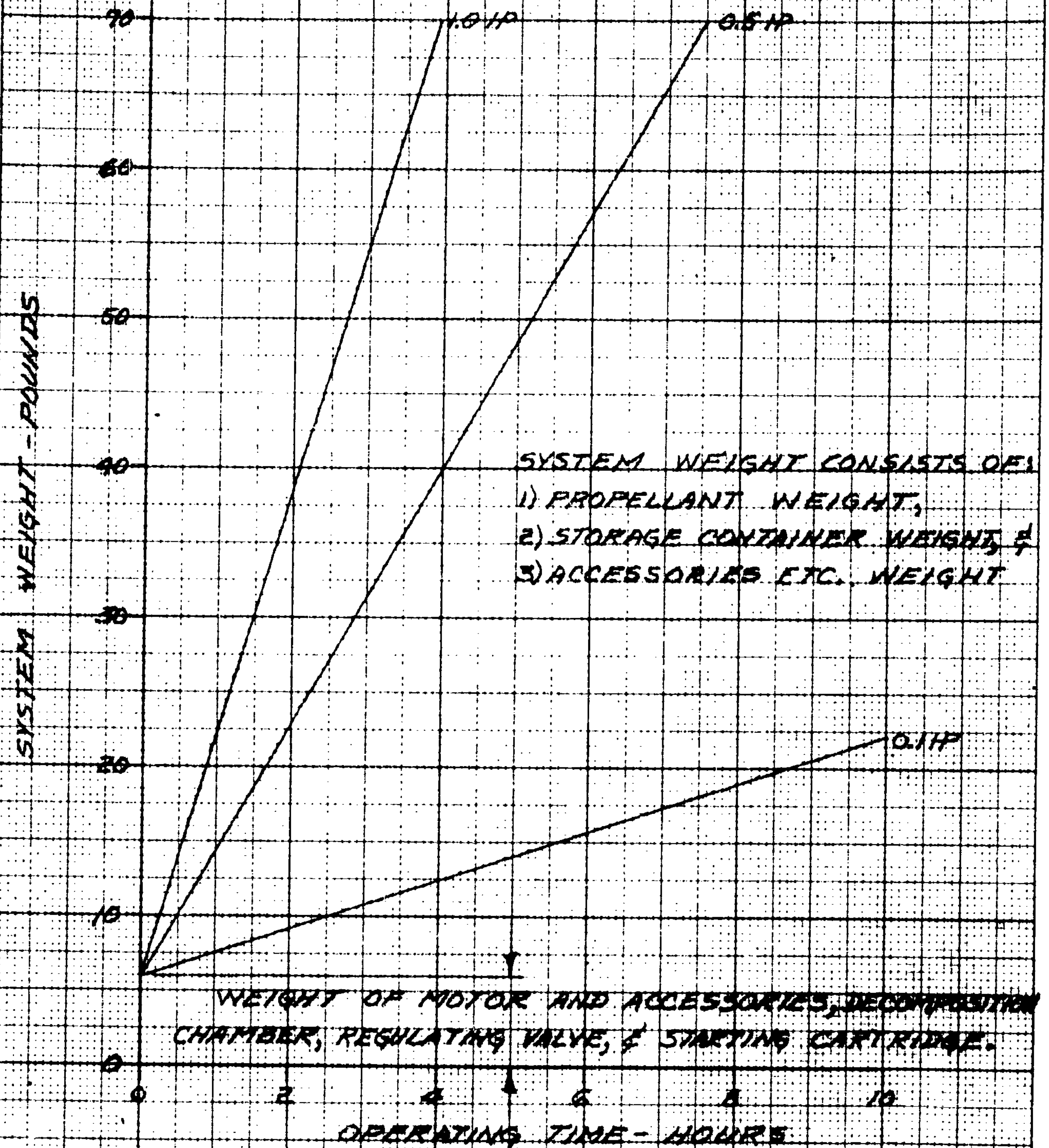

HOT GAS MOTOR SYSTEM WEIGHT

FIGURE 8

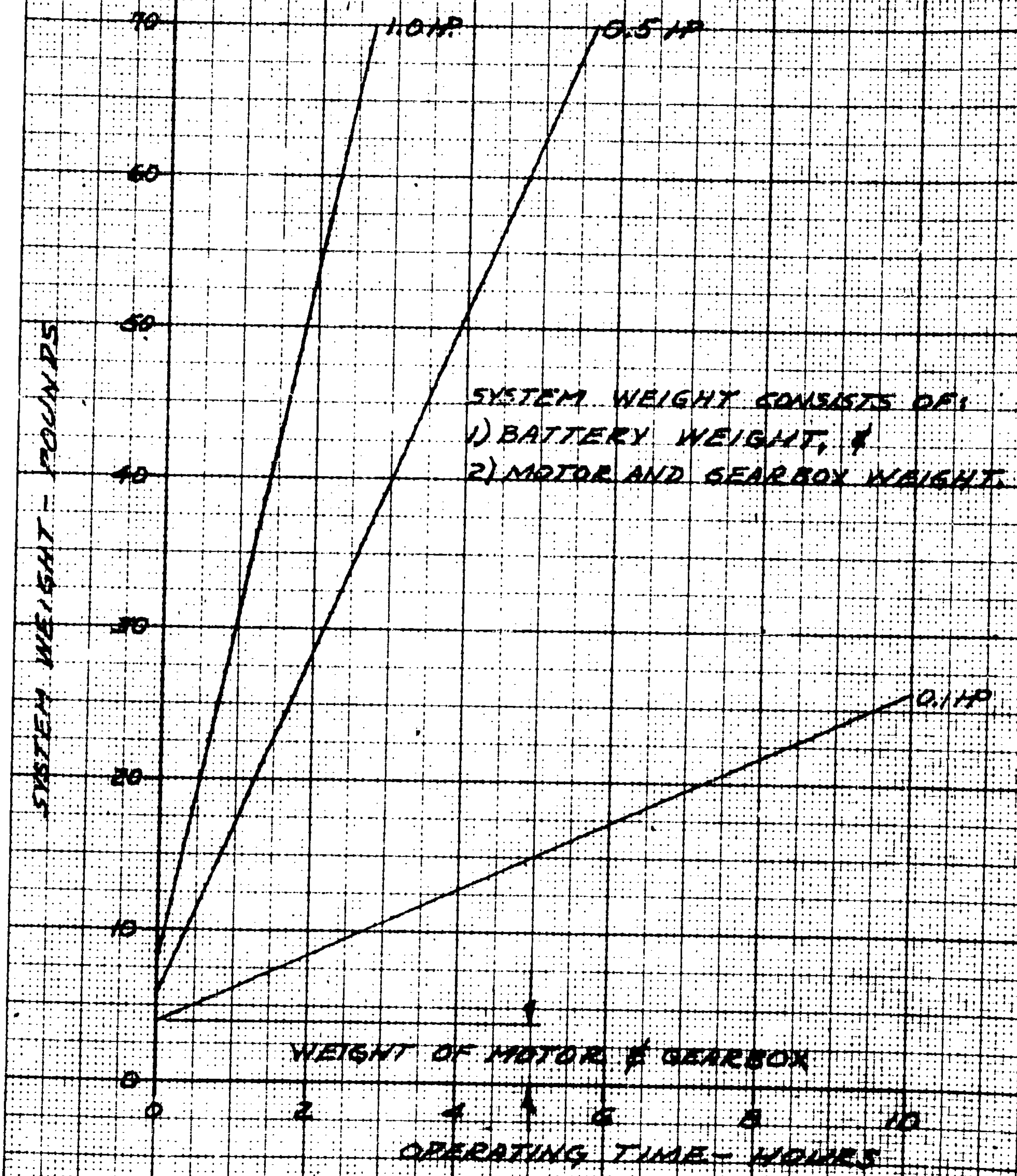

ELECTRIC MOTOR SYSTEM WEIGHT

FIGURE 9

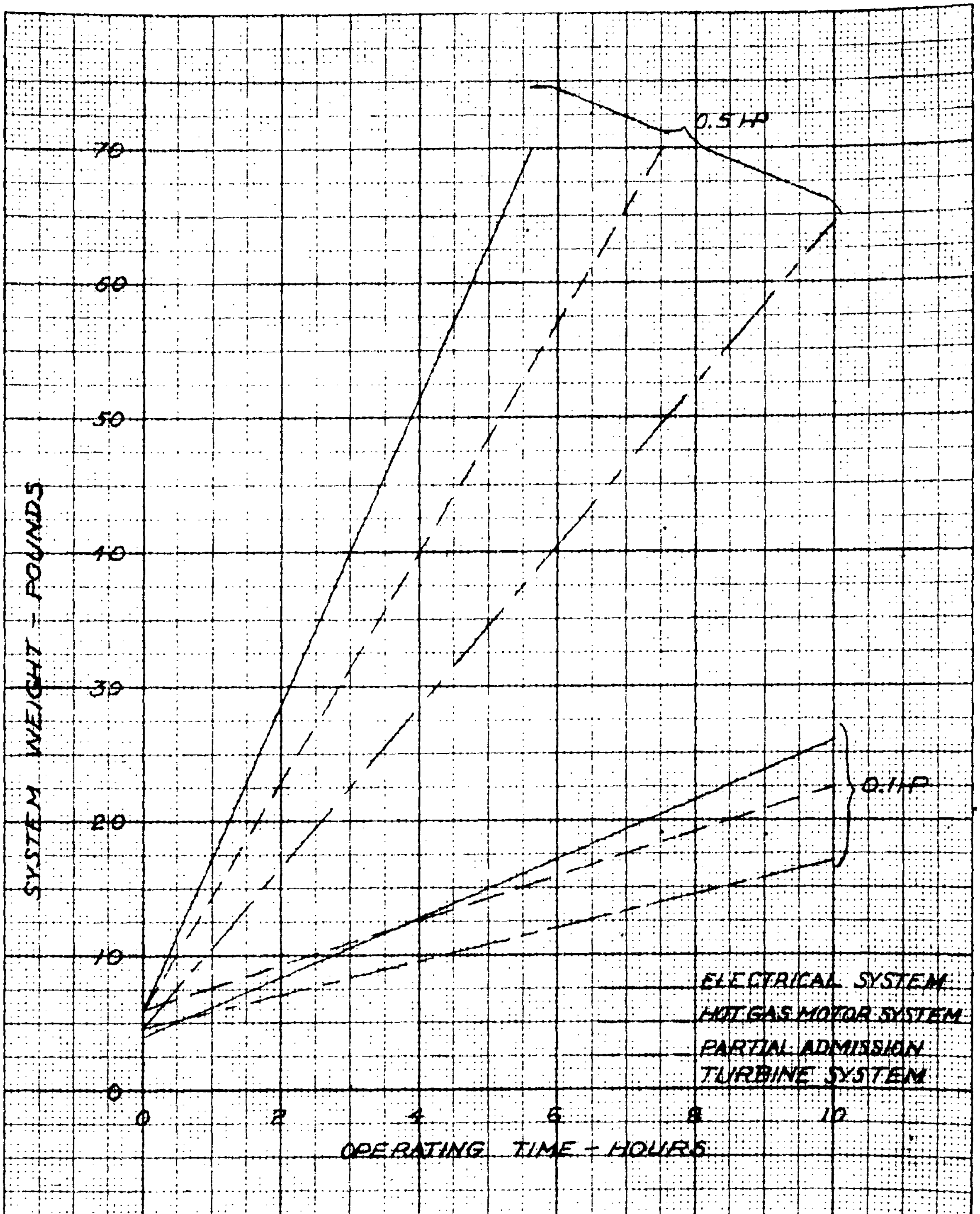

WEIGHT COMPARISON OF ROTARY DRIVE SYSTEMS

FIGURE 10

As seen from these curves, it appears that the gas turbine system would provide the minimum weight package, while the electric motor system would be the heaviest. However, there are several factors which must be considered before any final conclusion can be drawn. Some of these are:

a) The weight for the electric motor system is based on conservative estimates of units which have been available for several years. No effort has been made to push the so-called "state of the art" to minimize weight.

b) The estimates of the weights of the gas systems are optimistic; i.e., whenever the weight of a component was estimated, it was given the benefit of any doubt with the expectation that the weight might be achieved through a development program.

c) The gas systems require substantial development work. Both are predicated upon the possibility of extending their present range of applicability; e.g., to Foster-Miller's knowledge, no gas motor or turbine in this range has been operated successfully for as long as several hours in the anticipated environmental conditions.

d) Although great advances have been made in recent years in the reliability of liquid propellant systems, reliability is still a major problem.

e) The electric motor system is probably the most reliable. It is the least complicated and uses proven components. It can be readily turned on and off, or reversed.

From the preceding discussion, it appears that the electrical system will be the most reliable and probably not much heavier than the gas systems. Also it requires no appreciable development effort to become operational. However, if the operating time becomes large, as it appears it might because of the low thrusts which can be applied to the bit, a more thorough investigation should be made of the gas turbine system because of the weight savings indicated in Figure 10. Also, other electrical energy storage or generation systems should be investigated for extended operating times.

2.3. Advancing the Shaft

2.3.1. Shaft Configuration

The rotary shaft may be one or multi-piece. Unless there is a very good reason for having a short package axially, the arguments for a one-piece shaft on the grounds of simplicity and reliability are overwhelming. A one-piece shaft mechanism will also weigh less than a multi-piece shaft mechanism. A more important weight consideration, however, is the weight saving per unit length of hole in the rotary power system. This is possible because the minimum diameter of hole for a multi-piece (telescoping) system is larger than that for a one-piece shaft. This is clearly seen by examining the various mechanisms presented in Sheets 1 and 2 of the Lunar Drilling Mechanisms drawings. (See end of this Section II) Unfortunately, the depth to which a one-piece shaft can drill is limited to something less than the package length. If it is desired to go deeper, a multi-piece shaft is necessary.

Of the many possible multi-piece shaft configurations, the following three were examined.

2.3.1.1. Telescoping Shaft

This has the advantage that its package will occupy approximately the same volume as a one-piece shaft. The pieces are arranged on a common center line and need to be moved only axially. The primary disadvantage is, as mentioned above, that the hole size, and therefore the power required for drilling, will increase significantly for each added section.

2.3.1.2. Folding Shaft

Many folding arrangements are possible. They all have the disadvantage that they require more room for packaging; and result in added complexity of aligning and locking the segments together.

2.3.1.3. Assembled Shaft

This would consist of sections which are assembled as the hole is drilled. Again many possibilities are available, but they all have the disadvantage of added complexity and weight.

On the basis of the above discussion, it was decided to use a telescoping system if a hole deeper than that attainable with a single piece shaft is required.

The systems which were investigated are illustrated in the above-mentioned drawings of the Lunar Drilling Mechanisms and discussed in Section 3 below.

2.3.2. Methods of Feeding the Shaft

Two methods were considered for advancing the shaft: (1) pneumatically, i.e., pushing the shaft down by gas pressure; and (2) electromechanically, i.e., using an electric motor to actuate a mechanical device, such as a feed screw.

Both schemes are illustrated in the Lunar Drilling Mechanisms drawings, and are discussed in some detail in Section 3 below.

2.4. Removing the Chips

It is necessary to remove chips from the bottom of the hole to permit the bit to engage virgin surface and to avoid floundering of the bit and/or binding of the shaft. A hole can be drilled faster and with a minimum expenditure of energy if good cleaning is accomplished. Chips may be removed from the hole by two basic methods: (1) suspension in a moving fluid stream, e.g., gas transport; or (2) mechanical conveyor, e.g., a screw conveyor.

2.4.1. Gas Cleaning

In this system, gas passes down the center of a hollow drill shaft and through small holes in the bit out into the annulus between the shaft and the hole. The stream picks up chips off the bottom and conveys them to the surface, where part of the stream can be sampled. Gas cleaning requirements are examined in detail in Appendix C. The technique appears quite feasible and the required system appears to be relatively simple. An important result of the analysis is that by low pressure operation the gas mass flow requirements can be substantially reduced. Figure 11 shows transport system weights required as a function

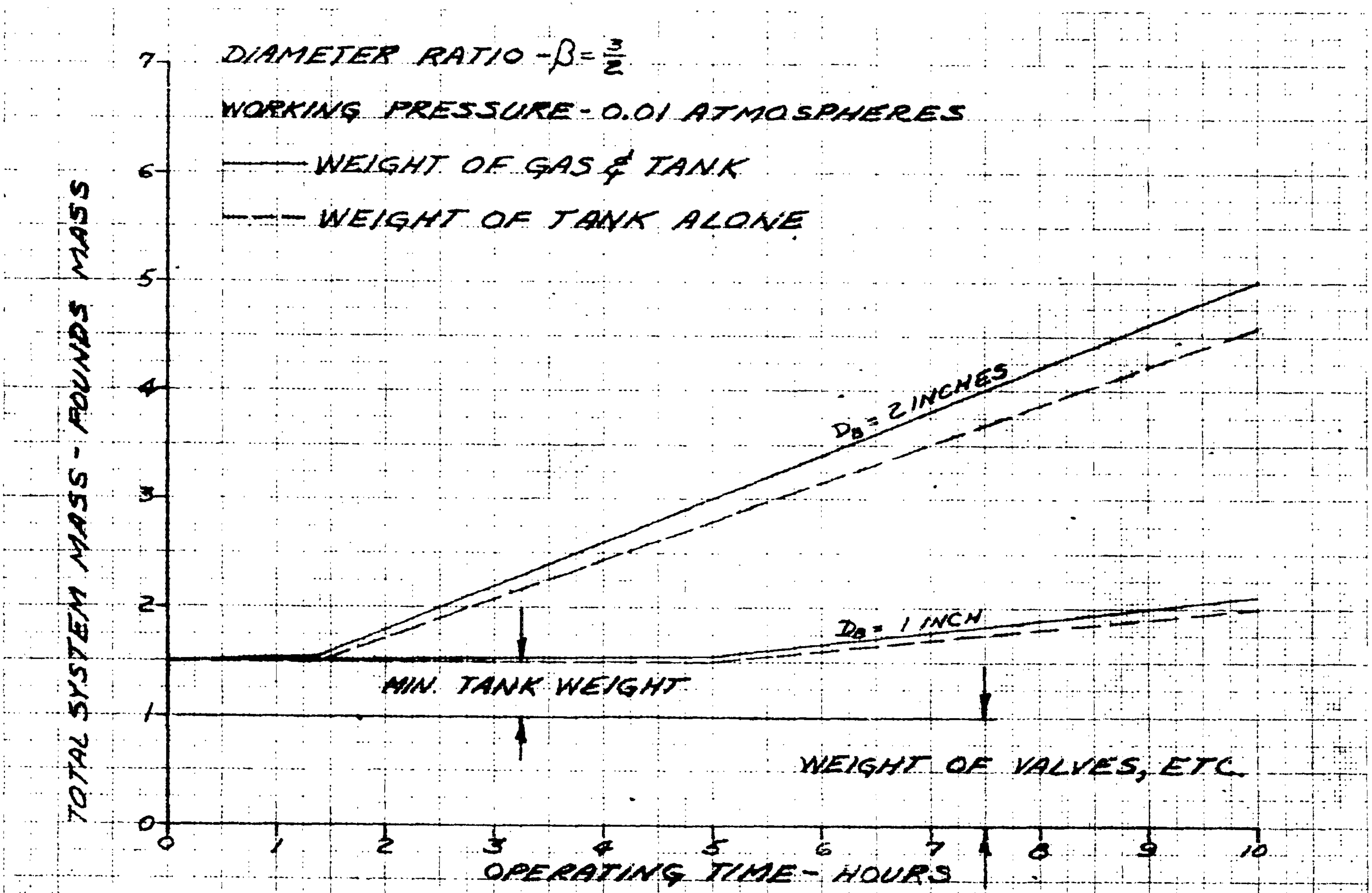

MASS OF HELIUM GAS TRANSPORT SYSTEM

FIGURE 11

of the time of operation when helium gas is used. The transport system includes: (1) the mass of gas, (2) the container or tank, and (3) accessories such as regulating valves, etc.

2.4.2. Mechanical Cleaning

In this system, the bit is designed to facilitate "scooping" up the chips from the bottom of the hole and conveying them up by means of a screw-feed type mechanism. Past experience with screw feed mechanisms indicates that frictional forces may prevent continuous transport of chips to the surface. The alternative, periodic retraction and "spinning off", would require an elaborate mechanical system. In view of these obvious difficulties, it appears that the gas cleaning system will be more simple and dependable and hence should be chosen for the application.

2.5. Providing Cooling for the Bit

Since most of the power required for diamond bit drilling goes into friction heat, some means is usually provided for cooling. Whenever possible, water is used. However, air may also be used, but the mass flow requirement is much higher than that required for cleaning. The various "heat sinks" available have been examined to determine their heat-dissipating capacity. (See Appendix B.) The analysis indicates that the bit will not overheat, even if no fluid cooling is used, provided the drilling power level is low, say 1/3 hp; and if good cleaning can be effected, i.e., the newly formed "hot" chips can be gotten out of the way.

3. Description of Drilling Mechanism

3.1 General Requirements

The general requirements for a lunar drilling system can be itemized as follows:

(a) Maximum reliability

(b) Ability to drill a hole in hard rock while functioning in a difficult environment.

(c) The entire package must be as light as possible

(d) The mechanism must be packaged as compactly as possible.

(e) Vibrations transmitted to the moon vehicle should be negligible.

(f) The package must not generate R-F electrical noise.

These requirements are presented in the order in which they should be considered to determine the final design.

The difficult environment existing at the surface of the moon, is one of very high vacuum with surface temperatures varying from over 200°F to less than -150°F during the lunar day. In addition, the gravitational force on the moon is one-sixth that of the earth.

These conditions present severe lubrication problems for those parts of the mechanism working in the vacuum. All high speed bearings must be hermetically sealed. Those bearings which must function in the vacuum must be designed with care and functionally evaluated.

The type and hardness of rock to be drilled is unknown; the mechanism, therefore, must be capable of drilling both very hard and soft materials. It has been assumed that the drilled material is granite. Since the mechanism will be instrumented, the nature of the material actually being drilled may be inferred from the rate of penetration.

The mechanism must also be designed so that provisions can be made to recover samples of the material being drilled. These samples will be analyzed.

When all the functional requirements are met, the problems of weight and volume can be attacked. The mechanism must be as light and as compact as possible while being capable of performing the assigned task.

3.2 Proposed Drilling Mechanisms

The drill rig considered in this section is a diamond rotary bit rotated by an electric motor. For holes of less than five feet depth, the shaft will be made in one piece; for deeper holes it will have telescoping sections. The drill can be advanced into the hole either mechanically or pneumatically. Similarly, the telescoping shaft can be extended and retracted either mechanically or pneumatically. The chips will be removed by a low-pressure gas cleaning system.

Several alternative systems to rotate and feed the bit are illustrated in the Sheet 1 and Sheet 2 drawings. For conciseness, the following abbreviations will be used on subsequent curve sheets.

PA - Pneumatic drill advance (pneumatic feed)
MA - Mechanical drill advance (mechanical feed)
PE - Pneumatic extension of telescoping shaft
ME - Mechanical extension of telescoping shaft.

3.2.1. Pneumatic Drill Advance (PA)

The pneumatic drill advance with a one-piece shaft is illustrated in the bottom picture on Sheet 1.

The drill bit motor, gear train and a supply of gas for advancing the drill are enclosed in a sealed piston which is inside the feed cylinder. The drill shaft extends through a bushing at the bottom of the cylinder. The gas reservoir for chip removal is attached to the shaft and rotates with it, thus eliminating the necessity of a dynamic shaft seal. The supply valve for this gas may be actuated by centrifugal force, opening when the shaft is rotated.

The piston and cylinder may have some cross section other than circular so that the bit reaction torque will be absorbed by the feed cylinder. The drill is advanced by introducing gas at a regulated pressure of a few psia into the space between the top of the piston and the end of the cylinder. This will feed the drill by a constant load allowing the penetration rate to vary as the rock hardness changes.

3.2.2. Pneumatic Drill Advance and Pneumatic Drill Shaft Extension (PAPE)

The pneumatic extension mechanism is shown at the top of Sheet 2. The gas used for cleaning is introduced into the top of the shaft, at a pressure of 200 to 400 psia, forcing the smaller inside shaft down relative to the outer shafts. The gas will be further reduced in pressure in passing through the bit to be used for chip transport. The two upper views in the drawing illustrate only the pneumatic extension. This method of extending a telescoping shaft could be used with a pneumatic feed to form a PAPE.

3.2.3. Mechanical Drill Advance (MA)

The mechanical advance or feed mechanism is illustrated in the middle of Sheet 1. The drill bit motor and gear train are mounted on a platform or enclosed in a case which has three equally spaced threaded holes around its edge. A lead screw runs through each hole. Both ends of each screw are fitted in bushings, which permit axial travel of the screw to limit thrust on the drill shaft. The upper end of each lead screw is spring loaded and has a sprocket fixed to it. A small drive motor rigidly attached to the exploration vehicle frame drives one of the lead screws through a small gear train. The other two screws are chain driven from this powered screw. The lead screws force the bit-rotating motor and shaft down. Any axial force on the drill bit is transferred to the lead screws and into the springs at their upper ends. When the load reaches a predetermined value the lead screws move upward enough to disengage the advance or feed gears. The speeds and forces involved in the lead screw drive motor are low enough to allow gear engagement and disengagement without gear tooth damage. An alternate method would be to use a torque limiting clutch or overload protection in the electrical circuit (neither is shown).

The gas reservoir for chip removal may or may not be rigidly attached to the drill shaft.

An alternate method of arranging the drill bit motor, gear train and gas reservoir for chip removal is shown at the top of Sheet 1. Here the drill bit motor is positioned on its side and the gas reservoir is remotely located. This arrangement has the advantage of getting maximum hole depth from the mechanism.

With a mechanical feed mechanism, the rate of penetration can be measured by counting the turns of the lead screw; and the force on the bit could be measured from the deflection of the springs at the upper end of the lead screws.

3.2.4. Mechanical Drill Advance and Pneumatic Extension (MAPE)

The mechanical advance, pneumatic extension mechanism

would consist of either MA system described above, coupled with the PE system illustrated at the top of Sheet 2 and described in Section 3.2.2.

3.2.5. Mechanical Drill Advance and Mechanical Extension (MAME)

The mechanical advance is described in Section 3.2.3. The mechanical extension (ME) is illustrated at the bottom of Sheet 2. A series of concentric threaded screws capable of being telescoped is surrounded by a series of concentric shafts also telescoping. The screws are the means of advancing the drill and the shafts rotate the bit. The outermost lead screw is rigidly attached to the lunar vehicle frame, and the outermost shaft is rotated by the last gear of the gear train. The shafts are splined so shafts and bit rotate together. This is clearly shown in the blown-up Detail A-A. The inner feed screw is driven through the clutch in the bit as long as the axial load does not exceed a preset value, say 50 pounds. When this value is exceeded the spring in the bit is compressed enough to disengage the clutch. The bit keeps rotating but does not advance since the inner screw is not rotated. This will continue until the axial load decreases and the spring extends to engage the clutch.

In the illustration, the motor does not advance with the drill as it does on Sheet 1. However, this feature may be added if desired. The MAME as shown requires remote location of the gas reservoir for chip removal, which necessitates a rotary seal. The gas bottle could be located around the outer shaft to avoid this problem.

This particular mechanism can be retracted by simply reversing the motor. The rate of penetration can easily be measured by counting lead screw revolutions. The force on the drill bit can be determined within limits from the clutch spring deflection.

3.2.6. Drill Retraction

The mechanical systems, MA or MAME, can be easily retracted by reversing the motors which drive the feed screws. In order to retract in the pneumatic systems, (PA, PAPE, or MAPE), the mechanism shown in the top illustration of Sheet 2 is suggested. A wire wound on a reel with one end fastened to the lower section of the shaft is unwound as the shaft is extended. For retraction, the gas supply is

shut off and the wire is rewound on the reel by a small electric motor. The device could be used for measuring penetration by counting the number of turns of the reel. The theoretical power required for drill retraction is very small, about 0.005 hp, provided the time of retraction is allowed to be a minute or two.

3.2.7. Comparison and Weight Analysis of Mechanisms

The weight of the mechanisms described in the preceding paragraphs is presented in Figure 12. These results do not include the weight of the drill bit motor and power supply (see Figure 10), or the cleaning gas and storage tank, (see Figure 11). Thus, only the weight of the mechanism for advancing the shaft and the shaft itself are included.

Eight configurations were analyzed and the weight of the mechanism was plotted against the range of depths the particular configuration would be able to drill. A one-piece shaft in a six foot package could drill to a depth of about five feet so the weight of the five-foot model was plotted against the range from zero to five feet. Weights were estimated using titanium as a construction material; and the shaft sizes were determined by buckling considerations, but in no case was a wall made thinner than one-sixteenth inch.

The results show that the mechanical advance (MA) seems to have a slight weight advantage over a pneumatic advance (PA). However, it is quite possible that slight changes in configuration could reverse this. For example, by using a planetary gear train, the cylinder diameter in the PA system could be reduced to about 3 or 4 inches. This would reduce the weight of the PA system to about 8.5 pounds. For estimating system weights, the results presented in Figure 12 will be used. The minimum bit sizes shown in Figure 12 are governed by the shaft sizes. A telescoping shaft will obviously require a larger bit as sections are added: and the mechanical extension, which is essentially a double telescoping system will require an even larger bit. The mechanical extension (ME) compares rather poorly because of higher weight and larger bit size.

For the calculation of system weights in the following section, the lightest weight mechanisms in Figure 12 will be used: i.e., MA or MAPE.

4. Overall System Weight

In previous sections, the weights of the various sub-systems

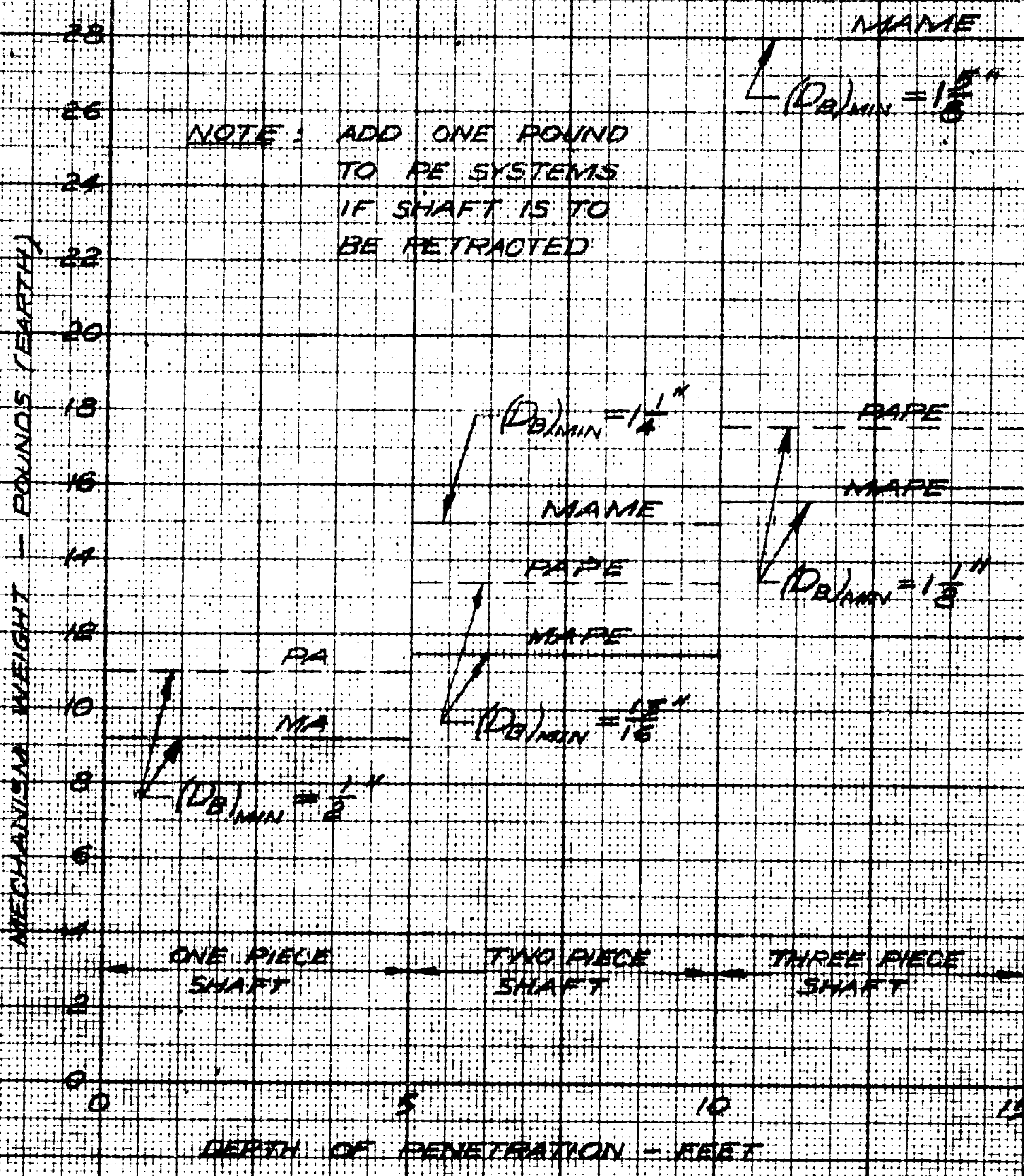

WEIGHT OF DRILLING MECHANISMS

FIGURE 12

were presented. These will now be combined to form an estimate of the total drilling system weight.

Of the various possibilities of sub-system configuration, the following were chosen:

a) Drill rotation - electric motor (0.1 horsepower) powered from silver-zinc storage batteries.

b) Chip transport - using helium at a working pressure of 0.01 atmospheres.

c) Drill Mechanism - mechanical advance with pneumatic extension of a multi-piece shaft (MAPE).

Two cases were investigated for the range of hole depths from zero to ten feet.* One with a drill bit of minimum size as determined by structural considerations; the other with a one inch diameter drill bit. The minimum bit size and mechanism weight were found from Figure 12. With bit size and power level (0.1 hp) known, Figure 5 yielded the penetration rate, from which the time of operation was found.** With the time of operation known, Figures 10 and 11 were used to find weights of the rotary power and gas transport systems, respectively. The results are presented in Figure 13.

The results show that the major part of the system weight is due to the storage batteries. With the system described above, it is possible to construct a drill rig within the weight limit of sixty pounds provided the depth is limited to five feet and the drill bit diameter does not exceed 3/4 inch; the time required to drill would be about 20 hours if the shaft power were 0.1 hp and 10 hours if the power were 0.2 hp. However, if there is no particular reason for making the hole 3/4" in diameter, a hole only 1/2" in diameter or a cored hole will result in a much lighter system as shown by Figure 13. The 1/2" hole

* Holes deeper than ten feet were not considered because the overall system weight became very large.

** The time of operation may be somewhat adjusted by varying the power level. Since the maximum load is set at 50 pounds, for a given bit size the power is determined by the rotary speed. However, heat dissipation and chip removal requirements at the bit set an upper limit of about 1/3 hp. Although the operating times can be reduced by increasing the power level, the total energy required (horsepower x time of operation) remains constant, so that the weights are not affected.

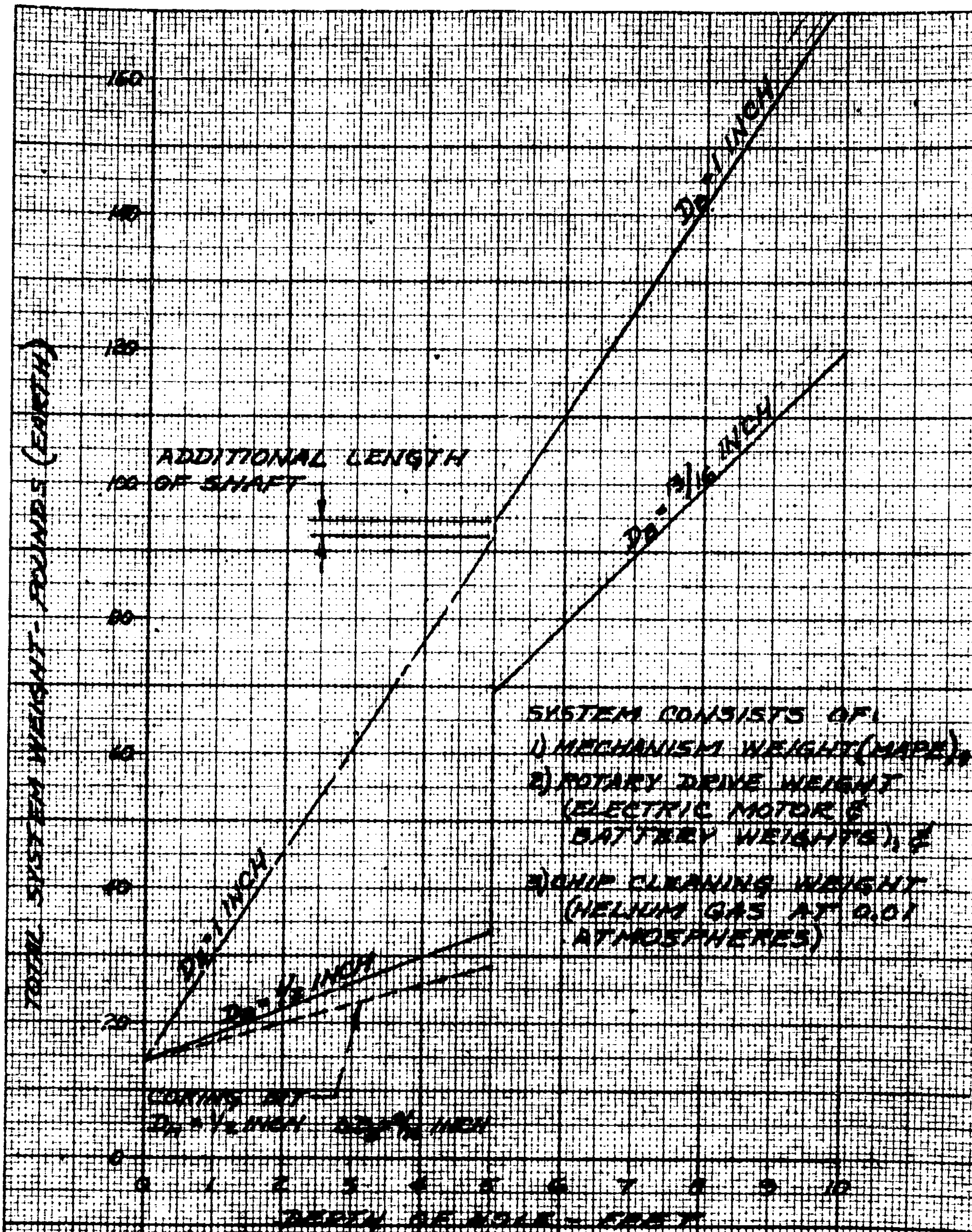

WEIGHT OF TOTAL DRILLING SYSTEM

FIGURE 13

-31-

system will weigh only 34 pounds for a hole depth of 5 feet; and the time required to drill would be about 8 hours if the shaft power were 0.1 hp.

A minimum size core bit (D_M = 1/2 inch, ΔD_B = 3/16 inch) can be used with a one-piece shaft which would result in a slightly lower energy requirement per foot drilled; and hence a slight weight saving. This configuration is not shown. It would be similar to the middle illustration of Sheet 1, except that it would use a core bit. The core will not be removed but will remain inside as drilling progresses. A core-bit used with an extendable shaft is not shown since a pneumatically extending coring shaft was not designed. Significant savings are not anticipated because of the size and complexity of the system.

If a much lighter source of power can be used, a system with much greater capabilities is possible; but in any event, drilling beyond ten feet (using a shaft with more than two pieces) does not appear feasible within the limit of an overall system weight of sixty pounds.

5. <u>In Conclusion</u>

Of the various possible mechanical systems, it appears that the most suitable diamond bit system, from the standpoint of weight and reliability, would consist of:

(a) An electric motor-storage battery combination for the rotary drive

(b) Helium gas for chip scavenging

(c) A mechanical or pneumatic advance (with pneumatic extension of a multipiece shaft)

as the basic drilling mechanism.

Using such a system, with a one-piece shaft, it should be possible to construct a drill rig which would weigh about sixty pounds and which would be capable of drilling a hole 3/4 inch diameter by five feet deep. The lightest system capable of making a hole five feet deep would weigh approximately half this, or about thirty pounds. It would make a 1/2 inch diameter full hole or a core hole having a 1/2 inch minimum diameter. The space requirements for any one of these systems would be a cylinder about six inches in diameter by six feet in length exclusive of batteries. The system appears to have reasonable growth

potential, i.e., a hole 13/16 inch diameter by ten feet deep could be drilled with an overall system weight of one hundred and twenty pounds. This is illustrated in Figure 13. Furthermore, the rig would not be subject to severe or intolerable vibration and, with appropriate electrical shielding, it is not expected to generate any R-F noise.

In arriving at the above conclusions, many "sticky" problems were examined analytically or by a minimum of experimental work. Some of the solutions which require additional attention are:

(a) The chip removal scheme appears quite feasible but it is yet to be proven in the laboratory.

(b) The drilling power requirements and penetration data were based on a very limited number of tests.

(c) The starting problems and the durability of the diamond bit must be examined in greater detail

(d) Although the diamond bit performs well in consolidated formations, its operation in loose, granular formations remains to be determined.

(e) The ability to design seals, bearings, etc., which will function properly in the environment existing on the moon remains to be proven.

(f) The predictions concerning bit cooling need to be checked in the laboratory.

It is anticipated that straightfoward engineering design and development will resolve all these problem areas with the possible exception of (c), diamond bit life. The laboratory tests made at Hughes Tool Company* with two J.K. Smit and Sons diamond bits were not encouraging. These bits consisted of a finite number of fairly large diamond points set in the surface of a sintered metal matrix. During the drilling tests, the individual diamonds dulled rapidly and/or came loose from the matrix. There is some question as to whether this was a "hard" or "soft" formation type bit. Considerably better performance was obtained with a Felker "Di-Met" core bit used by Foster-Miller Associates. This bit has a section of diamond dust impregnated material about 1/4 inch long which continues to drill until completely worn away.

---

* See Appendix 2, "Bi-weekly Report No. 3", submitted 26 August 1960; and Appendix E of this report.

Preliminary tests at Hughes have confirmed this. It is felt that the problem of bit life can be resolved with time and development.

In view of the foregoing, the conclusion regarding the feasibility of diamond bit drilling on the moon cannot be clear cut. However, the results of these preliminary studies indicate that the diamond bit is a promising contender. If the durability of these bits were established, the diamond rotary system would be recommended over the percussion drill, for certain combinations of hole diameter and depth, because of its inherently simpler and more reliable design. See Section III - 6 for further discussion on this point.

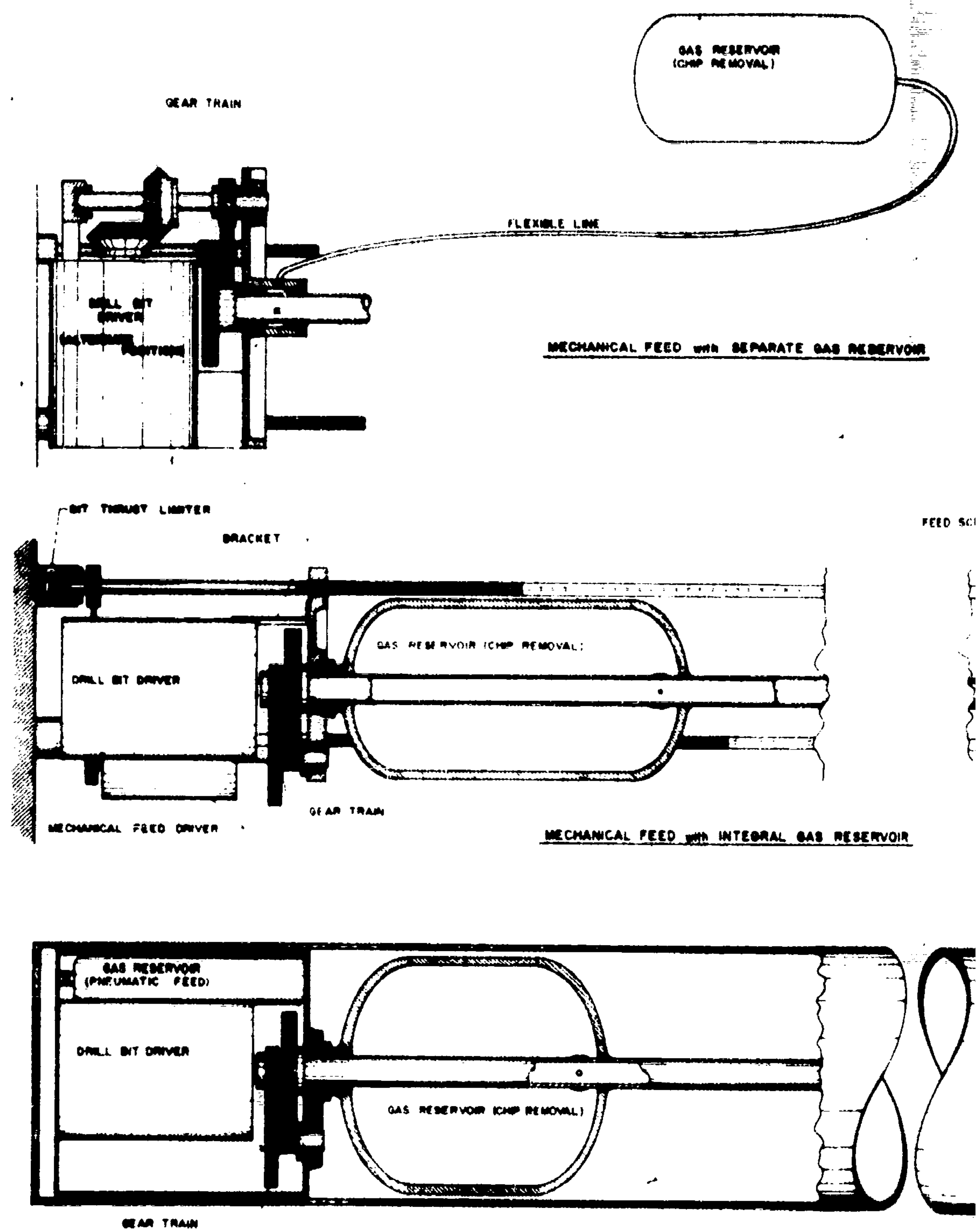

MECHANICAL FEED with SEPARATE GAS RESERVOIR

MECHANICAL FEED with INTEGRAL GAS RESERVOIR

PNEUMATIC FEED

1

LUNAR DRILLING MECHANISMS

FULL SCALE

ARTIST'S CONCEPTION

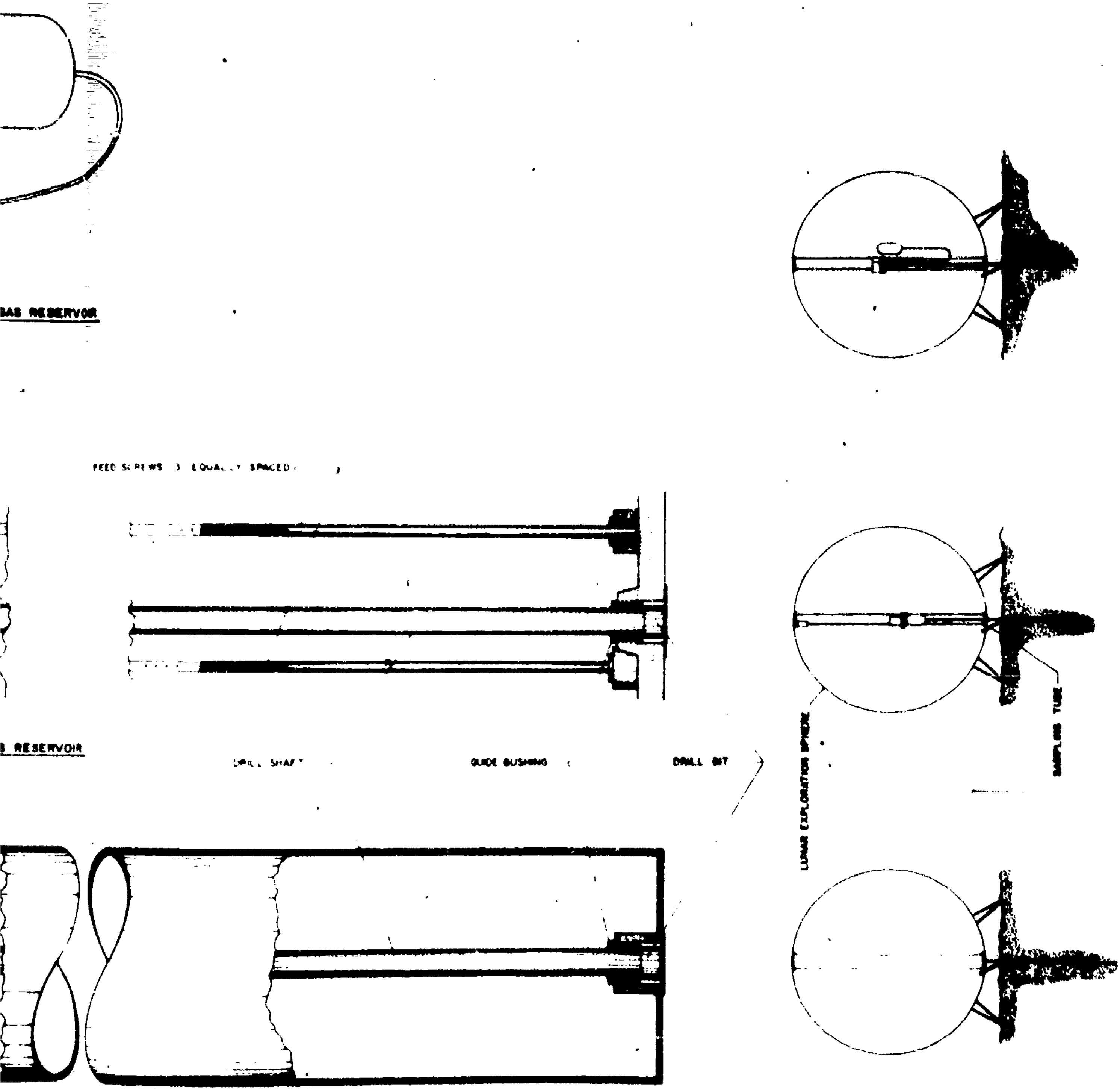

MECHANISMS

2

FOSTER-MILLER ASSOCIATES, INC.
WALTHAM, MASSACHUSETTS
AUGUST, 1960

SHEET 1 of 2

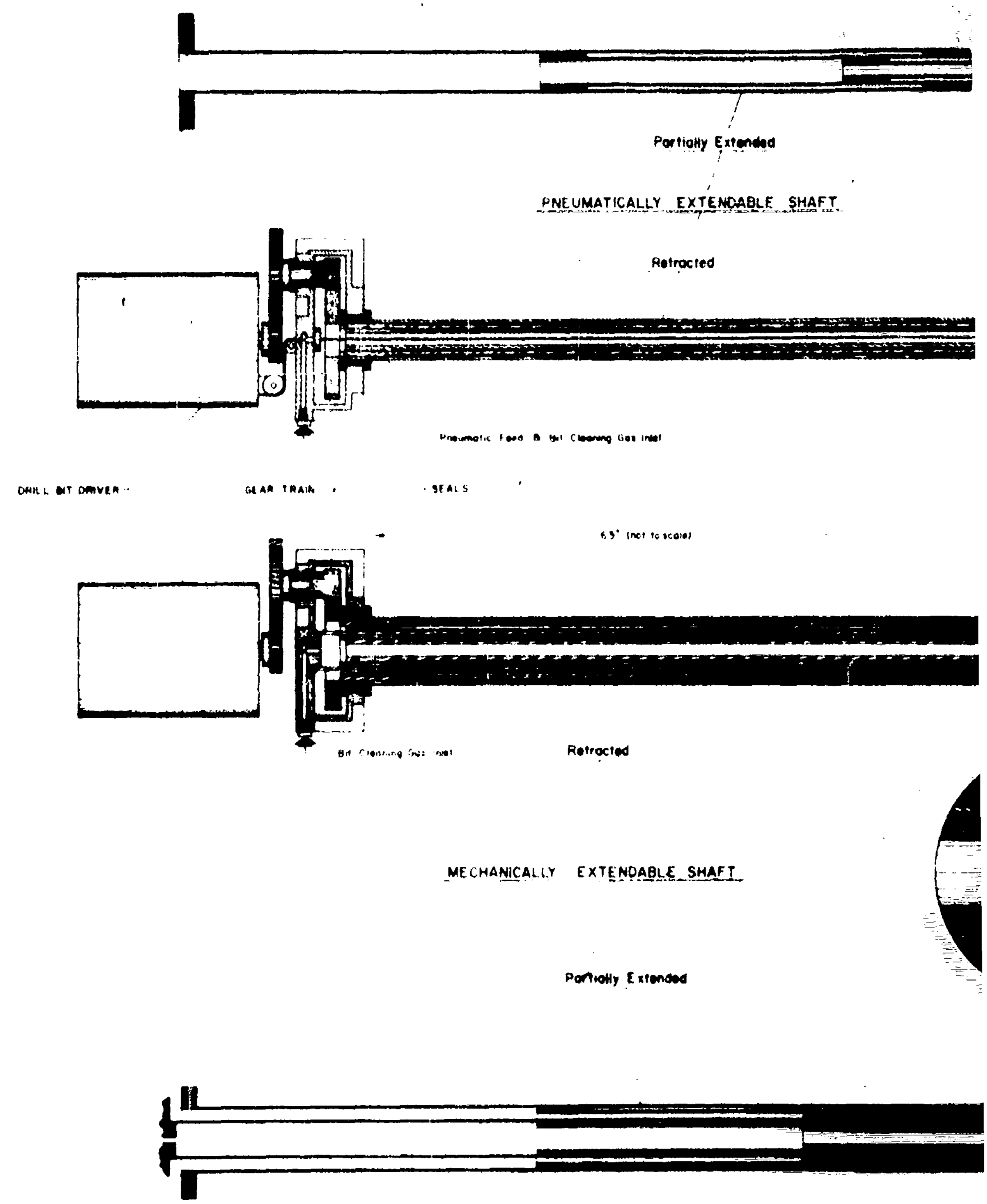

1

LUNAR DRILLING MECHANISMS

FULL SCALE

ARTIST'S CONCEPTION

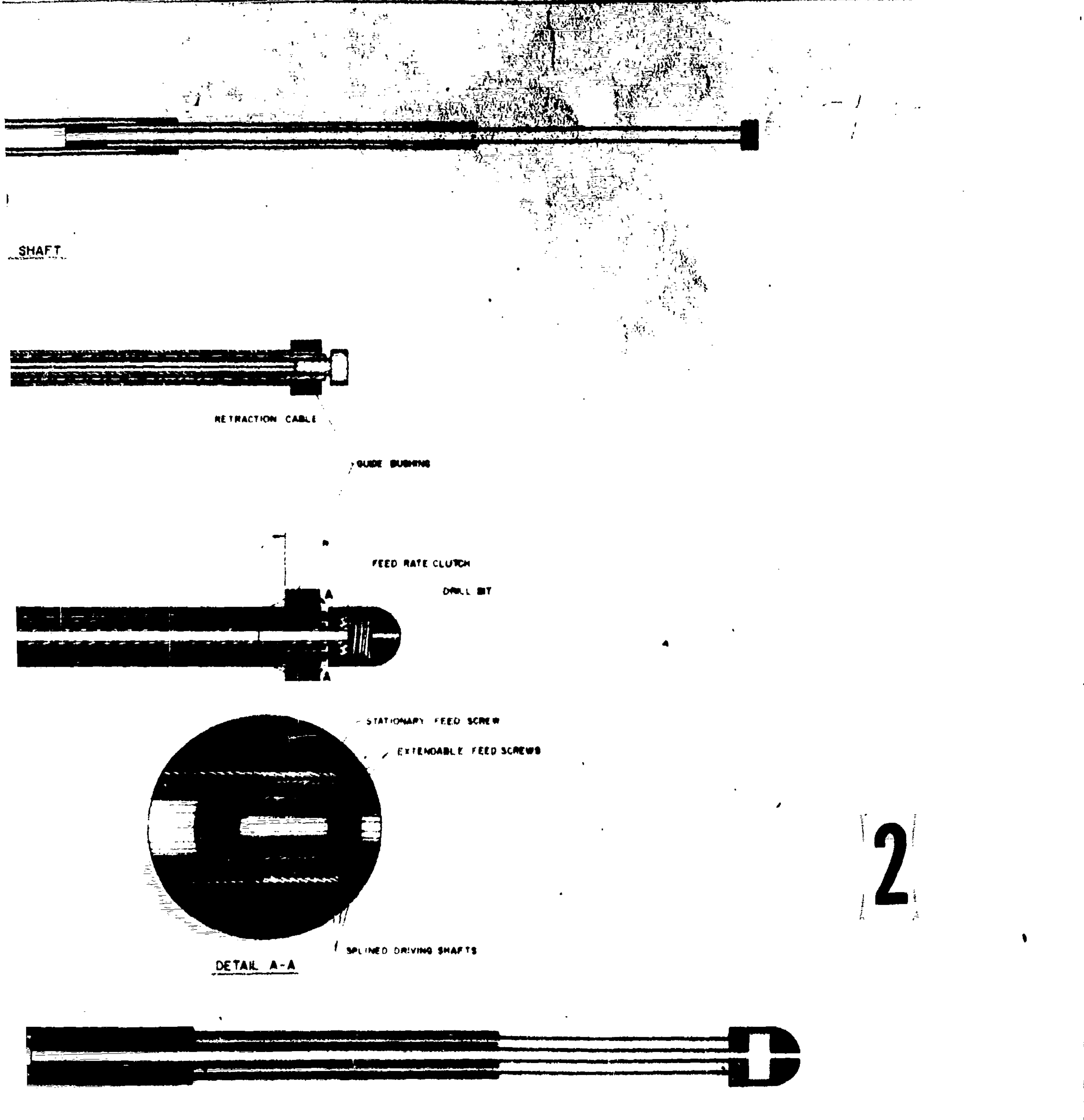

CHANISMS

FOSTER-MILLER ASSOCIATES, INC
WALTHAM, MASSACHUSETTS
AUGUST, 1960

SHEET 2 of 2

Section III

Percussion Drilling

1. Introduction

In the survey of drilling methods presented in Section I, percussion drilling appeared to be one of the two feasible methods of producing a hole in the moon. The other method, rotary diamond bit drilling, was discussed in Section II. This Section III is devoted to the percussion drill rig and it presents: (a) a discussion of the principle of operation of a percussion drill; (b) the several tasks which a percussion rig must perform, and various methods of accomplishing them; (c) a description of three of the most promising systems; and (d) preliminary weight estimates for those three systems.

2. Principle of Operation of a Percussion Drill

Although the mechanical design of percussion drills may vary markedly, their basic mode of operation will be the same. Energy is supplied to a mass or hammer over a relatively long period of time. Thus, a low-power source is able to store a fairly large amount of energy in the mass. Subsequently, the mass impacts with the rock either directly, or indirectly through a drill rod, and dissipates its energy over a very short period of time. This results in extremely large stresses (or strains) in the rock. These high stresses cause immediate fracture of the rock with relatively small energy losses due to friction between the tool and the rock*. This is in contrast to rotary diamond bit drilling where the friction energy losses associated with the drag between the tool and the rock surface are very large compared to the strain energy input to the rock which effects fracture.* Thus, impact drilling appears to be considerably more efficient.

Although the processes involved in fracturing rock are not thoroughly understood, the following characteristics of impact drilling are known:**

a. The amount of rock which is fractured by a blow from the hammer depends on the energy of the hammer and not its

* Note, however, that only a small fraction of the strain energy put into the rock is utilized to fracture rock. The remainder of the strain energy is dissipated in the rock as the bit load is removed. As this energy is distributed throughout a large mass of rock, no significant temperature rise occurs.

** "The Fundamentals of Rock Drilling". Paper 826-27-H by R. Simon, D.E. Cooper and M.L. Stoneman, Battelle Memorial Institute, Columbus, Ohio.

momentum.

b. The energy required to drill rock is proportional to the volume of material removed for a given chisel geometry, i.e.,

$$E_o = \frac{\pi}{4} D_B^2 h \sigma_c \tag{5}$$

where:

E_o = Energy input (in-lb)
D_B = Hole diameter (in)
h = Hole depth (in)
σ_c = Specific energy (in-lb/in^3)

The best available value for the specific energy of grey granite for an acute-angle, wedge-shaped bit is about 40,000 in-lb/in^3.*

c. A threshold energy per impact exists, depending on bit shape, below which the rock drilling process becomes very inefficient. For impact energies above the threshold value, relatively large chips are formed. Conversely, for energies below the threshold value, only local pulverization occurs, i.e., very small chips are formed; and since the volume of rock fractured is low, the apparent specific energy is several times that when large chips are formed. The best available value for threshold energy** is about 100 in-lb per inch length of a chisel bit having a cutting edge width of about 1/16".

3. Principal Tasks in Percussion Drilling

The block diagram of Figure 14 shows the principal functions which are required for drilling a hole with a percussion drilling rig on the moon. It is seen that they are:

a. Provision of reaction force
b. Hammer actuation
c. Tool advance
d. Chip removal
e. Bit rotation
f. Bit cooling

---

* Based on information from the Ingersoll-Rand Company and extrapolation of data given in Paper 826-27-H cit. Page 38.
** cit. Page 38.

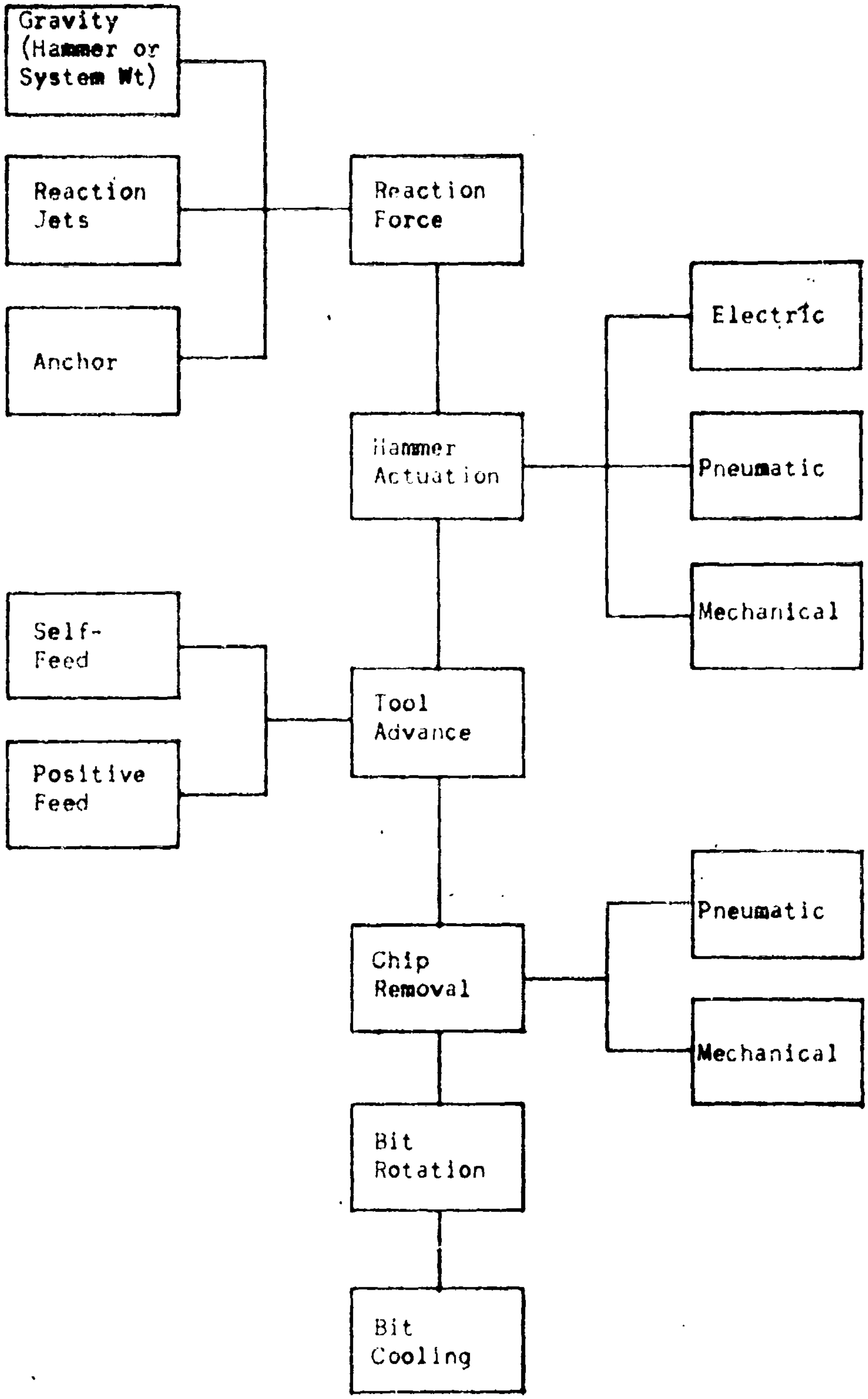

Principal Functions in Percussion Drilling

Figure 14

The various methods of fulfilling these requirements will now be examined and compared for relative feasibility. The specific mechanical design requirements and drilling systems will then be considered in Sections 4 and 5.

3.1. Provision of Reaction Force

In the operation of a percussor, an internal force is required to accelerate the hammer. If the casing of the percussor is not permitted to recoil, then the instantaneous external reaction force on the casing must be equal to or greater than the internal force. If, however, the casing is permitted to recoil, then the only requirement is that the average reaction force equal the average rate of momentum transfer to the hammer. In either case, some reaction force is required and may be supplied by: (a) external reaction forces applied to the casing; (b) the weight of the percussor exclusive of the hammer; or (c) inertia forces resulting from acceleration of the casing.

By reasoning similar to that employed in Section II - 2.1, it may be concluded that about 50 pounds of reaction force from the weight of the vehicle could be used to load a moon-drilling mechanism. It is undesirable, however, to use all the available weight of the capsule as reaction force because cyclic variation of this reaction force would tend to excite vibration of the capsule and its contents. These vibrations could, at the expense of added weight and complexity, be partially isolated from the capsule.

The most desirable source for reaction force is the weight of the impact tool itself. Since the tool will only weigh from two to six pounds on the moon, the percussor should be designed to operate with a small average reaction force. Analysis (Section II of Appendix F) shows that percussion drilling on the moon can be efficient with average reaction forces equal to the weight of the percussion tool, provided that the impact rate, hammer mass, and energy delivered to the rock per blow are properly matched. The amount of recoil can also be limited to reasonable values, typically less than one inch.

For the reasons outlined above, all percussion systems recommended in this study will utilize the tool weight to supply the reaction force necessary for impact drilling.

3.2 Hammer Actuation

Actuation of the percussor requires a hammer, a source of energy and means (a mechanism) of transforming this energy into mechanical motion of a hammer.

3.2.1. Energy Sources

Of the many possible energy sources, only three appear to be feasible for use in the present moon-drill system. These are:

a) Electrochemical (storage batteries)
b) High-pressure, stored gas
c) Liquid propellant hot gas

The silver-zinc type of storage battery is suitable for use on the moon and will typically provide 33 watt-hours of energy per pound of battery including case and connections. (See Section IV, Appendix D.) If η_1 is the overall energy conversion efficiency of the impact tool, and Equation (5) is used to express the energy required, the resultant battery weight, on earth, is

$$Wb = 0.746 \times 10^{-6} \frac{\sigma_c D_B^2 h}{\eta_1} \quad \text{(lbs)} \qquad (6)$$

where the symbols have the same meaning as before.

Stored high-pressure gas can be conveniently and directly utilized in a pneumatically-actuated percussor and can at the same time serve for chip scavenging. The requirements for gas and container mass and volume as determined in Section I of Appendix F for nitrogen and helium as working fluids show that the overall weight of the nitrogen source will be slightly less than that of the helium source. The weight of the stored-gas source is independent of the gas pressure and its volume is inversely proportional to pressure. The nitrogen system weight, Ws, on earth, can be expressed as

$$Ws = 1.11 \times 10^{-5} \frac{\sigma_c D_B^2 h}{\eta_1} \quad \text{(lbs)} \qquad (7)$$

This is based on the assumption that the initial stored mass of gas is sufficient to allow only a 25% drop in gas temperature. (See Section I of Appendix F for details.) Comparison of Equations (6) and (7) shows

that, for equal efficiency of operation, the stored-gas system is over ten times heavier than the battery system. The weight of the stored-gas system might be decreased somewhat, (possibly by 40%). by reducing the initial stored mass of gas. This may be accomplished by intermittent drilling to permit heat transfer from the surroundings to the gas to maintain reasonable temperature levels, but only at the expense of added complication. Figures F-3 and F-4 in Appendix F show the weight and volume of a nitrogen system, for a storage pressure level of 3000 psi, as a function of hole size and depth.

The third feasible energy source for moon drilling is a chemical, hot-gas generator. The simplest and most reliable gas generators are of either the solid fuel or the liquid monopropellant types. Bipropellant systems can provide higher energy outputs per pound of propellant, but only at the expense of added complexity and, hence, lower reliability. The liquid monopropellant is chosen over the solid propellant because: (1) the latter generates "dirty" gas, i.e., has solid, gummy particles in the gas stream, which tend to clog the small flow-control orifices; and (2) the grain has an excessively large ratio of length to diameter due to the low mass flow of gas and the relatively long time of operation required. Hydrazine, $N_2 H_4$, is a liquid monopropellant which decomposes to form a relatively clean gas at a generator temperature of 1960° R. It, therefore, appears to be feasible as an energy source for percussion drilling.

A detailed analysis of the hydrazine gas generator shows that the weight of a hot-gas system required for drilling a 5 foot hole 3/4" in diameter in grey granite (σ_c = 40,000 lb-in/in^3) is about 5.5 pounds. (See Section I of Appendix F.) To make the same hole, Equations (6) and (7) give the weight of the battery system as 2.5 pounds and of the stored-gas system as 30.2 pounds. Thus, it would appear that the battery or hot-gas systems should be chosen. However, it should be realized that hot-gas generators for extended times of operation are not within the present state of the art and would require considerable development before a practical and reliable system could be realized. Furthermore, the use of high-temperature gas in the percussor mechanism will require the solution of many difficult mechanical design problems connected with differential expansion, the sealing of high-temperature gases, and high-temperature metallurgy. Until the form of the actuation

mechanism is selected, it is not possible to choose between the above energy sources. This selection is considered below in Section 5.

3.2.2. Actuation Methods

The type of actuation, or the method used to accelerate the hammer mass in a percussion drill, will depend on the energy source employed and the degree of recoil desired.

3.2.2.1. Zero-Recoil Percussors

A detailed analysis was made of two general types of zero-recoil percussors; i.e., the gravity-force actuated system and the contact-force acceleration system. Both systems are awkward and complex mechanically and offer no weight advantage over the finite-recoil type of percussor. In addition, the zero-recoil systems would transmit time-varying forces to the moon capsule and, therefore, would tend to excite vibrations in that structure. The zero-recoil percussor mechanism is, therefore, eliminated from further consideration. (See Section II of Appendix F for details.)

3.2.2.2. Finite Recoil Percussor

In order to avoid transmitting vibratory (or even steady) forces to the moon capsule when recoil is permitted, the reaction force exerted on the percussor must be supplied by the casing weight. If the percussor earth weight is limited to about 16 pounds, the available reaction force on the moon is only about 2.7 pounds. Thus, the percussor must be designed to operate effectively under this small reaction force. A dynamic analysis was made of a percussion drill for two limiting modes of operation; i.e., intermittent percussion and continuous percussion. (See Section II of Appendix F.)

In the intermittent mode, the time interval between blows is large compared with the time for the recoil motion, caused by the blow, to die out. This mode of operation is limited only by the allowable recoil distance. For example, a small reaction force, large hammer mass and large blow energy result in large recoil distances. Also, an inherent inefficiency is present in the intermittent percussor because the recoil energy of the percussor casing is dissipated without doing useful work. Since the recoil energy is about 20% of the blow energy for a ratio of casing to hammer mass equal to 8 to 1, this loss

will typically be about 20%.

In the continuous percussion mode, the interval of time between blows is about twice the time required to reach maximum recoil height. If this condition exists, the recoil energy in the casing is not wasted as in the intermittent mode, but is utilized to help accelerate the hammer for the next blow. The recoil distance is then only half as large as in the intermittent mode. To maintain this steady, efficient mode of percussion requires that the impact rate be matched to the reaction force available according to the following relationship (See Section II of Appendix F.):

$$F_o = N \sqrt{2 E_b M_h} \qquad (8)$$

where F_o = Reaction force, lbs
N = Cyclic rate, blows/sec
E_b = Energy per blow, in-lb
M_h = Hammer mass, lb sec^2/in

Efficient energy transfer from hammer to drill rod will occur only if the hammer mass is of the same magnitude as the drill rod and bit, which is about 5 lb_m for a 5 foot hole 3/4" in diameter. Thus, a hammer mass of about 2 lb_m appears to be a realistic minimum. The minimum energy per blow is determined by the threshold energy for rock fracture and is about 100 in-lb/in for grey granite (see Section II). The casing mass will be of the order of 16 lb_m. Thus, the maximum impact rate is about 180 blows/min. This is in contrast with a conventional jack hammer which operates at about 2000 blows per minute*.

In summary, the continuous percussion system is inherently more efficient than an intermittent system. To operate in this efficient mode, the impact rate must be matched to the available reaction force. If matching is achieved, the minimum permissible reaction force is determined only by the allowable recoil distance.

3.2.3. Actuator Mechanisms

Two types of actuator mechanism have been found to be

* The results of tests by Hughes Tool Company on an Ingersoll-Rand Model J-10-A jack hammer operated at reduced loading showed good correlation with Equation (8). See Appendix 1, "Bi-weekly Progress Report No. 3", "Lunar Drill Study".

feasible for moon drilling; namely, pneumatic and mechanical.

The pneumatic system involves the use of gas pressure directly on the hammer in the same way as in commercial pneumatic drilling equipment. Gas is first ported to the top side of the hammer to accelerate it toward the drill rod. After thehammer strikes the anvil of the drill rod, the gas is automatically ported to the bottom side of the hammer to return it to the starting position. When the hammer reaches its starting position, gas is readmitted to its top side and the cycle repeats. This system will operate directly from a pressure-regulated source of gas.

A mechanical actuator employs mechanical means to accelerate and re-set the hammer after impact. The simplest and most reliable mechanism having a small-diameter casing is a cam-return, spring-actuated one. This mechanism is discussed in more detail in Section II of Appendix F.

3.3. Tool Advance

Either a positive feed or a gravity-feed may be used to advance the percussor into the rock. Since a positive feed would prevent recoil, it is ruled out. The gravity feed is possible and requires no mechanism other than guide rods; hence, it is recommended.

3.4 Chip Removal

In order to obtain efficient percussion drilling, the rock chips must be continuously removed from beneath the bit. If this is not done the initially large chips will be hit again and broken down into fine particles. This requires additional expenditure of energy without advancing the bit, and thus the drilling efficiency will drop. Chips may be removed mechanically or by gas transport.

3.4.1. Mechanical Cleaning

Mechanical cleaning was discussed in Section II-2.4.2 of the main body of this report and found to be impractical. For the reason presented there, plus the additional complications introduced by the oscillating shaft of a percussion tool, it is ruled out.

3.4.2. Gas Cleaning

An analysis of the requirements for gas chip transport

has been made, including estimates of the weight of such a system. (See Appendix C.) The calculations were based on the size of chips produced in diamond, rotary bit drilling. Since the size of chips formed in efficient percussion drilling will be considerably larger, the gas requirements for chip transport in percussion drilling will be greater than the values given in Appendix C. In order to obtain reliable information on gas requirements, it would be necessary to run tests to determine the size distribution and shape of the chips produced at low impact energy level by a percussion drill. Such tests were considered beyond the scope of this study, and the gas requirement has been assumed to be four times that required for rotary diamond bit drilling.

3.5. Bit Rotation

Effective percussion drilling requires that the bit be rotated after each blow so that a relatively uniform circular hole will be produced. The need for this rotation has been demonstrated by the manufacturers of commercial percussion drilling equipment.* In these commercial devices, bit rotation is accomplished by means of a simple ratchet mechanism during the recoil stroke. This technique could also be used for the moon drilling apparatus.

3.6. Bit Cooling

In Section II-2, it was concluded that the bit temperature levels in rotary diamond bit drilling would not be excessive if good chip cleaning were achieved and the shaft power level limited to less than 1/3 hp. In percussion drilling, frictional energy losses at the bit-rock interface will be a small fraction, one tenth or less, of that of rotary diamond bit drilling. Thus bit overheating will be much less of a problem in percussion drilling and no special provisions for bit cooling are anticipated.

4. Percussion Drilling Mechanisms**

4.1 Requirements

The general requirements for a lunar drilling mechanism

---

* "Rock Drill Data", Page 52. Ingersoll-Rand Company, New York, N.Y.

** The term "mechanism" is used to denote only the percussor case, hammer and anvil. The term "system" refers to these parts plus the energy storage source.

have been stated and discussed in Section II-3.1. Since the percussion drill involves vibratory motion, the requirement that the drilling mechanism must not transmit vibration to the moon capsule deserves special consideration. As discussed in the preceding section, a percussor can be designed which utilizes the percussor weight to supply the required drill reaction force. The percussor can then be freely mounted on guides so that no significant drilling forces will be transmitted to the capsule.

4.2. Feasible Percussion Mechanisms

On the basis of the discussion given in Section III and the analysis presented in Appendix F, two types of percussion mechanism have been selected as feasible for operation on the moon: (1) a pneumatically-actuated device; and (2) a cam-driven, mechanically-actuated device. Neither of these mechanisms has an appreciable weight or volume advantage over the other. (Note, however, that total system weights are significantly different.) (See Section 5, below.) The mechanical system will be more complex in terms of the number of components which are essential to its function, while the pneumatic system does not have positive actuation and is thus susceptible to sticking or jamming. Hence, neither mechanism appears to have the advantage in reliability.

5. Complete Drilling Systems, Configuration and Weight Estimates

Three percussion drilling systems have been found to be feasible, from a weight standpoint, for moon drilling. They are

a. Pneumatic Actuation, Stored Gas Energy Source
b. Pneumatic Actuation, Chemical (Hot Gas) Energy Source
c. Mechanical Actuation, Electrochemical (Battery) Energy Source

The estimated weights for these systems are based on drilling a hole in granite. For softer materials these estimates will be conservative.

It has been concluded that the percussion drill is competitive with the rotary diamond bit for depths up to five feet. Hole depths in the range five to ten feet are better done with a rotary diamond drill, since the use of a multi-piece drill rod is impractical in percussion drilling*

* If a large diameter hole in this range is required, the percussor again becomes feasible as the entire tool can be lowered into the hole.

However, for holes greater than ten feet deep, the bit diameter required for diamond drilling increases to the point where it becomes feasible to consider a percussion tool of small enough diameter which can be lowered into the hole. This study of percussion drilling was limited to saml1 diameter holes, 1/2 to 3/4 inch, of five foot depth.

5.1. Pneumatic Actuation, Stored-Gas Energy Source

Sheet 3 of Lunar Drilling Mechanisms* shows a schematic diagram of the pneumatic percussion system which appears best to satisfy the requirements for a moon drill. The percussor is loaded by the tool weight only and the actuation of the hammer is as described in Section 3.2.2.3. Weights for this system have been computed in Section II of Appendix F and are summarized in Table II for a five foot deep hole.

Table II

Component and Total Stored-Gas System Weights

System Components	1/2 Inch Diameter Hole	3/4 Inch Diameter Hole
Nitrogen Gas plus tank	13.5 lbs	30 lbs
Percussor	18.	18
Drill Rod and Bit	5.	5
Guides and Supports	4.	4
Regulator, etc.	3.	3
Total System Weight	43.5 lbs	60 lbs

The system considered is of the continuous percussion type (see Section 3.2.2.2.) and would require approximately 2.5 cubic feet of space (say, 6 inch diameter by 6 feet long). A five foot hole could be drilled in about 1.3 hours if the moon's surface is no harder than granite.

The weight estimates given in Table II are believed to be conservative, since no attempt has been made in this study to optimize system weight with respect to all the pertinent system variables.

* Sheet 3 is at the end of this Section III.

5.2. Pneumatic Actuation, Hot Gas Energy Source

If the stored gas supply tanks in the schematic diagram of Sheet 3 were replaced by a hydrazine generator, the system would represent a hot-gas pneumatic actuator. In Section I of Appendix F, a schematic diagram of the gas generator is presented along with design considerations. The hot-gas generator has a substantial weight advantage over the stored gas supply; it weighs 5.5 pounds, compared with 30 pounds for a stored gas energy source for drilling a five foot hole having a 3/4 inch diameter. However, since the hot gas (1960° R) cannot be used for chip removal, a separate stored gas chip cleaning system must be provided. The weights of the other components are the same as in the stored gas pneumatic system. The system weight is listed in Table III for a five foot hole.

Table III

Component and Total Hot-Gas System Weights

System Components	1/2 Inch Diameter	3/4 Inch Diameter
Hydrazine Gas Generator	4.5	5.5
Chip Transport System	2	2
Percussor	18	18
Drill Rod and Bit	5	5
Guides and Supports	4	4
Regulator, etc.	3	3
Total System Weight	36.5 lbs	37.5 lbs

The substantial weight advantage of the hot-gas system over the stored-gas system is effectively nullified by other considerations:

a) the probably unreliability of such a system

b) difficulties associated with a high-temperature working fluid

c) the great amount of effort and cost required for the development of a hot-gas system.

5.3 Mechanical Actuation, Battery Energy Source

Sheet 4 of Lunar Drilling Mechanisms* shows an artist's

* Sheet 4 is at the end of this Section III.

conception of a mechanically-actuated percussor which is driven by a storage battery and an electric motor. The motor drives a splined shaft through a gear train. The shaft in turn rotates the hammer which has a cam follower attached to it. As the hammer rotates, the cam follower moves up along the cam surface displacing the hammer upwards, compressing a spring. After 180° rotation of the shaft, the cam surface ends abruptly, allowing the spring to accelerate the hammer downwards toward the drill rod anvil. After the impact between hammer and anvil, the cam follower again engages the cam and the cycle repeats.

Many other methods of mechanical actuation are possible in addition to the scheme chosen here, but their weights would be comparable. This is because the total percussor weight is determined by the reaction force requirements and may be apportioned between casing, electric motor, etc. in any way desired.

The components and total system weights for the mechanically-actuated system aregiven in Table IV. Approximately 4 hours would be required on the moon to drill a 3/4 inch diameter hole five feet deep in rock similar to granite. The approximate volume required is about one cubic foot, exclusive of batteries.

Table IV

Component and Total Mechanically-Actuated System Weights

System Components	1/2 Inch Diameter	3/4 Inch Diameter
Battery	1.1	2.5
Percussor (includes Motor and Gearing)	18.0	18.0
Chip Transport System	2.0	2.0
Guides	4.0	4.0
Drill Rod and Bit	5.0	5.0
Miscellaneous	3.0	3.0
Total System Weight	33.1 lbs	34.5 lbs

5.4 Discussion of Mechanisms

Of the three possible percussion drilling systems deemed feasible, a mechanically-actuated device driven by an electric motor and

batteries appears to be best. Although the mechanical system has no appreciable weight advantage over the pneumatic, hot-gas system, the latter is likely to be less reliable and will require more development work. Hence, it is ruled out of consideration. The mechanical system, while having no great reliability advantage over the pneumatic, stored-gas system, has a substantial weight advantage; hence, it looks best.

It should be possible to design an electromechanical percussion drill system for moon drilling, which would weigh less than thirty-five pounds and which could drill a hole 1/2 to 3/4 inch diameter by five feet deep in granite-like rock in approximately four hours time. This system should transmit essentially zero vibration, or force, to the moon capsule. By adequate shielding of the motor, the generation of R-F noise could be eliminated. The rate of penetration of this drill could be measured to give an indication of the formation being drilled.

6.. In Conclusion

This study of percussion drilling has shown that the method is feasible for drilling a hole on the moon. Two types of percussion mechanism have been found to be suitable:

a) An electro-mechanical type which would weigh about thirty-five pounds and could drill a hole 1/2 to 3/4 inches in diameter by five feet deep in granite in about four hours time.

b) A pneumatically-actuated (stored-gas source) percussor which would weigh about forty-five pounds for a 1/2 inch diameter hole and about sixty pounds for a 3/4 inch diameter hole in granite, both holes being five feet deep.

The pneumatic system would be slightly less complicated than the mechanical system but would have no reliability advantage because it provides a less positive actuation of the hammer.

The conclusions reached have been based upon a limited analytical study and a minimum of experimental data. In order to reach a final choice regarding the best system, additional work should be done in the following areas:

a) The threshold energy required for efficient drilling should be investigated experimentally, at very low ambient pressures, in the range of blow momentum

anticipated for the moon drill system.

b) The specific energy of the rock, σ_c, should be verified experimentally at low pressures. A value of $\sigma_c = 40,000$ lb/in^2 was assumed in this study.

c) The chip removal system should be studied in more detail, analytically and experimentally.

d) Detailed, optimized mechanical designs of the percussor should be prepared.

e) The problem of seals, bearings, and lubricants for use in the anticipated environment should be investigated.

None of the above items appears to present an insurmountable problem. Essentially the same conclusion was reached regarding the diamond rotary rig which, however, had a possible limited bit life problem. Thus, a more thorough investigation is required before a positive decision can be made regarding the superiority of percussive or rotary drilling for making a hole in the moon. From the present study, however, it appears that:

a) For holes less than five feet deep and 1/2 inch diameter, the mechanical simplicity of the rotary system and low system weight, a rotary system with a diamond bit should be chosen.

b) For holes larger in diameter (3/4 inch to 4 inches) the percussor appears to be simpler, more reliable, does not depend on moon vehicle for weight to apply to bit and lighter in weight.

From the above discussion and that given in Section II - 5 it is apparent that on the basis of the preliminary studies the pneumatic percussion drill is superior for diameter and depth limitation for the first craft.

Further investigation of the problem areas outlined in Section II - 5 and III - 37 may bear out this conclusion, or may swing the balance to another tool.

Thus, it is recommended that further work be undertaken to more completely evaluate these systems before a final selection is made.

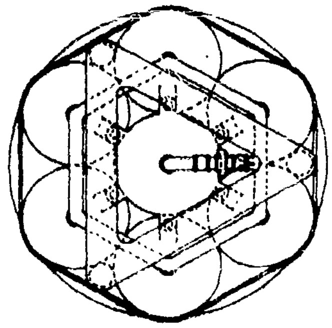

TOP VIEW

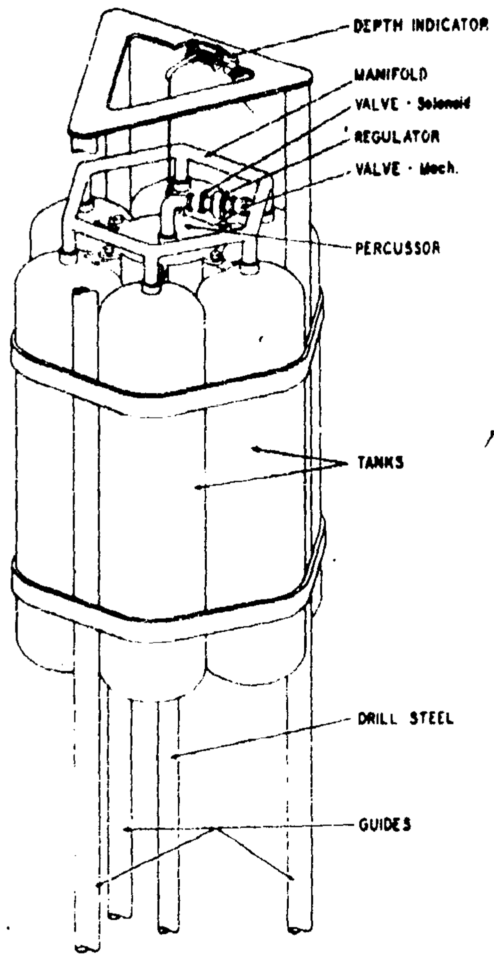

STORED-GAS-ACTUATED PERCUSSOR

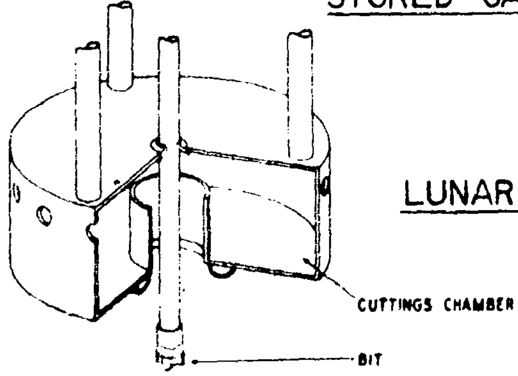

LUNAR DRILLING MECHANISMS

SHEET 3

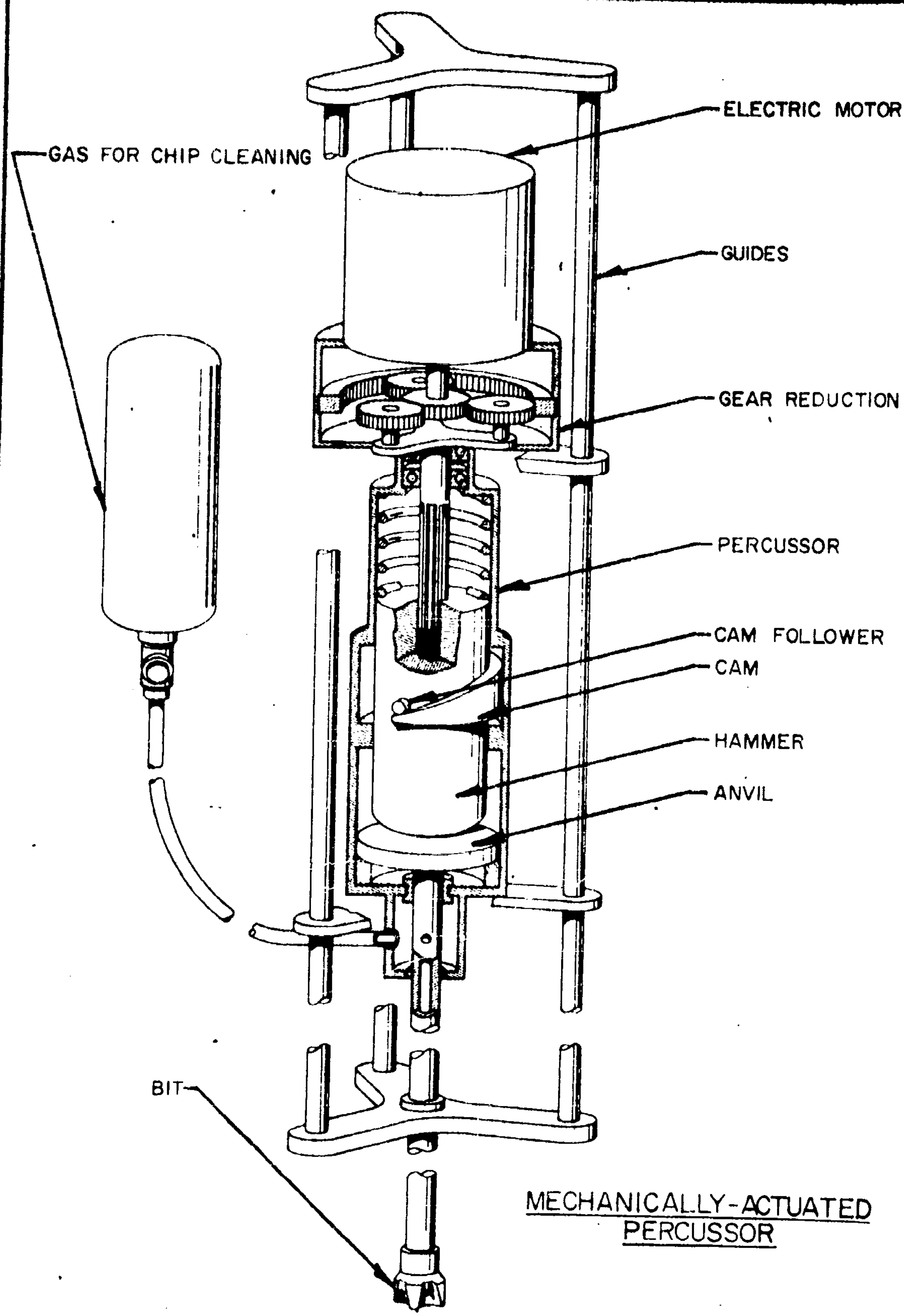

LUNAR DRILLING MECHANISMS

SHEET 4

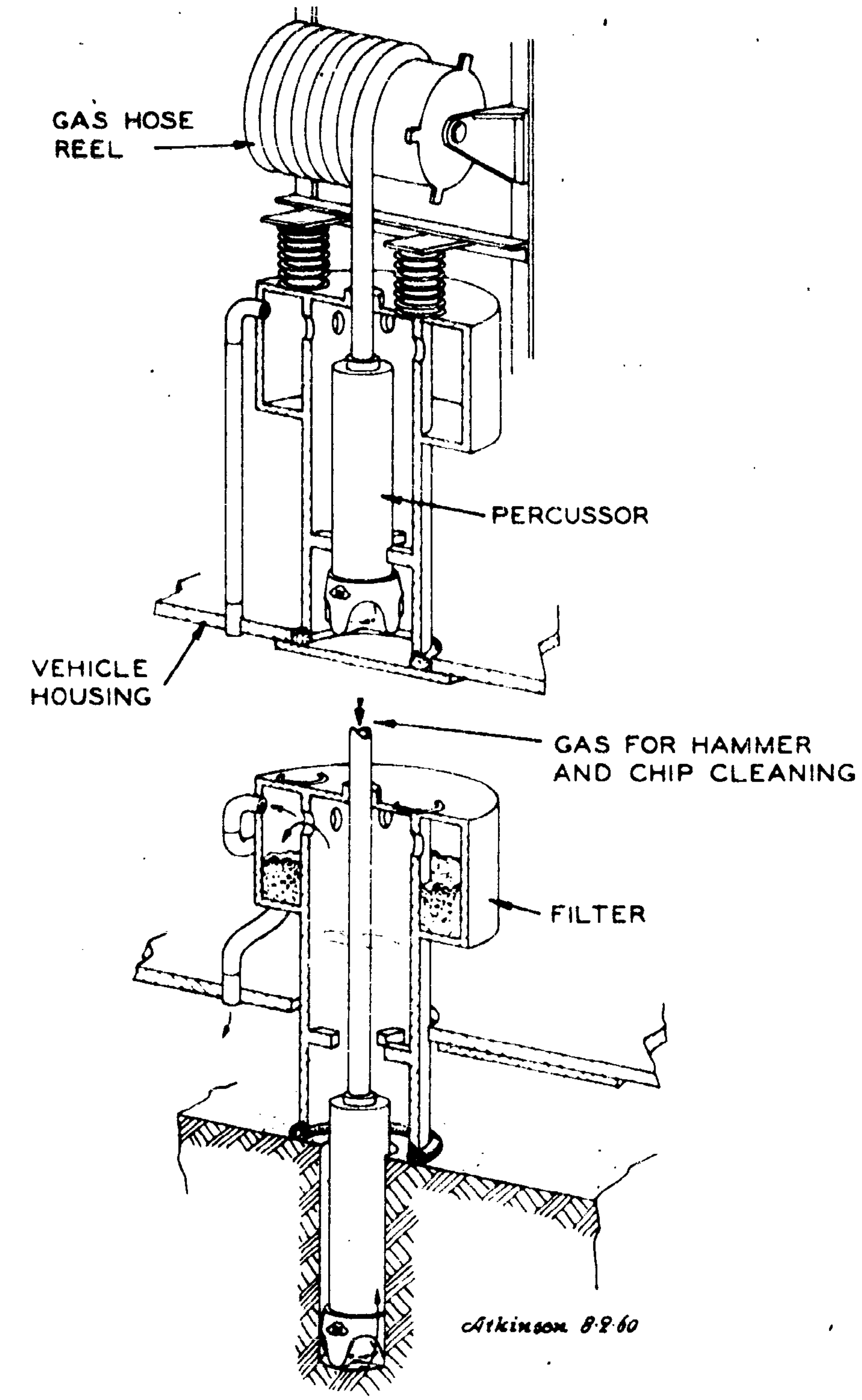

PNEUMATIC PERCUSSOR SYSTEM FOR DEEP HOLES

LUNAR DRILLING MECHANISMS

SHEET 5

Appendix A

Means of Providing Thrust

for

Drilling

1. Various Methods of Creating Thrust

If the drilling method employs a rotary-type tool (e.g., roller-cutters, diamond bits or augers), some provision must be made for loading the bit. The thrust required depends on the type of cutter used; i.e., a diamond cutter is a low-thrust, high-speed tool, while a roller cutter is a high-thrust, low-speed tool.

Several techniques may be used to provide thrust, such as: (a) the weight of the package, (b) the reaction thrust produced by expanding a high energy gas through a nozzle, and (c) some means of "anchoring" the package to the moon's surface, e.g., an explosive imbedment anchor; or using side thrust against the walls of a partially drilled hole. Until more complete knowledge of the composition of the moon's surface is available, only the first two methods will be considered here.

2. Weight of the Package

The estimated earth weight of the package is about 600 pounds, hence its moon weight will be about 100 pounds. Since the center-line of the bit cannot be located at the center of mass of the package, only a fraction of this weight will be available for loading the bit. If the mass of the package is symmetrically distributed about its geometrical center (i.e., if its center of mass coincides with its geometrical center), the available thrust will be one half, or more, of the package-weight. Thus, for purposes of estimating drill performance, the available thrust may be assumed at fifty pounds.

3. Reaction Thrust

Thrust may be produced by expanding a high-energy gas through a nozzle. Figure A-1 shows the mass flow requirements for a hot gas (produced by burning a solid propellant, OMAX 448A) to develop various magnitudes of thrust. The earth weight of the required fuel may be obtained by multiplying the mass flow requirements by the time interval during which thrust is desired.

NO. 340R-20 DIETZGEN GRAPH PAPER
20 X 20 PER INCH

EUGENE DIETZGEN CO.
MADE IN U.S.A.

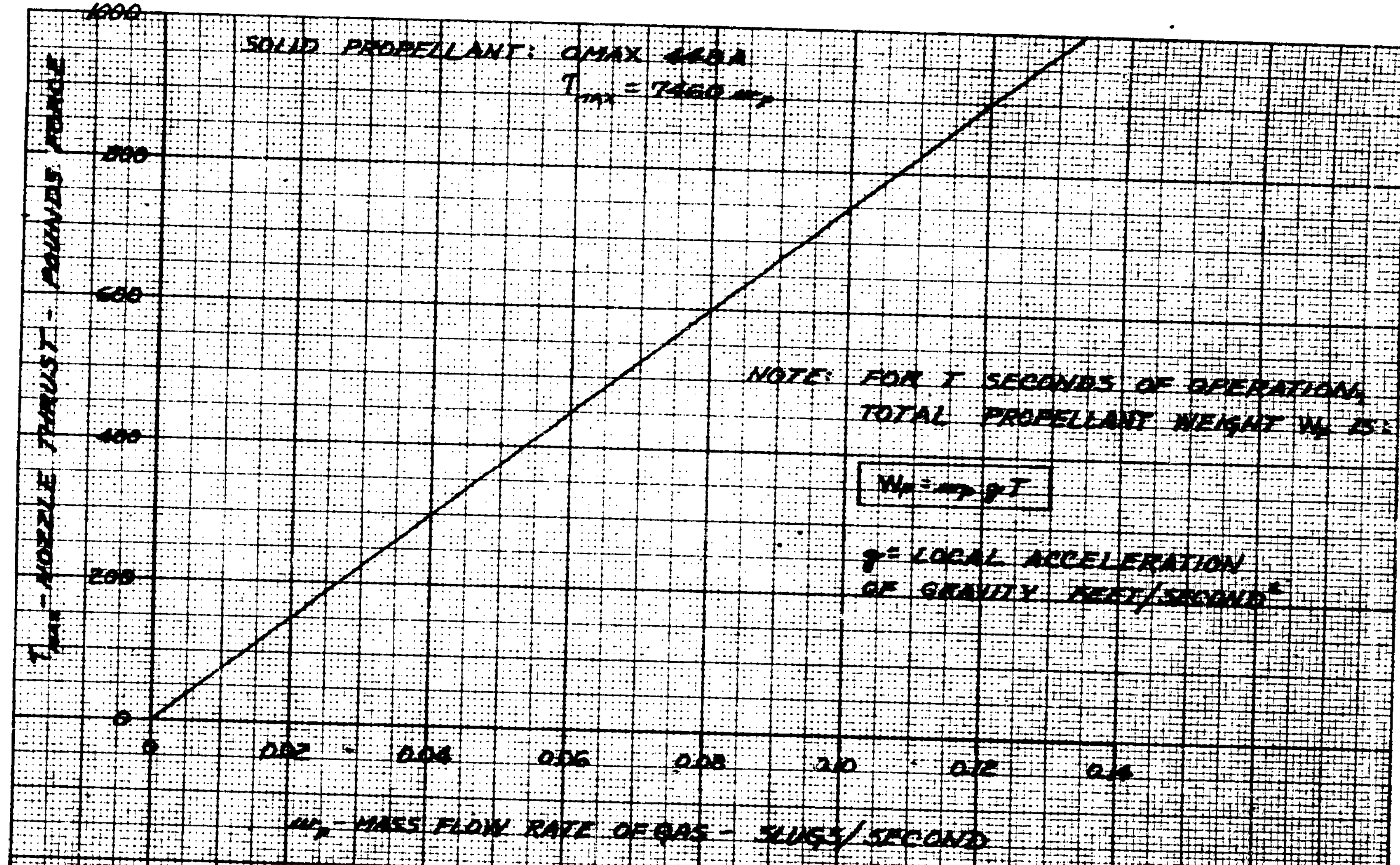

Maximum Nozzle Thrust Versus Mass Flow Rate of Gas

Figure A-1

The results plotted in Figure A-1 were obtained from the following thrust and mass flow equations for a nozzle*:

$$\frac{\tau_{max}}{P_o A_t} = k \sqrt{\frac{2}{(k-1)} \left(\frac{2}{k+1}\right)^{\frac{k+1}{k-1}}} \cdot \sqrt{1 - \left(\frac{P_a}{P_o}\right)^{\frac{k-1}{k}}} \tag{A-1}$$

and
$$w_p = \sqrt{\frac{k}{R} \left(\frac{2}{k+1}\right)^{\frac{k+1}{k-1}}} \cdot \frac{P_o}{\sqrt{T_o}} A_t \tag{A-2}$$

where

τ_{max} = maximum thrust, lb_f.

P_o and T_o = pressure, psia, and temperature, ^oR, of the generated gas.

P_a = ambient pressure, psia

A_t = cross-sectional area of nozzle throat, ft^2.

k = ratio of specific heats of the gas.

w_p = mass flow rate of propellant gas, slugs/second.

R = gas constant, ft $lb_f/slug/^oR$.

Recognizing that $P_a/P_o = 0$ on the moon, and combining Equations (A-1) and (A-2), yields

$$\tau_{max} = \sqrt{\frac{2\ k\ R}{k-1}} \sqrt{T_o} \cdot w_p \tag{A-3}$$

For a given gas and operating temperature (T_o), Equation (A-3) states that the available thrust is directly proportional to the mass flow rate of gas. The gas generated by burning OMAX 448A has a k of 1.29 and R of 2510 ft lb_f/slugs ^oR. Assuming T_o at 2500^oR, Equation (A-3) becomes

$$\tau_{max}\ (\text{OMAX 448A},\ T_o = 2500^oR) = 7460\ w_p \tag{A-4}$$

* See, for example, page 102 of "The Dynamics and Thermodynamics of Compressible Fluid Flow" by A.H. Shapiro. The Ronald Press Company, New York.

For example, to produce 235 pounds of thrust, the required flow rate is w = 0.031 slugs/sec. If the drilling tool operates for one hour, the total earth weight of fuel is about 3600 pounds. The moon weight will be 600 pounds which might more effectively be used directly to load the tool.

Appendix B

Cooling of the Drill Bit

1. Introduction

Since most of the power required for diamond bit drilling is converted into heat at the drill bit, some means is usually provided for cooling the bit to limit operating temperatures. The usual coolant is a circulating fluid, e.g., water. However, there are other heat sinks which can help to, or perhaps solely, dissipate the heat in the moon drill application. The possible heat sinks are:

a) Heat flow into the surrounding rock
b) Heat flow into the drill stem
c) Radiation from the drilling mechanism
d) Heat flow into the drilled material, i.e., the chips which are formed and which leave at a high temperature
e) Heat transfer to a circulating fluid

Even though there may be no circulating fluid, the other sinks will be available. Since their interaction is complicated, an estimate will be made of their heat absorption capacity as if each were present alone. Then an attempt will be made to draw some conclusions regarding the temperature levels at the bit.

2. Capacity of the Heat Sinks

2.1 Heat Flow into Surrounding Rock

Since the rock at great distances from the drilled hole is at a low temperature, part of the heat generated at the bit-rock interface will be conducted into the rock. The temperature rise in the rock will be small everywhere except near the drilled surface. To get an estimate of the heat capacity, it will be assumed that all the shaft power goes into the rock. Furthermore, the rock will be approximated as a semi-infinite medium with a hemispherical hole through which a constant heat flux (equal to the shaft power) passes as represented by Figure B-1(a). After the hole has been partially drilled, the actual state of affairs will be as in Figure B-1(b), i.e., the mass of rock above the local level will also absorb considerable heat. Hence, the answer obtained by this approximation will yield local surface temperatures which are somewhat higher than the actual ones.

Since there is a finite number of diamond points on a bit,

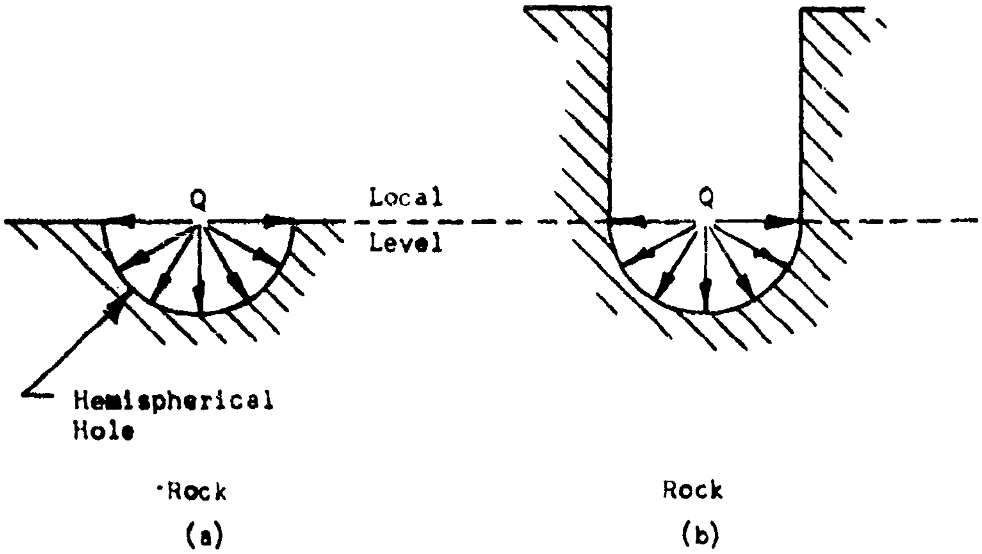

Models for Heat Transfer into Rock

Figure B-1

the heat is generated by a small percentage of the hemispherical bit area. The rock surface will be at some average temperature which is determined by the total heat flux, rock properties, and hole diameter. This average temperature will exist everywhere on the surface except in the immediate vicinity of the diamond points. The temperature at the diamond points (local hot spots), which is above the average rock surface temperature, is determined by the requirement that a fraction of the total generated heat has to pass through each diamond point that is in contact with the rock. The diamond temperature is, thus, the sum of the average rock interface temperature and the local temperature rise. Both of these are evaluated below.

2.1.1. Average Rock Surface Temperature

Consider a hemispherical surface of radius, a, in a semi-infinite solid with a constant heat flux Q_s (which is equal to the shaft horsepower, hp_B, divided by the surface area of the hemisphere). This is illustrated in Figure B-2. The differential equation for unsteady heat flow in this case is

$$\frac{\partial T}{\partial \theta} = \alpha \cdot \frac{1}{r^2} \cdot \frac{\partial}{\partial r}\left(r^2 \frac{\partial T}{\partial r}\right) \qquad (B\text{-}1)$$

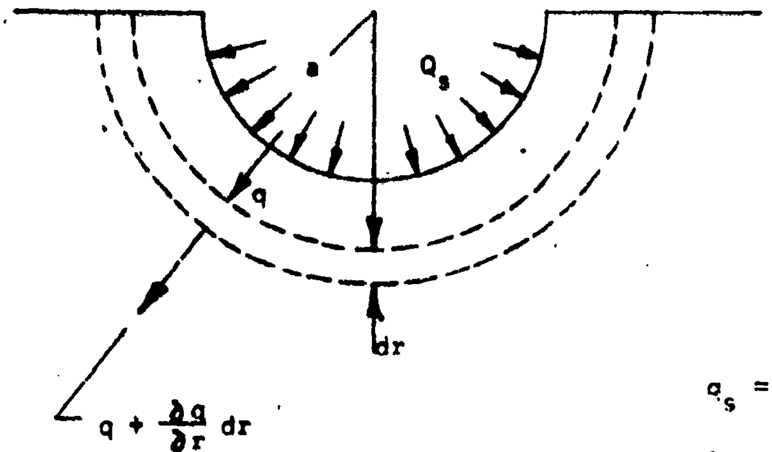

$$q_s = q_{r=a} = Q_s 2\pi a^2 \ (\frac{BTU}{hr})$$

$$Q_s = \frac{2544 \ hp_B}{2\pi \ a^2}$$

Heat Flow from Hemispherical Surface into Semi-infinite Solid

Figure B-2

The boundary conditions are

$\theta < 0 \quad T(r,0) = 0^{\circ}F$

$\theta > 0 \quad q(a,\theta) = q_s = \text{constant}$

where	T = Temperature at a point in the rock	($^{\circ}F$ or $^{\circ}R$)
	r = Radial distance	(ft)
	θ = Time	(hr)
	$\alpha = \frac{K}{\rho C}$ = thermal diffusivity	(ft^2/hr)
	K = Thermal conductivity of rock	(BTU/hr ft $^{\circ}F$)
	ρ = Density of rock	(lb_m/ft^3)
	C = Specific heat capacity of rock	(BTU/lb_m $^{\circ}F$)

The solution of the temperature distribution for times $\theta > 0$ is

$$T = \frac{Q_s a^2}{K \ r} \left[\text{erfc} \left(\frac{r-a}{2\sqrt{\alpha\theta}}\right) - \text{erfc}\left(\frac{r-a}{2\sqrt{\alpha\theta}} + \frac{\sqrt{\alpha\theta}}{a}\right) \exp\left(\frac{r-a}{a} + \frac{\alpha\theta}{a^2}\right)\right] \quad \text{(B-2)}$$

where

$$\text{erfc}(x) = 1 - \text{erf}(x) = 1 - \frac{2}{\sqrt{\pi}} \int_0^x e^{-x^2} \, dx \quad \text{(B-3)}$$

For large values of θ, Equation (B-2) becomes

$$T = \frac{Q_s a^2}{K r} \left[1 - \frac{2}{\sqrt{\pi}} \cdot \frac{r-a}{2\sqrt{\alpha\theta}} + \cdots\cdots - \frac{2}{\sqrt{\pi}} \frac{a}{2\sqrt{\alpha\theta}} \right] \tag{B-4}$$

and, as $\theta \rightarrow \infty$

$$T = \frac{Q_s a^2}{K r} = T_{ss} \tag{B-5}$$

which is the steady state temperature distribution. In particular at the surface of the rock, where $r = a$

$$(T_{ss})_a = \frac{Q_s a}{K} \tag{B-6}$$

The ratio of the steady state temperature at any point to that at $r = a$ is

$$\frac{T_{ss}}{(T_{ss})_a} = \frac{a}{r} \tag{B-7}$$

Equation (B-7) shows that the rock temperature falls off rapidly from that at the bit-rock interface.

The temperature at the rock surface at any time θ is found from Equation (B-2) by setting $r = a$. Thus,

$$\left(\frac{T}{T_{ss}}\right)_{r=a} = 1 - \frac{1}{\sqrt{\pi}} \left(\frac{a}{\sqrt{\alpha\theta}}\right) \left[1 - \frac{a^2}{2\alpha\theta} + \frac{3a^4}{4(\alpha\theta)^2} + \cdots \right] \tag{B-8}$$

which, when θ is large but not infinite, becomes

$$\left(\frac{T}{T_{ss}}\right)_{r=a} \approx 1 - \frac{a}{\sqrt{\pi\alpha\theta}} \tag{B-9}$$

Equation (B-9) is plotted as Figure B-3 for two values of K. If the steady state temperature is too high, this relationship may be used to determine the safe running times for a cyclic drill-stop-drill mode of operation. An example is given below.

Equation (B-7) is plotted as Figure B-4 to show the steady state temperature as a function of the shaft horsepower. For example, if $K = 2$ BTU/hr ft $^{\circ}$F and $a = 1/2$ inch, the curve $K_a = 1/24$ BTU/hr $^{\circ}$F shows $T_{ss} = 1950$ for a shaft horsepower of 0.2. If it is desired that

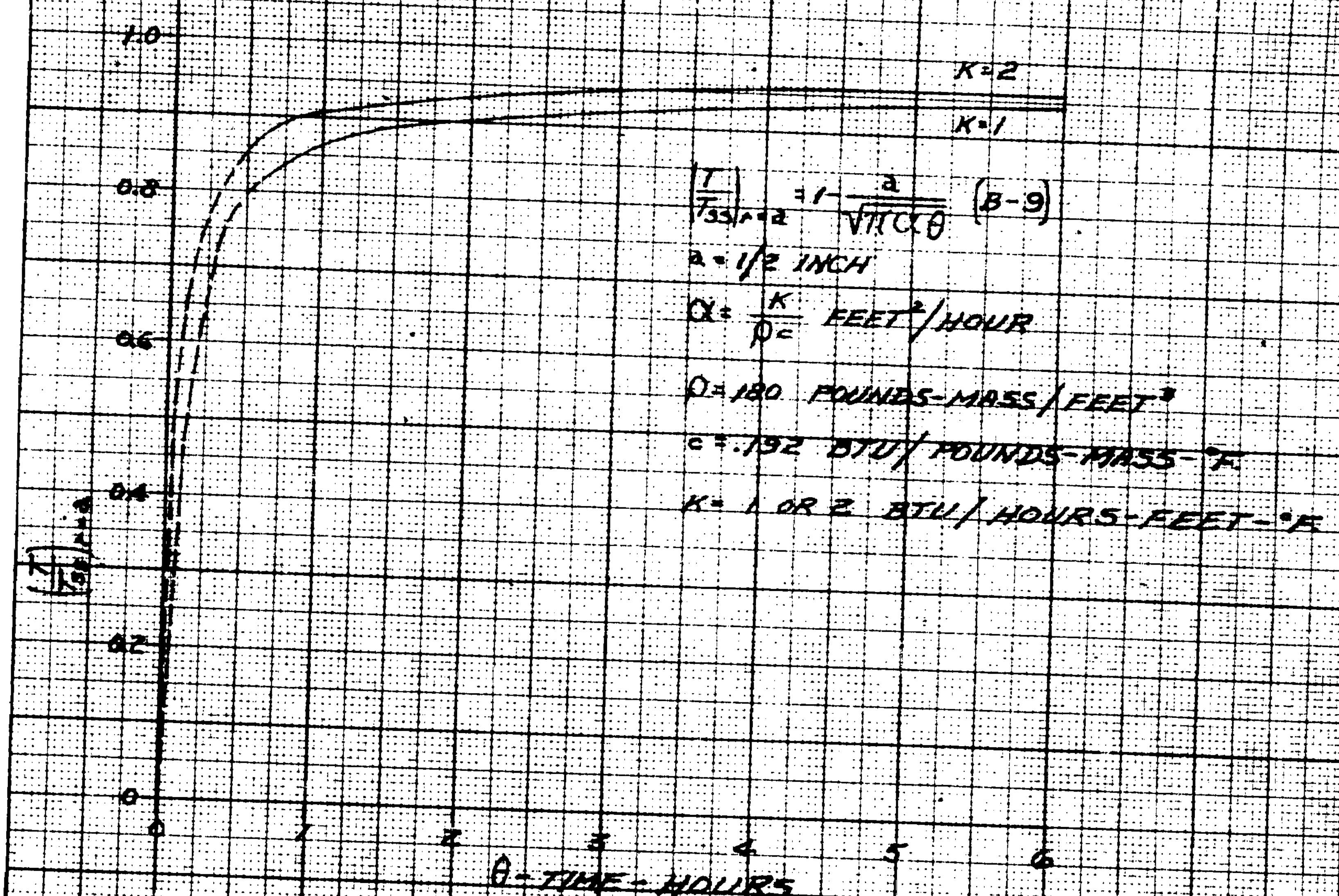

TEMPERATURE AT ROCK-BIT INTERFACE

FIGURE B-3

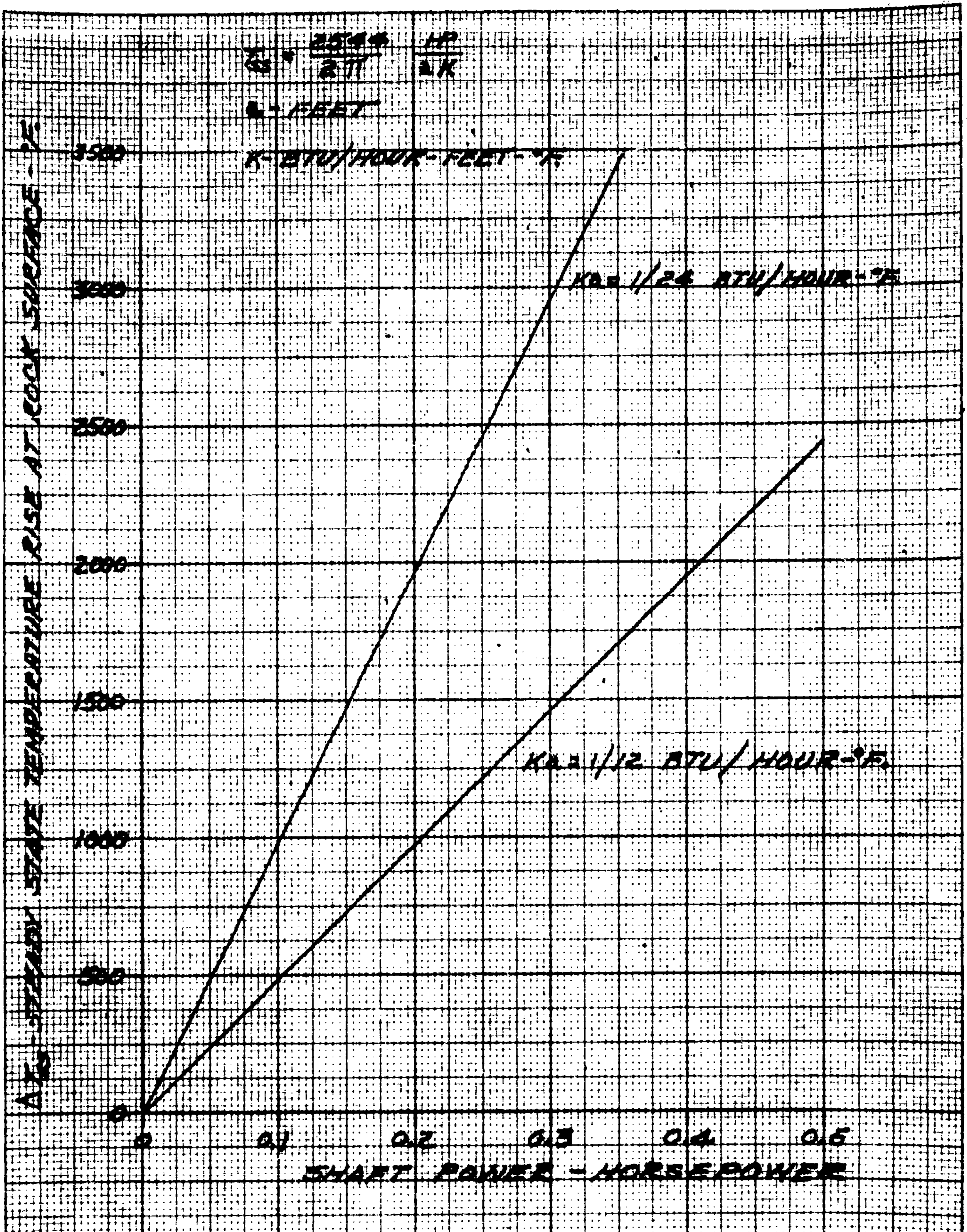

STEADY STATE TEMPERATURE RISE vs SHAFT POWER

FIGURE B-4

the bit temperature be limited to say $1500^{o}F$, * the time of operation may be determined from Figure B-3 as 15 minutes by noting that $(T/T_{ss})_{r=a}$ = 1500/1950. Hence, after operating for 15 minutes the bit must be stopped and allowed to cool down.

2.1.2. Local Hot Spots

The above results indicate what the rock surface temperature, and hence the bit temperature, would be if the heat is generated uniformly at all points of the rock surface. In fact, however, the heat is generated at a finite number of points, namely, at the diamonds. The local temperature near these points will be higher than the average surface temperature. The transients associated with this problem are very short, of the order of a few seconds. The maximum steady-state local temperature rise is given by

$$\Delta T_{local} = \frac{2\,Q_D}{K}\sqrt{\frac{2\alpha\,l}{\pi V}} \quad ** \qquad (B\text{-}10)$$

where:

ΔT_{local}	= Maximum local temperature rise above the average rock surface temperature	(^{o}F)
Q_D	$= \frac{2544\ hp_B}{n\ A_D}$ = Heat flux per diamond	$(BTU/hr\ ft^2)$
hp_B	= Shaft horsepower	(hp)
n	= Number of diamonds	(-)
$A_D = (2\,l)^2$	= Contact area of diamonds	(ft^2)
$2\,l$	= Length of "square" diamond contact area	(ft)
V	= Velocity of diamond	(ft/sec)

The other symbols have the same meaning as previously used.

Assuming $l = 1/64"$, $\alpha = 0.0281\ ft^2/hr$, $V = 2.0$ ft/sec (corresponding to a diamond 1/4" from center of bit rotating at 900 rpm), Equation (B-10) becomes

$$\Delta T_{local} = 11.4 \times 10^{-5}\,\frac{Q_D}{K} \qquad (B\text{-}11)$$

If the number of diamonds is assumed as n = 100, the heat flux per diamond becomes $Q_D = 37.5 \times 10^{3}\ hp_B$ and:

---

* The local temperature rise must be accounted for. In the following section it is shown that this is small, but if it were say $500^{o}F$, then T/T_{ss} = 1000/1950.

** E.L.Foster, ScD Thesis, May 17, 1954, Massachusetts Institute of Technology.

$$\Delta T_{local} = 428 \frac{hp}{K} \qquad \text{(B-12)}$$

Equation (B-12) indicates that the local temperature rise will be small compared to the rock surface temperature.

2.2 Heat Flow into the Drill Stem

Since the conductivity of diamond bits and steel are relatively high, an approximate calculation for the heat capacity of the drilling mechanism is

$$q \Delta \theta = m C_s \Delta T_{rise} \qquad \text{(B-13)}$$

or

$$2544 \text{ hp} \Delta \theta = m C_s \Delta T_{rise} \qquad \text{(B-13a)}$$

where

m	= Mass of drill stem	(lb_m)
C_s	= Specific heat capacity of drill stem	($BTU/lb_m\,^oF$)
ΔT_{rise}	= Temperature rise in drill stem	(^oF)
$\Delta \theta$	= Time interval for ΔT_{rise}	(hr)
hp	= Shaft horsepower	(hp)

If $m = 10\ lb_m$ and $C_s = 0.15 \ \frac{BTU}{lb_m\ ^oF}$

$$\frac{\Delta T_{rise}}{\Delta \theta} = 1700 \text{ hp} \qquad \text{(B-14)}$$

Thus if the shaft power is 0.1 hp, there will be a 170 ^oF temperature rise each hour, if all the heat goes into the drill stem.

2.3 Radiation from the Drilling Mechanism

If the drill stem gets hot it will radiate to the relatively cold rock walls. The governing equation, assuming black body radiation with emissivity equal to 1, is*

$$q = 0.173\ A_1 \left[\left(\frac{T_s}{100}\right)^4 - \left(\frac{T_R}{100}\right)^4 \right] \qquad \text{(B-15)}$$

or, the heat radiated per foot of shaft is:

$$\frac{q}{L} = 0.173\ \frac{\pi}{4}\ D_s^2 \left[\left(\frac{T_s}{100}\right)^4 - \left(\frac{T_R}{100}\right)^4 \right] \qquad \text{(B-15a)}$$

* McAdams, W.H., "Heat Transmission", 2 ed., McGraw-Hill Book Co., Inc., p.52.

where:

q = Heat rate (BTU/hr)
L = Shaft length exposed to rock (ft)
D_s = Shaft diameter (ft)
T_s = Shaft temperature (oR)
T_R = Rock temperature (^oR)

If $T_s = 1500^oR$, $T_R = 500^oR$ and $D_s = 1/24$ ft,

$$\frac{q}{L} = 12 \left(\frac{BTU}{hr\ ft}\right) = 4.7 \times 10^{-3} \quad \left(\frac{hp}{ft}\right) \tag{B-16}$$

If $T_s = 2000^oR$,

$$\frac{q}{L} = 14.8 \times 10^{-3} \quad \left(\frac{hp}{ft}\right) \tag{B-16a}$$

Hence, for a five foot length of shaft the amount of heat that could be dissipated (at $T_s = 2000^oR$) is about .074 hp. From Equation (B-14), if the shaft power input is 0.1 hp, the temperature of the stem after about 10 hours of operation will be approximately 1500^oF or 2000^oR. Thus, it appears that a good fraction of the input heat could be dissipated by radiation if the power inputs are low.

Note, however, that it is highly undesirable to let the shaft temperature rise much above 500^oF. Hence, both this sink and the previous one were included only for completeness. The physical connection between the bit and shaft should be such that the resistance to heat flow is high compared to that into the rock.

2.4. Heat Flow into the Drilled Material

The heat absorption capacity of the drilled material is

$$q = w_R C_R \Delta T = \rho_R A_B P_r C_R \Delta T \tag{B-17}$$

where:

w_R = Rate of generating rock chips (lb_m/hr)
ρ_R = Rock density (lb_m/ft^3)
A_B = Bit or hole cross-sectional area (ft^2)

P_r = Bit penetration rate (ft/hr)
C_R = Specific heat capacity of rock (BTU/lb_m °F)
ΔT = Temperature rise of rock chips (°F)

If the rock chips are assumed to leave after a 1000°F temperature rise, then

$$q = 0.074\ D_B^{\ 2}\ P_r \quad (hp) \tag{B-18}$$

where

D_B = bit diameter expressed in inches.

From Figure 5 of the main body of this report, the horsepower required for drilling is

$$hp_{drilling} = 0.667\ D_B^{\ 2}\ P_r \tag{B-19}$$

Thus about 10% of the heat input can be dissipated in this way if the chip temperature rise is 1000°F: and about 20% if the rise is 2000°F. Of course, good chip cleaning is essential for this sink to function properly.

2.5. Heat Transfer to a Circulating Fluid

If air is used as the circulating fluid, the minimum mass flow rate required to absorb a given heat flux is set by the First Law of Thermodynamics as

$$q = w_A\ C_p\ (\Delta T)_{rise} \tag{B-20}$$

If ΔT = 1000°F,

$$w_A = 10.6\ hp_B \quad (lb_m/hr) \tag{B-21}$$

Thus, the air mass flow requirements get to be large compared to what is required for cleaning, (see Appendix C). If the power input is 0.1 hp, the air flow required is 1.06 lb_m/hr. For 10 hours operation, the air mass needed is 10.6 lb_m. As mentioned above, this is the minimum air rate; in general a higher rate is necessary to achieve the required heat transfer coefficients.

3. Discussion

The foregoing analysis of the heat capacities of the various heat sinks indicate that their combined capacity is adequate to limit the bit temperature to something under 1500°F, provided that: (1) the shaft power input does not exceed 1/3 hp; and (2) good chip cleaning is accomplished. This power limitation appears to pose no problem when compared to the expected power levels and penetration rates anticipated for grey granite. (See Figures 2 through 6 in Section II of the main body of this report.)

APPENDIX C

CHIP TRANSPORT

1. Introduction

A major problem in rotary (diamond bit) or percussive drilling is chip removal from the bottom of the hole to permit the tool to engage virgin surface. Chips may be removed from the hole by: (1) gas transport; (2) mechanical means, e.g., screw conveyor; (3) a combination of these; e.g., a screw conveyor with gas flow to "lubricate" the particles. The requirements and problems associated with gas transport of chips produced by a diamond bit are examined in this appendix.

The ultimate purpose is to determine the gas flow system requirements, i.e., what total mass of gas, storage tank, and accessories will be required. These will depend on the size of particles produced, the size of hole to be drilled, the rate of penetration, the type of gas used, the operating density of the gas, etc.

The analysis presented below indicates that if the particles are small, say .01" diameter, and the gas density is low, the drag force on the particles will be independent of the gas density-a consequence of operating in the Stokes flow regime. Thus, the drag force will be a function of only the relative velocity between gas and particles; and the gas density can be reduced to whatever value that can be controlled readily, i.e., whatever value of pressure that can be maintained in the transport line. Hence, if the regime of operation is Stokes flow, the gas mass flow rate can be reduced by operating at reduced pressures and the required fixed volume flow rate. However, a lower limit on gas density will be set by the requirement that the mean-free path of the molecules should not get so large that the regime of fluid dynamic operation changes from a continuum to highly rarefied. Another limitation is to prevent the solids from "loading", i.e., the mass of solids per unit volume of space should stay below certain limits as required by flow stability considerations. These and other considerations are examined in the following sections.

2. Stability and Loading of the Gas Stream

W.C. Bauer* and others have reported that in dilute phase vertical up-transport the solid particles are by no means evenly distributed through the gas. Rather, the particles seem to be gathered into

*Bauer, W.C., ScD Thesis, Massachusetts Institute of Technology, (1949).

streamers, which fluctuate in location in the stream. Furthermore, there is a limitation on the quantity of solids that may be carried per unit volume of gas. If this limit is exceeded, the flow is no longer smooth and continuous but "slugs". The slugging phenomenon is characterized by alternate "packets" or slugs of particles and gas moving up the pipe. These packets span the diameter of the tube and may be from one to several diameters in length. For each gas velocity, there is a maximum solids rate (i.e., loading of solids in the gas stream) above which slugging will occur. If there is sufficient pressure drop available in the carrier gas, the solids can be transported in the slugging phase. However, this is a very inefficient mode of operation from the point of view of gas power requirements.

The phenomenon of slugging is not completely understood. Among other things, the effect of particle spacing on the drag coefficient is probably critical. If the particles are sufficiently far apart, as in very dilute phase transport, the drag coefficient may be calculated from single particle consideration. As the particle spacing decreases, the fluid flow pattern around a particle is affected by the presence of neighboring particles: the drag coefficient increases (continuously?) with decreased particle spacing. For the two extreme modes (i.e., particles very far apart or almost touching), drag coefficient information is available. Because of experimental difficulties in producing stable flows, and analytical complexity, the intermediate range is uncharted. However, that need not be considered here since the transport system will be designed to operate in the dilute phase, using information from workers like Bauer to specify the limits of loading that cannot be exceeded. Figure C-1, reproduced from Bauer, is just such a limit chart. Before this chart is examined in detail, consider some of the continuity requirements of the transport process.

3. Continuity Considerations

Consider a hole being drilled by a diamond bit, of diameter D_B, which is driven by a shaft of diameter D_s, as in Figure C-2. Call the hole cross-sectional area A_H and the annulus area A_N. Define the "spatial" or "apparent" density of the solid particles, ρ_B, as the

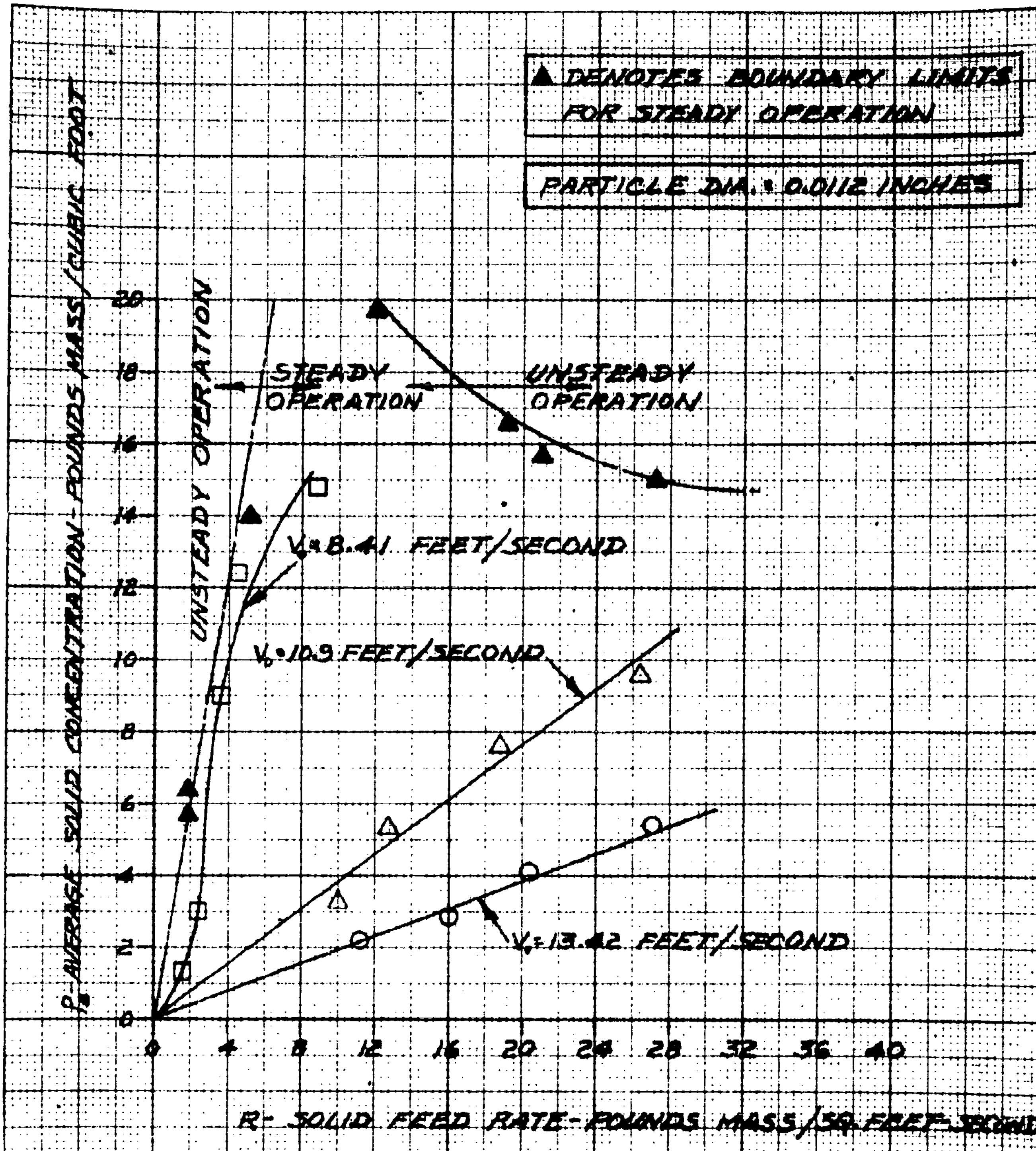

REGIME OF STABLE AND UNSTABLE OPERATION
IN VERTICAL GAS TRANSPORT

FIGURE C-1

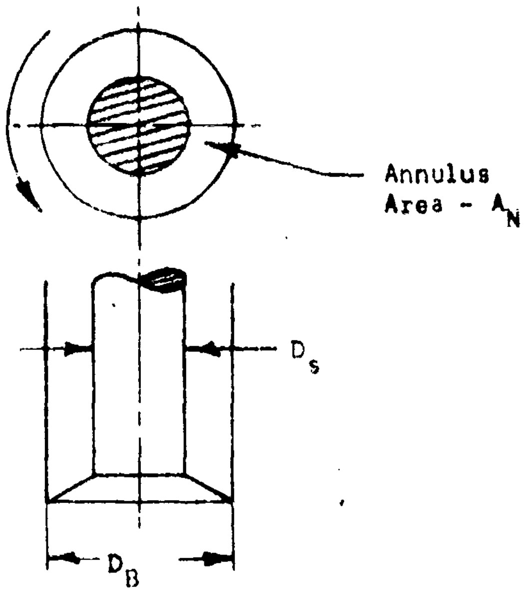

Geometry of Drilled Hole

Figure C-2

mass of particles per unit volume of space;* and the penetration rate of the drill as P_r. Then from solids continuity, the flow rate of solids up the annulus must be equal to the rate of generation of particles at the drill rock interface.

Thus,

$$\rho_B V_s A_N = \rho_s A_H P_r \qquad \text{(C-1)}$$

Or,

$$\rho_B V_s = \rho_s \frac{A_H}{A_N} P_r = \rho_s \frac{\beta^2}{\beta^2 - 1} P_r = R \qquad \text{(C-2)}$$

where R is the mass flow rate of solids per unit area up the annulus, V_s is the velocity of the particles, ρ_s is the true solids density, and $\beta = D_B/D_s$. From Equation (C-2)

$$\rho_B = \frac{1}{V_s} R \qquad \text{(C-3)}$$

---

*Note, ρ_B is related to (but not equal to) the true solids density, ρ_s, by the "voidage" factor, ε. Thus, $\rho_B = (1-\varepsilon)\,\rho_s$. The voidage is the void volume expressed as the fraction of the space not occupied by solid particles. $\varepsilon \approx 1$ indicates large particle spacing.

Thus, in Figure C-1 the slope of the curves for constant gas velocity, V_o, represents the reciprocal of the solids velocity. The curves for the higher gas velocities are straight lines, whereas the one for V_o = 8.41 ft/sec has varying slope and thus varying solids velocity. Using Figure C-1 and Equation (C-3), the solids velocity for V_o = 10.9 ft/sec is V_s = 2.7 ft/sec, yielding a relative velocity V_r = 8.2 ft/sec. Similarly, for V_o = 13.42 ft/sec, V_s = 5.32 ft/sec and the relative velocity is V_r = 8.1 ft/sec. This indicates: (1) the drag coefficient is a function of relative velocity only; and (2) that the drag coefficient does not vary significantly for the range of solids loading considered. For the curve marked V_o = 8.41 ft/sec, the slope varies, increasing at the higher loadings. This implies that the solids velocity decreases at higher loadings. Probably this variation is due to experimental errors or difficulties associated with operation at V_o almost equal to V_r.

Once the pertinent velocities are known, the gas flow requirements can be calculated. Thus, the gas volume flow rate is:

$$Q_f = V_o A_N \qquad ft^3/sec \tag{C-4}$$

Also

$$V_o = V_r + V_s \qquad ft/sec \tag{C-5}$$

and the gas mass flow rate is

$$W_f = \rho_f Q_f = V_o \rho_f A_N \tag{C-6}$$

Figure C-3(a) indicates how the solid feed rate varies with bit penetration rate for various ratios of bit diameter to shaft diameter, and Figure C-3(b) shows how the solids apparent density varies with solids feed rate for several values of solids velocity. Thus, if the relative velocity were known, Equations (C-5) and (C-6) could be used to calculate the gas mass flow requirements.

In Figure C-1, Bauer's results indicate that for 0.0112" diameter particles, if the apparent density is below 14 lb_m/ft^3, operation in the slugging regime will be avoided. From Equations (C-2) and (C-3), for β = 4/3 and V_s = 1 ft/sec, a value of ρ_B = 14 lb_m/ft^3 corresponds to a penetration rate of 140 ft/hr. This is much higher

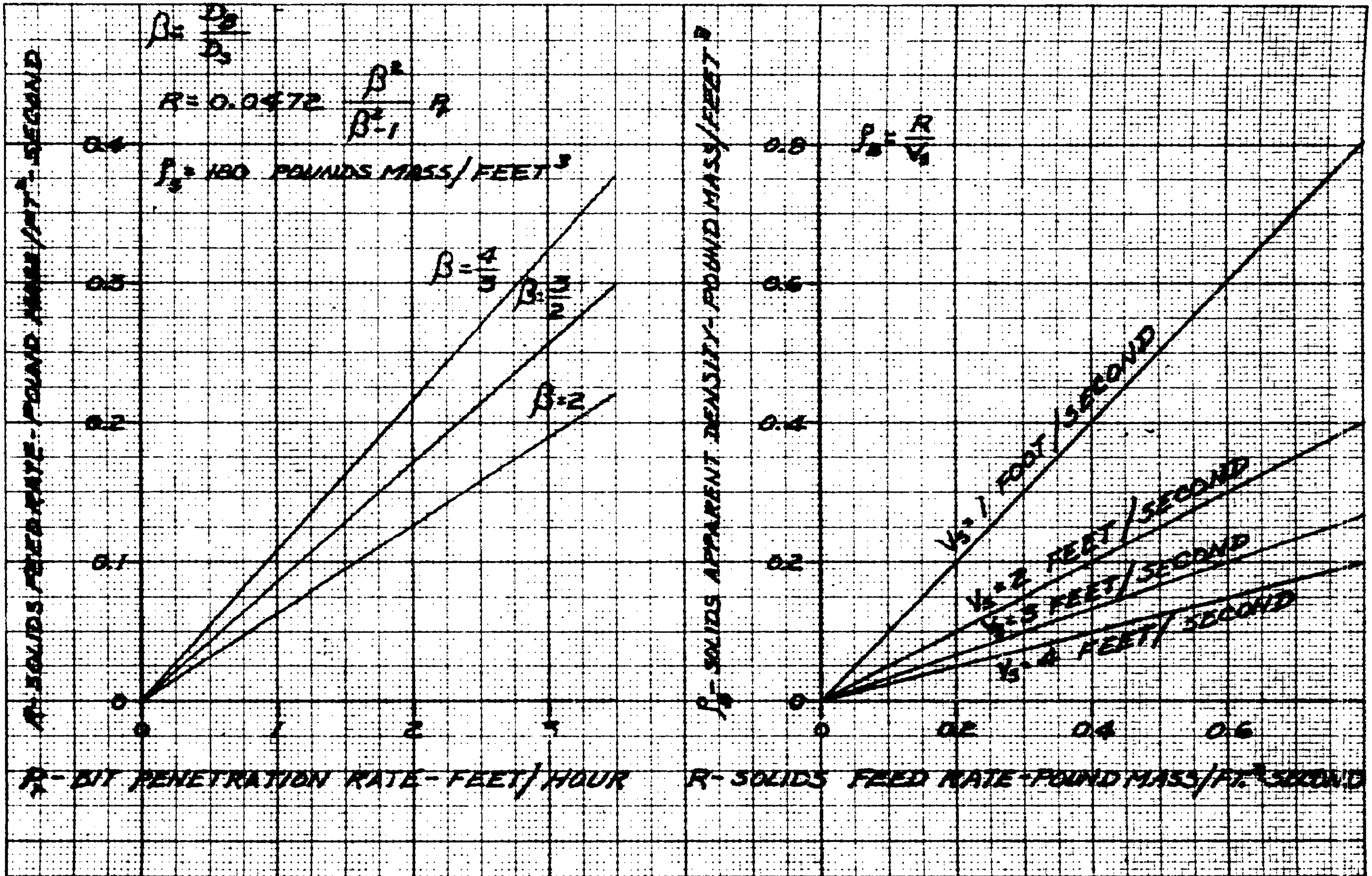

GAS TRANSPORT PARAMETERS AS A FUNCTION OF PENETRATION RATE

FIGURE C-3

than the anticipated penetration rate of the order of 1 ft/hr for diamond bits. Thus the solids apparent density will be of the order of 0.1 lb_m/ft^3.

Since the solids loading is so low, it would appear that drag coefficients may be calculated from single particle considerations. This permits evaluation of V_r, as presented in the following section, and consequently the gas mass flow requirements.

4. Relative Velocity Calculation

If the particle spacing is sufficiently large, single particle drag coefficients may be used to calculate the relative velocity required to transport particles.

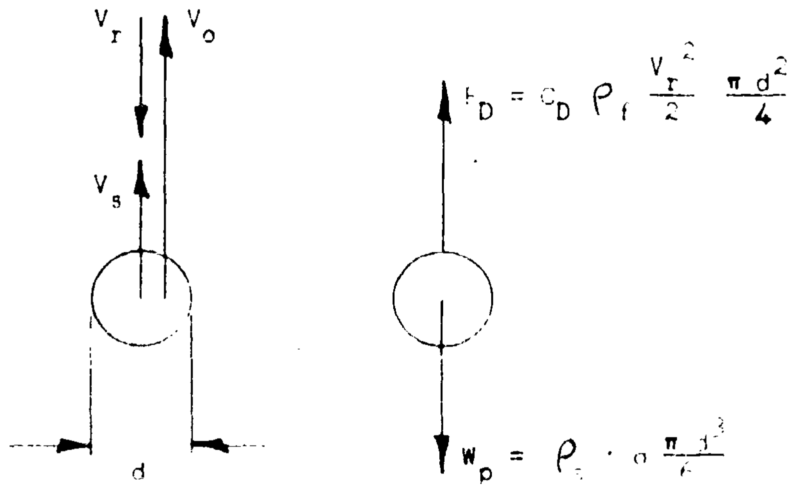

Forces Acting on Single Particle

in Fluid Stream

Figure C-4

Figure C-4 shows the velocities of and the forces acting on a particle in a vertical fluid stream. The fluid drag force is F_D and the particle weight is W_p. When V_r, the terminal velocity relative to the fluid, is reached the acceleration is zero and the fluid drag force balances the gravitational force. Thus,

$$C_D \; \rho_f \frac{V_r^2}{2} \; \frac{\pi d^2}{4} = \rho_s \cdot g \cdot \frac{\pi d^3}{6}$$

or,

$$V_r^2 = \frac{4}{3} \frac{\rho_s}{\rho_f} \frac{gd}{C_D} \qquad \text{(C-7)}$$

It should be noted that the densities are expressed in slugs/ft^3 and g is the local acceleration of gravity. Hence, for a given size and density of particle and equivalent fluid conditions, the required relative velocity on the moon is less than that on the earth by a factor of $(g_{earth}/g_{moon})^{1/2}$ or about $\sqrt{6}$.

In order to determine V_r from Equation (C-7), the drag coefficient must be known. The drag coefficient, C_D, is a function of the Reynolds Number, N_{RE}. Thus,

$$N_{RE} = \frac{\rho_f V_r d}{\mu} \qquad \text{(C-8)}$$

4.1 If $N_{RE} < 2$,

$$C_D = \frac{24}{N_{RE}} \qquad \text{(C-9)}$$

for a sphere. This corresponds to operation in the Stokes flow regime. Substituting Equation (C-9) into Equation (C-7) yields

$$V_r = \frac{\rho_s g d^2}{18\mu} \qquad \text{(C-10)}$$

a result which is independent of the gas density, ρ_f. This follows from the consideration that as ρ_f decreases, the Reynolds Number decreases; which has the physical significance that viscous forces become predominant over inertia (i.e., density-dependent) forces. This result is a very significant one because it indicates that only the volume flow rate of gas is important in chip transport if the regime of operation is Stokes flow. Thus, by reducing the gas density (by reducing the operating pressure) the required mass flow rate of gas and, hence, the total mass of gas for a given time of operation, may be substantially lowered. Since the viscosity of a gas does not vary appreciably as its density is lowered at constant temperature, this

mode of operation appears quite feasible. This is examined further in the following sections.

4.2. If $N_{RE} > 2$, the relationship between C_D and N_{RE} cannot be expressed as simply as in Equation (C-9). In fact, the most convenient form of presenting this information is graphically, e.g., as in Figure 10.13 on page 201 in Hunsaker and Rightmire's, "Engineering Applications of Fluid Mechanics".

Thus, in this regime, the calculation of V_r becomes a trial-and-error procedure in the following steps: (1) with an assumed value of V_r, N_{RE} can be calculated from Equation (C-8); (2) with this value of N_{RE}, a plot such as the above mentioned Figure 10.13 yields a value of C_D; (3) this value of C_D can be used in Equation (C-7) to determine V_r. In general, the resulting value of V_r will not be the same as assumed in step (1). Accordingly, a new value is assumed, being guided by the previous result, and steps (1) through (3) are repeated. This procedure is continued until the calculated and assumed values of V_r agree with each other.

4.3. Next calculate the relative velocity required to lift Bauer's 0.0112" diameter glass spheres with $\rho_s = 5.6$ slugs/ft^3. If air is the transport gas, $\mu = 3.77 \times 10^{-7}$ lb$_f$-sec/ft^2; and $\rho_f = 2.33 \times 10^{-3}$ slugs/ft^3 at atmospheric pressure and a temperature of 70°F. From Equation (C-10), assuming Stokes flow, $V_r = 23$ ft/sec. With this value of V_r, the Reynolds Number is 150. Obviously, this is not Stokes flow, so Equation (C-10) cannot be used to calculate V_r. (Note, however, that if $\rho_f = 2.5 \times 10^{-5}$ slugs/ft^3 at 1/100 of atmospheric pressure, then $N_{RE} = 1.5$ and the flow is Stokes flow.) By the trial-and-error process outlined above, it is found that $V_r = 8$ ft/sec, $N_{RE} \approx 52$ and $C_D \approx 1.5$.

This value, $V_r = 8$ ft/sec, agrees very well with that calculated from Bauer's curve in Section 3. Hence, the required values of relative velocity and flow may be calculated with confidence from single particle drag coefficient data.

5. Flow Requirements

The gas mass flow requirements may be calculated from Equations (C-5) and (C-6) if the solids velocity, V_s, and the relative velocity, V_r, are known. V_s may be set within a rather broad range provided only that ρ_B does not get too large. The value of V_r will depend on the regime of operation, e.g., Stokes flow; and the regime of operation will be determined by the density of the gas. The variation of relative velocity with gas density (or pressure) is shown in Figure C-5. This indicates that on the moon, if the gas pressure is 0.1 atm (1.5 psia) or less, the relative velocity required for nitrogen gas remains constant. Hence, the mass flow requirement can be reduced by operating at reduced pressure levels. Figures C-6 and C-7 show the volume and mass flow requirements, respectively, as a function of bit diameter for several density levels. These calculations were based on the assumption that $\beta = D_B/D_s = 3/2$.

It should be noted, as in Section 3 for Figure C-3, that the flow rates indicated in Figures C-6 and C-7 will transport all chips produced, assuming they are 0.0112" diameter, up to a penetration rate of 160 ft/hr. (The limit in Section 3 was 140 ft/hr because β was only 4/3.) At this penetration rate, the solids loading becomes $\rho_B = 14\ lb_m/ft^3$, which is the upper limit for stable operation. For example, consider a 1" diameter hole and set* the operating pressure as 0.01 atm. Assume a volume flow $Q_f = 0.015\ ft^3/sec$.** This requires a mass flow, w_f, equal to $1.15 \times 10^{-5}\ lb_m/sec$ of nitrogen or $1.5? \times 10^{-6}\ lb_m/sec$ of helium+ and will transport all chips produced up to a penetration rate of 160 ft/hr. (For a total time of operation of 10 hours, a total of 0.415 pounds mass of nitrogen or 0.056 pounds mass of helium would be needed.) However, at a given gas mass flow rate, as the loading, ρ_B, increases (corresponding to increased penetration rates) the required pressure drop increases as shown in Figure C-8. The total pressure drop indicated in Figure C-8 consists of:

1) The pressure drop required to accelerate the solid particles up to velocity,

---

* The requirements for setting the pressure level are examined below in Section 6.2.

** - From Figure C-6.

+ - From Figure C-7.

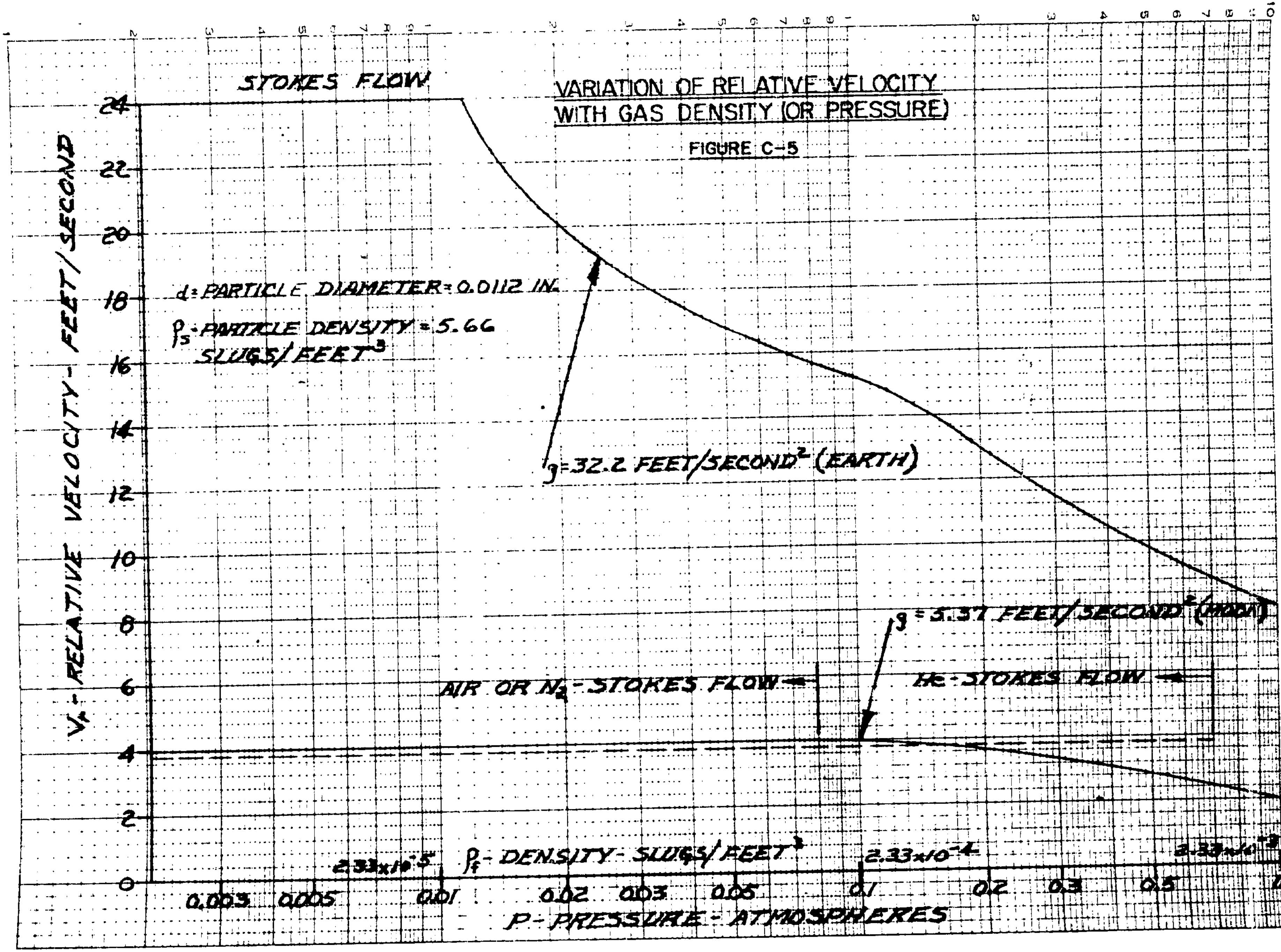

VARIATION OF RELATIVE VELOCITY WITH GAS DENSITY (OR PRESSURE)

FIGURE C-5

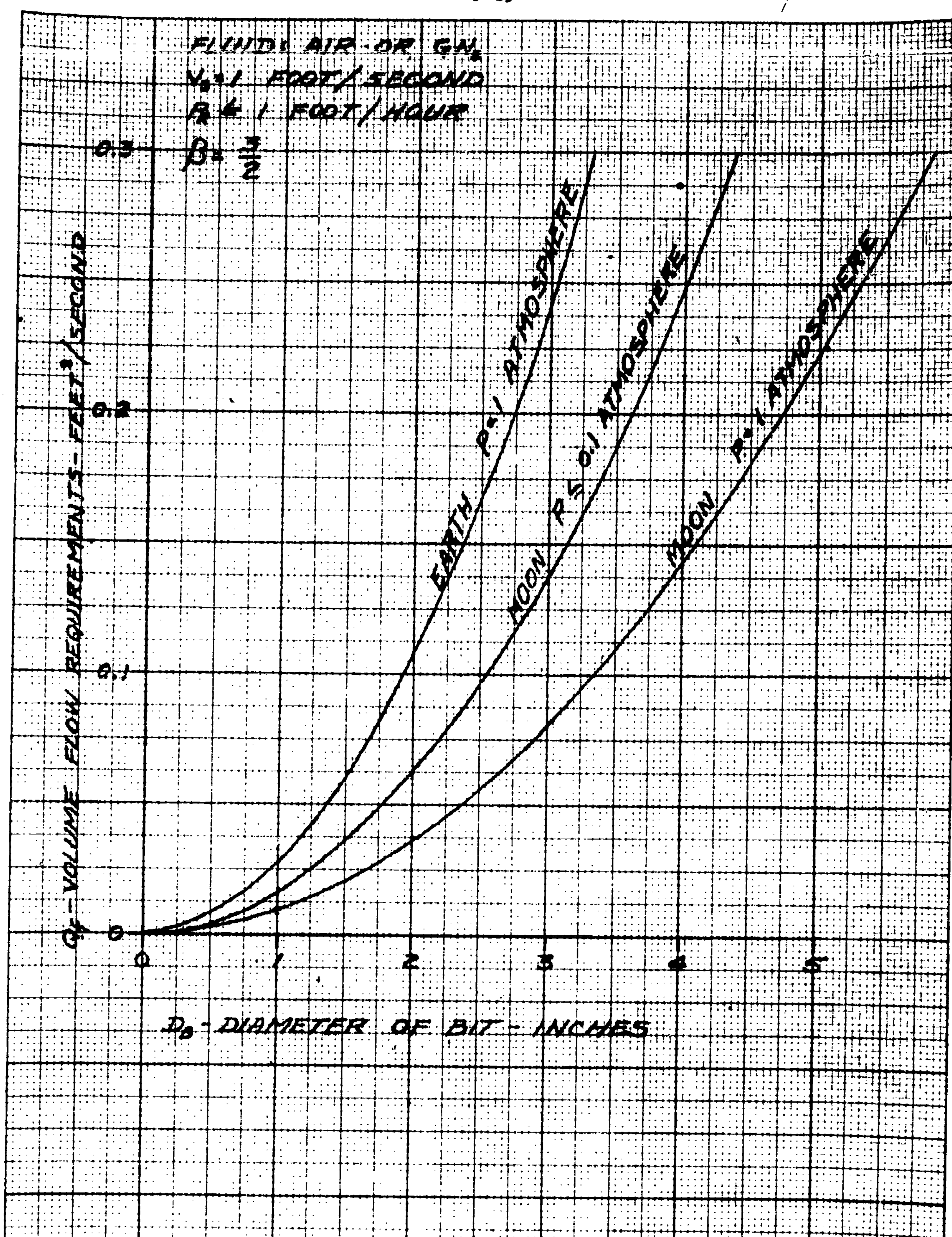

GAS VOLUME FLOW REQUIREMENTS

FIGURE C-6

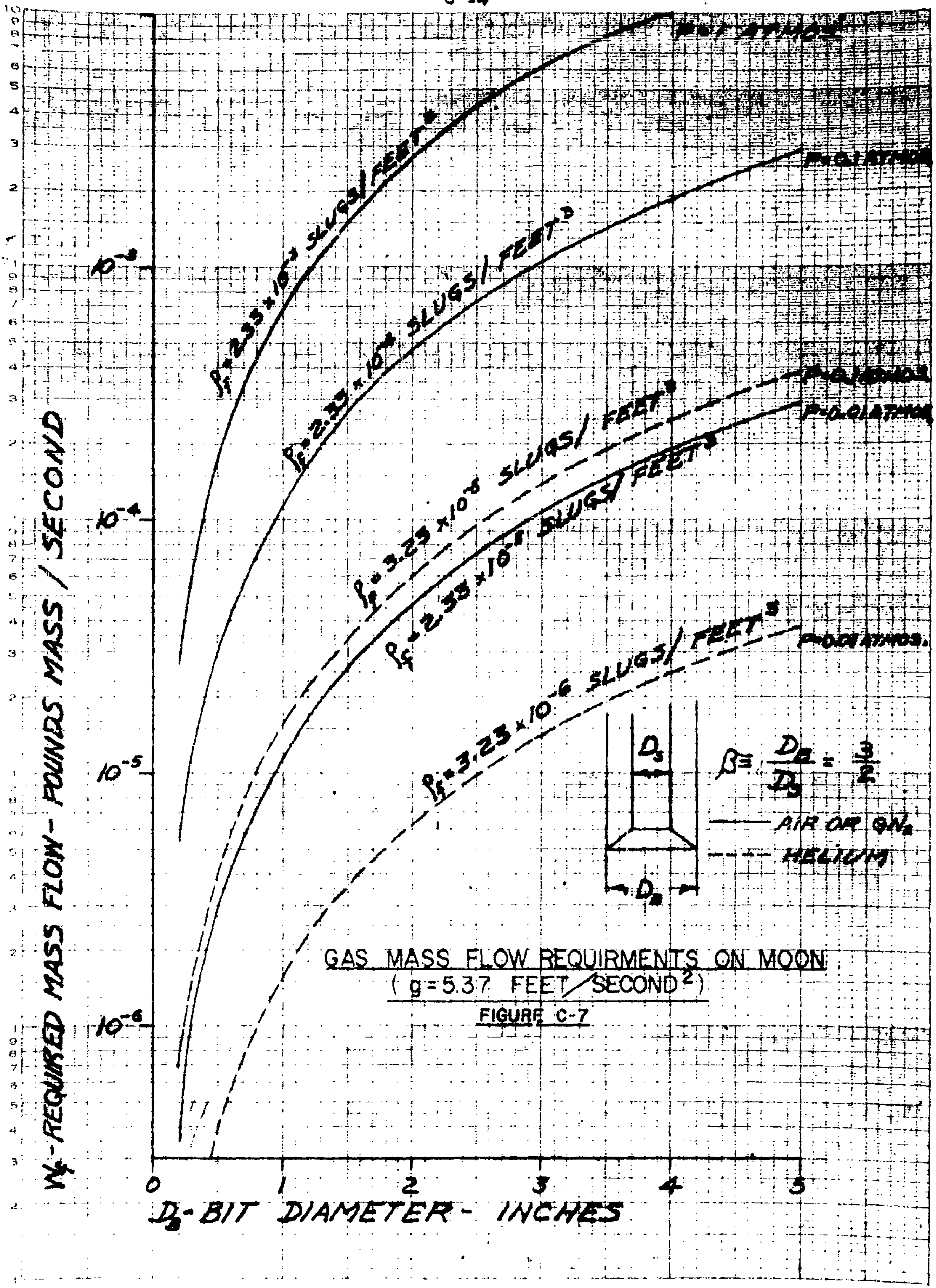

GAS MASS FLOW REQUIRMENTS ON MOON

(g = 5.37 FEET/SECOND^2)

FIGURE C-7

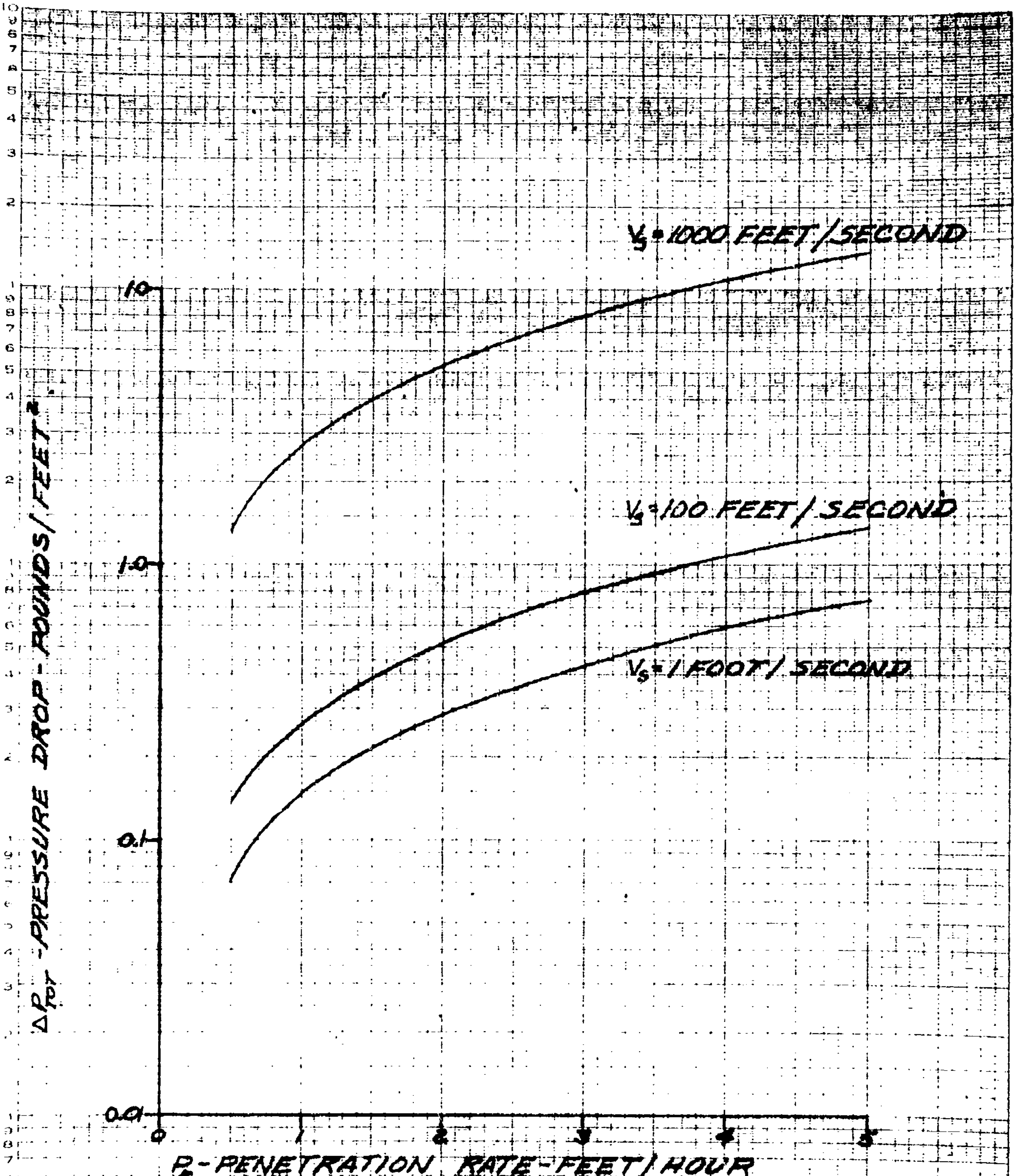

GAS PRESSURE DROP REQUIRED

FIGURE C-8

$$\Delta P_a = \rho_B V_s^2 = R V_s \qquad \text{(C-11)}$$

(Note: ρ_B is expressed in slugs/ft^3)

2) The pressure drop due to the static head of solids,

$$\Delta P_s = \rho_B g L = \frac{R}{V_s} g L \qquad \text{(C-12)}$$

Where L is the height of the transport column and g is the local acceleration of gravity.

The frictional pressure drop along the wall has been neglected because at low gas velocities and densities it is negligible compared to the other terms. From the results of Figure C-8, and noting that the pressure drop is expressed in lb/ft^2, it would appear that the pressure drop will not be a limiting consideration.

6. Low Density Operation and Controls

In the preceding section, the advantages of low-density operation were shown. Questions arise, however, as to what is the limit of density reduction and how the density is to be set. In this section, these questions will be briefly examined.

6.1 Low Density Limits

As the gas density or pressure is reduced, the number of gas molecules per unit volume of space decreases, i.e., the mean free path of the gas molecules increases. The question here is "How good is the assumption of a continuum?" The continuum is implicit in the Stokes flow analysis. If a continuum does not exist, then the concept of density as here used is no longer true, since in a given small volume of space the average number of molecules may vary markedly with time. Thus the pertinent question is "How small a volume of space must be used to test the constancy of the number of molecules?" This "test volume" should be small compared to the volume of a solid particle; i.e., the mean free path should be small compared with the particle diameter. From kinetic theory considerations* the ratio of particle diameter, d, to the mean free path, l, is approximately equal to the ratio of the Reynolds Number to the Mach Number. Thus

* See page 57, A.H. Shapiro, "Compressible Fluid Flow", Vol. 1, The Ronald Press Co., New York.

$$\frac{d}{l} \approx \frac{N_{RE}}{M} \tag{C-13}$$

For example, with nitrogen gas at a pressure of 0.01 atm, temperature of 72°F, and V_o = 10 ft/sec, d = 0.0112",

$$\frac{N_{RE}}{M} = \frac{0.582}{0.087} = 67$$

Thus, at this pressure there appears to be no problem.

In Volume 3, Chapter H of "Fundamentals of Gas Dynamics", Princeton Series, the following relationship is given for the variation of drag coefficient, C_D, at slightly rarefied operating conditions:

$$\frac{C_D}{(C_D)_{Stokes}} = \frac{1+2\ \frac{2-\sigma}{\sigma}\ \frac{2l}{d}}{1+3\ \frac{2-\sigma}{\sigma}\ \frac{2l}{d}} \tag{C-14}$$

Here,

σ = The fraction of molecules not reflected specularly, i.e., reflected diffusely. This is usually close to unity and in general lies in the range $0.8 < \sigma < 1$.

$$l = \text{Mean free path} = 1.26\ \frac{\mu\sqrt{R_g T}}{P} \tag{C-15}$$

d = Particle diameter

This relationship is plotted in Figure C-9 for air at 32°F and indicates that at 0.01 atm, the error by assuming a continuum is only 5%. Equation (C-14) approaches a limit of 2/3 as the mean free path increases. At a pressure of 10^{-4} atm, $C/C_{D_{Stokes}}$ = .68. Hence, the equation probably should not be used much below this pressure.

6.2. Pressure Level Regulation

The advantages of low density operation can only be realized if the pressure level in the annulus between the drill shaft and rock wall can be maintained at desired values. Figure C-10 shows schematically how this might be done. The rock granules are lifted by a helix to a point on the bit where a gas blast from one or more small orifices picks them up and transports them up the annulus. The pressure upstream of the small orifices is regulated to a value $P_1 \gg P_2$, which, together with the gas temperature and orifice area, determines the mass flow rate.

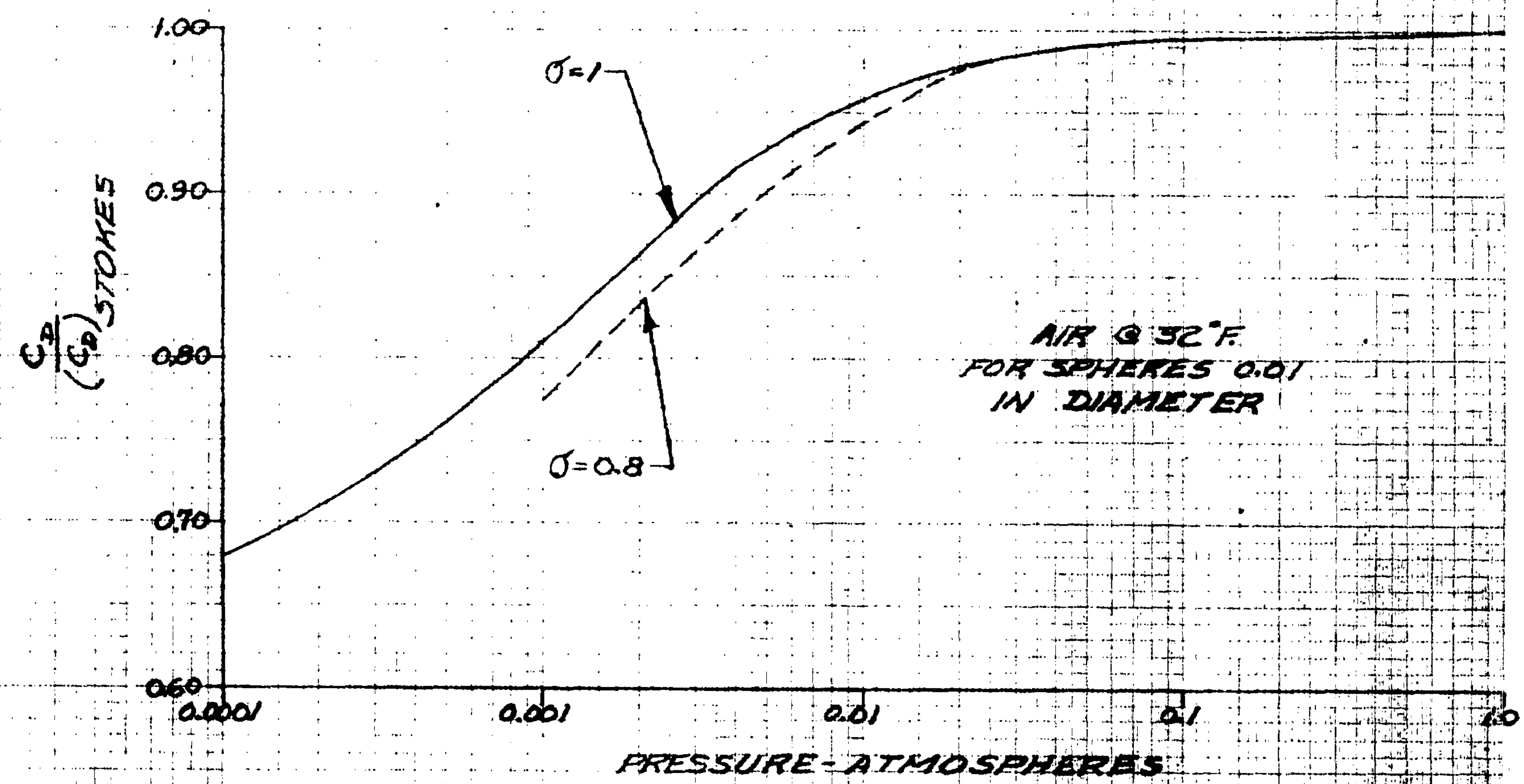

EFFECT OF SLIGHTLY RAREFIED CONDITIONS ON DRAG COEFFICIENT

FIGURE C-9

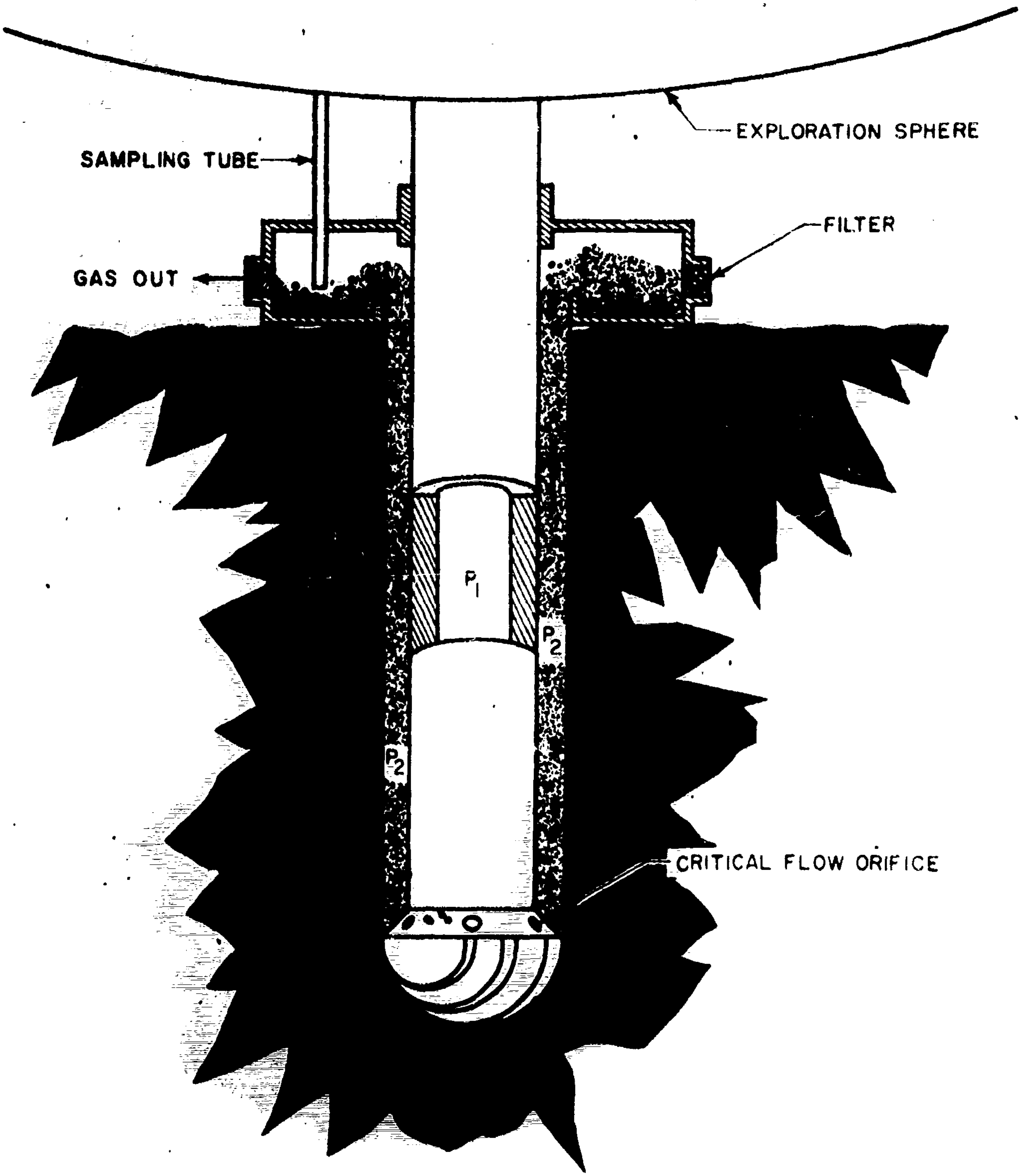

GAS TRANSPORT FOR SCAVENGING BIT

FIGURE C-10

Thus, a fixed mass flow rate is introduced into the annulus. The annulus is capped with a filter to catch the particles and provide a flow resistance. By setting the resistance to flow, the desired pressure level in the annulus may be established.

Unfortunately, this scheme requires that the gas be forced to pass through the filter, i.e., that there be no leakage into the surrounding rock or by sealing surfaces. Since the structure of the rock is unknown, it can only be assumed impervious to gas flow. To ascertain the effect of an imperfect seal at the filter, consider what happens if the annulus discharges directly to the vacuum on the moon.

A model for this case is shown schematically by Figure C-11. The gas flows into a chamber through a critical flow orifice. Since the

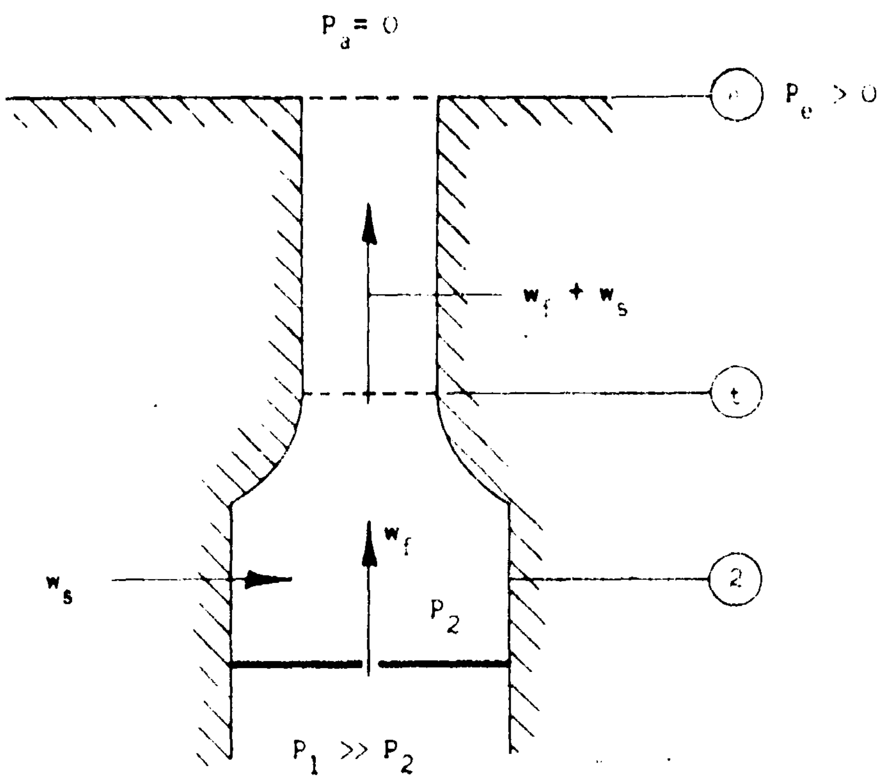

Schematic of Tube Discharging to Vacuum

Figure C-11

pressure upstream of the orifice, P_1, is much greater than that downstream, P_2, the flow w_f is independent of P_2, i.e., for a fixed value of P_1, the flow w_f is also fixed. Assume that a fixed mass flow of

solids (set by the penetration rate and hole diameter) is injected into the chamber and mixes thoroughly with the gas stream to form a uniform mixture. Before examining the state changes occurring as the mixture flows up the tube, a brief review of the process will be made for pure gas flow.

When a gas discharges into a region of extremely low pressure, the flow adjusts so that "choking" (the local Mach Number equals 1) occurs somewhere in the system. For the situation being considered ($w_s = 0$), since the gas flow w_f is fixed, the chamber pressure P_2 and the exit plane pressure P_e will be set by the system geometry and boundary conditions. Let the length of the tube be 100 inches and its diameter 1/2 inch, so that L/D equals 200.

Several causes can produce a change of state between the chamber (State 2) and the exit plane (State e), such as: (1) an area change, e.g., a nozzle; (2) wall friction; (3) heat transfer to the fluid; (4) the acceleration of a stream of particles. Consider the first two causes:

Cause 1. If there is an isentropic (no friction, no heat transfer) area change, say a converging nozzle, followed by a frictionless, constant-area tube, the stream will accelerate reaching some velocity at the throat, or section of minimum area. The state of the fluid in the tube will not change, i.e., $P_t = P_e$, and $T_t = T_e$. However, there will be an expansion shock at the exit. The ratios P_t/P_2 and R_t/T_2 are fixed by the gas properties and are about 0.528 and 0.8[illegible], respectively, for both air and nitrogen, Since $T_1 = T_2$ = the stagnation temperature of the gas, if w_f and the tube area are known, P_t is set by continuity requirements, i.e., $w_f = \rho_t V_t A_t$; $P_t = \rho_t R T_t$; and V_t = sonic velocity at temperature $T_t = \sqrt{kR_g T_t}$. Thus, the pressure P_2 can be determined.

Cause 2. If there is an isentropic converging nozzle feeding an adiabatic constant area tube having friction, the stream will accelerate through both the nozzle and the tube reaching sonic velocity at the exit plane. The pressure and temperature distributions, which are strongly influenced by friction, may be found from thermodynamic considerations. For air, this procedure has been formalized into working tables. In particular, if the variable $4f\ (L/D)_{max}$ is known, the state changes are

readily obtained from Shapiro's Table B.4. Some of these states will be calculated assuming $4f = 0.02$, and a typical value for L/D as 200. This yields $4f(L/D)_{max} = 4$. From Shapiro's Table B.4

$$\begin{aligned} P_t/P_e &\approx 3.1 \\ T_t/T_e &= 1.17 \\ M_t &= 0.35 \\ V_t/V_e &= 0.38 \end{aligned} \qquad \text{(C-16a)}$$

From an Isentropic Flow Table, e.g., Shapiro's Table B.2, the Mach Number M_t may be used to determine the properties at State 2 as

$$\left.\begin{aligned} P_t/P_2 &= 0.9187 \\ T_t/T_2 &= 0.987 \end{aligned}\right| \text{ at } M_t = 0.35 \qquad \text{(C-16b)}$$

Thus, the pressure at point t is three times that at the exit and most of the acceleration occurs in the tube. The above, together with w_f and the continuity relation, sets the pressure levels at various locations.

Return now to the gas stream carrying particles. If there is no heat transfer between the mixture and its surroundings, two limiting cases may be considered: (1) Isentropic expansion of the mixture in a section of varying area with no further state change in the duct, i.e., although there is friction between the two phases of the mixture, there is no friction between the mixture and the walls of the nozzle or tube. (2) Isentropic expansion of the mixture in a constant area section. In the former case choking will occur at the throat; while in the latter case, choking will occur in the exit plane.

The actual state of affairs will lie somewhere between these two extremes since wall friction will not be zero. However, to get a rough idea of the state changes it is desirable to approximate the situation by one of the above limiting cases. Which case represents the better approximation is determined by the time required for the mixture to achieve thermal equilibrium, e.g., as the system accelerates, the gas temperature will tend to drop but the relatively large heat capacity of the solid particles will counteract this tendency. Estimates of the time required for heat transfer indicate that there is not sufficient time for the gas and solids temperatures to reach equilibrium while the

mixture is in a nozzle; hence the mixture discharging into the constant-area tube will not have attained that equilibrium. However, the time required for the mixture to pass through the tube is large compared to that required for heat transfer. Thus, Case 2 will be chosen as representing the better approximation.

For this case, choking will occur at the exit. If the mixture properties are assumed uniform at any cross section, e.g., $T_{2f} = T_{2s}$, $T_{tf} = T_{ts}$, $V_{tf} = V_{ts}$, etc., the First Law of Thermodynamics yields:

$$w_f \left[c_{pf} \left(T_2 - T_e\right) + \frac{V_{2f}^{\,2} - V_{ef}^{\,2}}{2} \right] + w_s \left[c_{ps} \left(T_2 - T_e\right) + \frac{V_{2s}^{\,2} - V_{es}^{\,2}}{2} \right] = 0 \tag{C-17}$$

Which, by rearranging and recognizing $V_{2f} = V_{2s} \approx 0$, becomes

$$\left(1 + \frac{w_s}{w_f}\frac{c_{ps}}{c_{pf}}\right) \cdot \left(T_2 - T_e\right) = \frac{V_e^{\,2}}{2\, c_{pf}} \cdot \left(1 + \frac{w_s}{w_f}\right) \tag{C-18}$$

Substituting $V_e^{\,2} = C_e^{\,2}$ (sonic velocity at exit conditions) $= kR_gT_e$, $\alpha = w_s/w_f$ and appropriate perfect gas relations, results in

$$\frac{T_e}{T_2} = \frac{1}{1 + \frac{(k-1)}{2} \dfrac{1 + \alpha}{1 + \alpha \dfrac{c_{ps}}{c_{pf}}}} \tag{C-19}$$

From Figure C-7, $w_f = 1.15 \times 10^{-5}$ lb_m/sec of nitrogen when drilling a 1" diameter hole. Assuming a penetration rate of 1 ft/hr, Figure C-3(a) gives the solids flow rate, $R = 0.085 \dfrac{lb_m}{ft^2 - sec}$ for $\beta = 3/2$. Then $w_s = R \times A = 46.3 \times 10^{-5}$ lb_m/sec.

Hence, if $k = 1.4$, and $c_{ps}/c_{pf} = 0.8$, then

$$\frac{T_e}{T_2} = 0.80 \qquad (P_r = 1\,ft/hr)$$

$$\frac{T_e}{T_2} = 0.83 \qquad (P_r = 0.1\,ft/hr) \tag{C-20}$$

The mixture temperature at the tube entrance, T_2, will depend on the temperature of the rock particles. Examination of the temperatures at the diamond-rock interface indicates that to dissipate the power input

the temperature levels may reach 2000°F. Thus, it seems reasonable to assume $T_2 = 1600°R$.

The velocity at the tube exit is

$$V_e = C_e = \sqrt{k\ R_g T_e} = 49\sqrt{.81 \times 1600} = 1760 \text{ ft/sec} \qquad (C\text{-}21)$$

From continuity requirements

$$\rho_e V_e A_e = w_f \qquad (C\text{-}22)$$

Substituting the perfect gas relation

$$P_e = (R_g T_e) \frac{w_f}{V_e A_e} = 0.135 \text{ lb/ft}^2 = 0.6 \times 10^{-4} \text{ atm} \qquad (C\text{-}23)$$

The pressure drop, $P_2 - P_e$, may be found from Equation (C-11) using the solids flow rate, $R = 0.085/32.2 \frac{\text{slugs}}{\text{ft}^2 - \text{sec}}$ and $V_s = 1700$ ft/sec

Thus,

$$P_2 - P_e = R\ V_s = 4.5 \text{ lb/ft}^2 \qquad (C\text{-}24a)$$

or

$$P_2 = 4.64 \text{ lb/ft}^2 = 2.2 \times 10^{-3} \text{ atm} \qquad (C\text{-}24b)$$

Comparing the pressure drop required to accelerate the particle (see Equation (C-24a)) with that resulting if pure gas were flowing in the tube (see Equation (C-16a)), it is seen that the latter is much smaller. Thus, the assumption neglecting wall friction appears reasonable.

The above results for $P_2 = 2.2 \times 10^{-3}$ atmos and $P_e = 0.6 \times 10^{-4}$ atmos, together with Figure C-9 indicate that no special seals will be required for nitrogen even though the drag coefficient at the entrance is only $0.83\ (C_D)_{Stokes}$ and at the exit only $0.66\ (C_D)_{Stokes}$; because the increase in relative velocity will easily make up the difference. Similar calculations using helium gas indicate that $P_2 \approx 8.75 \times 10^{-3}$ atmos and $P_e \approx 0.14 \times 10^{-4}$ atmos. Thus, it will probably present no special problem.

The scheme illustrated in Figure C-10 may be used to sample the particles whether a filter cap is used or not.

7. System Weights

As shown in Figure C-10, the gas transport system consists of:

(1) a storage tank; (2) the transport gas; (3) a pressure regulator; (4) means for getting the gas to the point of chip generation, the drill shaft, rotary seal, orifices, etc.; and (5) a sealing and/or sampling tube. In this discussion, Items (3), (4) and (5) will be referred to as "the accessories". It will be assumed that the accessories, exclusive of the drill shaft, have a mass of 1/32.2 slugs. Hence, to estimate the system weight, only the weight of the storage tank and the mass of gas are required. It is shown below that both of these are proportional to the time of operation.

If the working stress, σ_w*, is set, the storage tank weight is directly proportional to its volume; which in turn is directly proportional to the mass of gas at a given pressure and temperature. Thus for a spherical tank

$$W_{tank} = \frac{3}{2} \frac{\rho_t g}{\sigma_w} PV \tag{C-25}$$

Substituting $PV = M_f R_g T$

$$W_{tank} = \frac{3}{2} \frac{\rho_t g}{\sigma_w} \cdot M_f \cdot R_g T \tag{C-26}$$

where

- P = Gas pressure in tank
- V = Tank volume
- σ_w = Working stress = 120,000 psi
- R_g = Gas constant
- T = Gas temperature
- M_f = Mass of gas initially in tank
- ρ_t = Density of tank material

The mass of stored gas, M_f, is determined by:

1) The gas mass flow rate, see Figure C-7, and the operating time. Ordinarily this figure might be doubled to provide a margin of safety, but sample cuttings from a diamond tool are considerably smaller than the assumed value of 0.01" diameter. This provides an adequate margin of safety.

---

* Note $\sigma_w = \frac{Pr}{2t}$, where r is the radius and t is the thickness of the spherical tank.

2) The final gas temperature will be approximately 75% of the initial temperature when one half the initial gas mass remains in the tank.* Thus, the mass of gas in the tank should be doubled.

Hence, the initial stored mass of gas should be twice that required by the flow considerations shown in Figure C-7.

Figures C-12 and C-13 show for nitrogen and helium, respectively: (1) the weight of the entire system; and (2) the system weight minus the gas weight. It is noted that Item (2) is the same for both gases since the product MR_g is the same, i.e., although the mass of helium required is less than that of nitrogen, the volume required to store the former is greater. In calculating the tank weight, Item(2), when the wall thickness required to satisfy strength considerations was less than 0.035", the latter value was arbitrarily used to insure adequate rigidity. Also, it was assumed that the minimum tank weight was 0.5 lb_m. This accounts for the constant value portions of the curves in Figures C-12 and C-13. Hence, as shown in these figures, the over-all weight of the helium system is not substantially lower than the nitrogen system even though the mass of helium required is substantially less.

8. Conclusion

From the foregoing analysis, it appears that a gas transport system is feasible, simple and relatively lightweight. It appears that no special pressure level control system will be required, i.e., the transport gas may discharge directly to the moon's "atmosphere". A small sampling tube put in this stream can be used to guide part of it to a sampling device.

---

* If an isentropic process is assumed as the gas is bled from the tank,

$$\frac{T_{final}}{T_{initial}} = \left[\frac{M_{final}}{M_{initial}}\right]^{k-1}$$

where k = ratio of specific heats

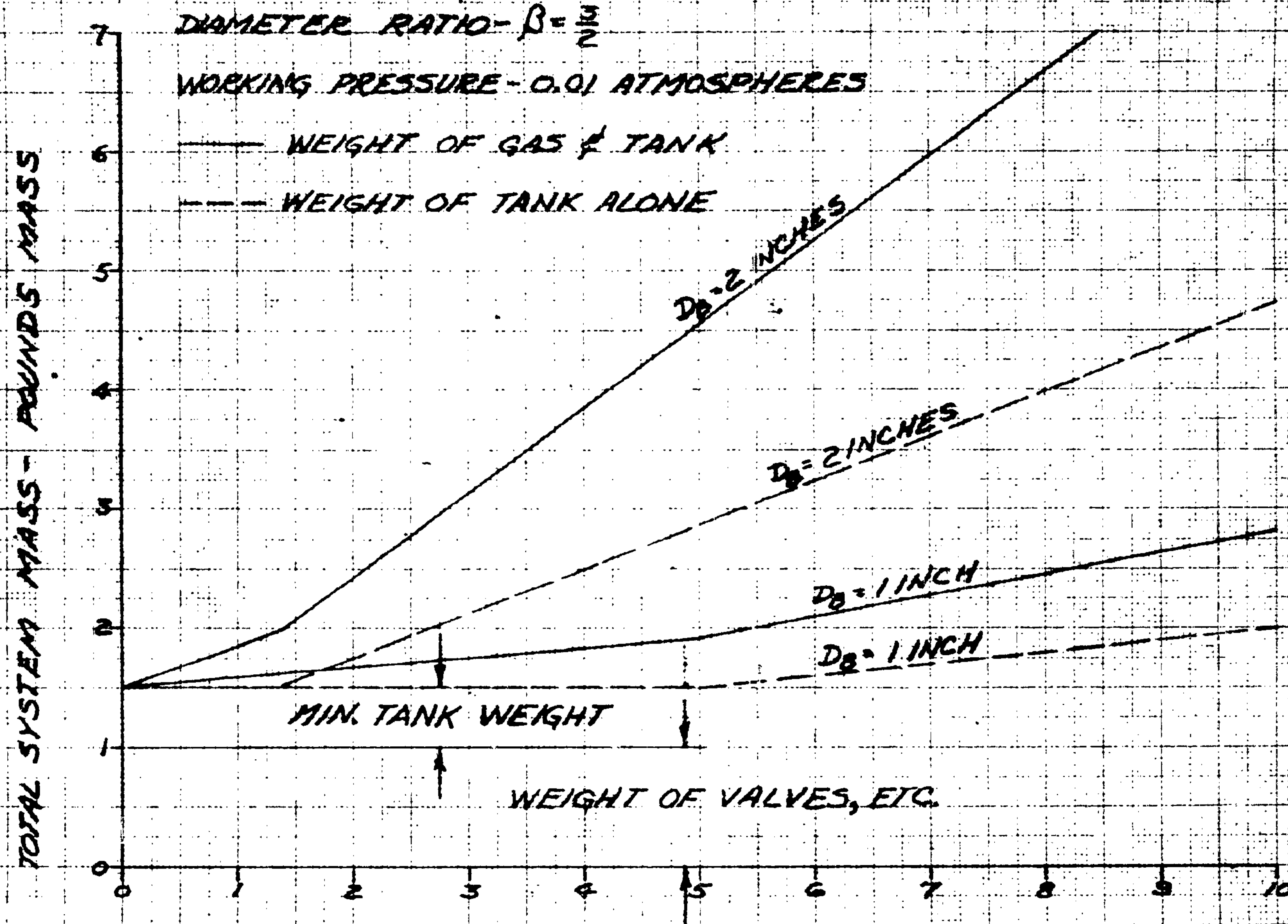

MASS OF AIR OR NITROGEN GAS TRANSPORT SYSTEM

FIGURE C-12

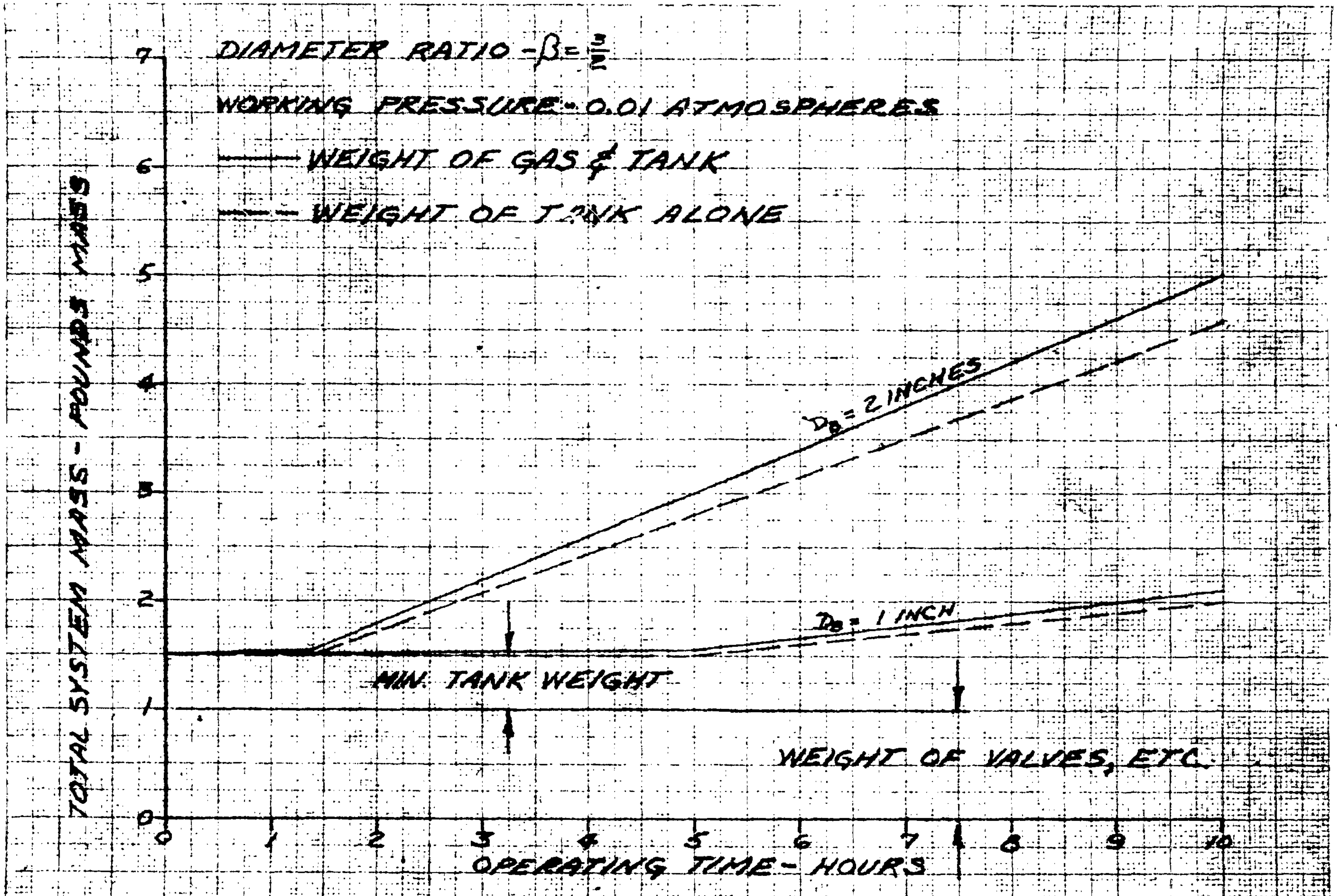

MASS OF HELIUM GAS TRANSPORT SYSTEM

FIGURE C-13

Appendix D

Means for Rotating the Drill Bit

Section 1

Gas Turbine Design Considerations

1. Introduction

One of the possible methods of driving the drill bit is by means of a partial admission turbine supplied by hot gas from the combustion of a solid propellant. This appendix will describe the partial admission turbine and give sample design calculations for one particular size. The method employed in the design is based upon "Fuels and Prime Movers for Rotating Auxiliary Power Units", Report Number 121, dated September 30, 1958, by R.W. Mann of the Dynamic Analysis and Control Laboratory, Massachusetts Institute of Technology.

1.1 General Design Features of Partial Admission Turbines

Partial admission turbines employ one or more nozzles which direct gas into an impulse wheel around a fraction of its circumference. In operation, high pressure gas is generated in a separate chamber at a pressure, P_{oo}. The gas expands through a nozzle (or nozzles) to essentially ambient pressure before entering the blades of the wheel. It passes through the blades and is deflected by them without any change in pressure or relative velocity, excluding frictional losses. The arrangement is represented schematically by Figure D-1. The velocity diagram and blade configuration are shown by Figures D-2 and D-3, respectively. The various symbols used throughout this appendix are defined in the nomenclature at the end of each section.

As indicated in Figure D-3, fluid enters over an arc of circumference of length, a. Normally, when operating on the earth, relatively stagnant fluid is present in the remaining pockets of the wheel, and so must be accelerated by the gases discharging from the nozzle. The losses connected with this acceleration process, make this type of turbine less efficient than its full admission counterpart. However, in operating on the moon, the back pressure would be so low, that very little gas would remain in the turbine blading (i.e., scavenging would be practically complete) and this loss would be negligible for a partial admission machine. The high pressure ratio which would be experienced on the moon, does cause difficulties in the nozzle. This high ratio results in a supersonic nozzle and, with the low flow rates required by the turbine, gives laminar flow in the nozzle. This nozzle would certainly be less efficient than the sonic, turbulent-flow type usually employed in partial admission turbines.

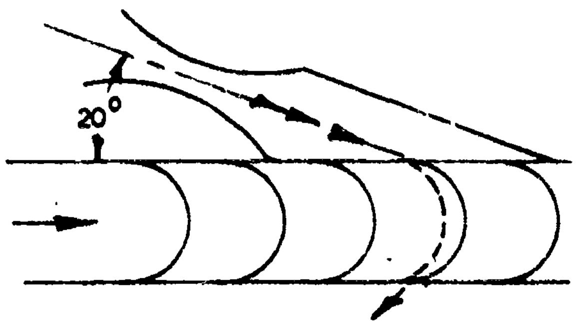

Impulse Turbine and Nozzle

Figure D-1

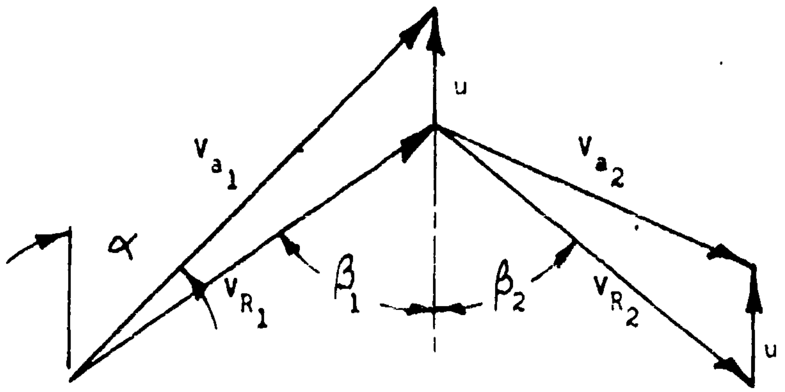

Velocity Diagram for Impulse Turbine

Figure D-2

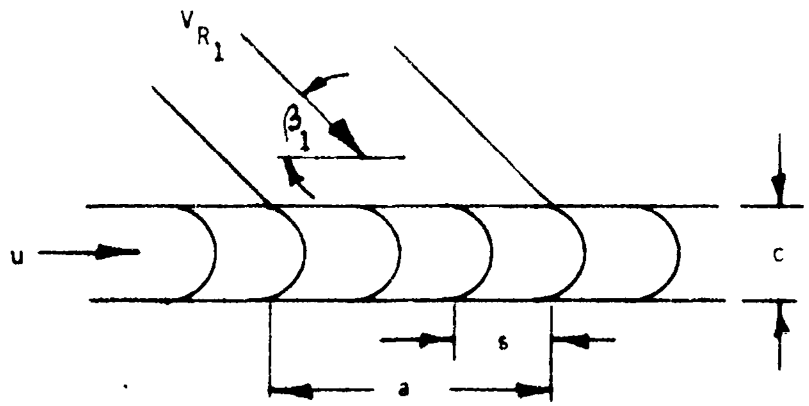

Impulse Turbine Blade Configuration

Figure D-3

2. Design Calculations

2.1 Design Point

A family of partial admission turbines will be designed for a power output range from 0.1 to 1.0 horsepower.

The solid propellant will be OMAX 448A, a product of the Olin-Mathieson Chemical Corporation. It has the following properties:

Specific heat, c_p = 0.461 BTU/lb/^{o}F

Ratio of Specific heats, k = 1.29

Molecular weight of gases, MW = 19.2 lb/mole

Since the ambient pressure on the moon is essentially zero, the pressure ratio available to the turbine is infinite. Thus, it would be advantageous to employ a slow-burning propellant, such as OMAX 448A, and set the chamber pressure as low as possible. A chamber pressure of 200 psia was selected. A back pressure of 0.2 psia was chosen so as to insure reasonable area ratios in the nozzle. This back pressure can be maintained by means of a suitable restriction down-stream of the turbine. The chamber temperature of the propellant gases is 1950^{o}F.

2.2 Assumptions

The following values have been assumed for the variables which influence partial admission turbine design:

a. Nozzle entrance temperature, T_{oo} = 1950^{o}F or 2410^{o}R

b. Nozzle entrance pressure, P_{oo} = 200 psia

c. Nozzle exit pressure P_2 = 0.2 psia

d. Turbine nozzle efficiency, η_N = 0.70

(This value was selected since the nozzle will be operating in laminar flow and supersonic exit velocities. Thus, a nozzle efficiency of greater than 70% would not be probable.)

e. Rotor velocity coefficient, $K = V_{R_2}/V_{R_1}$ = 0.85

f. Tip leakage factor, p = 0.95

g. Wheel speed, u = 1200 ft/sec

h. Mixing loss coefficient, f = 1.4

(This value is probably very conservative since the back pressure is so low that the gas trapped in the blades is easily scavenged.)

i. Blade Spacing, s. The minimum blade spacing which can milled is approximately 1/16 inch. This is probably satisfactory for a 1 HP turbine but not adequate for the lower powers. There are electrolytic etching methods available by which spacings down to 1/32 inch can be attained.

j. Ratio of blade width to blade spacing, c/s = 2.0

k. Nozzle angle, $\alpha = 20^{\circ}$

2.3 Design Procedure

In order to demonstrate the design procedure, a detailed analysis will be presented for the turbine with a horsepower output of 0.1.

The mass flow rate may be obtained from the definition of partial admission turbine efficiency, η_{tp}. Thus,

$$\eta_{tp} = \frac{\text{work output}}{\text{ideal work}} \tag{D-1}$$

where work output = output horsepower x 0.707 BTU/sec/horsepower

and ideal work = $w \times \Delta h_s$

Since the total enthalpy drop occurs in the nozzle,

$$\Delta h_s = c_p T_{oo} \left[1 - \left(\frac{P_2}{P_{oo}}\right)^{\frac{k-1}{k}} \right] \tag{D-2}$$

Equation (D-1) may be written as

$$w = \frac{0.707 \times (\text{output horsepower})}{\eta_{tp} \Delta h_s} \tag{D-3}$$

The efficiency of the partial admission turbine is not known at this stage of the calculation, and the design must be performed on a trial and error basis. As a first approximation, a turbine efficiency based upon full admission will be determined. This is given by

$$\eta_t = 2 \, p \, \eta_N \, n \, (\cos \alpha - n) \quad (1+K) \tag{D-4}$$

where,

$$n = \frac{u}{V_{a_1}} \tag{D-5}$$

and

$$V_{a_1} = \sqrt{\eta_N}\ V_{a_{1_s}} \tag{D-6}$$

$$V_{a_{1_s}} = \sqrt{2g_o\ J\ \Delta h_s} \tag{D-7}$$

For the case at hand,

Δh_s = 875 BTU/lb

$V_{a_{1_s}}$ = 6620 ft/sec

V_{a_1} = 5550 ft/sec

n = .216

and η_t = .385

Substituting this value of η_t for η_{tp} in Equation (D-3) yields

$w = 2.1 \times 10^{-4}$ lbs/sec.

This flow rate determines nozzle geometry and, hence, the variables which will be used to determine partial admission efficiency.

Since the nozzle is choked at the given pressure ratio, the throat area may be found from compressible flow relationships as

$$A^* = \frac{w\sqrt{T_{oo}}}{P_{oo}} \left[\frac{k\ g_o}{R} \left(\frac{2}{k+1}\right)^{\frac{k+1}{k-1}} \right]^{-\frac{1}{2}} \tag{D-8}$$

$= 1.22 \times 10^{-4}$ sq in

The nozzle throat diameter corresponding to this area is

$$d^* = 1.25 \times 10^{-2} \text{ in}$$

The exit area is obtained from the isentropic flow relationship

$$\frac{A}{A^*} = \frac{1}{M} \left[\frac{2}{k+1} \left(1 + \frac{k-1}{2} M^2\right) \right]^{\frac{k+1}{2(k-1)}} \tag{D-9}$$

where

$$M^2 = \frac{2}{k-1} \left[\left(\frac{P_{oo}}{P_2}\right)^{\frac{k-1}{k}} - 1 \right] \tag{D-10}$$

For the case at hand,

$$M = 5.08$$

and

$$\frac{A}{A^*} = 54.7$$

giving an exit area

$$A = 6.67 \times 10^{-3} \text{ sq in}$$

The nozzle is inclined at an angle of 20° to the plane of rotation, so that the projected area in this plane is

$$A_{exit} = \frac{A}{\sin 20^\circ} \tag{D-11}$$

$$= .0195 \text{ sq in}$$

The height of the blades is equal to the exit diameter. Thus

$$d = \sqrt{\frac{4}{\pi} A} \tag{D-12}$$

$$= .0924 \text{ in}$$

The arc length covered by the nozzle exit plane is

$$a = \frac{A_{exit}}{d} = .211 \text{ in} \tag{D-13}$$

and $\frac{s}{a} = \frac{.03125}{.211} = .148$

The partial admission turbine efficiency, η_{tp}, can be expressed as a function of the full admission turbine efficiency, η_t; geometric parameters, c/s, s/a, and α ; nozzle efficiency, η_N; velocity ratio, u/V_{a_1}; rotor velocity coefficient, K; tip leakage factor, p; and mixing loss coefficient, f. Thus,

$$\eta_{tp} = \frac{1 + K\ (1-\frac{s}{a})}{1 + K}\ \eta_t - \frac{f\ p\ \eta_N}{\sin\alpha} \left(\frac{u}{V_{a_1}}\right) \left(\frac{c}{s}\right) \left(\frac{s}{a}\right) \qquad \text{(D-14)}$$

The foregoing assumed and derived values may be substituted into Equation (D-14) to obtain the efficiency of the partial admission turbine as .351 for the first trial design.

This value of η_{tp} may be substituted back into Equation (D-3) to obtain a new flow rate for which the entire set of calculations may be repeated. In general, one iteration is found to be sufficient.

3: Results and Discussion

3.1 0.1 Horsepower Turbine

As shown in the preceding section the partial admission turbine with a 0.1 horsepower output will have the following dimensions and design factors.

flow rate, w = 2.30×10^{-4} lb/sec
nozzle throat diameter, d^* = 0.0131 inches
blade height, d = 0.097 inches
blade spacing, s = 0.03125 inches
admission arc length, a = 0.227 inches
turbine efficiency η_{tp} = 0.352
wheel width, c = 0.0625 inches
aspect ratio, AR = 1.55

3.2 1.0 Horsepower Turbine

In a similar manner, the partial admission turbine with 1.0 horsepower output will have design parameters of

flow rate, w = 2.37×10^{-3} lb/sec
nozzle throat diameter, d^* = 0.0415 inches
blade height, d = .311 inches

blade spacing, s = 0.125 inches
admission arc length, a = 0.71 inches
turbine efficiency, η_{tp} = .344
wheel width, c = 0.25 inches
aspect rates, AR = 1.24

3.3 Intermediate Sizes of Turbine

Between these two limiting sizes of turbine, the flow rate can be assumed to vary linearly. This is a good assumption since the turbine efficiency will not vary appreciably. Thus, Figure D-4 is a plot of flow rate versus power output in the range of 0.1 HP to 1.0 HP. Figure D-5 is a plot of total fuel weight required versus operating time for various power output and total energies.

3.4 Turbine Weight

The weight of the turbine can be estimated from its size, assuming a solid disc. Thus, the turbine weight is given by

$$W_t = \frac{\pi}{4} d_t^2 \, c \, \rho_{steel} \quad \text{(D-15)}$$

If the wheel diameter is considered to be 3" resulting in a speed of about 90000 RPM for a blade speed of 1200 ft/sec, Equation (D-15) can be simplified to

$$W_t = 2.12 \, c \text{ lbs} \quad \text{(D-16)}$$

The wheel thickness is assumed to vary linearly from 1/16" for 0.1 HP to .25" for 1.0 HP. Actual fabrication of the wheel would not necessarily result in a constant thickness disc but rather in a webbed disc. However, when the weight of the nozzle block and supports are added, the final weight should be about the same as for the solid disc. Figure D-6 is a plot of turbine weight versus power output.

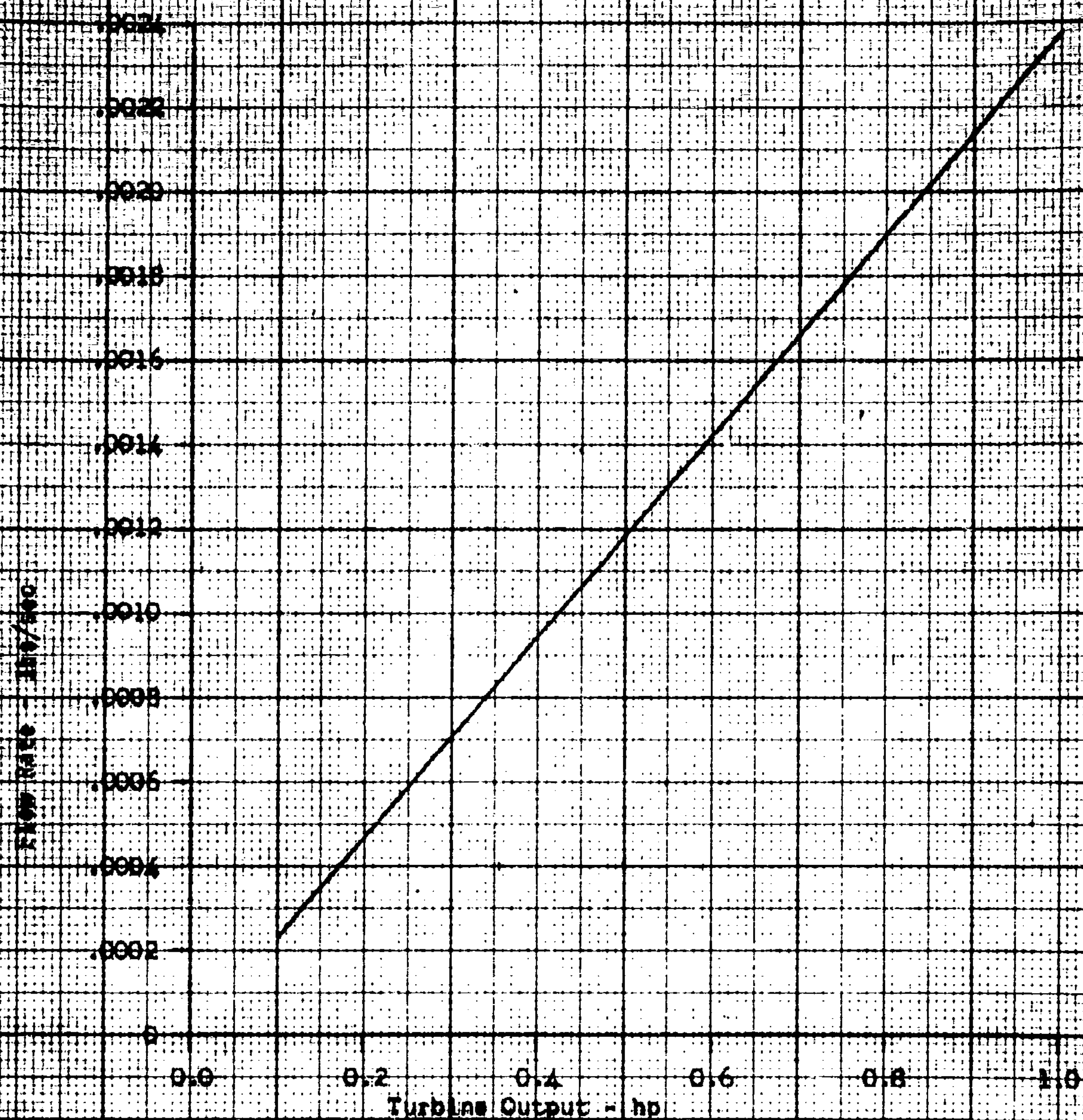

Flow Rate as a Function of Turbine Output

Figure D-4

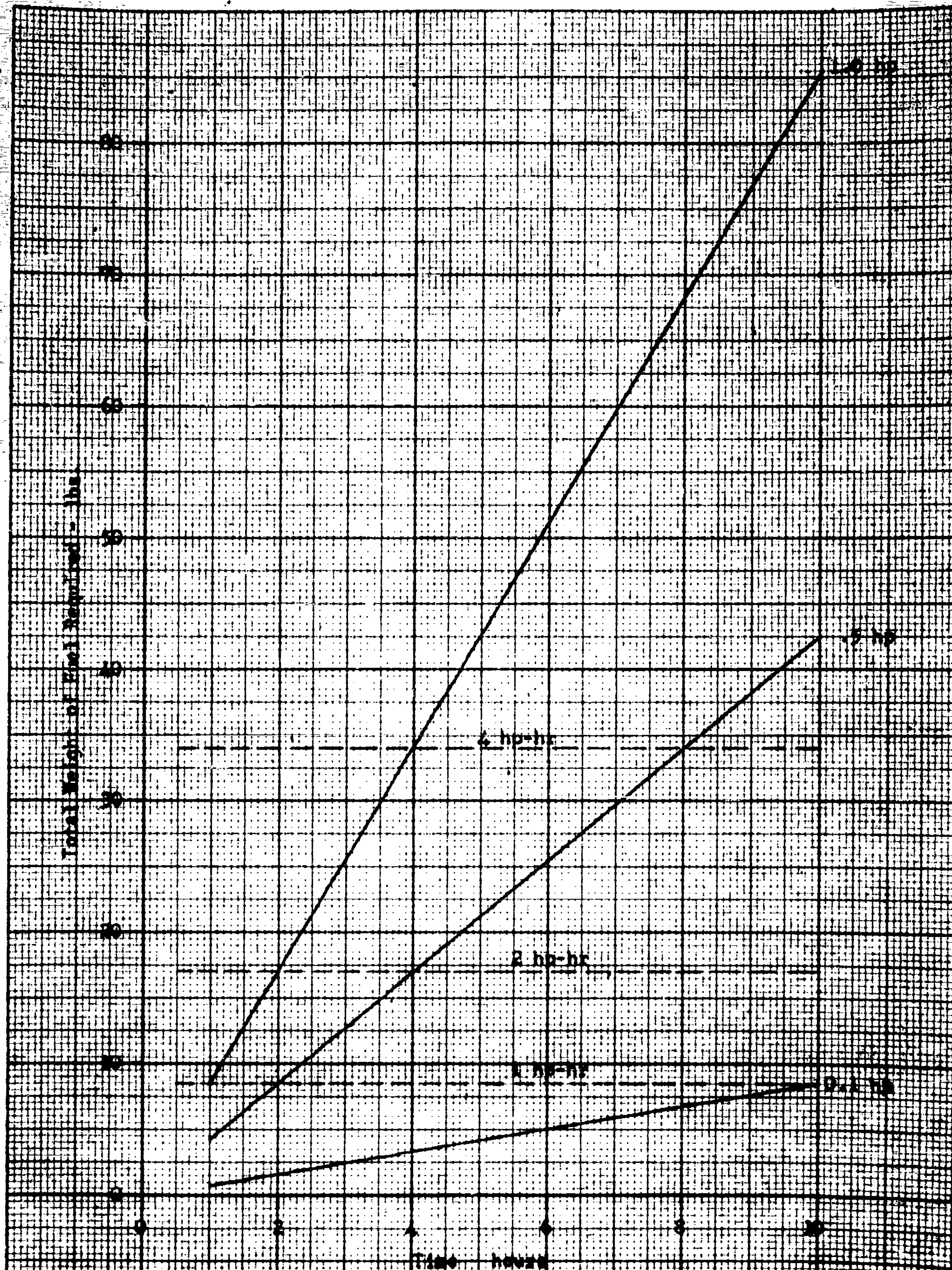

Fuel Weight as a Function of Operating Time
Figure D-5

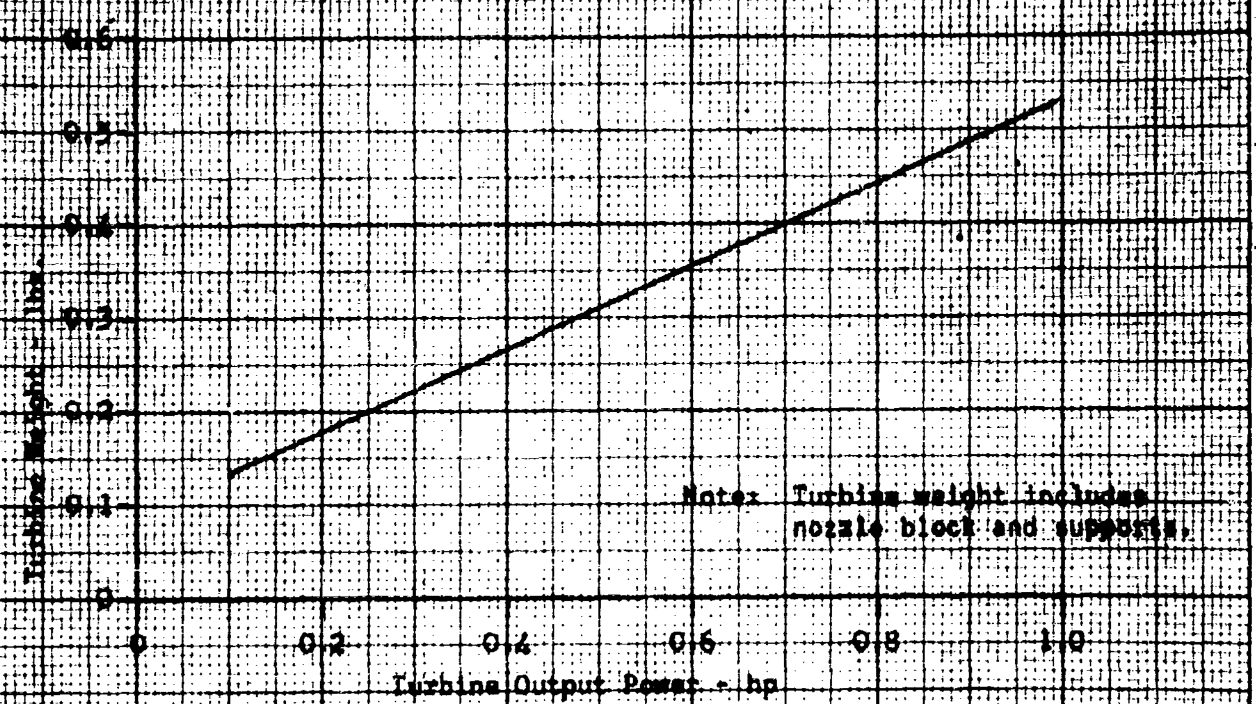

Turbine Weight versus Output Power

Figure D-6

Nomenclature

Partial Admission Turbine

A	Exit area of nozzle	in^2
A^*	Area in nozzle where M = 1	in^2
AR	Aspect ratio, d/c	-
A_{exit}	Projected exit area of nozzle in plane of rotation	in^2
a	Arc length covered by nozzle exit plane	inches
c	Rotor disc width	inches
c_p	Specific heat	BTU/lb/^oF
d	Exit diameter of nozzle	in
d_t	Turbine wheel diameter	in
f	Mixing loss coefficient	-
g_o	Proportionality constant, 32.2	ft lb_m/sec^2 lb_f
J	Mechanical equivalent of heat	ft lb/BTU
K	Rotor velocity coefficient, V_{R_2}/V_{R_1}	-
k	Specific heat ratio	-
M	Mach Number	-
MW	Molecular weight	lb/mole
n	Velocity ratio, u/V_{a1}	-
P_{oo}	Nozzle entrance pressure	psi
P_2	Exhaust pressure	psi
p	Tip leakage factor	-

s	Blade spacing	inches
T_{oo}	Supply gas temperature	^oR
u	Blade speed	ft/sec
V_{a_1}	Absolute velocity at blade entrance	ft/sec
V_{a_2}	Absolute velocity at blade exit	ft/sec
$V_{a_{1_s}}$	Isentropic nozzle velocity	ft/sec
V_{R_1}	Relative velocity at blade entrance	ft/sec
V_{R_2}	Relative velocity at blade exit	ft/sec
W_t	Turbine weight	lb
w	Flow rate	lb/sec
α	Nozzle angle	degrees
β_1	Angle of flow (relative to wheel) entering blades	degrees
β_2	Angle of flow (relative to wheel) leaving blades	degrees
Δh_s	Isentropic enthalpy drop	BTU/lb
η_N	Nozzle efficiency	-
η_t	Full admission turbine efficiency	-
η_{tp}	Partial admission turbine efficiency	-
ρ_{steel}	Density of steel	lb/in^3

Section II

Positive Displacement Gas Motor Design

1. Introduction

Previous studies of auxiliary power units have shown that compared with turbine drive there is the possibility of a weight saving by using a positive displacement motor at low power outputs. Thus, a brief survey is here made of its use as a drive for the drilling rig.

Data on hot gas actuated positive displacement motors were obtained from Clevite Corporation (Ordnance Division). However, since the design point for the motor needed here is so far removed from the range with which Clevite are concerned, their data must be extrapolated and checked independently. Thus, a thermodynamic analysis is made and the results compared with the Clevite equation.

Unfortunately, the performance of a piston device is not analytically predicted with as much confidence as for a turbine unit. This is due to the fact that mechanical design details affect the final performance to a much greater degree.

2. Design Considerations

2.1 Comparison with the Clevite Motor

The load is to be driven in a speed range of 1000-2000 rpm. The range of power outputs from the motor is to be 0.1 to 1.0 hp with operating time ranging from 1 to 10 hours. These are generally lower powers and speeds and longer operating times than the normal Clevite motor application which is usually several horsepower over a period of several minutes. At low powers and long operating times, efficiency and cooling become more important than in the normal application. To achieve high efficiency in such a motor, large volumetric expansion must be provided between intake and exhaust. In addition, it is necessary to keep mechanical, pumping, and leakage losses minimal. Mechanical design controls all of these factors, particularly valve timing which affects the expansion ratio to a great degree. Even though these engines have normal operating speeds and pressures much higher than required for this application, there appears to be no reason why proper valve timing could not be achieved to insure high efficiency. Moreover, it is possible to match the output speed of the

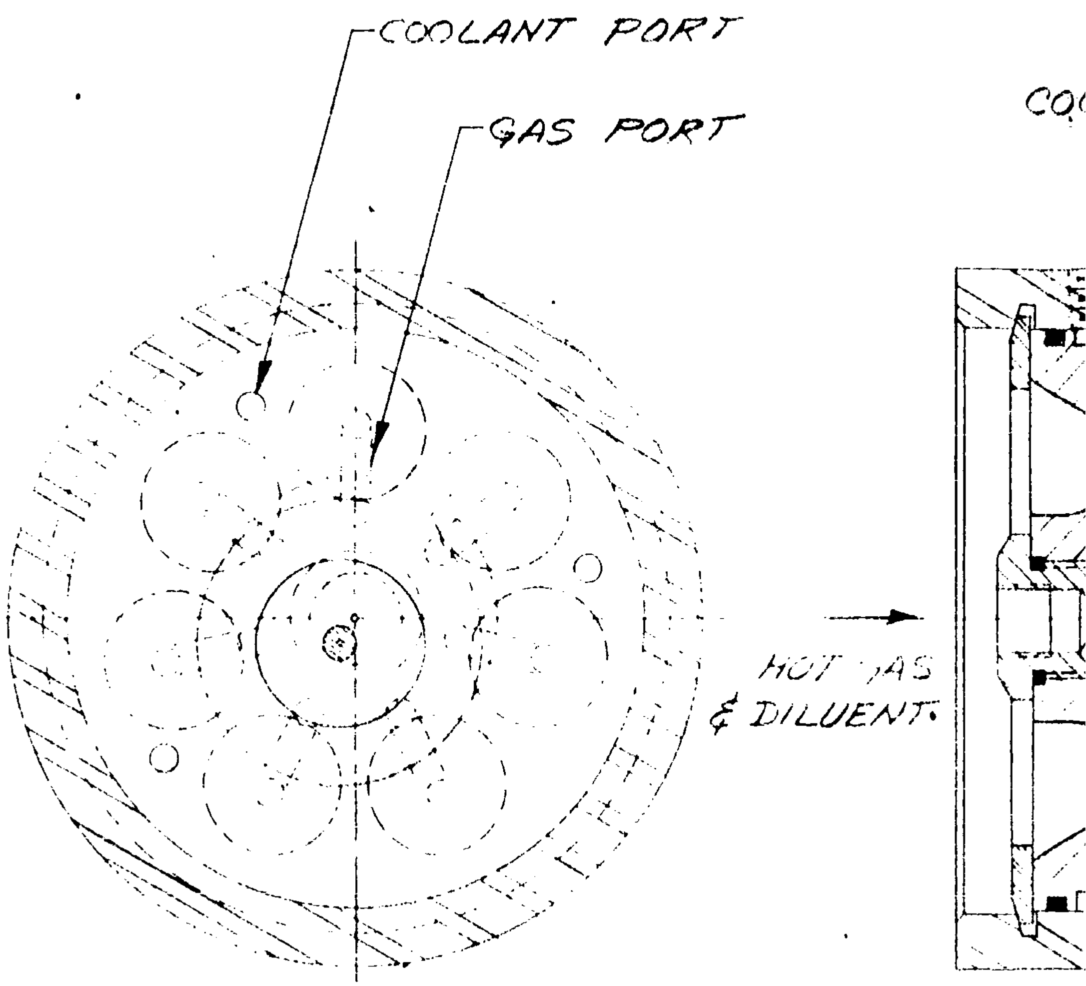

ENGINE SPECIFICATIONS:

HP - 7 1/2
RPM - 12,000
BORE - .563 IN.
STROKE - .576 IN.
CYINDERS - 7
DISPLACEMENT - 1.003 $IN.^3$
PSI - 700
RUN TIME - 150 SECONDS

1

NOTE: COPY OF CLEVITE ORDNANCE DWG. #B-2013

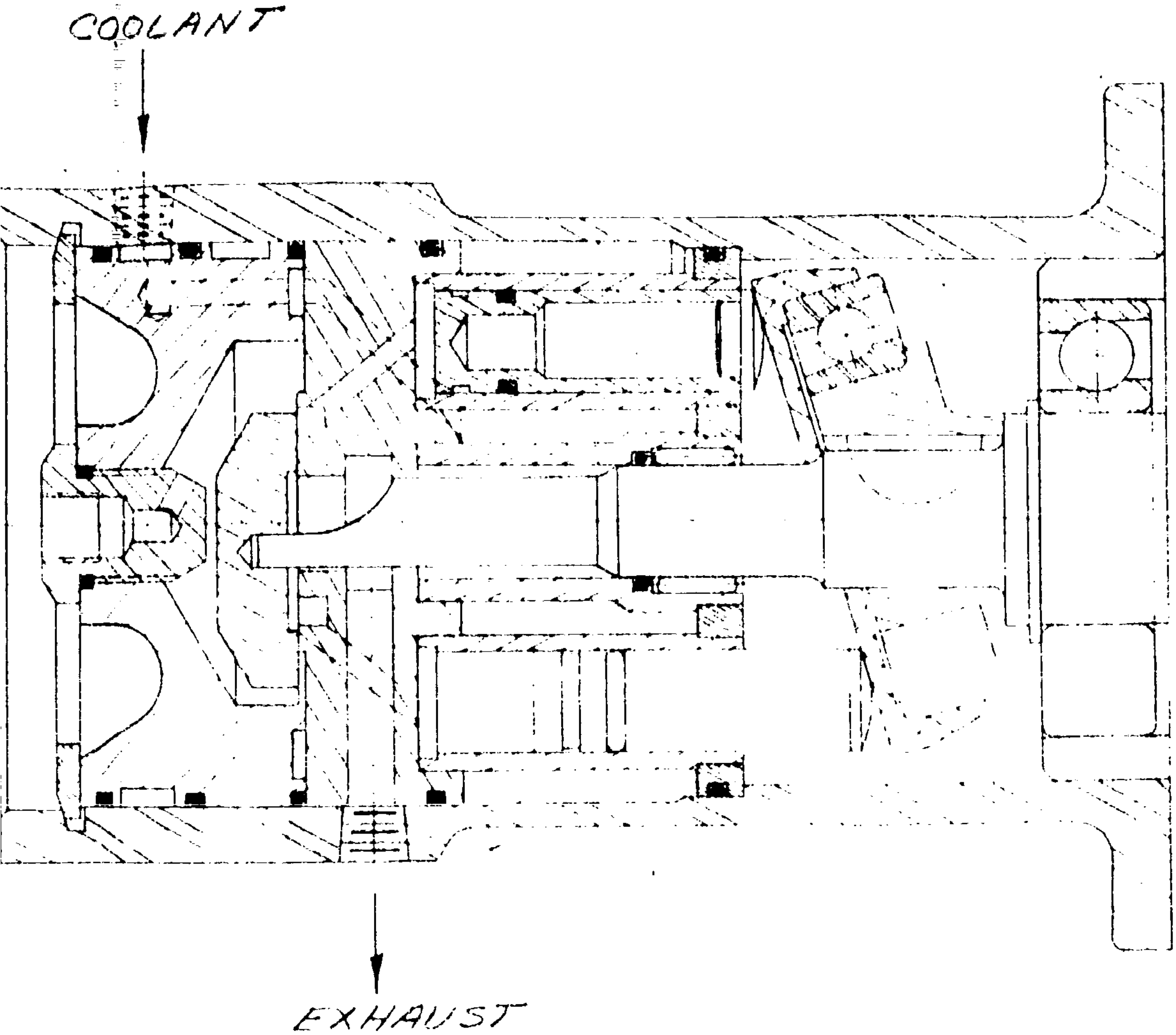

2

HOT GAS MOTOR ASSEMBLY

3-20138

FIGURE D-7

motor to the load so as to make use of a direct drive, thereby eliminating reduction gearing.

Another problem peculiar to the Clevite motor is that of heat transfer. Since there is intimate contact between the inlet passages and the cylinder walls, the latter will heat up quickly, giving rise to the need for a gas coolant. This may be accomplished by either the addition of a diluent in the hot gas, such as ammonium chloride; or by external cooling with another fluid.

Most small gas or hydraulic motors (the Clevite motor being a typical example) are constructed as a "barrel engine", with five or more cylinders arranged axially about a common shaft; and the power is transmitted through a "wobble plate" on the shaft. Flow is controlled through ports by a rotating cut-off valve. A typical assembly of a Clevite motor is shown by Figure D-7.

2.2 Assumptions

The following assumptions are made in analyzing the positive displacement motor:

(a) The motor is directly connected to the load.

(b) Supply pressure will not exceed 2000 psi.

(c) The supply gas is that obtained from the burning of OMAX 448A solid propellant. Its properties are

$c_p = 0.461$ BTU/lbs ^oR

$k = 1.29$

MW = 19.2 lbs/mole

(d) Ammonium chloride is to be used as a diluent in the proportions of 1 part to 2 parts OMAX 448A. This will lower the supply temperature to 1200°F but not change the gas properties appreciably.

2.3 Calculations

As a first approximation, consider an ideal engine - one in which the gas expands isentropically, has zero clearance, operates with zero back pressure, and has no throttling loss through the valves.

For such an engine, the ideal work output per pound of gas, W_i, is given by the area under the constant pressure line and adiabatic expansion curve. This area is shown cross-hatched in Figure D-8.

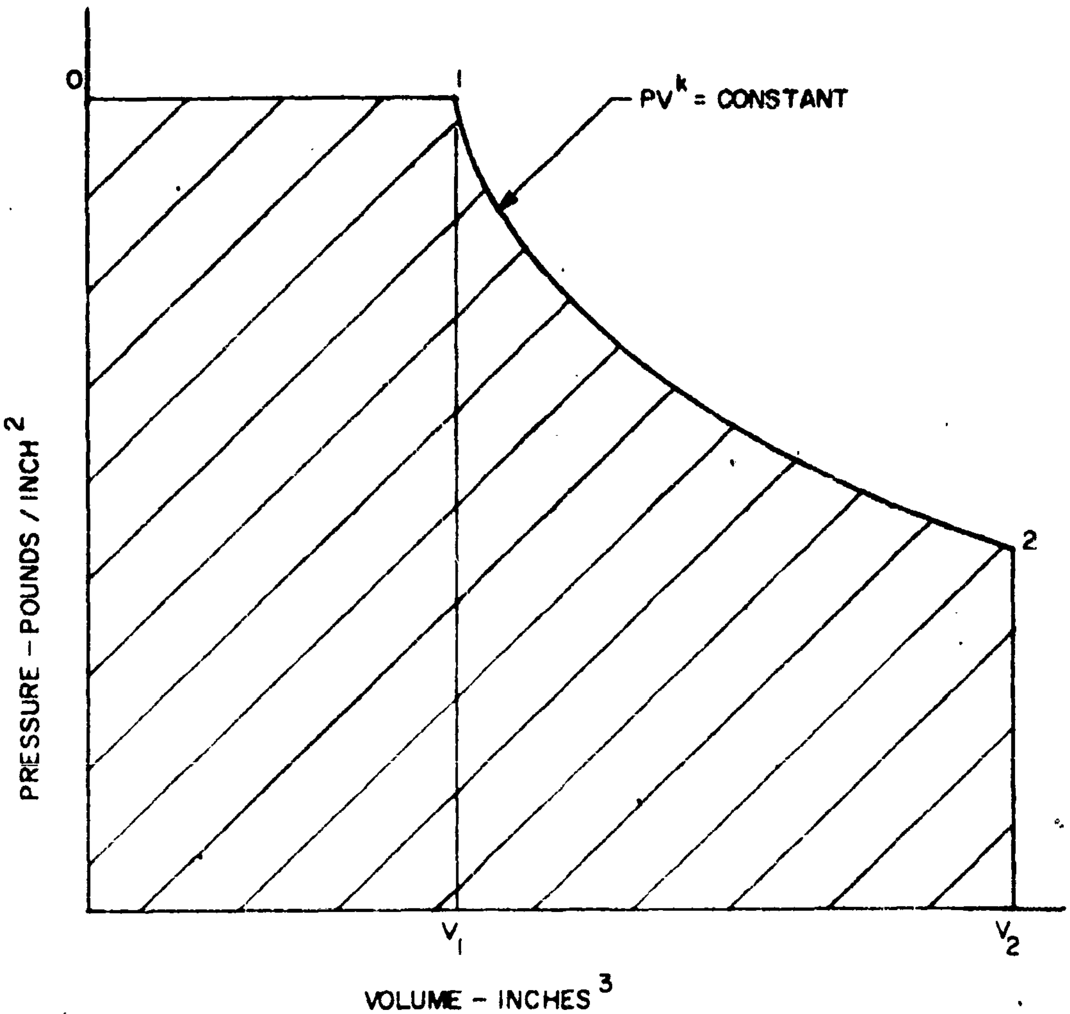

IDEAL WORK OUTPUT

FIGURE D-8

The work output per pound of gas is

$$W_i = \frac{c_p T_o J}{k} \left[k - \left(\frac{V_1}{V_2}\right)^{k-1} \right] \qquad \text{(D-17)}$$

and the power output is obtained by multiplying by the flow rate, w_i,

$$hp = \frac{w_i W_i}{550} \qquad \text{(D-18)}$$

Thus, the ideal flow rate required is

$$w_i = \frac{550\ hp}{W_i} = \frac{550\ hp}{\frac{c_p T_o J}{k} \left[k - \left(\frac{V_1}{V_2}\right)^{k-1} \right]} \qquad \text{(D-19)}$$

The effect of volumetric expansion ratio on the flow rate is shown in Figure D-9 for an entrance temperature of $1660^{\circ}R$ and a range of output powers from 0.1 to 1.0 hp. Previous work with this type of motor has shown that expansion ratios (V_2/V_1) from about 1.5 to 5.0 are possible in this power range. It is seen from the figure that the ideal flow rate does not vary appreciably beyond an expansion ratio of 5.

The ideal piston displacement can be calculated from the flow rate and expansion ratio to be

$$(PD)_i = \frac{V_2}{V_1} \frac{w_i}{P_o} \frac{R T_o}{N} \ (12 \times 60)\ in^3/rev \qquad \text{(D-20)}$$

Figure D-10 is a plot of Equation (D-20) showing the ideal piston displacement per revolution as a function of the expansion ratio. Curves are shown for 0.1 hp, 0.5 hp and 1.0 hp. For all curves the speed is 2000 rpm and inlet pressure 1000 psia.

The actual flow rate can be estimated from the ideal flow rate by dividing the latter by the product of mechanical efficiency and indicated efficiency. Thus,

$$w = \frac{w_i}{\eta_M \eta_i} \qquad \text{(D-21)}$$

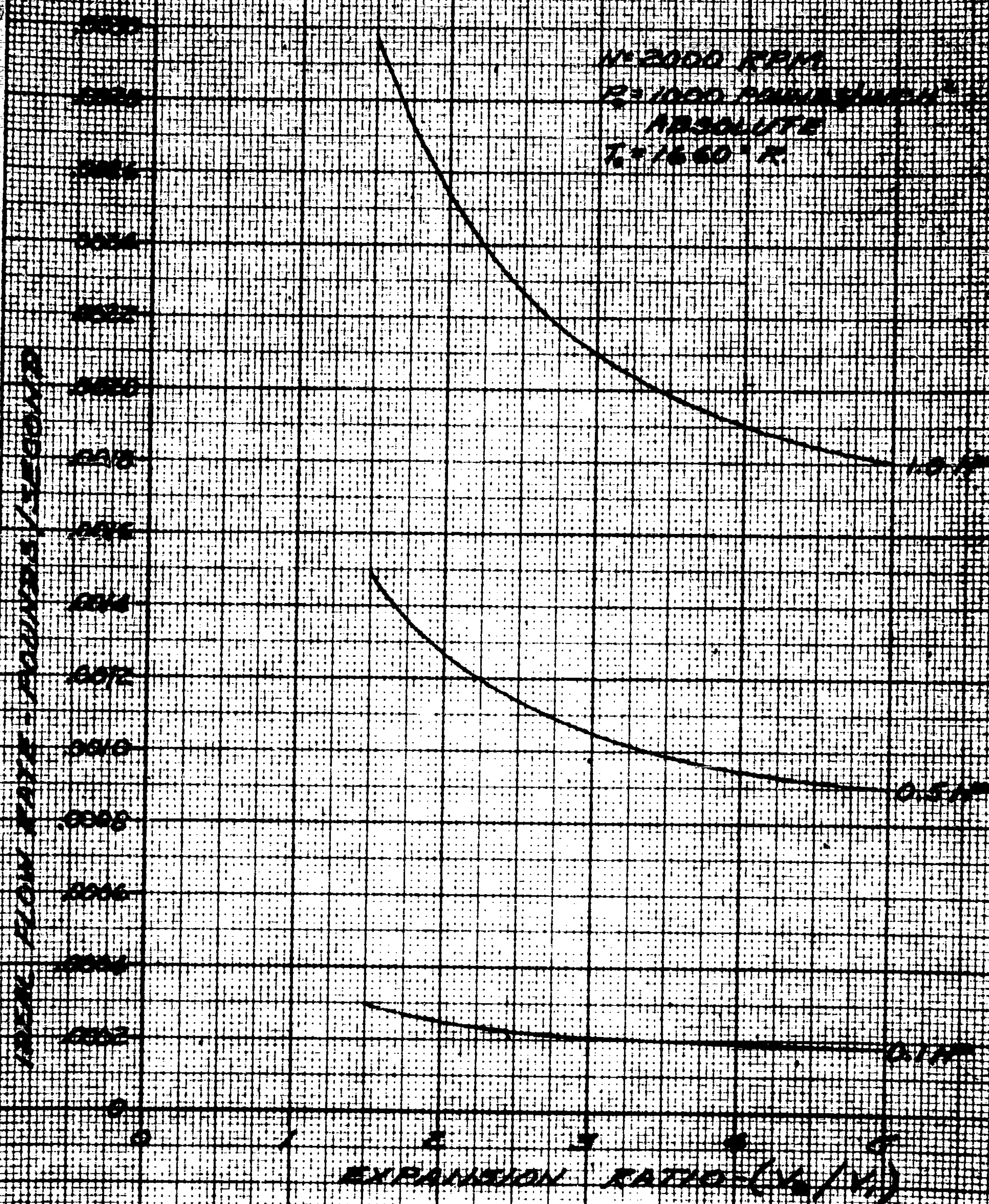

IDEAL FLOW RATE AS A FUNCTION OF EXPANSION RATIO

FIGURE D-9

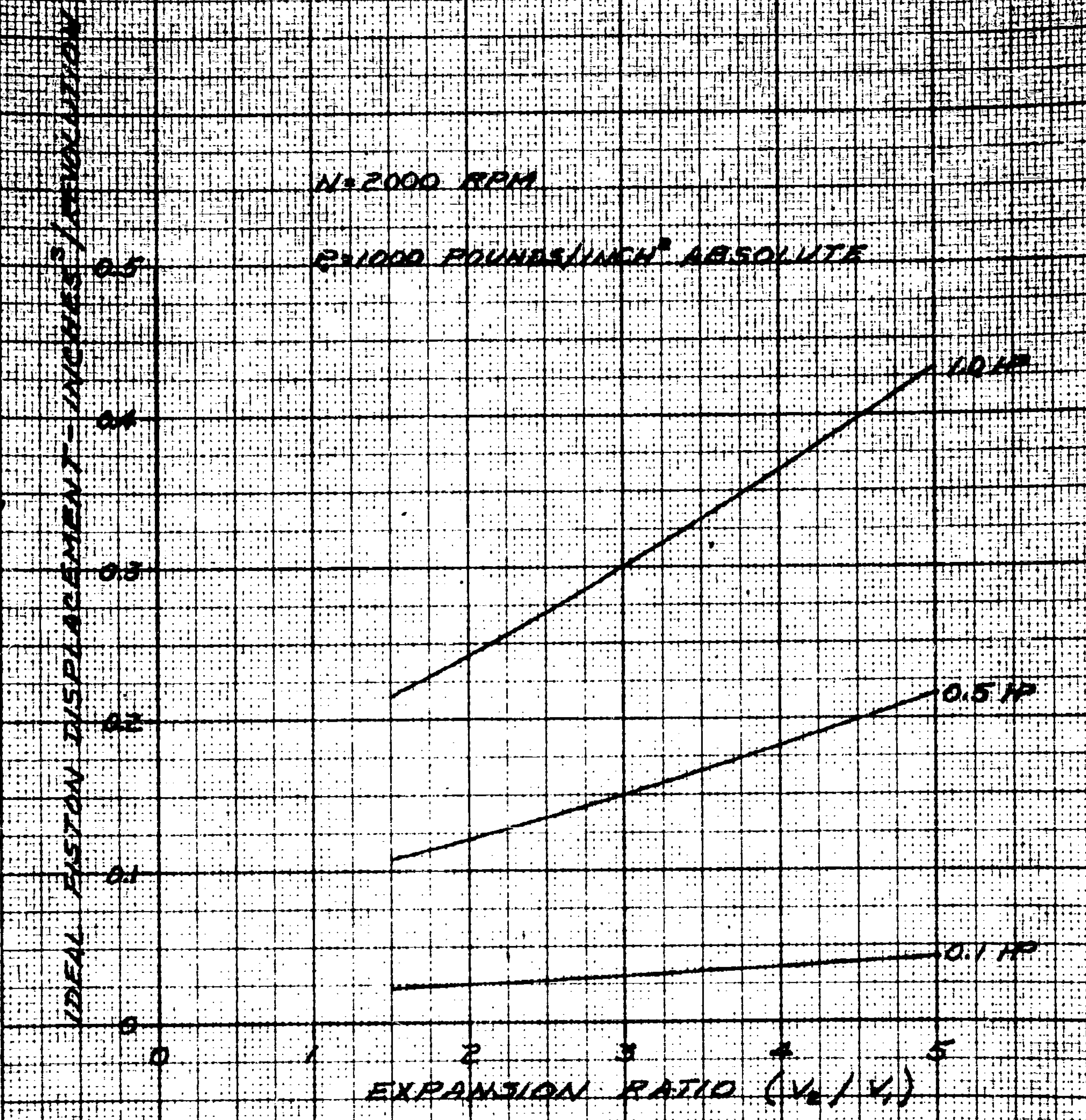

PISTON DISPLACEMENT PER REVOLUTION vs EXPANSION RATIO

FIGURE D-10

Tests results and indicator card studies for the Clevite engine result in values of $\eta_M \times \eta_i$ equal to about 0.66. Thus, the actual piston displacement per revolution should be about 50% more than the indicated values.

Equations (D-19) and (D-20) can be combined with (D-21) to give

$$w = \frac{550 \text{ hp}}{\frac{c_p T_o J}{k} \left[k - \left(\frac{V_1}{V_2}\right)^{k-1} \right] \eta_M \eta_i} \tag{D-22}$$

and $$(PD) = \frac{V_2}{V_1} \frac{w}{P_o} \frac{R T_o}{N} (12 \times 60) \frac{in^3}{rev} \tag{D-23}$$

Thus, it appears that for the range of powers contemplated (from 0.1 to 1.0 hp), a 1/4" to 1/2" bore and stroke is adequate. This is in the same range as those units presently constructed and hence offers no serious problems.

The operating torque can be expressed as a function of the output power and the rotary speed.

$$T_q = 63000 \frac{hp}{N} \tag{D-24}$$

Figure D-11 is a plot of this relationship for 1000 and 2000 rpm. As seen from these curves, even at the low powers the operating torque does not appear to be low enough to present serious design difficulty.

The total weight of propellant and diluent required can be calculated from Equation (D-22) multiplied by the operating time. These results are plotted in Figure D-12 for an expansion ratio of 2.5 at which this motor will probably operate.

These estimated values of flow rate and total weight of propellant can be compared to that obtained by extrapolation of Clevite data by using the following relationship.

$$w = \frac{550 K_1 P_o \text{ hp}}{\eta_M (K_T P_o - P_2) R \left[T_o - K_2 (T_o - 530) \right]} \tag{D-25}$$

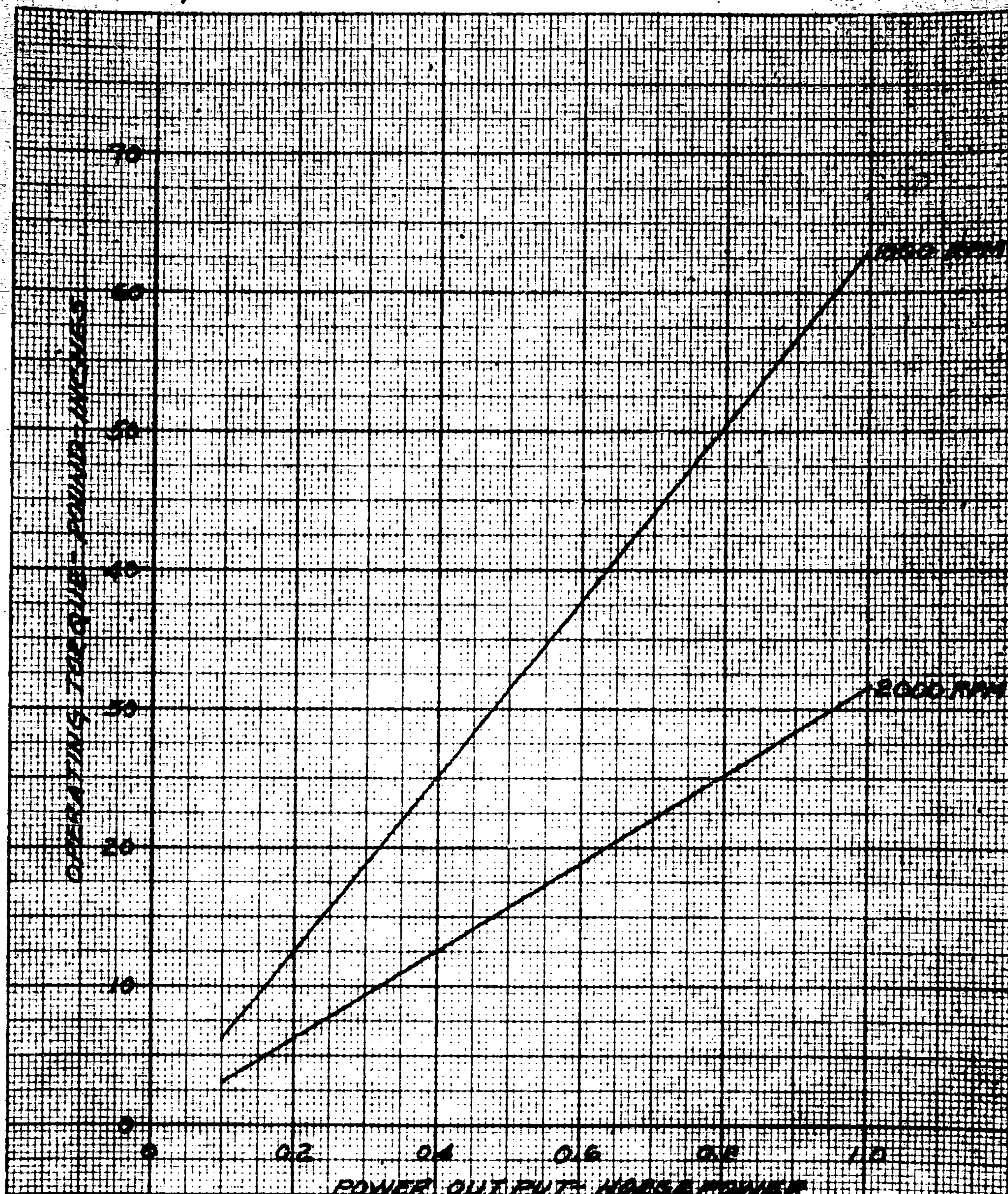

OPERATING TORQUE vs. POWER OUTPUT

FIGURE D-11

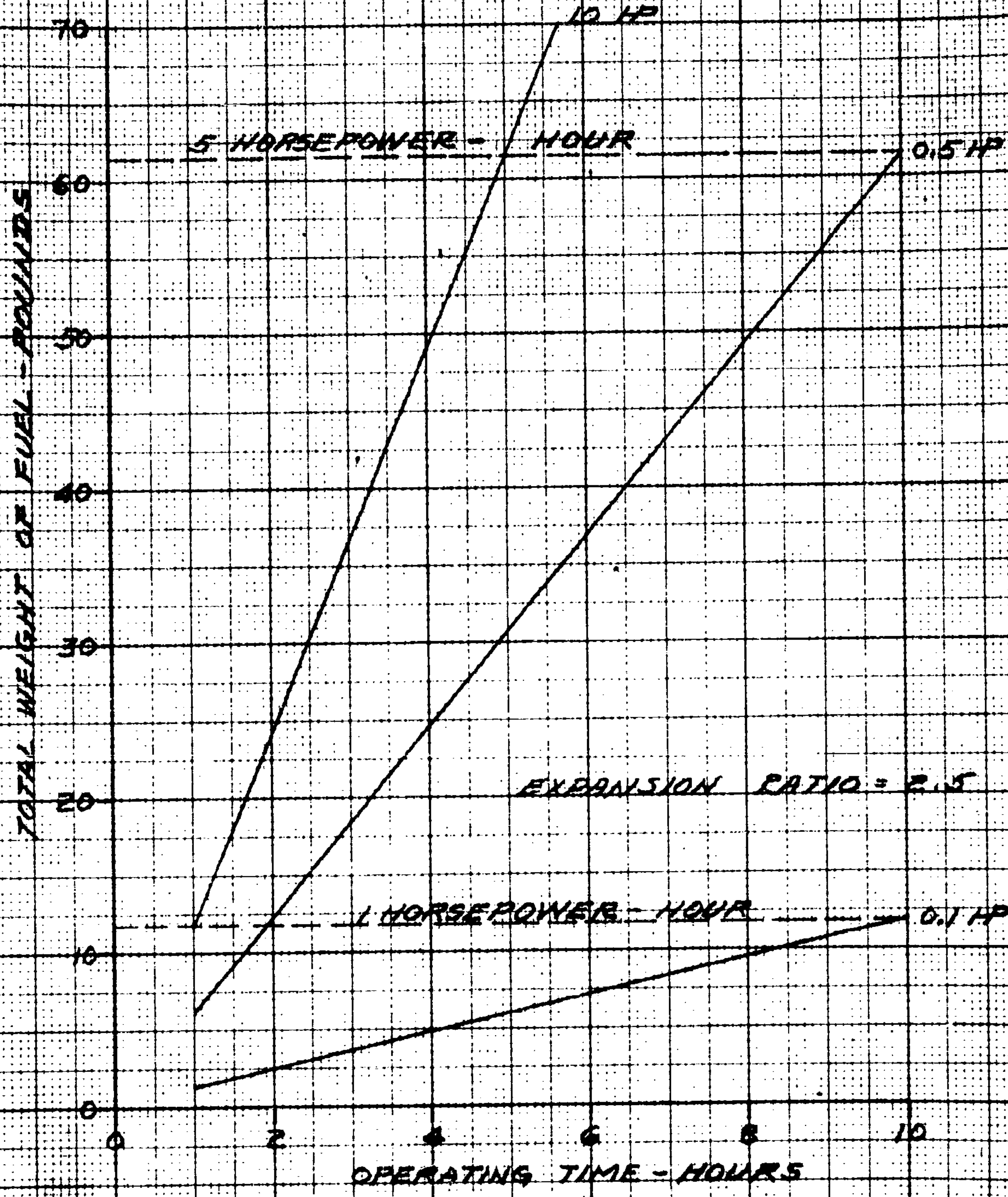

WEIGHT OF PROPELLANT AS A FUNCTION OF TIME

FIGURE D-12

With

$$K_1 = 0.20$$

$$K_2 = 0.05$$

$$K_T = 0.33$$

$$\eta_M = 0.85$$

$$P_o = 1000 \text{ psia}$$

$$P_2 = 50 \text{ psia}$$

$$T_o = 1660^\circ R$$

Equation (D-25) reduces to

$$w = (3.59 \times 10^{-3}) \text{ hp} \tag{D-26}$$

This is plotted in Figure D-13, along with that from the foregoing analysis for an expansion ratio of 2.5.

It is seen that the results of the two analyses compare very well and so the use of the Clevite equation is valid in this range of operation.

3. Weight of Motor

From previous experience in the design of these motors, it can be estimated that the weight of the motor components will probably not exceed 3 pounds. This compares favorably with the weight of the turbine and its necessary gear box.

4. Conclusions

The results of this analysis show that the weight of propellant is greater than that required by a partial admission turbine. This fact, together with the complexity of the motor as compared to the turbine; and the need for a development program to determine motor characteristics beyond the range presently investigated; weigh heavily against its selection. Also, to our knowledge, no small gas motor has yet operated successfully over any extended period of time because of the cooling problem.

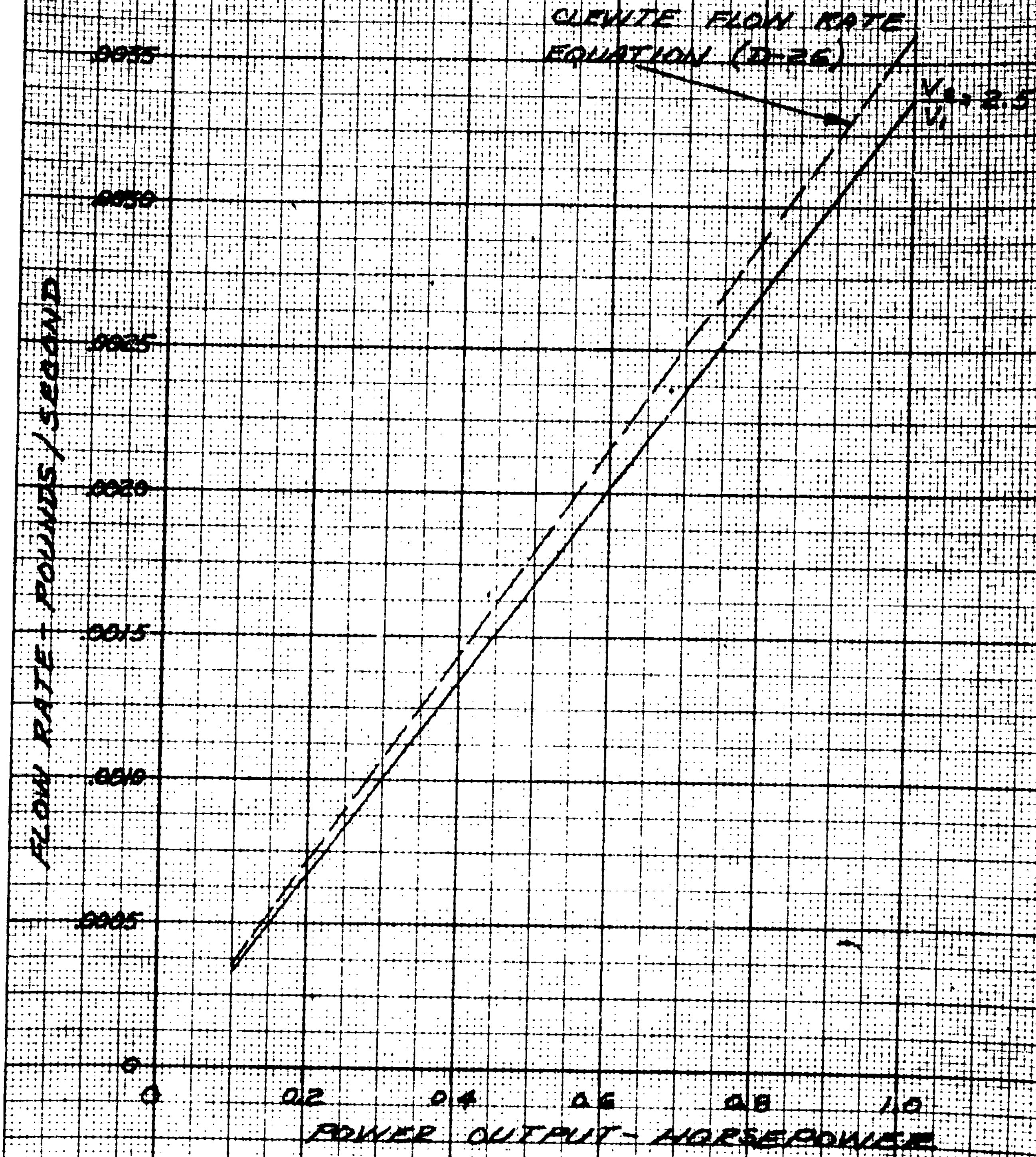

COMPARISON OF FLOW RATES OBTAINED BY ANALYSES

FIGURE D-13

Nomenclature

Positive Displacement Motor

c_p	Specific heat	$BTU/lb^{o}R$
hp	Horsepower output	hp
J	Mechanical equivalent of heat	ft lb/BTU
K_T	Ratio of mean power during power stroke to P_o	-
K_1	Constant used in Clevite Flow Equation	-
K_2	Constant used in Clevite Flow Equation	-
k	Specific heat ratio	-
MW	Molecular weight	lbs/mole
N	Rotary speed	rpm
(PD)	Piston displacement	in^3
P_o	Supply pressure	psi
P_2	Cylinder pressure during inlet or exhaust flow	psi
R	Gas constant	$ft\ lb/lb^{o}R$
T_o	Supply temperature	^{o}R
T_q	Operating torque	lb-in
V_1	Cylinder volume prior to expansion	in^3
V_2	Ctlinder volume after expansion	in^3
W_i	Ideal work	ft lb/lb
w_i	Flow rate	lb/sec
η_i	Indicated efficiency	-
η_M	Mechanical efficiency	-

Section III

Gas Generator Design Considerations

1. Introduction

The gas generator as described in this section includes the powder grain, or liquid fuel, its containing pressure vessel, and the appurtenances necessary to hold and ignite the charge. It includes the squib and igniter, grain insulation, and inhibiter. In the following section, the assumptions and methods employed to evaluate the size and weight of each of these components will be discussed for the solid propellant, compressed gas, and liquid monopropellant arrangements.

Briefly, the results show that due to the low flow rates and long operating times necessary for this application, the required size and shape of the propellant grain are such as to require considerable development work to fabricate. In addition, various schemes which might be used to overcome this difficulty would pose a reliability problem, in that many successive firings of the propellant are required.

For the case of compressed gas, the study shows that nothing is to be gained from its use since it requires a larger, heavier pressure vessel than the other systems.

Finally, the liquid monopropellant appears to offer a minimal weight package and most convenient shape.

In the following sections, the three systems will be considered in detail.

2. Solid Propellant Grain

2.1 Size and Shape

The size and shape of the grain have been determined by the usual procedures for design of solid propellant grains. The material selected is OMAX 448A, a product of the Olin-Mathieson Chemical Corporation.

Its properties are as follows:

Density of Solid, ρ = 0.0530 lb/in^3

Specific Heat Ratio, k = 1.29

Molecular Weight of Gases, MW = 19.2 lbs/mole

Chamber Temperature, T_c = 1950°F

Since burning rates are strongly affected by the temperature at which the propellant grain has been stored and the chamber pressure at which

it burns, it is important to know how this propellant performs under a wide range of both. Figure D-14 presents burning rates as a function of soak (storage) temperature and chamber pressure. These data have been derived from the manufacturer's data sheet by extrapolating to temperatures below $-65^{\circ}F$ and above $165^{\circ}F$, and pressures below 300 psia. The manufacturer has successfully fired this propellant at pressures ranging downward to atmospheric pressure and temperatures as low as $-90^{\circ}F$ and as high as $200^{\circ}F$. For ignition at low temperatures (i.e., less than $-65^{\circ}F$), they recommend the use of a more vigorous igniter.

The conditions on the moon are such that the soak temperature can be selected at either $+ 200^{\circ}F$ or $- 200^{\circ}F$ depending upon whether the drilling is done during the lunar day or night. In order to keep the length of the grain as low as possible, it is felt that ignition at $- 200^{\circ}F$ would be desirable. Certainly, this would provide the minimum length grain. From Figure D-14 at a soak temperature of $-200^{\circ}F$, the burning rate of OMAX 448A at a chamber pressure of 200 psia is seen to be 0.023 in/sec.

The rate of gas production is proportional to the cross-sectional area which is burning at any instant. Ideally, in a cylindrical grain, the entire end of the cylinder should be ignited and the flame front should proceed along the grain axis, shortening the cylinder as it goes. Since there is a one to one correspondence between the weight of the gases generated and the weight of propellant burned, the gas generation rate is directly proportional to the burning rate (i.e., the rate of progress of the flame front through the solid).

The rate of gas production based upon a soaking temperature of $-200^{\circ}F$ is given by

$$w = \frac{\pi}{4} d^2 \cdot r_{p_{-200^{\circ}F}} \rho \qquad \text{(D-27)}$$

where

ρ = density of the propellant grain, lbs/in^3

$r_{p_{-200^{\circ}F}}$ = burning rate at $-200^{\circ}F$ and the selected burning pressure, in/sec

d = grain diameter, in

Equation (D-27) may be used to determine the diameter of a grain

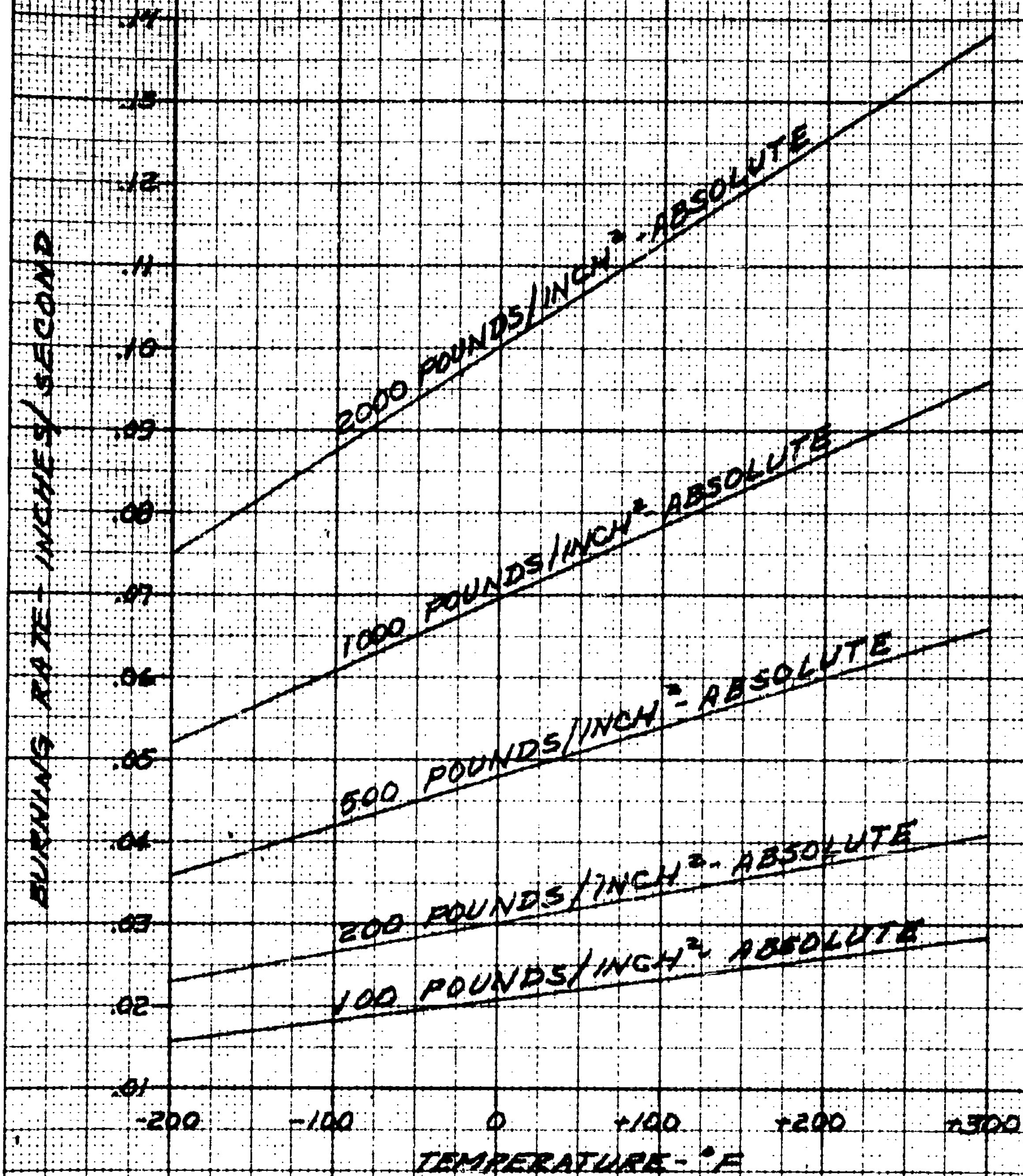

BURNING RATE OF OMAX 448A vs.
TEMPERATURE AT VARIOUS CHAMBER PRESSURES

FIGURE D-14

required to produce a flow rate, w (lbs/sec) at a chamber pressure, p. Thus,

$$d = 4.89 \sqrt{\frac{w}{r_{p_{-200^\circ F}}}} \tag{D-28}$$

The length of time during which gas will be supplied by the gas generator is directly proportional to the length of the propellant grain. It is equal to the time required for the flame front to travel from one end of the grain to the other. Grain length is given by

$$L = t \times r_{p_{-200^\circ F}} \tag{D-29}$$

where

l = length of grain, inches

t = burning time, seconds

The total weight of the grain is given by

$$W_g = \frac{\pi}{4} d^2 L \rho \tag{D-30}$$

or

$$W_g = w \times t \tag{D-31}$$

Figures D-15 and D-16 summarize these results for a range of sizes of turbine of between 0.1 hp and 1 hp output at a total energy consumption of 1 hp-hr.

As can be seen from these results, although the total weights of propellant are about the same (since the total energy is the same) the length of the grain varies from 6.9 feet long for the 1 hp unit to 69 feet long for the 0.1 hp unit!

In the space available, the latter length might be attained by means of a coiled tube. Thus, if the coil diameter is 3 feet, the 69 foot length could be attained with 7.3 loops. Although, casting of such a long length of propellant does not present any serious problem, there are numerous problems associated with burning the long, thin grain. Such problems are the support and insulation of the grain, the heat transfer from the tube over the long burning period, and pressure drop in the tube itself. Considerable development time might be required for their solution.

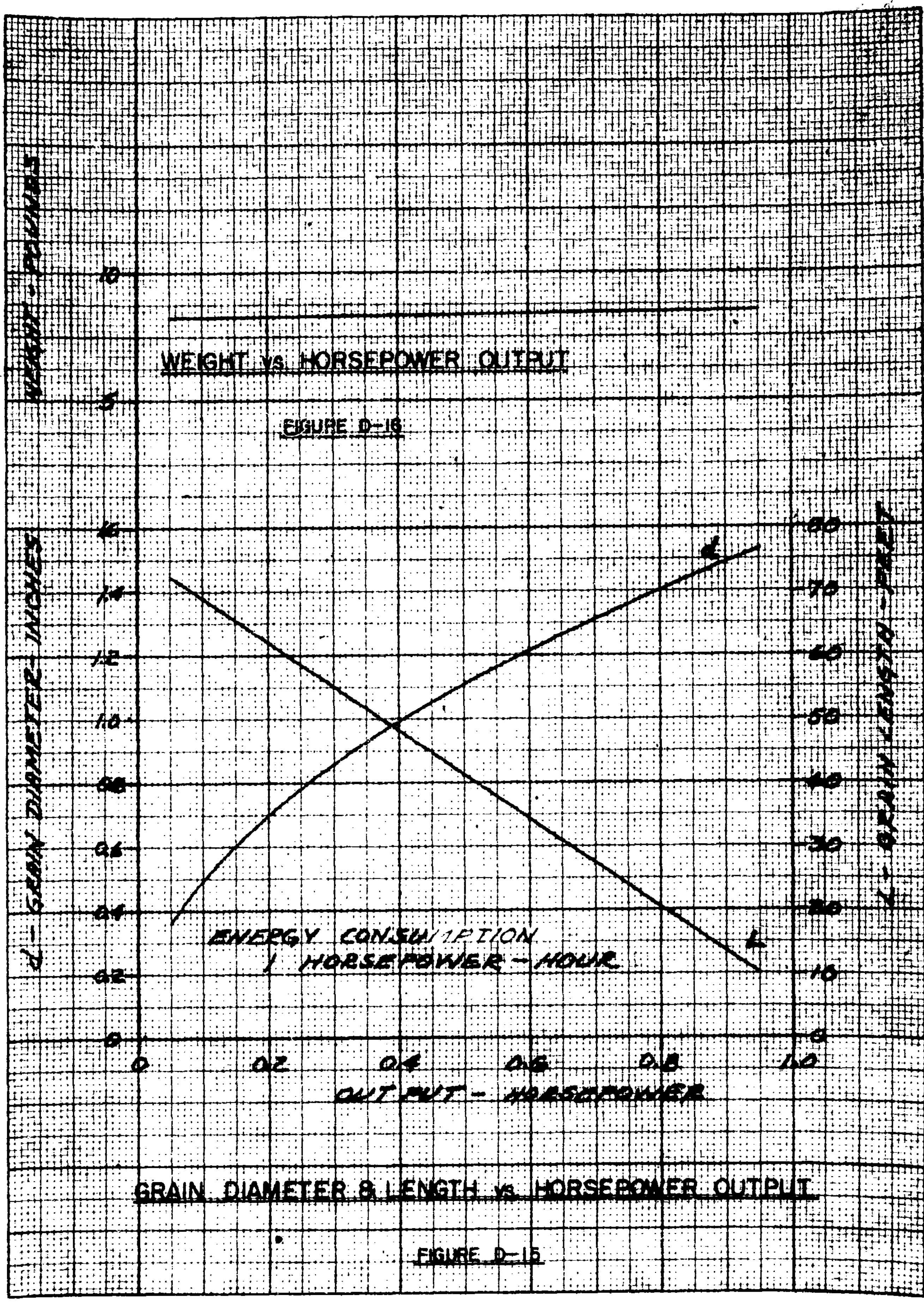

WEIGHT vs. HORSEPOWER OUTPUT

FIGURE D-16

GRAIN DIAMETER & LENGTH vs. HORSEPOWER OUTPUT

FIGURE D-15

Another possible configuration would be banks of short propellant grains which are fired sequentially into a central discharge chamber. This is shown in Figure D-17.

The firing of each grain could be governed by a pressure-actuated device which senses the chamber pressure and fires the grains in a predetermined sequence when the chamber pressure drops to some base level. This system is more complex than that of the usual solid propellant application and requires many individual igniters, a pressure sensor, a firing sequencer, and the added weight of the manifold. Although the sequential firing of solid propellant grains has been accomplished, this arrangement is not an off-the-shelf item and would require development work to ensure reliability.

Where shorter operating times are required as in the 1 hp unit, the fabrication of the gas generator pushes the "state-of-the art" only slightly. Even though the length is only 6.9 feet, it is too much for the space limitations of the package. However, a "folded" grain is possible. This configuration is shown in Figure D-18. By proper use of inhibiter and baffling, this allows the grain to burn "down" one half and "up" the other, thus, effectively doubling its length.

With such an arrangement, the overall length of the grain need only be a little more than 3 feet.

2.2 Pressure Vessel

In any system which employs a solid propellant, the casing which holds the propellant stick must also be a pressure vessel. It must be capable of withstanding the pressures and temperatures resulting from the combustion process, and also rigid enough to withstand rough handling and high acceleration forces.

Since the pressure at which the hot gases are to be supplied is a moderate 200 psia, the wall thickness required from stress considerations is small. Therefore, the primary criterion upon which the wall thickness is based is one of rigidity. This depends upon such factors as the wall thickness required to withstand denting resulting from rough handling, and the size and shape of the propellant grain, e.g., coil, bank, or folded stick. Thus wall thicknesses are based upon

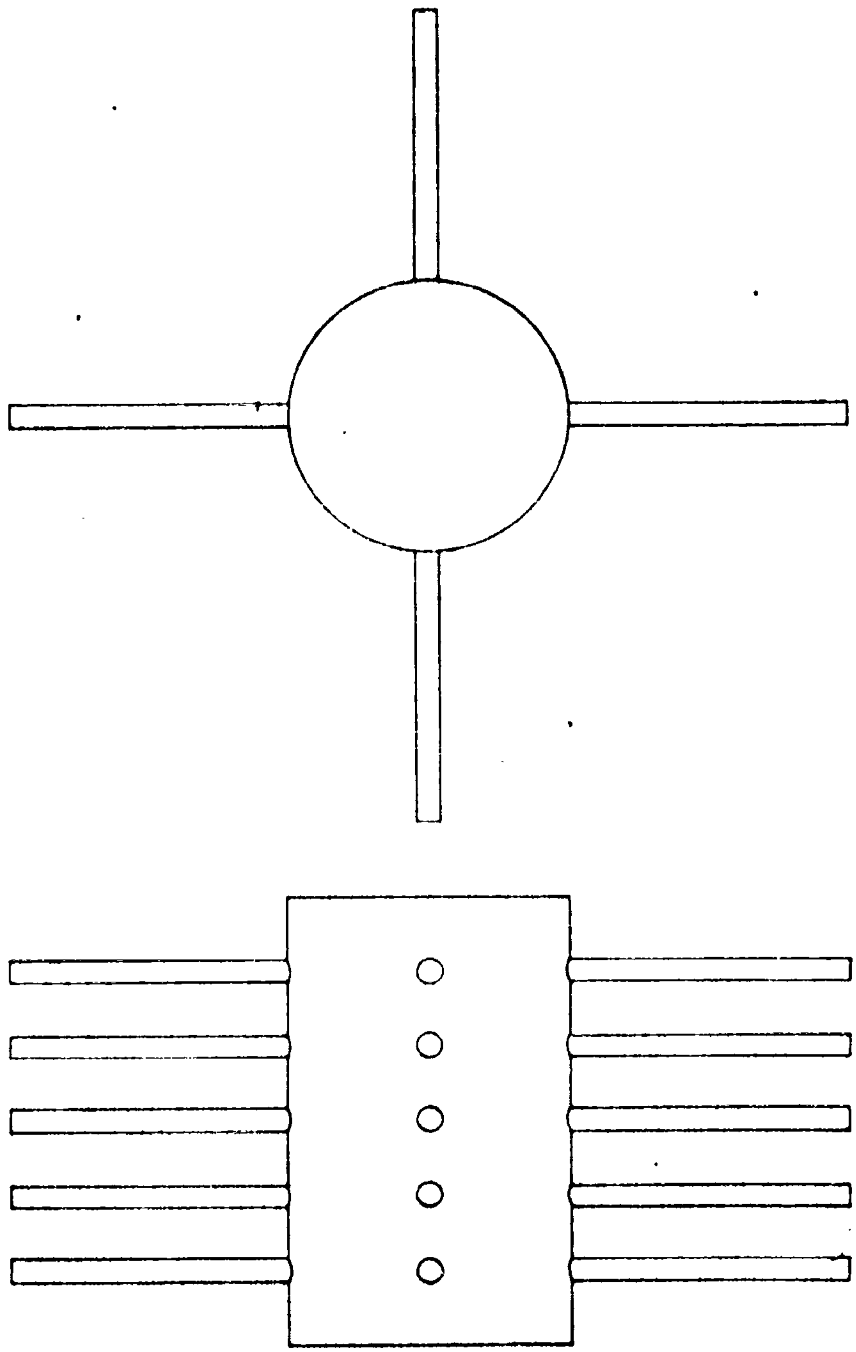

BANK CONFIGURATION OF GRAIN

FIGURE D-17

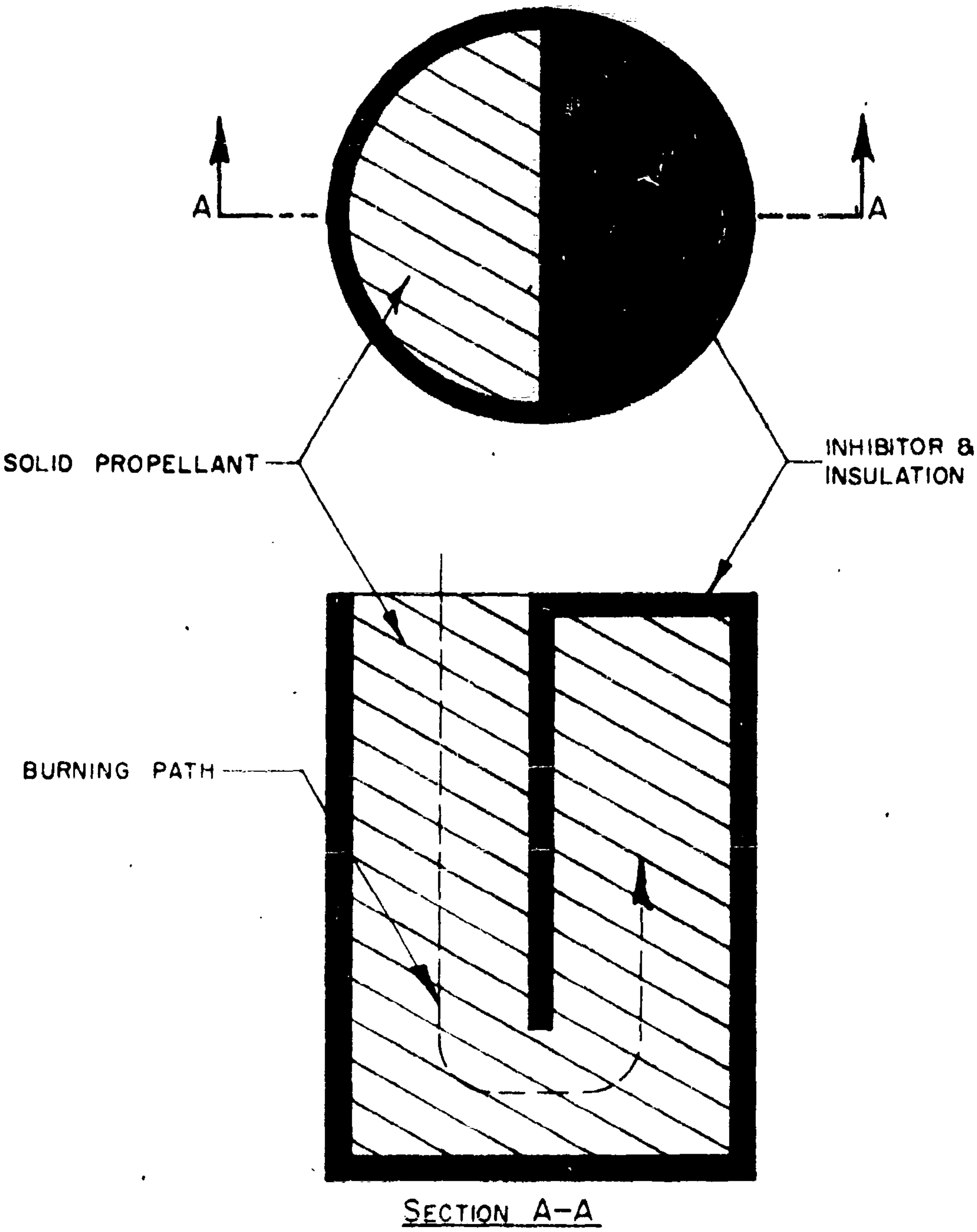

"FOLDED" PROPELLANT GRAIN

FIGURE D-18

design judgement, making no attempt to justify the selection analytically. In the range of propellant grain diameters from 0.4" to 1.5", the following schedule has been used for the pressure vessel wall thicknesses.

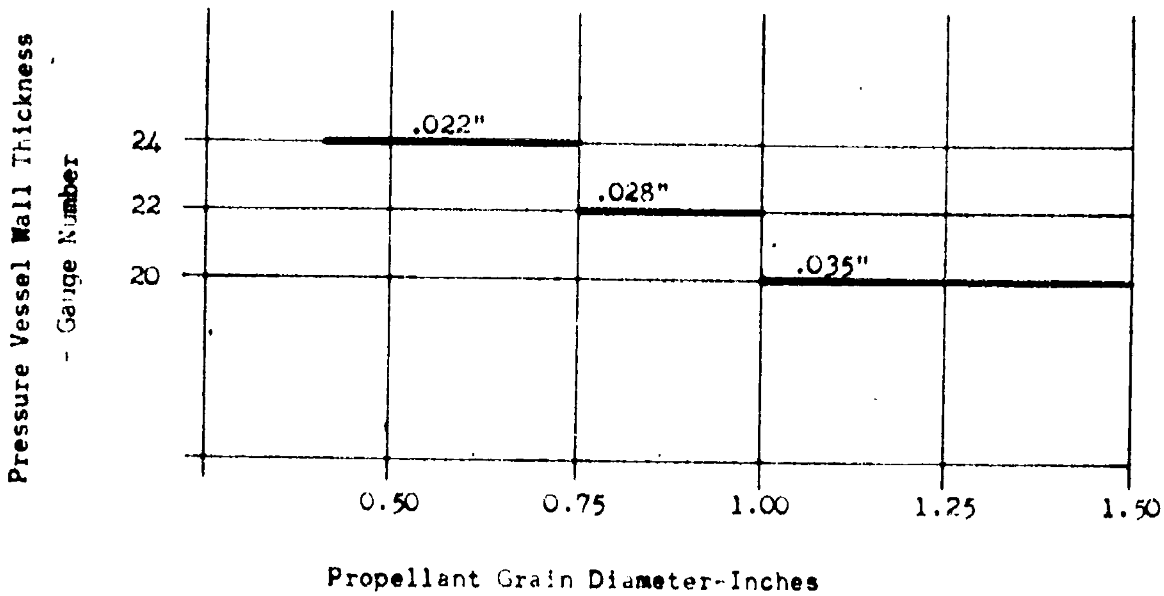

Pressure Vessel Wall Thickness

Figure D-19

In estimating the weight of the pressure vessel, only a single cylinder with ellipsoidal heads will be considered. This would be a reasonable approximation for any one of the grain configurations previously discussed.

The ellipsoidal ends are to have the same thickness as the cylinder for ease of fabrication. To maintain equal stress levels in both the ends and the cylinder, the minor axis of each end is made equal to one-half the major axis.

Adequate space must be allowed between the walls of the pressure vessel and the powder grain for supports at the ends of the grain; for the inhibiter and insulation around the periphery of the grain; and for the squib and igniter at the starting end of the grain. The

The arrangement is shown in Figure D-20. The exact space allocated to each item is problematical, since it will depend upon the shape of the grain, running time, shock loads, etc.

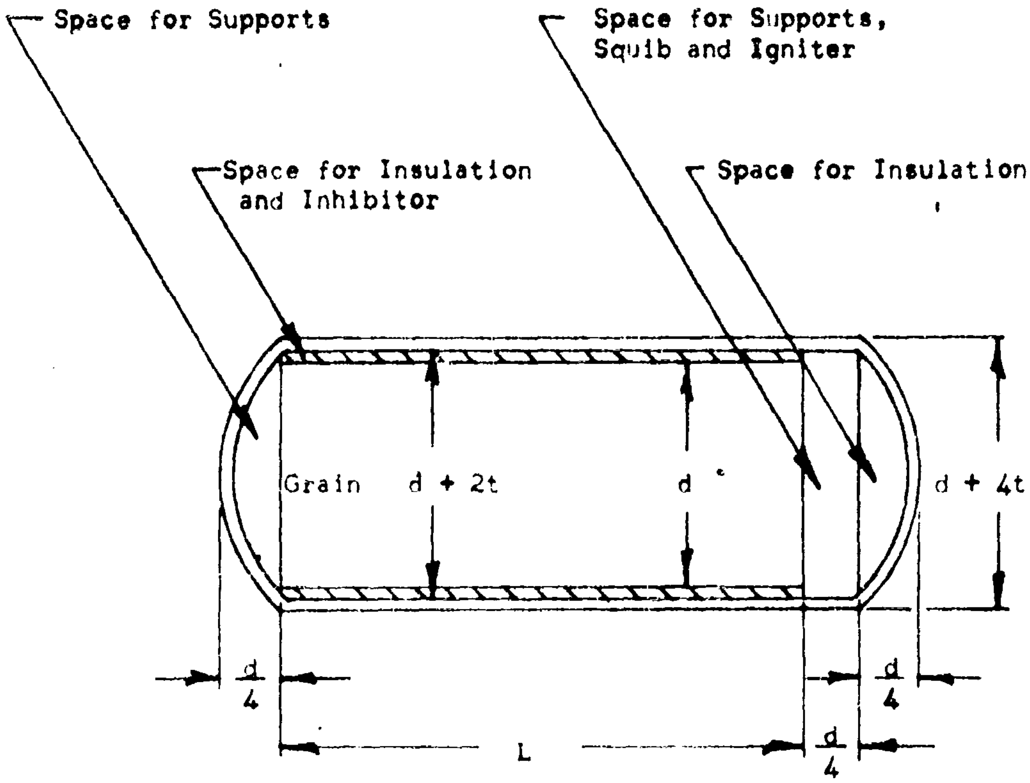

Pressure Vessel

Figure D-20

The insulation thickness is assumed to be equal to the wall thickness and to have a density one tenth that of steel.

The squib, igniter, and holding devices are assumed to have the weight of one of the ellipsoidal ends. This is optimistic since for small diameter grains, there is probably some minimum weight for these items. In addition, where multiple grains are to be used each grain will require its own squib and igniter plus means for sequence firing.

The total weight of the pressure vessel may now be found as follows:

Since the wall thickness is small compared with the other dimensions of the casing, the weight of the unit may be found by

multiplying its surface area by the wall thickness, t, and the density of steel, ρ_s.

The surface area of one end is found to be approximately

$$A_e = (d + 3t)^2 \qquad \text{(D-32)}$$

and that of the cylindrical section is

$$A_c = \pi (d + 3t) (L + \frac{d}{4}) \qquad \text{(D-33)}$$

Tabulating the weights for each component gives

Cylindrical Section $= \pi \rho_s t (d + 3t) (L + \frac{d}{4})$
Ellipsoidal Ends $= 2\rho_s t (d + st)^2$
Squib, Igniter and
Holding Devices $= \rho_s t (d + st)^2$
Insulation (approximately) = 10% of above

The above items are combined algebraically and simplified, to give,

$$W_c = 0.97 t (d + 3t) (L + 1.20 d + 2.85 t) \qquad \text{(D-34)}$$

where t is obtained from Figure D-19; L and d from Figure D-15.

The results of this computation are shown in Figure D-21 as a function of turbine output power for a total energy dissipation of 1 hp-hr. This plot indicates that the weight of the pressure vessel peaks at an output of about 0.4 hp. This is due to the fact that even though the lower power units are much longer, the wall thickness is less. The steps in the curve correspond to the steps in the increments of wall thickness previously selected. However, the weights for these low powers are optimistic in that they do not include the weights of other squibs, igniters, sequencer and controls which might be needed for a banked configuration; or the weights of extra insulation and holding devices needed for a coil configuration.

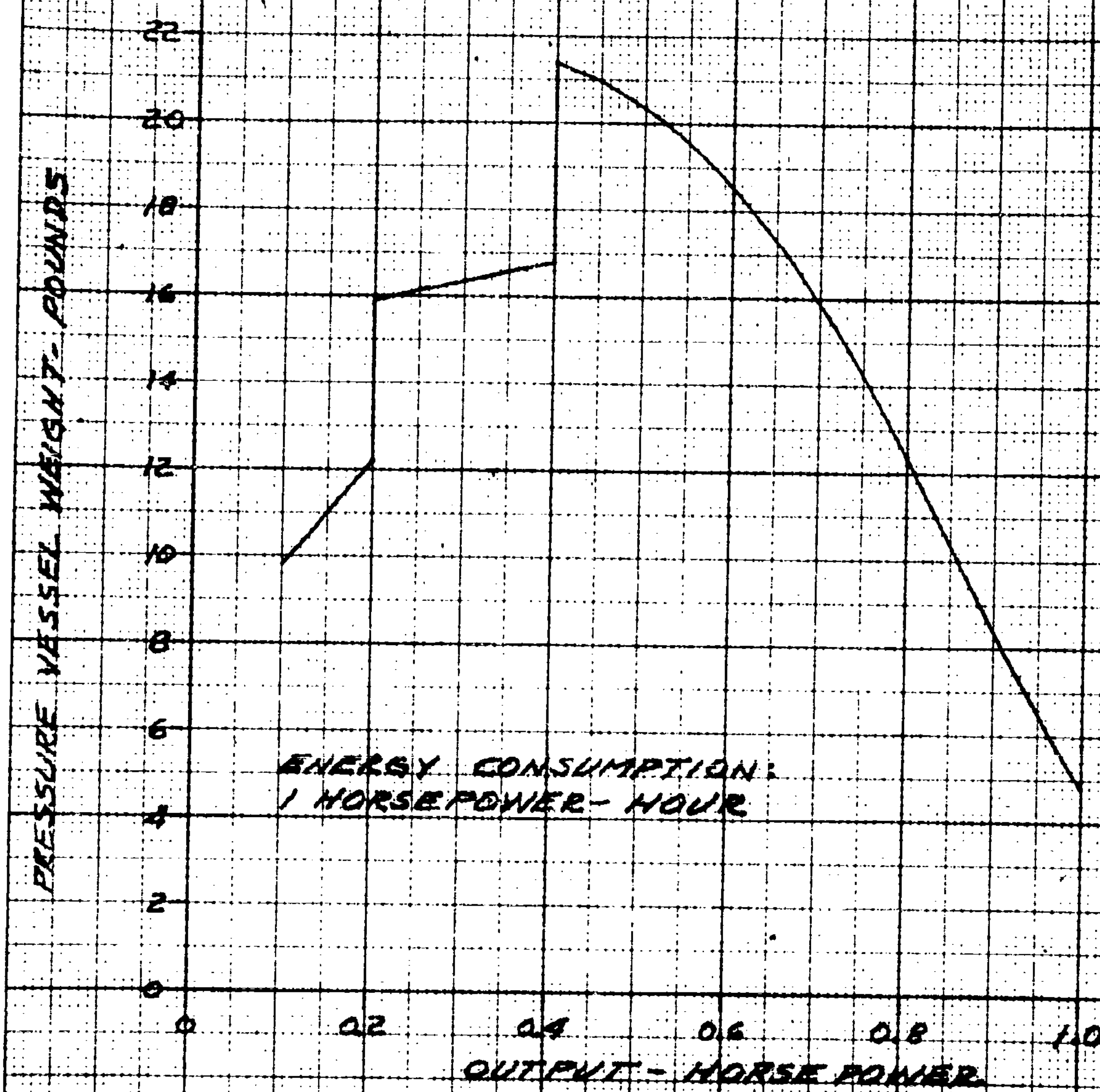

PRESSURE VESSEL WEIGHT vs. POWER OUTPUT

FIGURE D-21

3. Compressed Gas System

Another method of supplying gas to the turbine is by means of a compressed gas system. This system consists of a pressure vessel, propellant charge, and pressure regulator. The propellant charge is burned in a fraction of the running time of the drill bit and the gases generated are stored at high pressure in the pressure vessel.

The limiting condition for this system is the weight of the pressure vessel. If it is arbitrarily set at a maximum of 20 lbs, the maximum size of spherical pressure vessel that can be used for gas storage at 3000 psi can be computed.

The weight of a spherical vessel is given by

$$W = \rho_s V \tag{D-35}$$

where

V = volume of material in shell, in^3

If its wall thickness is small compared with its diameter, Equation (D-35) can be simplified to

$$W = \rho_s 4 \pi R^2 t \tag{D-36}$$

where

R = radius of sphere, inches

t = wall thickness, inches

The wall thickness, t, is determined by the container pressure, P_1, and the sphere radius. Thus,

$$t = \frac{P_1 R}{2\sigma} \tag{D-37}$$

where

σ = allowable stress in the shell material, psi.

Combining Equations (D-36) and (D-37) yields

$$W = 2\pi \rho_s \frac{R^3 P_1}{\sigma} \tag{D-38}$$

and, solving for the radius

$$r = \sqrt[3]{\frac{W}{2 \pi \rho_s P_i}} \qquad \text{(D-39)}$$

If the allowable stress of the shell material is 120,000 psi, container pressure is 3000 psi, and the maximum weight is 20 pounds, Equation (D-39) gives a maximum sphere radius of 7.7 inches.

The volume of such a vessel is

$$V = \frac{4}{3} \pi R^3 = 1910 \text{ cubic inches}$$

and the mass of gas that can be contained in such a volume (assuming the gas is the result of burning a propellant similar to OMAX 448A at a temperature of 1950°F) is

$$W = \frac{P_i V}{R T} = 2.46 \text{ lbs}$$

But from Section II, the 1 hp gas turbine would require a gas flow rate of 2.37×10^{-3} lb/sec. Thus, for 1 hp-hr total energy dissipation, the sphere can store only a small fraction of the total gas requirement. In addition, this system needs a larger mass of gas than is used by the turbine to make up for the loss in internal energy associated with the process by which the gas in the vessel forces some of itself out through an orifice or valve.

4. Liquid Monopropellant Gas Generator System

4.1 General Arrangement

As shown in previous sections, although the design of partial admission turbines for this application is straightfoward, the design of the solid propellant grain and its pressure vessel presents some serious development problems due to the long operating times required. Use of a liquid monopropellant eliminates many of these difficulties.

The gas generator for a liquid monopropellant system is shown schematically in Figure D-22. A fuel control valve senses pressure in the decomposition chamber and adjusts the flow of fuel to maintain that pressure. The fuel is stored in a chamber having one end closed by a differential area piston. This arrangement permits the gas generator to maintain "bootstrap" operation, once gas generation has started. A high pressure nitrogen cartridge provides initial pressurization for starting.

4.2 Calculation of Weight of Gas Generator and Fuel Storage Container

A typical liquid monopropellant is hydrazine, which will be used for the purposes of calculation.

For a total energy usage of 1 hp-hr, the mass of gases required is approximately 8.5 pounds. Since there is a one-to-one correspondence between the weight of the gases and the weight of liquid propellant, an equal mass of liquid must be stored in the container.

The density of hydrazine is approximately that of water, hence

$$\rho_H = 0.0365 \text{ lb/in}^3$$

Therefore, the volume of liquid to be stored is

$$V_i = \frac{8.5 \text{ lb}}{.0365 \text{ lb/in}^3} = 233 \text{ in}^3$$

The weight of the storage container, W_c, can be calculated from the geometric relationships and from strength considerations. Designate the gas end of the container by the subscript "g" and the fuel end by the subscript "L". Assume that there is a 50 psi pressure differential between the ends for bootstrap operation. Then since the force on the piston faces must be the same

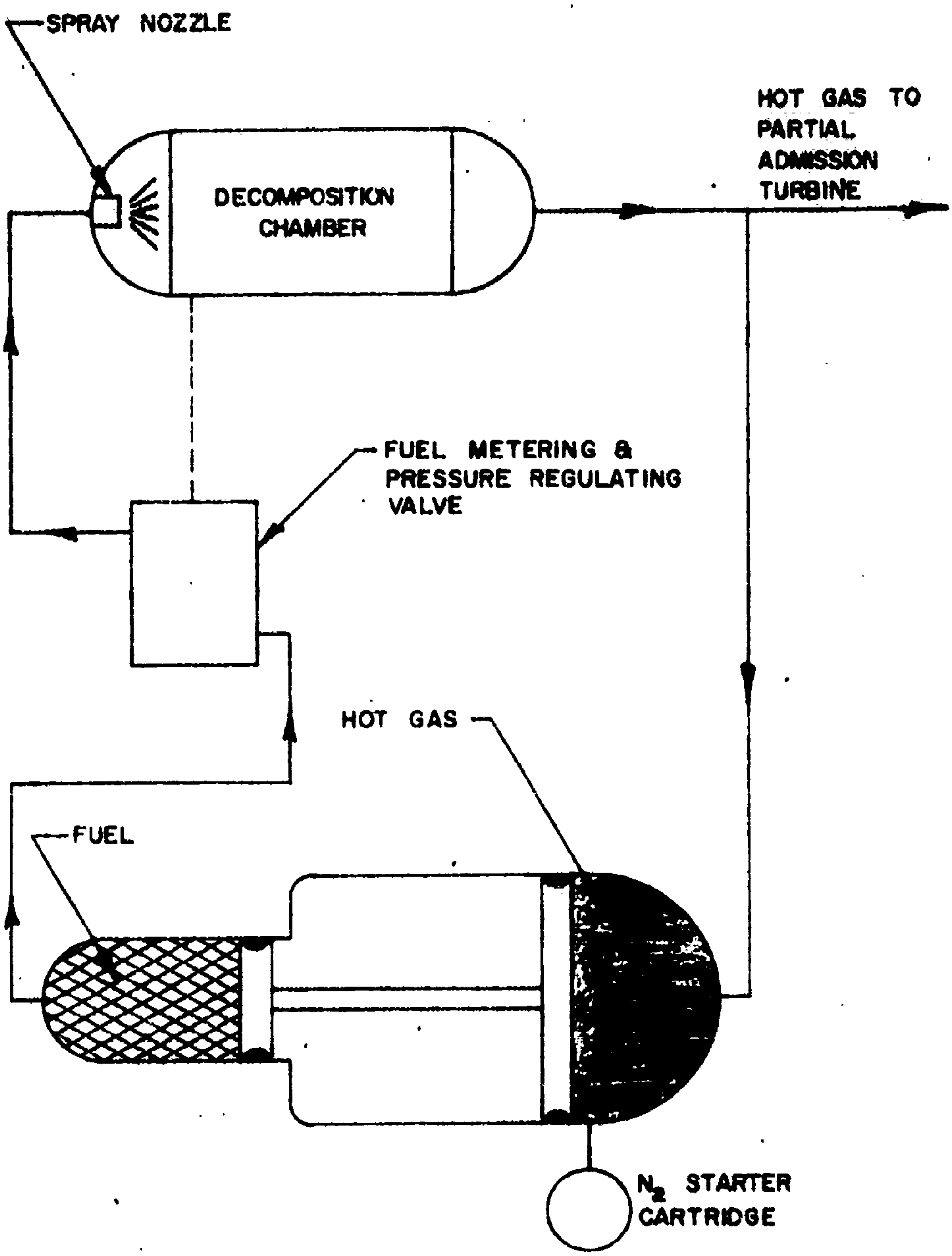

SCHEMATIC OF LIQUID MONOPROPELLANT HOT GAS GENERATOR

FIGURE D-22

$$A_L P_L = A_g P_g \tag{D-40}$$

Thus,

$$\frac{A_g}{A_L} = \frac{P_L}{P_g} = \frac{250 \text{ psia}}{200 \text{ psia}} = 1.25$$

and the ratio of diameters,

$$\frac{d_g}{d_L} = \sqrt{1.25} = 1.12 \tag{D-41}$$

The weight of the container on the liquid side is given by the sum of the weights of the cylindrical section and ellipsoidal end. In order for the stress in the end to be about the same as that in the cylindrical portion, the ellipsoid has its minor axis equal to one-half its major axis and the stress is given by

$$= 1.128 \frac{P_L d_L}{2 t} \tag{D-42}$$

Assuming an allowable stress to be 120,000 psi, and a liquid pressure of 250 psi,

$$t = .00118 \, d_L \tag{D-43}$$

For a 6" diameter cylinder, the required wall thickness is only .0071". This is too thin for sufficient rigidity of the container, so a wall thickness of 0.035 inches (number 20 gauge) will arbitrarily be selected.

In addition the piston stroke, L, must be the same on both ends. Since the thickness is small compared with the other dimensions, the shell volume can be found by multiplying the surface area at a mean radius by the wall thickness. Thus, the weights of the various components are:

Cylindrical Section (liquid end) = $\rho_s \pi (d_L + 3\,t)\, L \times t$

Ellipsoid (liquid end) = $\rho_s (d_L + t)^2 \times t$

Cylindrical Section (gas end) = $\rho_s \pi (d_g + t)\, L \times t$

Ellipsoid (gas end) = $\rho_s (d_g + t)^2 \times t$

Summing these components algebraically and making the appropriate substitution of Equation (D-41) yields for the weight of the container

$$W_c = \rho_s\, t \left[2.12\, \pi\, d_L\, L + 2\pi\, L\, t + 2.25\, d_L^2 + 4.24\, d_L\, t + 2t^2 \right] \qquad \text{(D-44)}$$

The length of the stroke L is related to the volume of fuel, V, which must be supplied by

$$V_L = A_L \quad L$$

or

$$L = \frac{V_L}{A_L} = \frac{932}{\pi d_L^2} \qquad \text{(D-45)}$$

Substitution of this relationship into Equation (D-44) yields

$$W_c = \rho_s\, t \left[\frac{1975}{d_L} + \frac{932}{d_L^2} + 2.25\, d_L^2 + 4.24\, d_L\, t + 2t^2 \right] \qquad \text{(D-46)}$$

For steel of $\rho_s = 0.28$ lb/in^3; and for a wall thickness of 0.035 inches

$$W_c = .0098 \left[\frac{1975}{d_L} + \frac{32.6}{d_L^2} + 2.25\, d_L^2 + .1485\, d_L + .00245 \right] \qquad \text{(D-47)}$$

In order for this size of container to have a reasonable shape, d_L should be about 6". Then

$$W_c = 4.03 \text{ lbs}$$

This excludes the weight of the pistons, the decomposition chamber, and the regulating valve. The weight of these components will certainly be less than that of the pressure vessel. Thus, this gas generator would weigh no more than about 8 pounds and so appears attractive from a

weight standpoint.

4.3 Discussion of the Liquid Monopropellant System

Probably the greatest single problem with the liquid monopropellant system is encountered in the fuel metering and pressure regulating valve where the orifice sizes become very small at the flow rates required for the range of turbine sizes from 0.1 to 1.0hp.

As an example, the orifice size required at each end of this horsepower range will be determined.

The flow through an orifice can be expressed as

$$w = CA \sqrt{2\ g\ \rho_H \triangle P} \qquad \text{(D-48)}$$

where

w = weight flow rate, lbs/sec

C = orifice coefficient, assumed to be equal to 1.0

ρ_H = liquid density, lbs/in^3

$\triangle P$ = pressure drop across orifice, psi

A = orifice area, in^2

The pressure drop across the metering orifice is limited to 20 psi. Then solving for the metering orifice area, yields

$$A = \frac{w}{C\ \sqrt{2g\ \rho\ \triangle P}} \qquad \text{(D-49)}$$

In Section II of this Appendix, the flow rates for the 0.1 hp and 1.0 hp turbines were calculated at about 2.3×10^{-4} and 2.3×10^{-3} lb/sec, respectively. Substitution of these values into Equation (D-49) yields for the metering orifice areas

$$A_{0.1\ hp} = 9.7 \times 10^{-6}\ in^2$$

$$A_{1.0\ hp} = 9.7 \times 10^{-5}\ in^2$$

and the corresponding diameters

$$d_{0.1\ hp} = .00352\ in$$

$$d_{1.0\ hp} = .0111\ in$$

These are extremely small orifices and only the larger appears to be feasible for good flow regulation.

5. Conclusions

This section has shown that there are many difficulties and development problems which must be surmounted before a gas generator for a partial admission turbine can be designed.

It appears that the use of a solid propellant grain is feasible only for a short run (about 1 hour). Longer operating time presents problems in weight as well as design of the propellant stick and its pressure vessel.

Use of a compressed gas appears to offer no advantage over the solid propellant grain since the weight of pressure vessel required to hold the mass of gas needed for this application becomes prohibitive.

The use of a liquid propellant appears to offer the best solution from the standpoint of shape and weight. However, it too presents some difficulty in providing proper regulation at the low flow rates at which these systems must operate.

Thus, if the partial admission turbine is to be used as a source of rotating power, the use of a liquid propellant seems to offer the minimum weight and most conveniently shaped package for the gas generator.

Nomenclature

Gas Generator

A	Orifice area	in^2
A_c	Surface area of cylindrical section of pressure vessel	in^2
A_e	Surface area of end of pressure vessel	in^2
A_g	Area of piston in gas end of storage container	in^2
A_L	Area of piston in liquid end of storage container	in^2
C	Flow coefficient	-
d	Propellant grain diameter	in
d_g	Diameter of piston in gas end of storage container	in
d_L	Diameter of piston in liquid end of storage container	in
g_c	Proportionality constant	$\frac{lb_m}{lb_F}\ \frac{ft}{sec^2}$
k	Specific heat ratio	-
L	Length of propellant grain	in
MW	Molecular weight	lb/mole
P_i	Container pressure	psi
P_g	Pressure in gas end of storage container	psia
P_L	Pressure in liquid end of storage container	psia

R	Gas constant	ft-lb/lb °R
$r_{p_{-200°F}}$	Propellant burning rate at -200°F and pressure, p	in/sec
T	Temperature	°R
T_c	Chamber temperature	°R
t	Burning time	sec
t	Wall thickness	in
V	Volume	in^3
V_L	Liquid volume	in^3
W	Weight	lb
W_c	Weight of container	lb
W_g	Weight of propellant grain	lb
w	Flow rate	lb/sec
ΔP	Pressure drop across orifice	lb/in^2
ρ	Density of solid propellant	lb/in^3
ρ_H	Density of hydrazine	lb/in^3
ρ_s	Density of steel	lb/in^3
σ	Allowable stress	psi

Section IV

Electric Motor System

1. Source of Energy

A third method of providing rotational power to the bit is by means of an electric motor which obtains its energy from some energy storage or conversion device. This may be a storage battery, fuel cell, thermoelectric generator, solar cell, or even a thermonuclear device such as a SNAP-type unit.

For the case at hand, the use of storage batteries is considered as typical of this type of energy source. In addition, batteries require no extensive development work to achieve a lightweight and compact configuration since this has already been achieved in applying them to missiles.

2. Weight Considerations

This section presents the weight of an electric motor system including the motor, storage battery and case, gear box, and necessary accessories. Figure D-23 is a block diagram of such a system.

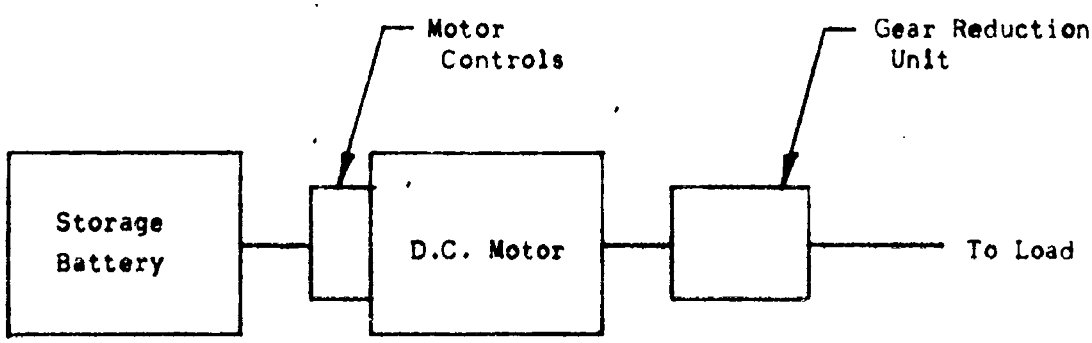

Electric Motor System

Figure D-23

In selecting the proper type of storage battery, weight considerations rule out all but the zinc-silver and mercury batteries. Mercury batteries are sensitive to temperature extremes and would not discharge satisfactorily

at the extreme temperatures which might be encountered on the moon. Silver-zinc batteries, although slightly heavier, are insensitive to variations in ambient temperature and current drain. They are quite rugged and are used extensively in missile applications.

A typical silver-zinc battery will provide 33 watt-hours of energy per pound of unit (including case and connections)*.

Figure D-24 presents the weights of electric motor systems as a function of operating time and at various power levels. It is seen that the weight of the system at zero time includes only the weight of the motor and the gear reduction unit. The system weight at any other time is the sum of this value and the weight of the batteries required to operate at that power level.

3. Conclusion

The system weights predicted here are probably on the conservative side in that they are based on units that were available and in use as of November 1958. No attempt has been made in this estimate to optimize weight or project the "state-of-the art".

* Hamer, W.J. "A Review of the State of the Art and Future Trends in Electrochemical Battery Systems - The More Common Systems". Proceedings of Seminar on Advanced Energy Sources and Conversion Techniques, Pasadena California November 1958. O.T.S P.B. 151461.

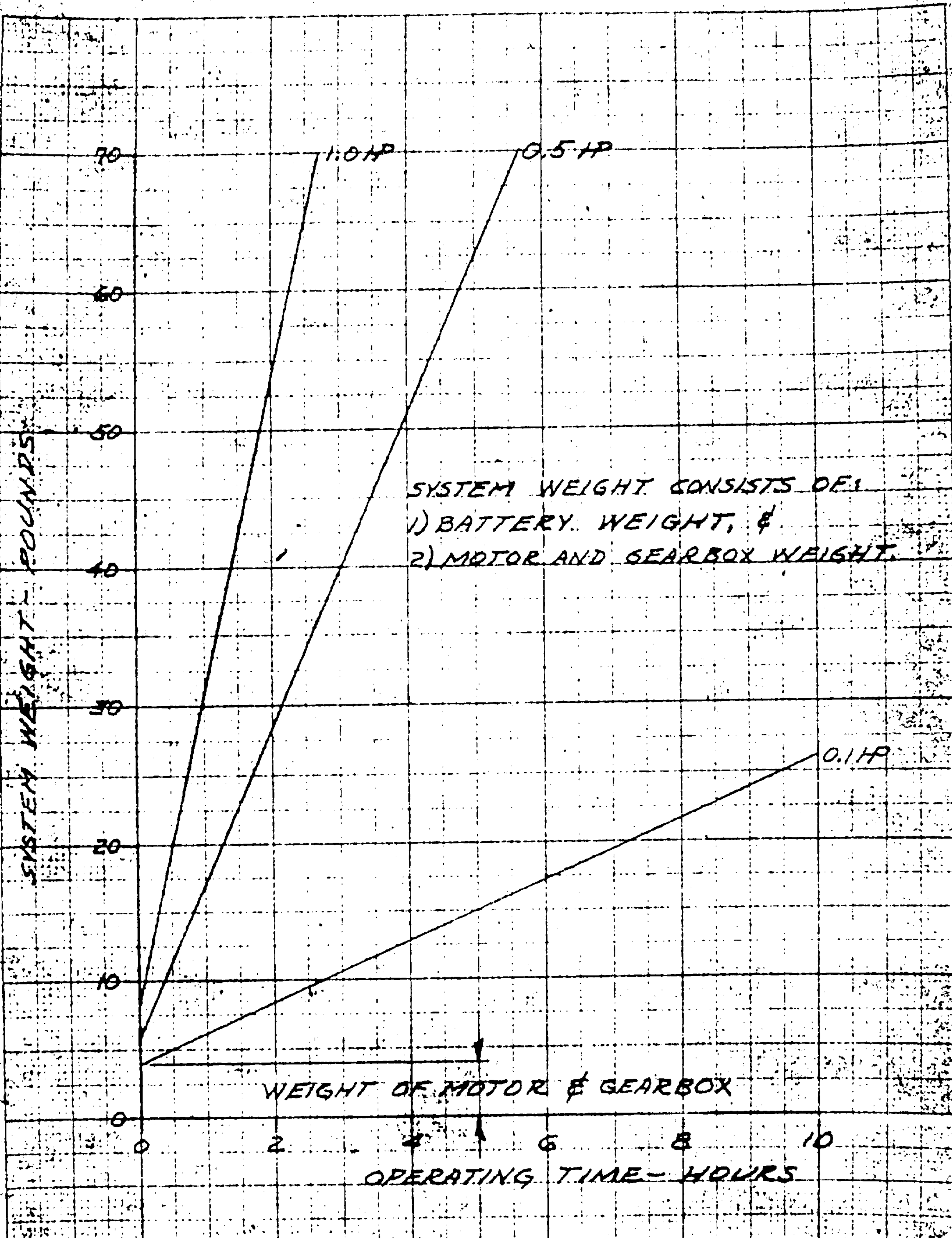

ELECTRIC MOTOR SYSTEM WEIGHT

FIGURE D-24

Appendix E

Performance Characteristics of Diamond Bits

1. Introduction

To determine the feasibility of diamond bit drilling on the moon it is necessary to know, or to be able to predict, its performance characteristics; i.e., how the penetration rate and shaft power requirements vary with the pertinent parameters. These parameters are:

a) Bit load
b) Bit rotary speed
c) Bit configuration, i.e., solid or core bit and type of matrix-diamond structure
d) Bit size
e) Type of rock being drilled
f) Chip scavenging

Another important consideration is bit life; i.e., footage that can be obtained before discard. Bit life is a strong function of chip scavenging and the operating temperature level. The temperature problem was examined in Appendix B where it was concluded that reasonable temperature levels would result with good cleaning and low shaft power operation, say 1/3 hp or less. In Appendix C, gas chip scavenging was examined and found to be feasible.

The Hughes Tool Company ran some laboratory tests to determine the performance of one size of solid and core bits in various rocks using air for chip removal. They investigated the effect of chip scavenging on penetration rate, with other factors held constant, and found that poor cleaning substantially reduced the penetration rate. The range of loads examined was very narrow, but a wide range of rotary speeds was investigated. These results were included as Appendix 2 of "Bi-Weekly Report No. 3" submitted to the Jet Propulsion Laboratory at Caltech on August 26, 1960. Hence, those results will not be repeated here. The pertinent conclusion reached was that the particular type of bit structrue used in the tests was not suitable for drilling the rocks under test because of rapid wear or dulling of the bit. Since there was some question as to whether this was a "soft" or "hard" formation bit, the results do not preclude the possibility of other bit structures being able to do the job. This has to be further examined in the laboratory.

However, even if a bit could be found which had sufficient life, its performance might rule it out as a tool for the moon drilling project.

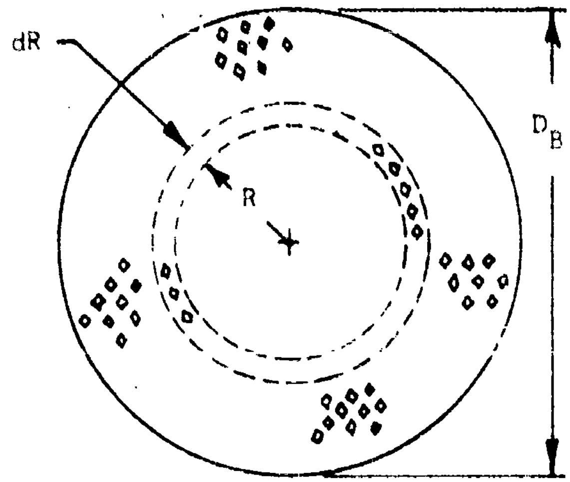

a) Bottom view showing uniform diamond spacing in bit.

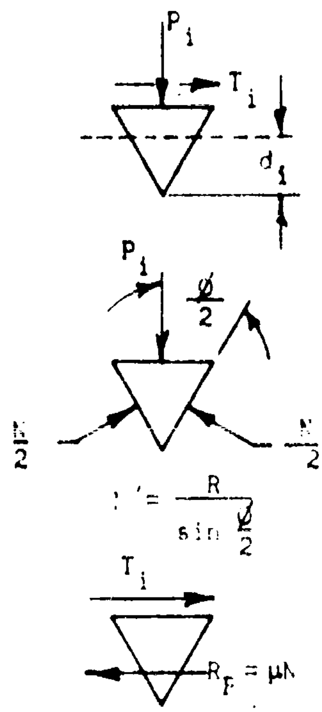

b) Radial view of bit showing forces from drill stem on diamond.

c) Tangental view of bit showing reaction forces from rock on diamond.

d) Radial view of bit showing friction force on diamond.

Schematic Views of Bit and Diamond Forces

Figure E-1

Nevertheless, it was assumed that a suitable tool could be found and the weight and volume of a diamond bit rotary system were investigated.

In order to do this, a knowledge of the performance of diamond bits outside the range investigated by Hughes was needed. To acquire this experimentally would require a prohibitive amount of work; i.e., investigating a range of bit sizes, loads, and rotary speeds in several rocks. What is desired is the functional relationships between these variables so that a limited number of tests with one bit size in various rocks could be used to predict the performance of other sizes over ranges of load and rotary speed. In the following sections, a simplified analysis of diamond bit performance is presented and used to predict bit performance over a range of the operating variables.

2. Analytical Model of the Bit

In order to extrapolate a limited amount of diamond bit data, it is necessary to determine how the penetration rate and rotary power requirements vary with bit load, rotary speed, and diameter. To determine this, the diamond bit drilling process will be approximated by a model having the following characteristics:

a. There is a finite number of diamonds uniformly spaced so that the number per unit area, λ, is constant over the entire surface of the bit. See Figure E-1.

b. The diamonds are conical or pyramidal in shape and the load-deflection relation for each diamond is

$$P_i = \sigma d_i^2 \qquad \text{(E-1)}$$

where

P_i is the load on each diamond

σ is the rock strength number

d_i is the depth of penetration.

c. The tangential force required to push a diamond through the rock is due to friction and to the work required to fracture the rock.

Referring to Figures E-1 (c) and E-1 (d), it is seen that the frictional work is

$$R_F \; Rd\theta = \mu \; NRd\theta = \mu \frac{P_i}{\sin\frac{\phi}{2}} \; Rd\theta = \frac{\mu\sigma d_i^{\,2}}{\sin\frac{\phi}{2}} \quad Rd\theta \qquad \text{(E-2)}$$

where

μ = coefficient of friction

ϕ = angle of diamond point

R_F = frictional force on diamond

N = normal force on diamond

The energy to fracture rock is

$$\gamma \times \text{volume} = \gamma \times \text{area} \times Rd\theta = \gamma \tan\frac{\phi}{2} d_i^{\,2} \; Rd\theta$$

where γ = energy per unit volume required to fracture the rock. Combining these expressions gives

$$T_i = \left(\frac{\mu\sigma}{\sin\frac{\phi}{2}} + \gamma \tan\frac{\phi}{2}\right) d_i^{\,2} = K_F \; d_i^{\,2} \qquad \text{(E-3)}$$

where

T_i = the horizontal force on one diamond

K_F = a constant depending on the type of rock.

From the foregoing model, the penetration rate, P_r, and the shaft power, hp_B, can be derived.

3. <u>Penetration Rate</u>

As a single diamond point at radius R rotates through $d\theta$ degrees, the volume of rock it sweeps out is

$$dV_i = A \; Rd\theta = d_i^{\,2} \tan\frac{\phi}{2} \quad Rd\theta \qquad \text{(E-4)}$$

where

A = projected area of the penetrating diamond point

Since there are $\lambda \, 2\pi RdR$ diamond points in a differential annulus, the volume swept out by all the diamonds in the annulus is:

$$dV = dV_i \quad (\lambda \, 2\pi RdR) = (d_i^{\,2} \tan\frac{\phi}{2}) \; (\lambda \, 2\pi RdR) \; Rd\theta \qquad \text{(E-5)}$$

The average penetration of the differential annulus, d*, is equal to the volume of material removed divided by the annulus area. Thus

$$d^* = \frac{dV}{2\pi RdR} = (\lambda \tan\frac{\phi}{2} d_i^{\,2}) \quad Rd\theta \qquad \text{(E-6)}$$

The penetration per revolution is $(d_R^*)_{d\theta} = 2\pi$

$$d_R^* = \lambda \tan \frac{\phi}{2} \; 2\pi R \; d_i^{\,2} \qquad \text{(E-7)}$$

Substituting from Equation (E-1) and recognizing that the total load on the differential annulus, dP, is $2\pi \, RdR \, \lambda \; P_i$, Equation (E-6) becomes

$$d_R^* = \frac{1}{\sigma} \tan \frac{\phi}{2} \; \frac{dP}{dR} \qquad \text{(E-8)}$$

For a solid bit, d_R^* is constant at all radii, hence

$$d_R^* = \frac{1}{\sigma} \tan \frac{\phi}{2} \; \frac{P}{R} \qquad \text{(E-9)}$$

Thus,

a) <u>For a Solid Bit</u>

$$(d_R^*)_s = K_{PR} \frac{P}{D_B} \qquad \text{(ft/rev)} \qquad \text{(E-10)}$$

$$(P_r)_s = d_R^* \, N = K_{PR} \frac{PN}{D_B} \qquad \text{(ft/hr)} \qquad \text{(E-11)}$$

where K_{PR} = a penetration rate constant for a given rock

P_r = penetration rate

b) <u>For a Core Bit</u> (having a radial cutting dimension $\Delta R = \frac{1}{2} \Delta D_B$, see Figure E-2)

$$(d_R^*)_c = K_{PR} \frac{P}{\Delta D_B} \qquad \text{(ft/rev)} \qquad \text{(E-12)}$$

$$(P_r)_c = d_R^* \, N = K_{PR} \frac{PN}{\Delta D_B} \qquad \text{(ft/hr)} \qquad \text{(E-13)}$$

where

$$K_{PR} = \frac{2}{\sigma} \tan \frac{\phi}{2} \qquad \text{(E-14)}$$

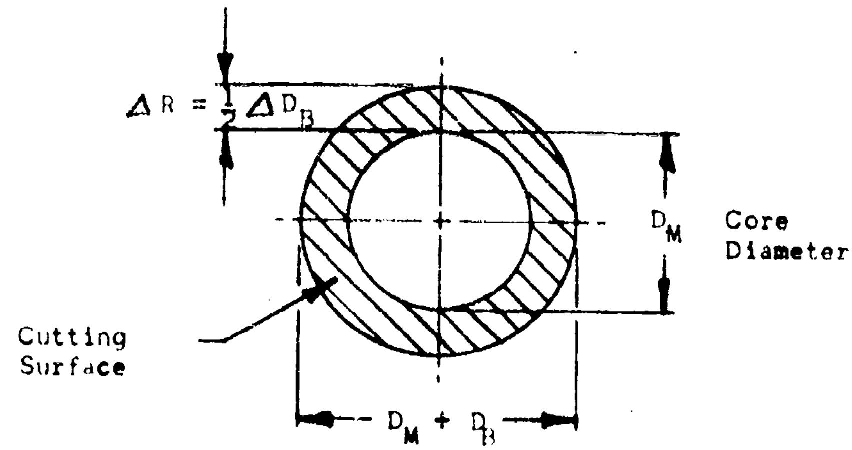

Core Bit Nomenclature

Figure E-2

4. Shaft Power Requirement

The power input to a differential annulus of radius R is

$$d(hp) = T_i \; RN \quad 2\pi \; R \lambda \; dR \tag{E-15}$$

Substituting Equations (E-1), (E-2), (E-7) and (E-8) yields

$$d(hp) = K_F \tan \frac{\phi}{2} \; d_R{*} \;\; N \; RdR \tag{E-16}$$

For a solid bit,

$$(hp)_s = K_F \tan \frac{\phi}{2} \; d_R{*} \;\; \frac{N \; D_B{}^2}{8} \tag{E-17}$$

For a core bit,

$$(hp)_c = K_F \tan \frac{\phi}{2} \; d_R{*} \; N \cdot \frac{D_M \Delta D_B}{4} \tag{E-18}$$

Substituting from Equations (E-10) and (E-12), Equations (E-17) and (E-18) become, respectively

$$(hp)_s = K_{hp}\ P\ N\ D_B \tag{E-19}$$

and

$$(hp)_c = 2\ K_{hp}\ P\ N\ D_M \tag{E-20}$$

where

$$K_{hp} = \frac{1}{8} K_{PR}\ K_F \tan \frac{\phi}{2}$$

D_M = core diameter

ΔD_B = twice the width of the finite cutting annulus

5. Experimental Results

Test data from three sources were used to check the foregoing analyses and to determine the constants K_{PR} and K_{hp} for several rocks. The results are summarized in Table E-1.

5.1 Discussion of Test Data

Since the data used were obtained under a variety of conditions and degrees of accuracy, some comment on their meaning is required.

5.1.1. Hughes Tool Company Data

The Hughes Tool Company obtained drilling performance data on several types of rock (see Table E-I) using two bits manufactured by J.K. Smit and Sons, Inc. of Murray Hill, New Jersey. Both bits were 1 7/8" O.D. (AX size). One was a core type, manufacturer's number FX-99, having D_M = 1 1/4" and ΔD_B = 5/8". The other was a concave-face, full-hole type, manufucturer's number FY-1 having D_B = 1 7/8". Figure E-3 is a photograph of these bits. It is noted that these bits consist of a finite number of uniformly - spaced diamond points set in the surface of a powdered metal matrix material. The points project about 1/32 to 1/16" from the matrix surface which has grooves for the cleaning fluid to pass out to the hole annulus.

The test setup used by Hughes Tool is described in Appendix 2 of

Table E-I

Test Drilling Data for Solid and Core Bits

Rock	Source	Bit Type	K^*_{PR} $\left(\frac{ft}{hr} \cdot \frac{in}{lb\text{-}rpm}\right)$	K^*_{hp}	Remarks
Berea Sandstone	H.T.	Core Bit $D_M = 1\ 1/4"$ $\Delta D_B = 5/8"$	$(90-180) \times 10^{-6}$	-	Bit wore rapidly. Air Cleaning
		Solid Bit $D_B = 1\ 7/8"$	140×10^{-6}	-	Bit wore very rapidly: rate dropped to a small fraction of this after drilling a few inches of hole. Power readings very unreliable because of large loss in packings.
Rush Springs Sandstone	H.T.	Core Bit (Same as above)	5×10^{-6}	-	This bit had already worn appreciably before start of test.
Virginia Limestone	Phillips	Solid Bit $D_B = 6\ 5/8"$	25×10^{-6}	3.8×10^{-6}	Water cooling. Very large load and power operating condition.
		Core Bit $D_M = 4"$ $\Delta D_B = 2\ 5/8"$	30×10^{-6}	3.2×10^{-6}	Water cooling and chip removal.
Rush Springs Sandstone	Phillips	Solid Bit $D_B = 6\ 5/8"$	40×10^{-6}	3.8×10^{-6}	Water cooling and chip removal.
		Core Bit	40×10^{-6}	3.2×10^{-6}	Water cooling and chip removal
Grey Granite	H.T.	Core Bit	4×10^{-6}	-	Bit practically worn out. No appreciable penetration could be made.
	FMA	Core Bit $D_M = 1"$ $\Delta D_M = 3/16"$	1.5×10^{-6}	1×10^{-6}	Limited number of tests. Bit type substantially different from Hughes Tool or Phillips.

					drilling a few inches of hole. Power readings very unreliable because of large loss in packings.
Rush Springs Sandstone	H.T.	Core Bit (Same as above)	5×10^{-6}	-	This bit had already worn appreciably before start of test.
Virginia Limestone	Phillips	Solid Bit $D_B = 6\ 5/8''$	25×10^{-6}	3.8×10^{-6}	Water cooling. Very large load and power operating condition.
		Core Bit $D_M = 4''$ $\Delta D_B = 2\ 5/8''$	30×10^{-6}	3.2×10^{-6}	Water cooling and chip removal.
Rush Springs Sandstone	Phillips	Solid Bit $D_B = 6\ 5/8''$	40×10^{-6}	3.8×10^{-6}	Water cooling and chip removal.
		Core Bit	40×10^{-6}	3.2×10^{-6}	Water cooling and chip removal
Grey Granite	H.T.	Core Bit	4×10^{-6}	-	Bit practically worn out. No appreciable penetration could be made.
	FMA	Core Bit $D_M = 1''$ $\Delta D_M = 3/16''$	1.4×10^{-6}	1×10^{-6}	Limited number of tests. Bit type substantially different from Hughes Tool or Phillips.
	Phillips	Solid Bit $D_B = 6\ 5/8''$	$(5\text{-}10) \times 10^{-6}$	1.4×10^{-6}	Report bit wore very rapidly when drilling grey granite.
		Core Bit	$(2.5\text{-}6) \times 10^{-6}$	1.3×10^{-6}	Same comment as above.

*For solid bit, $(P_r)_s = K_{PR} \dfrac{PN}{D_B}$ and $hp_s = K_{hp}\, PND_B$

For core bit, $(P_r)_c = K_{PR} \dfrac{PN}{\Delta D_B}$ and $hp_c = 2K_{hp}\, PND_M$

Where P = Axial load on bit, lb

N = Shaft speed, rpm

D_B = Diameter of solid bit, in

D_M = I.D. of core bit, in

ΔD_B = Difference between O.D. and I.D. of core bit, in

2

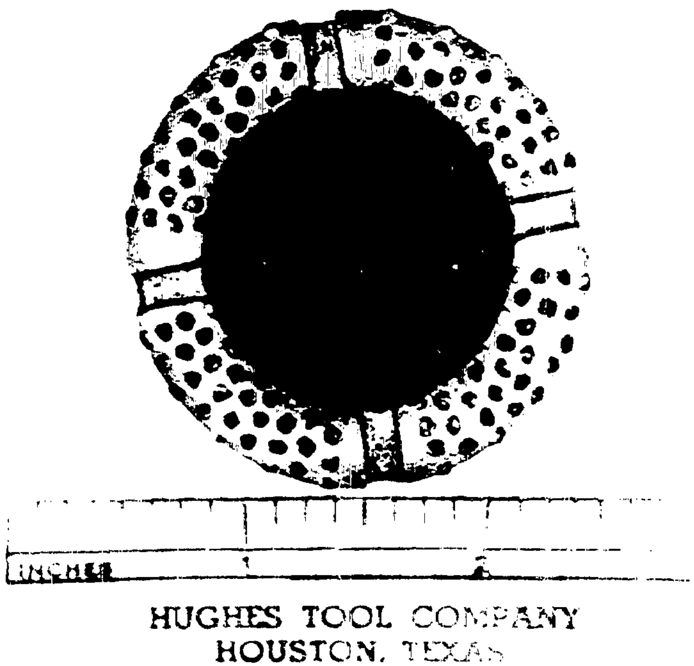

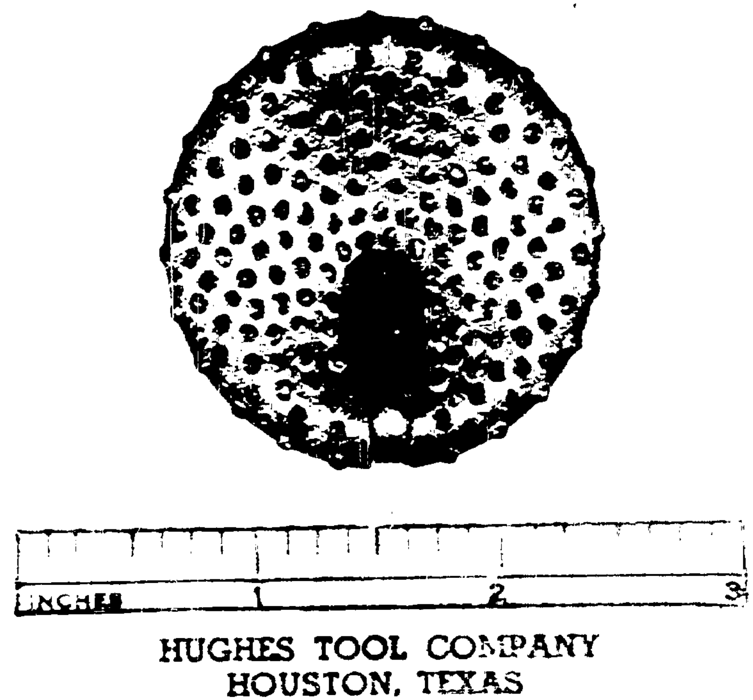

Smit and Sons, Core and Full-hole Type Diamond Bits .

Figure E-3

"Bi-Weekly Report Number 3". That report also presents the test data and results. It should be noted that all the data, for each type of bit, was obtained with the same bit. As the tests progressed, the diamond points dulled badly and many came out of the matrix. Thus, the meaning of these tests is questionable; however, they were used to calculate the drilling constants presented in Table E-I. In all cases, the data for the highest cleaning air flow rate were used. Since the method of obtaining power data gave unreliable results*, values for the power constant, K_{hp}, were not included.

There is some question as to whether these bits were designed for "hard" or "soft" formation drilling. At any rate, they did not stand up well and are considered unsuitable for drilling in the formations tested.

5.2.2. Phillips Petroleum Data

The Phillips Petroleum Company ran extensive laboratory tests, in cooperation with the Hughes Tool Company,** to evaluate the drilling performance of diamond bits in several formations*** (see Table E-I). They used two bits manufactured by the Christensen Diamond Bit Company of Salt Lake City, Utah. Both bits were 6 5/8" O.D. One of these was a core type, manufacturer's number B 12 B, having $D_M \approx 2$ 5/8". The other was a concave-face, full-hole type, manufacturer's type SHF. Figure E-4 is a photograph of these bits. These bits appear similar in construction to those used by Hughes, and described in Section 5.1.1, except that the fluid courses are of a different design.

These tests were run on a full-scale drilling rig at the Hughes Research Laboratory. Measurements of load, rotary speed, penetration rate, and rotary torque were made. The accuracy of these measurements is not known; in the tabulated test data, the same value of rotary torque is reported for a rotary speed range of 60 to 150 rpm at constant axial load. This raises some doubts about the accuracy of the torque values. In calculating the power constant, K_{hp}, for Table E-I, the test values for a rotary speed of 100 rpm were used since it is in the middle of the range.

The following significant differences in operating conditions between

* Since the tests were run on an available high-pressure drilling test stand which had very high power dissipation in the shaft pressure packings, the bit power requirements were a very small fraction of the power required to rotate the drill stem.

** Tests were run by Hughes personnel at Hughes Research Laboratory for Phillips.

*** Phillips Memorandum: Project No. 4 "Application and Performance of Diamond and Chert Bits", by R.S. Hoch, Feb. 23, 1954.

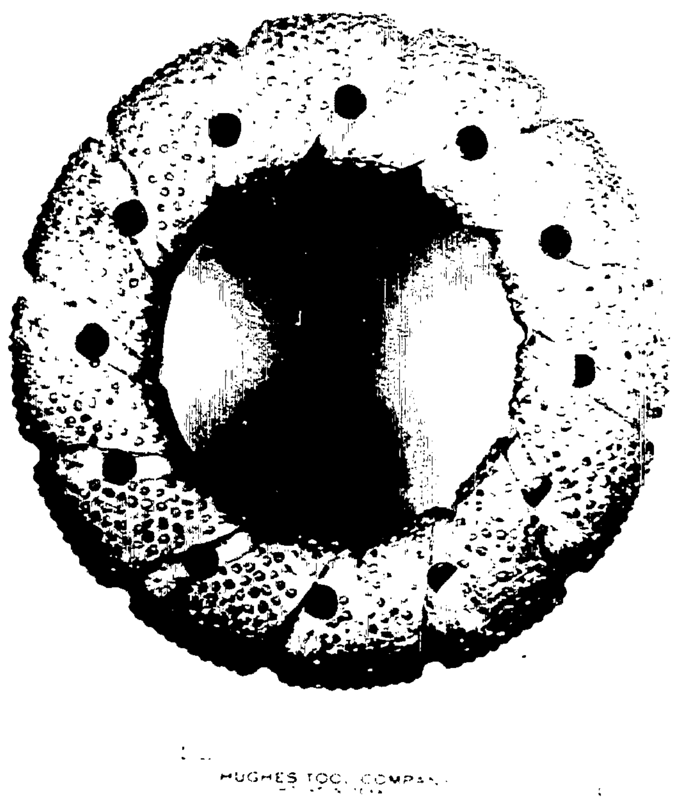

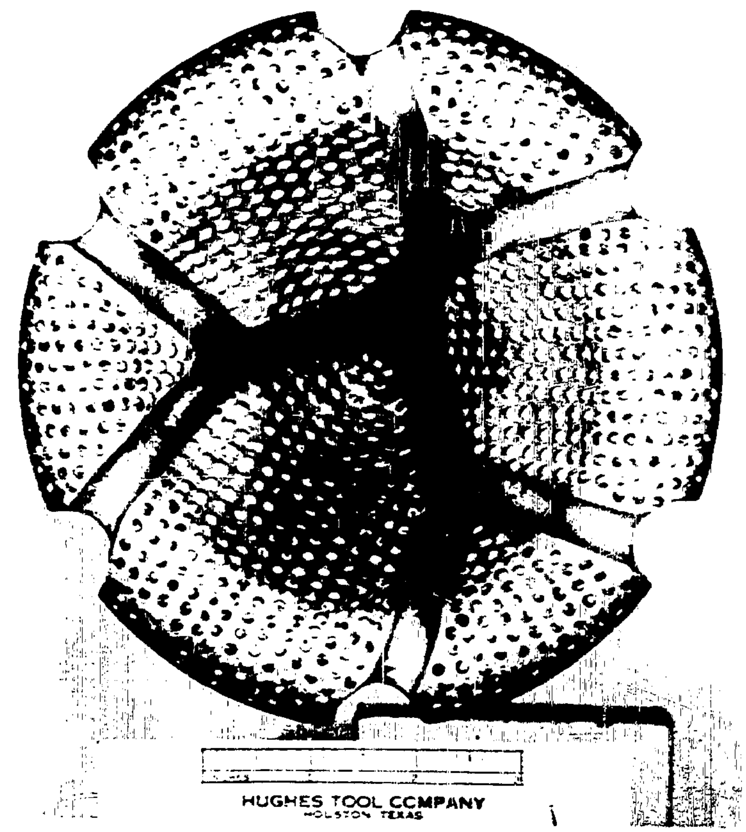

Christensen, Core and Full-hole Type Diamond Bits

Figure E-4

the Phillips and Hughes tests should be noted:

a. Phillips used 6 5/8" bits versus Hughes' 1 7/8".

b. Phillips used water (and "mud") for chip cleaning instead of air.

c. Phillips loaded their bits with several thousand pounds compared to fifty pounds.

d. Phillips ran rotary speeds in the range of 60 to 150 rpm as compared to Hughes' 90 to 1140 rpm.

The Phillips results, because of their extensive nature, are well suited for checking the analytical predictions; e.g., do the values of K_{PR} or K_{hp} determined from solid-bit tests check those determined from core-bit tests. However, Phillips' significantly different operating conditions exclude the use of the values of K_{PR} and K_{hp} based on their data to predict the performance of the moon diamond bit.

5.1.3. Foster-Miller Associates Data

Since the Phillips operating conditions were so different from the anticipated moon drill requirements and no power data was obtained by Hughes, Foster-Miller Associates ran a limited number of tests using a Felker "Di-Met" coring bit having a 1 3/16" O.D., D_M = 1" and ΔD_B = 3/16". This bit is photographed in Figure E-5. It is considerably different from those used by Hughes and Phillips. The Felker bit had a section of diamond-impregnated matrix about 1/4" long which continues to drill until completely worn away. It is similar to abrasive grinding wheel material.

The Foster-Miller tests were run on a rig shown schematically in Figure E-6. The core bit was mounted in a drill press and loaded by hanging a weight on the drill shaft feed arm. The rock to be drilled was mounted on a low-friction rotary platform which in turn was set on a platform scale to permit direct measurement of the bit load. A spring scale hooked on an arm of the rotary platform was used to determine the bit torque. The bit rotary speed was measured with the aid of a Strobotac. High pressure air was supplied for chip cleaning, but no attempt was made to measure the air flow rate. The results of these tests are presented in Table E-II.

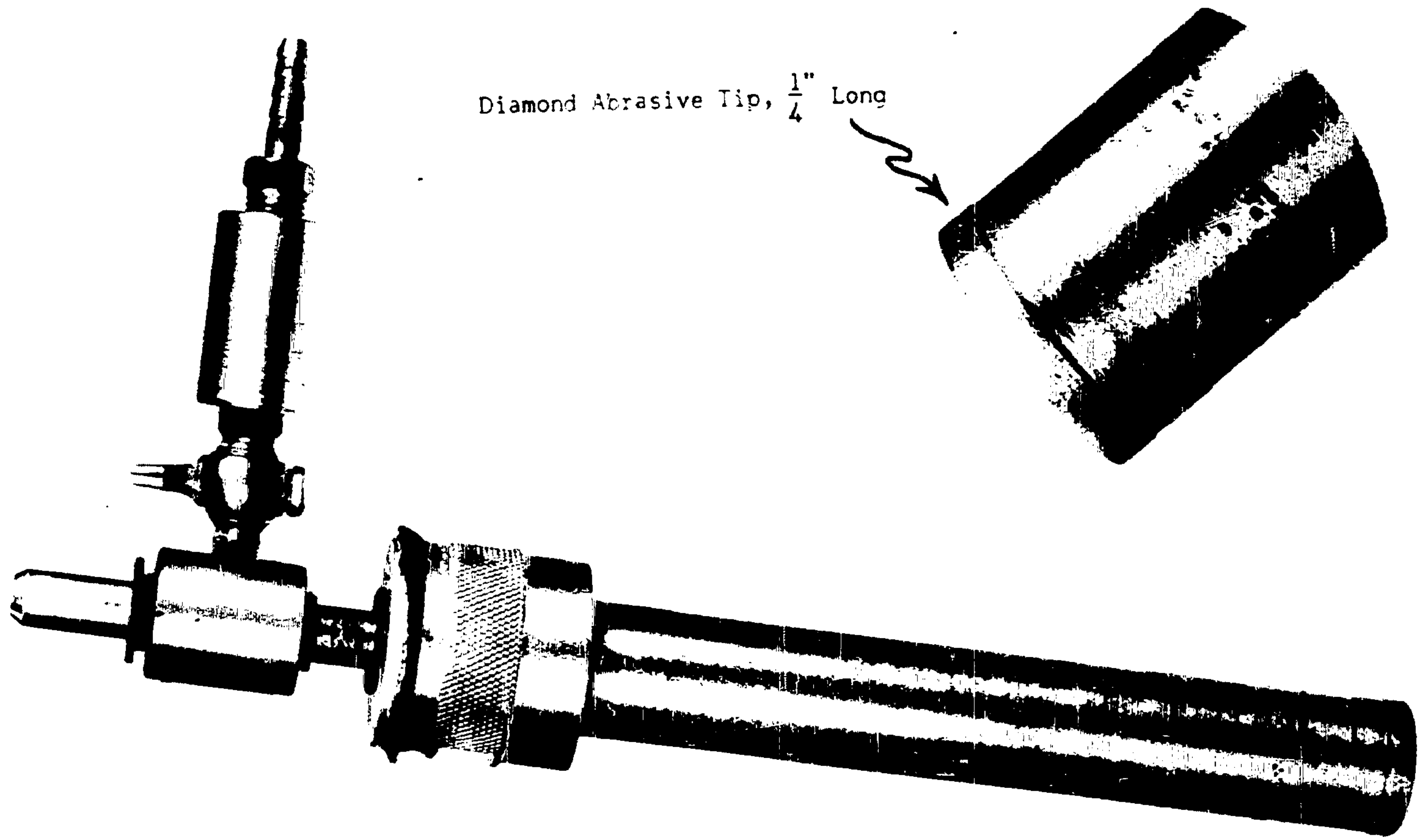

Felker, "Di-Met" Core Type Diamond Bit

Figure E-5

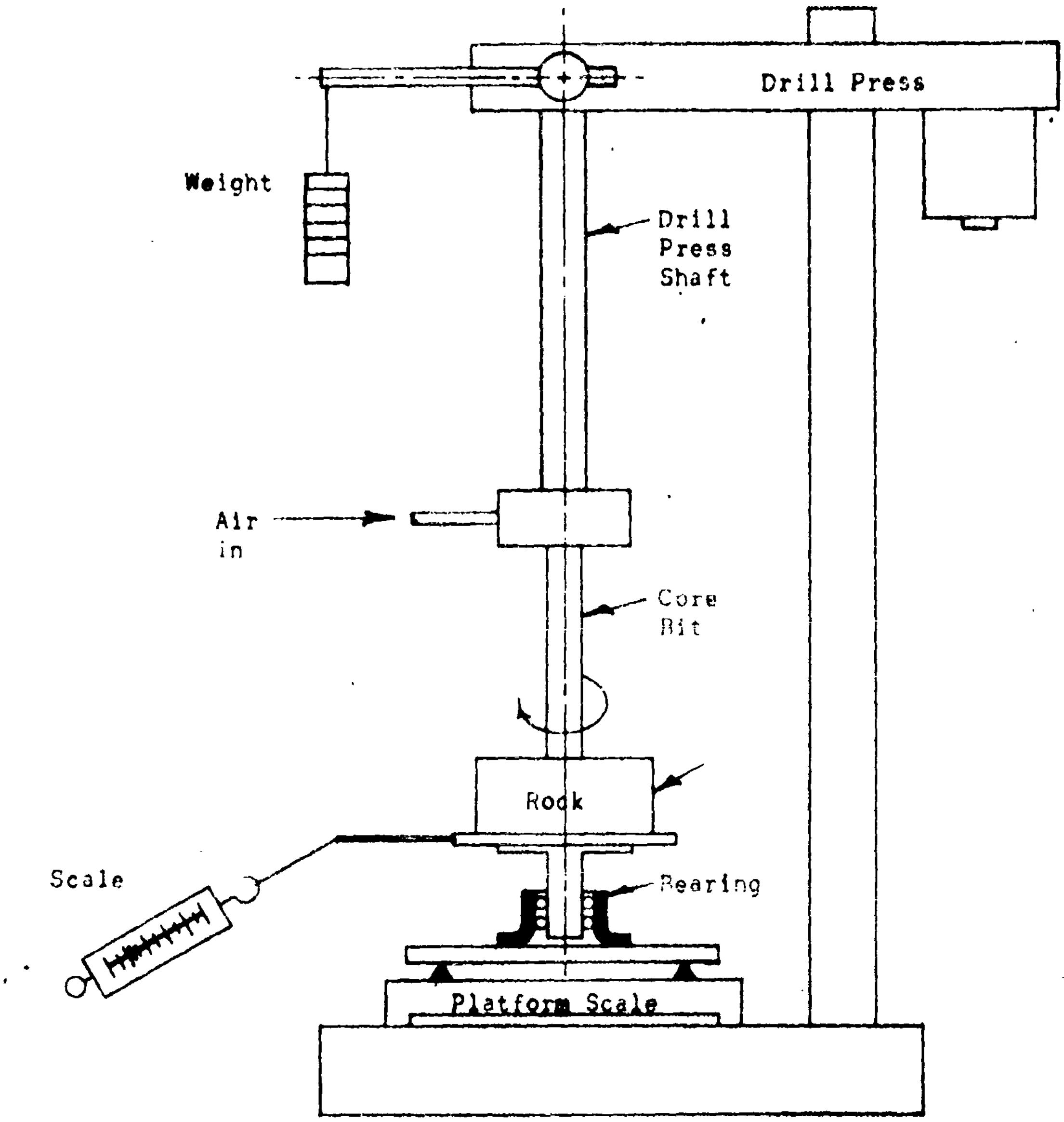

Foster-Miller Associates' Laboratory Drilling Rig

Figure E-6

Table E-II

Results of Foster-Miller Core Bit Tests

Load	Speed	Penetration Rate	Power	Penetration Constant	Power Constant
P	N	P_r *	hp *	K_{PR}	K_{hp}
(lbs)	(rpm)	(ft/hr)	(hp)	$\left(\frac{ft}{hr}\ \frac{in}{lb\ rpm}\right)$	$\left(\frac{hp}{lb\ in\ rpm}\right)$
70	560	0.28	0.055	1.33×10^{-6}	0.7×10^{-6}
70	920	0.62	0.105	1.80×10^{-6}	0.82×10^{-6}
90	560	0.32	0.128	1.20×10^{-6}	1.30×10^{-6}
90	920	0.69	0.164	1.58×10^{-6}	1.00×10^{-6}
			Average	1.5×10^{-6}	1.0×10^{-6}

* Average value of three tests; most values were within 20% of average.

6. Predicted Bit Performance

The Phillips data for Virginia limestone and Rush Springs sandstone (see Table E-I) indicate that the form of the derived drilling equations is probably right since the values of K_{PR} and K_{hp} obtained from data for solid and core bits check so well. Furthermore, the value of K_{hp} obtained from the Phillips data agrees fairly well with that obtained from the Foster-Miller results. However, the value of K_{PR} obtained from the Phillips data is several times larger than the Foster-Miller value. Since the Foster-Miller tests were run under conditions contemplated for moon drilling, their values will be used to estimate the diamond bit performance. Using the average values of the drilling coefficients for grey granite, the following formulae result:

a) Solid Bit (drilling grey granite)

$$(P_r)_s = 1.5 \times 10^{-6} \frac{PN}{D_B} \qquad \text{(ft/hr)} \qquad \text{(E-21)}$$

$$(hp)_s = 1.0 \times 10^{-6} P\,N\,D_B \qquad \text{(hp)} \qquad \text{(E-22)}$$

b) Core Bit (drilling grey granite)

$$(P_r)_c = 1.5 \times 10^{-6} \frac{PN}{\Delta D_B} \qquad \text{(ft/hr)} \qquad \text{(E-23)}$$

$$(hp)_c = 2.0 \times 10^{-6} \; P \; N \; D_M \qquad \text{(hp)} \qquad \text{(E-24)}$$

These results are plotted as Figures 2 through 6 in Section II of the main body of this report.

7. In Conclusion

The analysis presented herein permits extrapolation from a limited number of tests with a diamond bit for a given rock. Actually, if the rock properties σ and μ (strength number and coefficient of friction) were known, the results from one material could be extrapolated to other materials.

Since these formulations have been checked over a rather limited range of operation, extrapolation to very different conditions should be done with caution.

Furthermore, these relationships assume a constant diamond point condition, i.e., no dulling during the run. As the bit dulls, its performance drops. The rate of dulling and its effect on performance must be determined experimentally for each material to be drilled. However, Equations (E-21) through (E-24) should give a reasonable estimate of bit performance on grey granite as long as the bit is sharp; this will be particularly true for the Felker Di-Met type bit.

It is interesting to note that Equation (E-11) and (E-13) indicate that the "equivalent" solid bit for a given core bit (i.e., one which has the same penetration per revolution when loaded the same) has a diameter equal to twice the core bit annulus width. This is illustrated graphically in Figure 2 of the main body of this report.

Appendix F

Percussion Drilling

Section I

Energy Sources

1. Introduction

In this section the energy source requirements for driving a percussion-type moon drill are considered. The assumption is made here that the required energy must be brought to the moon from the earth in stored form; i.e., direct-conversion devices such as solar cells or thermoelectric converters are excluded from consideration. If these latter devices should be admissible, some savings may be possible in the total source weight over the amounts estimated in this section.

Three types of energy sources appear feasible for the moon drill from the standpoints of time of operation required, magnitude of source weight, reliability, and the amount of development required to realize a practical system. These are:

a. A compressed gas
b. A chemical fuel
c. An electro-chemical source

In the compressed gas system, two gases are investigated; a low molecular weight gas, helium, and one with high molecular weight, nitrogen.

In the chemical fuel system, a monopropellant gas generator (hydrazine) is investigated.

The only electro-chemical source considered is a storage battery. Fuel cells are possible sources of electric power, but, from the limited data available, appear to be heavier than batteries for the power levels and time of operation involved in a percussion moon drill.

In Section II of this appendix, it is shown that for the minimum weight percussion drill systems, the source weight is a rather small fraction of the system weight. Thus, an extremely accurate estimate of the source weight is not essential for a reasonable estimate of the drilling system weight.

2. Compressed Gas System

A gas supply system is assumed which consists of stored, high-pressure gas in a spherical tank, and a pressure regulator.

2.1. Gas Requirements

The following assumptions are made regarding the gas-

supply system:

1) The tank is adiabatic; no heat is transfered into the tank during use of the gas. This assumption is conservative since less gas will be required for drilling if heat transfer into the tank occurs.

2) The maximum temperature which the gas in the tank may reach is 200°F, which corresponds to the maximum ambient temperature on the moon.

3) The gas is utilized at a regulated pressure, P_r in a fixed-displacement device.

4) The fluid energy can be related to the energy required to fracture and remove rock.

5) The maximum allowable ratio of final gas temperature to initial gas temperature is 0.75.

Figure F-1 is a schematic diagram of a gas-operated impact system.

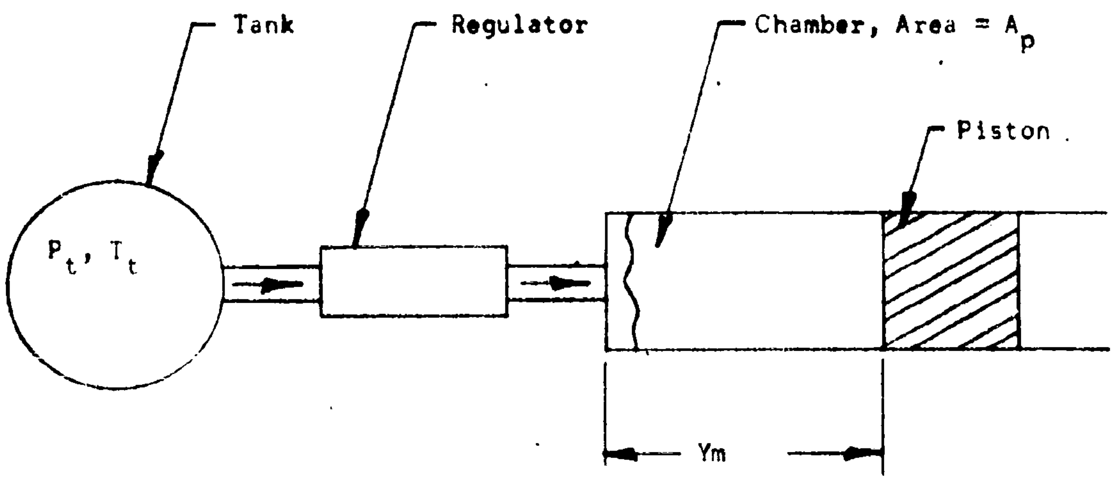

Schematic Diagram of Gas-Actuated Impactor

Figure F-1

In this study, the effects of leakage in the impactor, friction, and losses associated with scavenging the gas chambers and returning the piston in preparation for the next stroke will be lumped into an efficiency. That is, an "effective pressure" P_m, for the impact device is assumed. Exact calculations of this effective pressure cannot be carried out without a detailed design of the impactor which is beyond the scope of this preliminary study.

Let E_o = total energy required to remove the desired volume of rock. For impact drilling, this energy can be expressed as:

$$E_o = \frac{\sigma_c \pi D_B^2 h}{4} \tag{F-1}$$

where σ_c = energy of rock removal/unit volume = 40,000 in-lb/in^3,
D_B = hole diameter in inches, and
h = hole depth in inches.

The effective pressure P_m, is expressed in terms of an efficiency factor, η_i, and the regulated pressure, P_r:

$$P_m = \eta_i P_r \tag{F-2}$$

The energy, E_g, supplied by the gas must then be

$$E_g = \left[\int P_r A_p \, d(y) \right]_{n \text{ cycles}} = n P_r A_p Y_m = E_o/\eta_i \tag{F-3}$$

where A_p is the piston area, Y_m is the length of stroke, and n is the number of blows required to deliver the total energy E_o to the rock.

The incremental mass of gas supplied to the impactor is

$$d(M_r) = \rho_r A_p \, d(y) \tag{F-4}$$

where ρ_r is the gas density at the regulated pressure P_r and at temperature T_r. Since the regulator of Figure F-1 is isenthalpic, $T_r = T_t$. Using the perfect gas law, Equation (F-4) can be written in the form

$$d(M_r) = \frac{P_r A_p \, d(y)}{R_g T_t} \tag{F-5}$$

Equations (F-3) and (F-5) may be combined to give

$$d(M_r) = \frac{d(E_o)/\eta_i}{R_g T_t}$$

or

$$\int_{M_s}^{M_f} R_g T_t \, d(M_r) = \frac{E_o}{\eta_i} \tag{F-6}$$

The quantity of gas M_f which must be left in the tank is greater than zero because the pressure and temperature drops in the tank must be limited. Figure F-2 (a) and (b) shows the supply tank at time t and at time t $+\Delta t$, an instant later. During the time Δ t, the amount of gas ΔM_r, shown shaded in Figure F-2 (a), flows out of the tank, allowing the remaining gas to experience a reversible adiabatic expansion. The mass of gas remaining in the tank during the efflux of mass ΔM_r is constant, and thus

$$\frac{P_{t1}}{P_{t2}} = \left(\frac{V_{t2}}{V_{t1}}\right)^k = \left(\frac{T_{t1}}{T_{t2}}\right)^{\frac{k}{k-1}} \qquad \text{(F-7)}$$

where V_t is the volume of gas excluding that gas which flows out during the interval Δt; i.e., the control volume shown in Figure F-2.

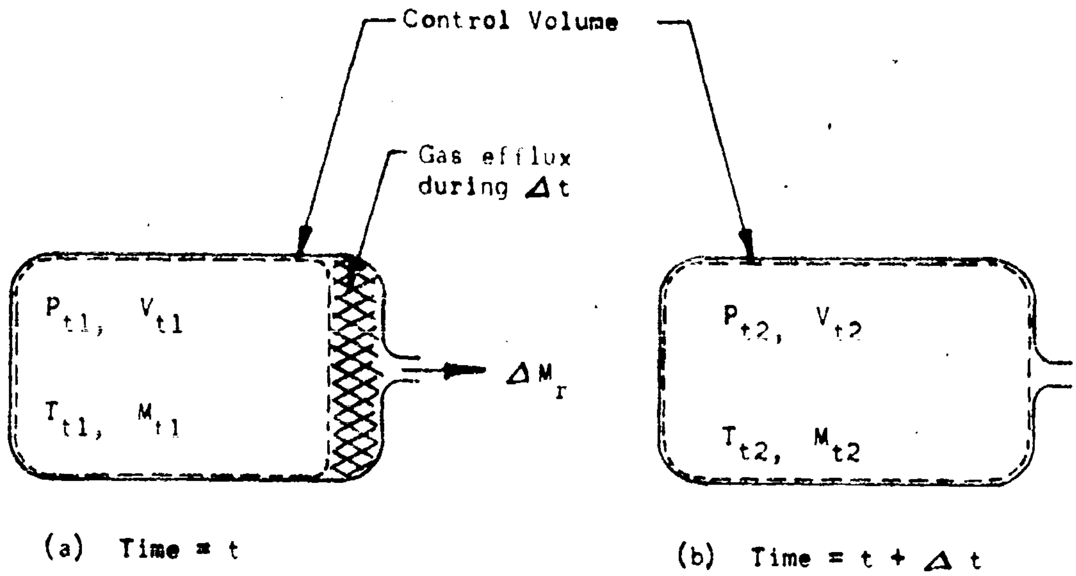

Supply-tank Discharge Process

Figure F-2

$$\Delta M_r = \bar{\rho}_t (V_{t2} - V_{t1}) \qquad \text{(F-8)}$$

or, in the limit,

$$\frac{d(M_r)}{dt} = -\rho_t \frac{dV_t}{dt} = -\frac{P_t}{RT_t} \quad \frac{dV_t}{dt} \tag{F-9}$$

or

$$-\frac{d(M_t)}{M_t} = \frac{dV_t}{V_t} \tag{F-9a}$$

For the control volume V_t, from Equation (F-7),

$$\frac{dV_t}{V_t} = -\frac{1}{k} \frac{dP_t}{P_t} = -\frac{1}{k-1} \frac{dT_t}{T_t} \tag{F-10}$$

When Equations (F-9a) and (F-10) are combined,

$$\frac{d(M_t)}{M_t} = \frac{1}{k} \frac{dP_t}{P_t} = \frac{1}{k-1} \frac{dT_t}{T_t} \tag{F-11}$$

$$\ln \left(\frac{M_t}{M_s}\right) = \frac{1}{k-1} \ln \left(\frac{T_t}{T_s}\right)$$

$$\frac{M_t}{M_s} = \left(\frac{T_t}{T_s}\right)^{\frac{1}{k-1}}$$

or,

$$\frac{T_t}{T_s} = \left(\frac{M_t}{M_s}\right)^{k-1} \tag{F-12}$$

Since $d(M_r) = -d(M_t)$, Equation (F-12) can be substituted into Equation (F-6) to give a relationship for M_r

$$\int_{M_s}^{M_f} R_g T_s \left(\frac{M_t}{M_s}\right)^{k-1} d\left(\frac{M_t}{M_s}\right) M_s = E_o/\eta_i \tag{F-13}$$

$$-\frac{M_s R_g T_s}{k} \left[\left(\frac{M_t}{M_s}\right)^k\right]_{M_s}^{M_f} = -\frac{M_s R_g T_s}{k} \left[\left(\frac{M_f}{M_s}\right)^k - 1\right] = E_o/\eta_i$$

But $\dfrac{M_f}{M_s} = \left(\dfrac{T_f}{T_s}\right)^{\frac{1}{k-1}}$

therefore,

$$\frac{M_s R_g T_s}{k}\left[\left(\frac{T_f}{T_s}\right)^{\frac{k}{k-1}} - 1\right] = - E_o/\eta_i$$

$$M_s R_g T_s = - \frac{kE_o}{\eta_i\left[\left(\frac{T_f}{T_s}\right)^{\frac{k}{k-1}} - 1\right]} \tag{F-14}$$

Two gases will now be considered, namely, nitrogen and helium. For helium, $k = 1.66$, and $R_g = 386$ ft-lb$_f$/lb$_m$ ^oR, and from Equation (F-14) .

$$M_s R_g T_s = P_s V_s = 3.22\ E_o/\eta_i \tag{F-15}$$

For nitrogen, $k = 1.4$ and $R_g = 55.2$ ft-lb$_f$/lb$_m$ ^oR, and

$$M_s R_g T_s = P_s V_s = 2.10\ E_o/\eta_i \tag{F-16}$$

The mass ratio is

$$\frac{(M_s)_{He}}{(M_s)_{N2}} = \frac{(R)_{N2}}{2.10} \times \frac{3.22}{(R)_{He}} = 0.219 \tag{F-17}$$

and the volume ratio at equal pressures is

$$\frac{V_{He}}{V_{N2}} = 1.53 \tag{F-18}$$

2.2 <u>Container Requirements</u>

In the following analysis a spherical container is assumed.

The tensile stress σ_t in a spherical shell of radius r, thickness t, and which has internal pressure P_t is

$$\sigma_t = \frac{P_t r}{2t} \tag{F-19}$$

If the gas is stored at 3000 psia and 100°F, then the maximum tank pressure, assuming a maximum ambient temperature of 200°F, will be

$$(P_t)_{max} = 3540 \text{ psi}$$

It is noted that the tank weight depends only on the product $P_t V_s$ for a given tank shape, allowable stress, and material density. Therefore, only the tank volume (and not its mass) will be affected by the pressure selected. Similarly, the gas mass required is independent of supply pressure.

For a steel tank, with an allowable stress σ_t = 120,000 psi, and density γ = 0.28 lbs/in^3, the tank weight, W_t, is

$$W_t = 4\pi r^2 t \gamma = \frac{2\pi r^3 (P_t)_{max} \gamma}{120,000} \tag{F-20}$$

$$= 0.0506 r^3 \tag{F-20a}$$

or, since the tank volume is

$$V_s' = \frac{4}{3} \pi r^3, \tag{F-21}$$

the weight is

$$W_t = 20.8 \quad V_s \tag{F-22}$$

where V_s is in ft^3 and W_t is in lbs.

2.3 Combined Weight and Volume of Container and Gas

2.3.1. Helium System

From Equations (F-15) and F-1),

$$(V_s)_{He} = \frac{3.22 \pi \sigma D_B^2 h}{4\eta_1 \ P_s} \tag{F-23}$$

or, for P_s = 3000 psi and σ_c = 40,000 in-lb/in^3

$$(V_s)_{He} = \frac{0.234\ D_B^2\ h}{\eta_i} \tag{F-23a}$$

where V_s is volume in ft^3 at 3000 psi and 100°F, D_B is the hole diameter in inches, h is the hole depth in ft., and η_i is the efficiency factor defined by Equation (F-2). The volume of "free" helium at standard pressure and temperature is then

$$(V_o)_{He} = 193\ (V_s)_{He} = 45.2\ \frac{D_B^2\ h}{\eta_i} \tag{F-24}$$

From the perfect gas law, the mass of gas is

$$(M_s)_{He} = \frac{P_s\ V_s}{R_{He}\ T_s} = 2.0\ V_s \text{ lbs} \tag{F-25}$$

When Equations (F-22), (F-23a), and (F-25) are combined, the following expression for the weight W_s of the helium source is obtained.

$$(W_s)_{He} = 5.35\ D_B^2\ h/\eta_i \tag{F-26}$$

2.3.2 Nitrogen System

From Equations (F-16) and (F-1),

$$(V_s)_{N2} = \frac{2.10\ \pi\ \sigma_c\ D_B^2\ h}{4\ \eta_i\ P_s} \tag{F-27}$$

or

$$(V_s)_{N2} = 0.153\ \frac{D_B^2\ h}{\eta_i} \tag{F-27a}$$

The volume of "free" nitrogen is then

$$(V_o)_{N2} = 29.5\ \ D_B^2\ h/\eta_i, \tag{F-28}$$

and the mass of nitrogen is

$$(M_s)_{N2} = 14\ V_s \text{ lbs} \tag{F-29}$$

and the total source weight is

$$(W_s)_{N2} = 5.31\ D_B^2\ h/\eta_i \qquad (F\text{-}30)$$

It is seen by comparison of Equations (F-30) and (F-26) that, for equal efficiencies, the nitrogen system has a slight weight advantage over the helium system. This is because the helium requires a larger diameter tank, due to the volume ratio as seen from Equation (F-18), thus adding more weight in tank material than is saved due to the reduced weight of gas.

Figures F-3 and F-4 show weights and volumes of nitrogen supply systems as functions of penetration and hole diameter, and for efficiencies of 0.5 and 0.7 According to Ingersoll-Rand Corporation, the efficiency of 0.5 is conservative for a pneumatic high-rate impact drill. For a slow rate drill, it is estimated that a somewhat higher efficiency, about 0.7, will be possible. For a nitrogen source capable of producing a 3/4 inch hole five feet deep in granite, the system weight is about 30 pounds, assuming η_i as 50%.

3. Liquid-Fuel, Hot-Gas System

Hydrazine (N_2H_4) is a possible energy source for a percussion drill It is a liquid monopropellant which decomposes at about 1960°R to form relatively clean gas.

3.1. System Configuration

Section III of Appendix D contains a description of a hydrazine gas generator, and Figure D-22 is a schematic of its system configuration. This system employs the "bootstrap" method of pressurizing the liquid fuel. The fuel is metered by a regulating valve into a decomposition chamber where gas is produced at 1960°R. This hot gas is fed back to the bootstrap cylinder and to the utilization device, as shown in Figure D-22. A starter cartridge of high-pressure nitrogen provides for initiation of bootstrap operation.

3.2. System Design

3.2.1. Fuel Requirements

A combustion pressure of 200 psia is selected and an efficiency factor η_i =0.5 for the hot-gas percussor is assumed.

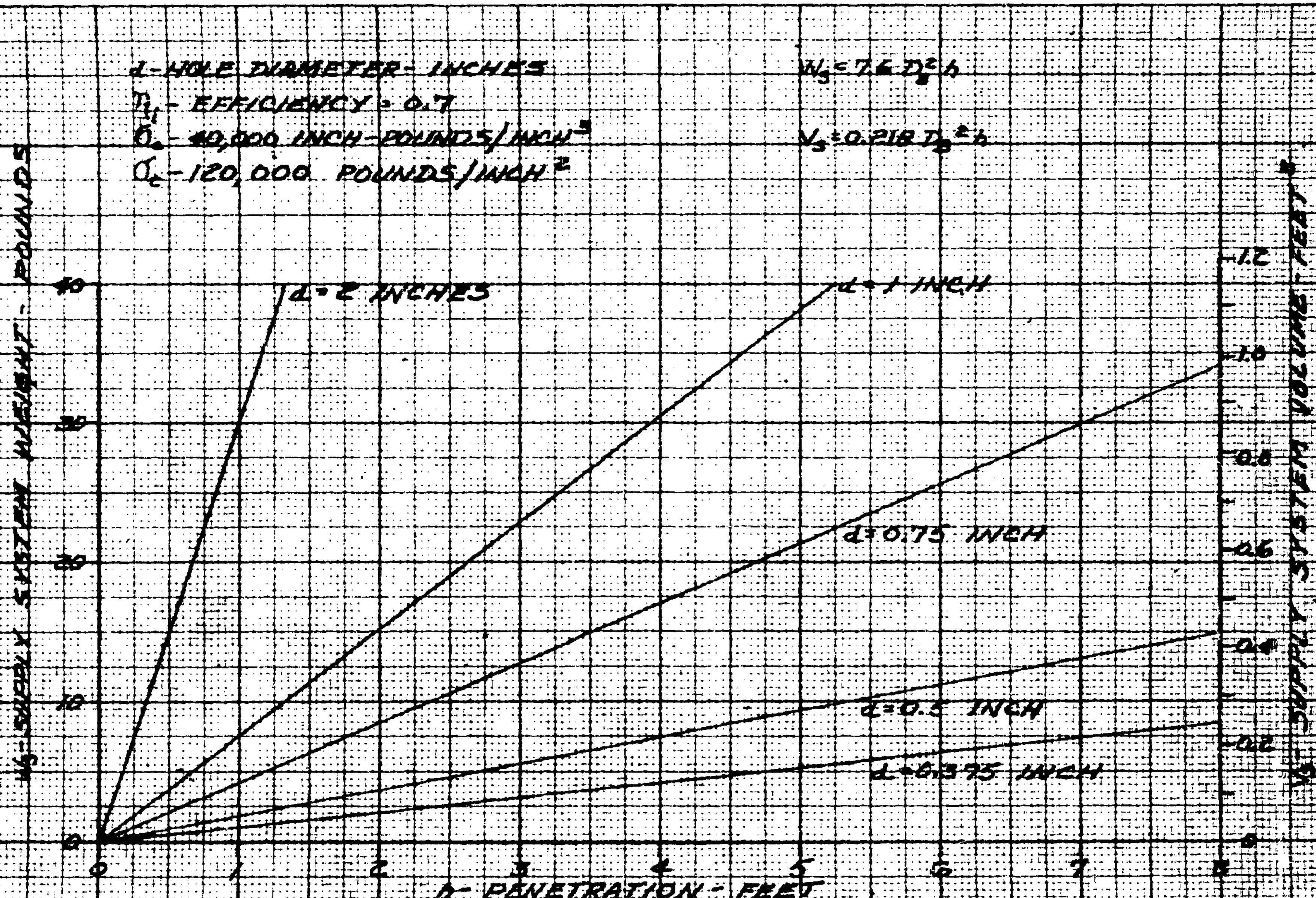

NITROGEN SUPPLY SYSTEM WEIGHT & VOLUME vs. PENETRATION & HOLE DIAETER ZERO RECOIL PERCUSSOR

FIGURE F-3

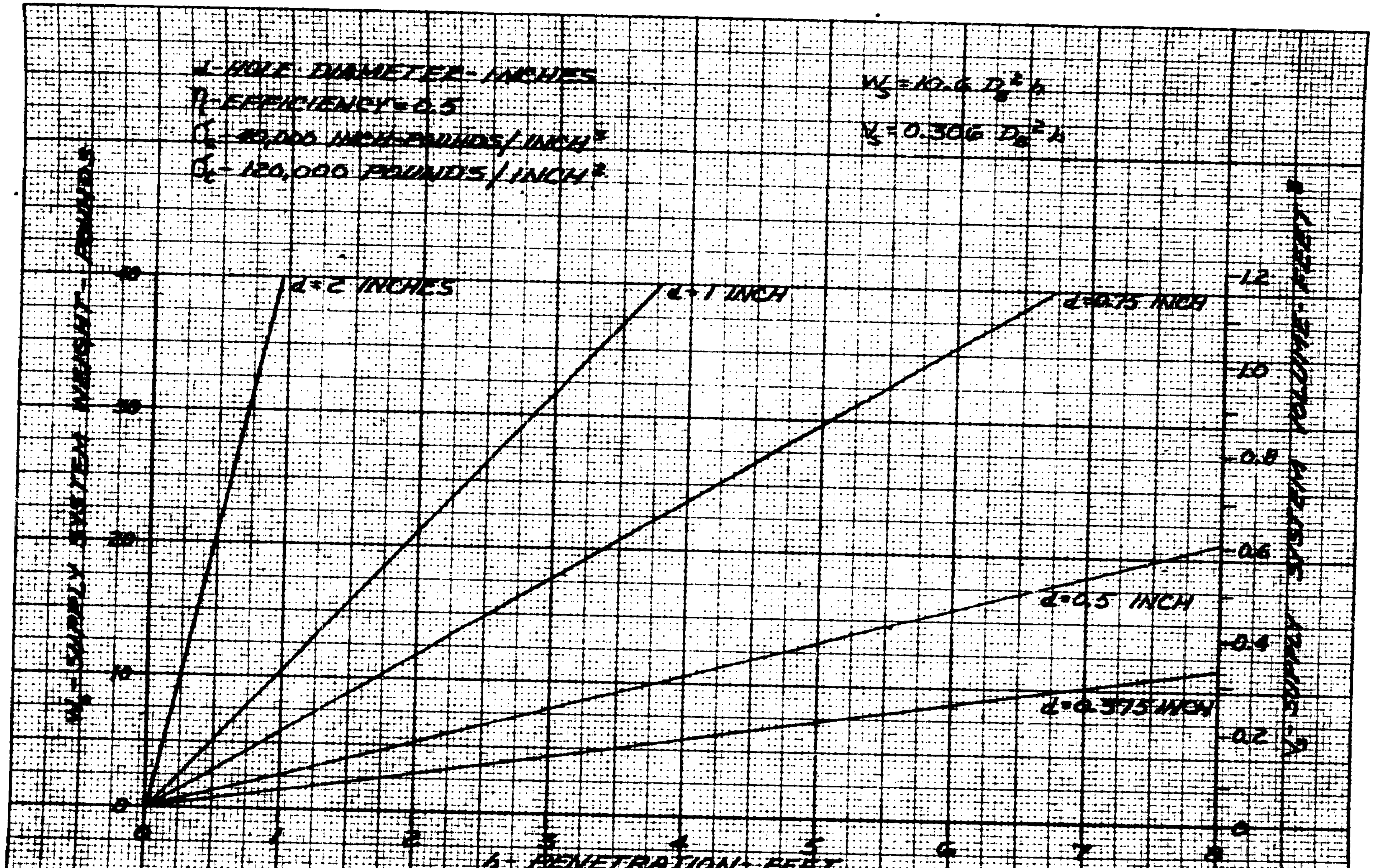

NITROGEN SUPPLY SYSTEM WEIGHT & VOLUME VS. PENETRATION & HOLE DIAMETER: CONTINUOUS IMPACT

FIGURE F-4

If the fuel flow to the decomposition chamber is regulated, and if the time constant of the decomposition chamber pressure with respect to changes in flow demand is large compared with the time between blows of the percussor, then only the average gas flow demand of the percussor must be supplied by the hydrazine generator.

$$\bar{Q}\, P_r\, t_o = E_o/\eta_i = \frac{\pi D_B^{\,2}\, h\, \sigma_c}{2} \tag{F-31}$$

where

$\bar{Q}$ = average volume flow to impactor, in^3/sec

P_r = regulated pressure, psia

E_o = energy required to drill a hole in rock, in-lb

t_o = drilling time, sec

η_i = efficiency factor

D_B = hole diameter, in

h = hole depth, in

σ_c = energy per unit volume required to remove rock in-lb/in^3

The regulator will be essentially isenthalpic, therefore the rate of efflux of mass from the gas generator is

$$\dot{M}_g = dM_g/dt = \bar{Q}\,\rho_g = \frac{\bar{Q}\; P_r}{R_h\; T_r} \tag{F-32}$$

Combining Equations (F-31) and (F-32) yields

$$M_g = \dot{M}_g\, t_o = \frac{\pi\, D_B^{\,2}\, h\, \sigma_c}{2\;\eta_i\; R_h\; T_g} \tag{F-33}$$

For a 3/4 inch diameter hole five feet deep in granite, and using R_h = 80.7 ft-lb_f/lb_m °R, the required mass is 1.12 pounds. If about 10% additional mass is included for "dead" volume, $M_g \approx$ 1.25 pounds.

Since hydrazine has about the same density as water, the volume, V_e, is approximately 34.6 in^3.

3.2.2. Fuel Tank and Bootstrap Unit

A fuel tank and pressure-boost system, as shown in Figure D-22, was designed to accomodate the required 1.25 pounds of hydrazine, and to provide a pressure difference of 50 psi between the fuel supply and the decomposition chamber. A decomposition chamber pressure of 200 psia was specified. Using a minimum wall thickness of 0.035 inches (20 gauge), the weight of the tank and piston assembly is 2.34 pounds. The tank is approximately 16 inches long with a maximum diameter of about 3 inches, and a volume of about 100 cubic inches.

3.2.3. Decomposition Chamber

The decomposition chamber should have a time constant for a change in flow rate which is large compared with the percussion tool cycle time. For a rate of 180 blows per minute, the time, T_i, between blows is 0.33 seconds. Therefore, the decomposition chamber is designed for a time constant of 3 seconds. From ASTIA Report Number AD142322,

$$\tau = \frac{\bar{P}_o \ V_o}{1.5 \ w_{fo} \ R_h \ \bar{T}_o} \qquad \text{(F-34)}$$

where

τ = time constant, sec

$\bar{P}_o$ = average chamber pressure, psi

V_o = chamber volume, in^3

w_{fo} = average fuel flow rate, lb_m/sec

R_h = gas constant, in-lb_f/lb_m ^oR

$\bar{T}_o$ = average chamber temperature ^oR

For a drilling time of 78 minutes, the average fuel flow rate is 0.027 pounds per minute. From Equation (F-34) the required chamber volume for a three-second time constant is 20.5 in^3.

A chamber is selected which has diameter D, and which is composed of a cylindrical section of length 3D closed by ellipsoidal ends of

height D/4. In order to provide the required volume, the diameter must be 3 inches. If the minimum wall thickness is taken to be 0.035 inches, then the chamber weight is 0.95 pounds.

3.2.4. Source Weight and Volume

The component and total weights of the hydrazine source are given in Table F-I. Note that one pound is allotted for valving, starter cartridge, catalyst, tubing, and a pressure regulator.

Table F-I

Hydrazine Source Weights

System Components	Weight (lbs)
Hydrazine fuel	1.25
Fuel tank and Booster	2.34
Decomposition Chamber	0.95
Valves, Catalyst, etc.	1.00
Total System Weight	5.54 lbs

The volume of this source is less than 0.1 cubic foot.

3.3 Discussion of the Hydrazine Hot-Gas Generator

The weight of the hydrazine system is much less than the weight of a stored-gas system. For example, the nitrogen source weight for a 3/4 inch diameter, five foot deep hole in granite is 30 pounds, compared with 5.5 pounds for a hydrazine source. However, the following problems associated with a hot-gas generator cast considerable doubt on the desirability of such a system for moon drilling:

a. Flow Metering. The orifice area required to meter 0.027 pounds of hydrazine per minute, with a 50 psi pressure differential, is only about 1.86×10^{-5} in^2. This means a diameter of about 0.0049 inches. Metering orifices of this size would be impractical, and although reduction of the pressure difference would permit a larger metering area to be used, a decrease of the pressure drop from 50 psi to 5 psi would only increase the area to 5.9×10^{-5} in^2. This corresponds to the area of an 0.0087 inch diameter circular orifice. Furthermore, a pressure drop across the inlet to the decomposition chamber of the order of 50 psi

is desirable to promote atomization of the propellant. Thus, fuel metering is a difficult function to accomplish in the liquid propellant gas generator.

b. Temperature Level. A hot-gas generator would be a heat source within the moon capsule and would tend to aggravate the problem of temperature control of instruments or other equipment associated with the capsule.

c. Development Costs. Although some hydrazine generators are now used, the design of such systems is far from straightfoward, and the development of a hydrazine-powered moon drill would be much more costly in time and money than to use a more conventional, well-developed type of energy source.

4. Batteries

As discussed in Section IV of Appendix D, silver-zinc storage batteries are insensitive to variation in ambient temperature and current drain, are rugged, and have been used extensively in missile and satellite applications. A typical silver-zinc battery will provide 33 watt-hours of energy per pound mass including the case and connectors.

The weight of a battery source, W_b, for driving a moon drill can therefore be expressed by the following equation

$$W_b = 0.746 \times 10^{-6} \frac{\sigma_c D_B^2 h}{F_i} \tag{F-34}$$

where the symbols are as previously defined.

Thus, for an overall efficiency of 40%, the battery weight for drilling a 3/4 inch diameter hole to a depth of five feet in granite is only about 2.5 pounds. This should be compared with 30 pounds for a stored-gas system and 5.5 pounds for a hydrazine hot-gas generator.

5. Discussion of Energy Sources

Of the energy sources examined above, the battery is definitely superior because of its substantial weight advantages, and also because it is less complex and more reliable than either a stored-gas or hot-gas generator source. However, no definite conclusions regarding choice of an energy source can be drawn without consideration of the complete

percussion drill system. Section II of this appendix is concerned with the drilling systems as a whole, and presents weight and volume estimates for several types.

Section II

Types of Percussion Drills

and

Weight and Volume Estimates

1. Introduction

There are many different types of systems possible for percussion drilling. In this section, the two general classifications of percussion drill systems, zero-recoil and finite-recoil, are examined. It is concluded that finite-recoil operation is preferable for moon drilling, and two limiting modes of finite-recoil percussion, intermittent and continuous, are considered. The conclusion is reached that maximum drilling efficiency occurs when reaction force and cyclic rate are properly matched in continuous percussion drilling.

Weight estimates are presented for three percussor systems: (1) a stored-gas pneumatic; (2) hot-gas pneumatic; and (3) a battery-source mechanical percussor.

2. Zero-Recoil Percussion Systems

In an impact drill, a force internal to the percussion mechanism acts on a hammer mass over a relatively long period of time, thus storing energy in the mass. The hammer is then allowed to strike a drill rod which is in contact with the rock being drilled, thereby dissipating its energy in a very short period of time and causing rock fracture. If a reaction force, equal to the internal force which imparts energy to the hammer mass, is supplied to the percussor mechanism as a whole, then the percussor case will remain stationary during the drilling process; i.e., no recoil of the percussion system will occur during or following a hammer blow. In a zero-recoil impactor, the forces which accelerate the hammer may be gravitational, or contact forces which act directly on the hammer (and thus react on the percussor case).

2.1. Gravity-Force Actuated System

Figure F-5 is a schematic diagram of a gravity-fall impactor.

The hammer, of mass m_h, is lifted through height Y_m by a force F_i, which might be a cable force derived from an electric motor, or which might be supplied by a regulated gas pressure, P_r, acting on the area, A_h, of the hammer. The work done by the moon's gravitational field on the mass as it drops through the distance Y_m is

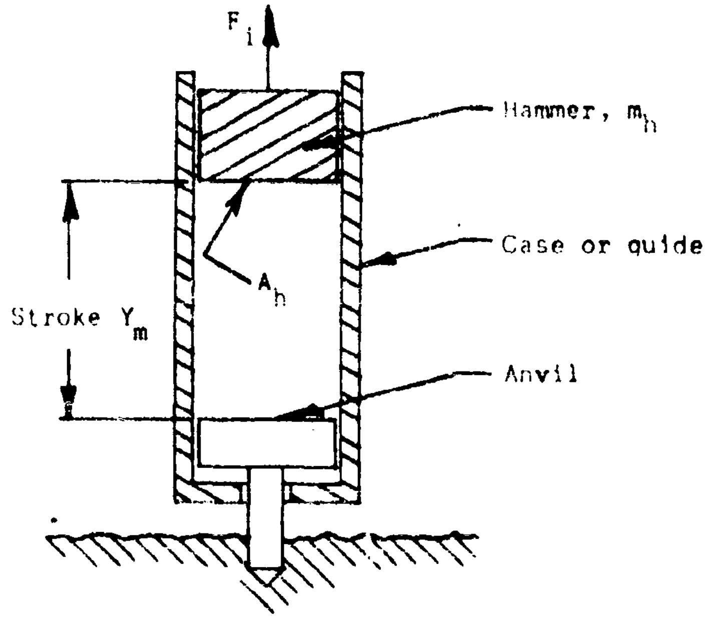

<u>Schematic Diagram of Gravity-Force Actuated Percussor</u>

<u>Figure F-5</u>

$$E = m_h\, g_m\, Y_m \tag{F-35}$$

Assuming a 10% loss of this energy due to friction and other effects in the cylinder, the energy per blow transferred to the rock will be

$$E_b = 0.90\, m_h\, g_m\, Y_m \tag{F-36}$$

In order to produce rather large chips and to obtain a high degree of drilling efficiency in granite, a threshold energy E^* of approximately 100 in-lbs/inch of bit diameter must be supplied to the drill bit during each blow. If the bit diameter is D_B inches, then

$$g_m\, m_h\, Y_m \geq 111 D_B \text{ in-lb} \tag{F-37}$$

In terms of earth weight, W_h, of the hammer,

$$W_h\, Y_m \geq 666 D_B \text{ in-lb} \tag{F-38}$$

If the maximum hammer weight is taken to be 16 lbs earth weight, and the minimum hole diameter to be 0.75 inches, then the minimum stroke is

$$Y_m \gtrapprox 31.2 \text{ inches}$$

Since the drill package length must be less than six feet, a telescoping, cylinder arrangement is required to produce a hole depth greater than about 1 ft. From a design standpoint, this is awkward because of the valving of fluid, (if fluid is used as the source of energy), and because of the mechanical difficulties of extending the telescope and of providing a reasonable seal between the hammer and telescoping members of different diameters. Figure F-6 shows one possible configuration for such a telescoping impactor, upon which approximate weight and volume estimates can be based. This arrangement will permit a hole of about 5 feet depth to be drilled.

Details such as valving and means for rotating the drill bit will not be considered at this stage of the study. Rotation would be provided on the up-stroke of the hammer by means of a ratchet mechanism.

A minimum tube diameter of 3 inches and maximum hammer length of 6 inches are assumed. From Figure F-6, and with 1/16" thick steel tubes, the approximate tube weight is $W_{tube} \approx 20$ lbs, and the approximate weight of the drill rod is $(W)_{rod} \approx 51$ lbs.

It is seen that the drill impactor assembly must be extended prior to the start of drilling. Thus, its upper end would protrude from the top of the moon capsule by about four feet. Under these conditions the implementation of an electric system would be very difficult. In addition, some method of cleaning the rock chips away from the bit must be provided. The most feasible method of chip removal appears to be by means of a gas flow (see Appendix C). This suggests that gas be used as the means of lifting the hammer. The gas used to raise the hammer can be exhausted through the drill bit prior to dropping the hammer, thereby providing chip removal without added weight penalty.

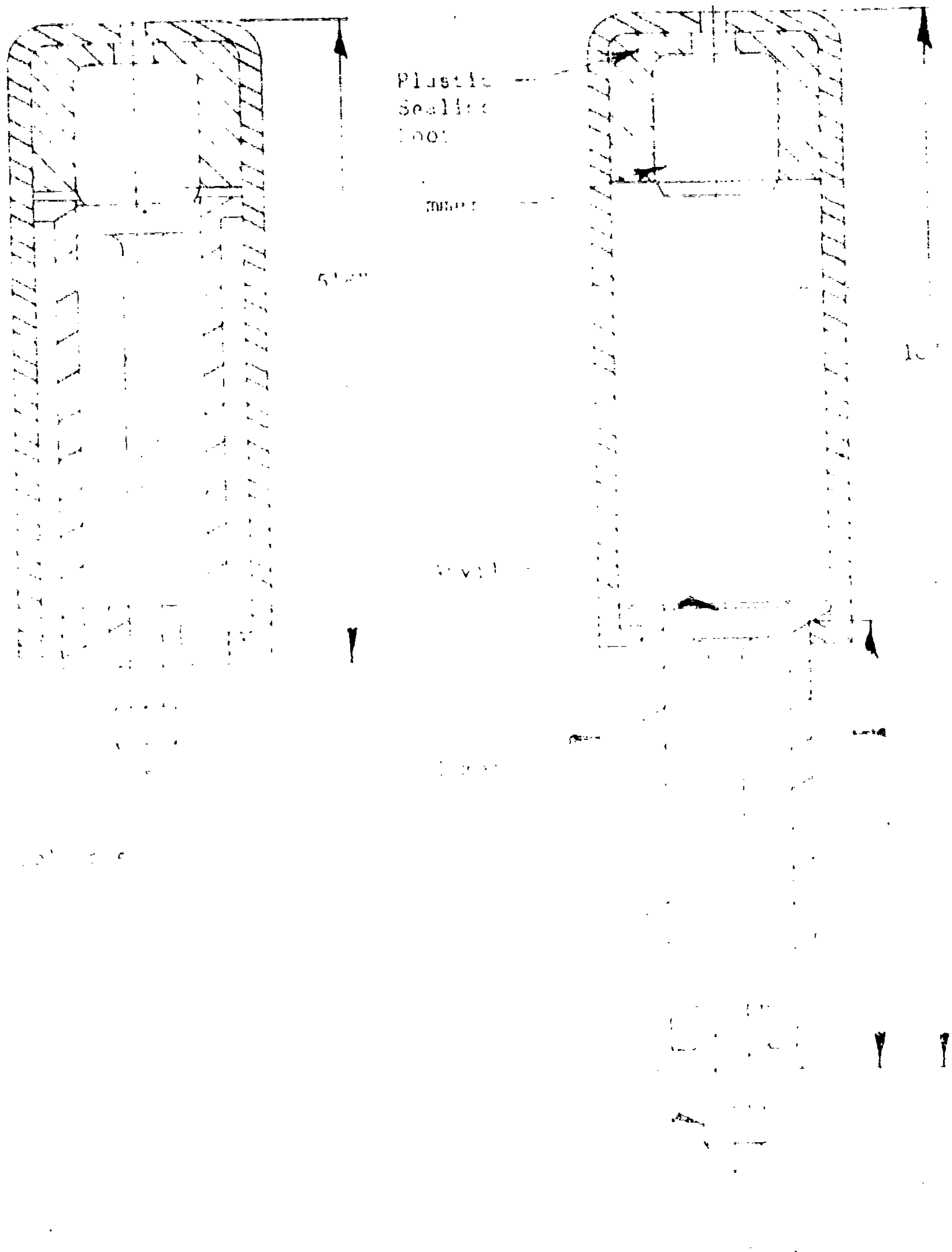

Weight requirements for the gas (nitrogen) and cylinder are given in Figure F-3. For a five foot deep, 3/4 inch diameter hole in granite,

$$W_s = 21.4 \text{ lbs}$$

For a hole diameter of 1/2 inch,

$$W_s = 9.5 \text{ lbs.}$$

An added weight, W_r, of 3 lbs. is provided for valves, a regulator, and support members for the drill assembly.

The total estimated weights for the gas-operated, gravity-fall system are

$$W_t = W_{tube} + W_{rod} + W_r + W_s + W_{hammer} \qquad \text{(F-39)}$$

For a 3/4" diameter and a 5 foot deep hole, $W_t \approx 65.4$ lbs. A 1/2" diameter reduces the (earth) weight to about 53.5 lbs.

The total approximate volumes of the system, when collapsed, are,

$$V_t = V_{hammer} + V_s + 0.25$$

(The 1/4 ft^3 covers valving, regulator and other small parts). For a 3/4" diameter and a 5 foot deep hole, $V_t \approx 1.4\ ft^3$. A 1/2" diameter reduces the volume to

$$V_t \approx 1.0\ ft^3$$

The drilling time, allowing 10 sec/cycle will be

$$T = (\text{Number of blows}) \times (\text{time per blow})$$

The energy required to drill a five-foot hole is

$$E_o = \frac{\pi D_B^2 h}{4} \times 40{,}000 = 6\pi D_B^2 \times 10^5 \text{ in-lb}$$

where $40{,}000 = \sigma_c$ = rock removal/unit volume.

Then, if E_b = energy/blow from Equation (F-36),

$$T = 1.51 D_B^{2} \text{ days.}$$

For a 0.75" diameter hole five feet deep.

$$T \approx 0.85 \text{ days}$$

and for 0.50" hole,

$$T \approx 0.38 \text{ days}$$

2.2 Zero-Recoil, Contact-Force Acceleration Impactor

Figure F-7 shows a second type of recoilless impact drill.

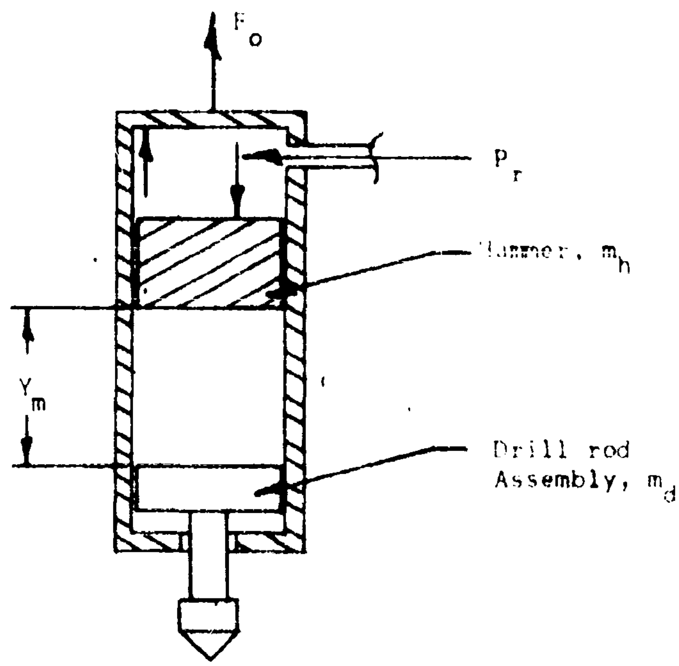

Schematic Diagram of Contact-Force Recoilless Impactor
Figure F-7

This device would be suspended from the moon capsule by a force F_o, and would function as follows. Regulated gas pressure, P_r, is admitted above the hammer, m_h, causing it to accelerate downwards and

strike the tool. Valve sequencing is arranged so that the source pressure is shut off just prior to impact. After impact, the upper cylinder chamber is ported to the lower chamber, and most of the gas confined in the cylinder exhausts through the bit, thus removing chips from the hole. When the chamber pressure approaches zero, the upper chamber is ported to zero pressure, allowing the fluid below the piston to return the hammer to the raised position. The exhaust port above the piston is then closed, the regulated pressure P_r is again admitted to the upper cylinder, and the cycle repeats. Bit rotation can be provided on the return stroke by means of a ratchet mechanism as in the gravity-fall system. Assuming that no compressive force is transmitted to the moon vehicle, the condition for no recoil is

$$F_i < m_c \, g_m, \tag{F-41}$$

where F_i is the maximum internal force in the hammer cylinder, and m_c is the case mass. Since F_i also acts on the hammer mass m_h,

$$m_h \ddot{y} \leqq m_c \, g_m \tag{F-42}$$

or integrating from $y = o$ to $y = Y_m$, and $\dot{y} = o$ to $\dot{y} = \dot{y}_h$,

$$E_b = \frac{1}{2} m_h \, \dot{y}_h^{\,2} \leqq m_c \, g_m \, Y_m \tag{F-43}$$

If a 10% loss for friction is assumed, then the maximum energy per blow which can be delivered to the rock is

$$E_b = 0.90 \, m_c \, g_m \, Y_m \tag{F-44}$$

Note that Equation (F-44) is identical with Equation (F-36) for the free-fall system, except that the pertinent mass here is the case mass rather than the hammer mass. Thus, this system has an advantage over the free-fall system in that advantage may be taken of the weight of the hammer case, while the mass of the hammer itself may be small. The hammer mass should, however, be approximately the same size as the anvil and drill rod in order to facilitate good energy transfer between these elements.

In the gravity system, the hammer and case weights totalled 36 lbs, if the hammer weight were limited to 16 pounds. In the present system, guides must be provided to align the drill with the moon capsule during drilling and to maintain the hole essentially vertical. The weight of these elements cannot be included in m_c.

If the case weight is limited to 30 lbs, then the minimum stroke to supply the threshold energy of 100 in-lb/in is

$$m_c \, g_m \, Y_m = 111 D_B$$

$$Y_m = 22.2 D_B \text{ inches} \qquad \text{(F-45)}$$

for 0.75" diameter,

$$Y_m = 16.6 \text{ in}$$

Therefore, the minimum length of stroke for the contact-force acceleration system is about half that of the free-fall system. However, a telescoping arrangement is still necessary to permit the drilling of a five-foot deep hole. Furthermore, since guide rails and a feeding device must be incorporated in this system, the complete mechanism appears to have only a slight advantage over the free-fall system either in terms of weight or complexity. Therefore, it will not be considered further in this study.

2.3. Summary

A zero-recoil percussion drill is possible for operation on the moon. It is not recommended, however, due to the mechanical problems of implementing such a system.

A free-fall impactor capable of drilling a five-foot deep, 3/4 inch diameter hole in granite would weigh about 66 pounds on earth including a gas-supply system. The required drilling time would be approximately 20 hours.

3. Finite-Recoil Percussion Systems

If recoil of the percussor assembly is permitted, it is possible

to deliver a larger amount of energy per blow to the rock, for any given reaction force and percussor mass, than is possible when recoil is prevented. This advantage occurs because the net impulse delivered by the reaction force to the hammer is distributed over a longer period of time than in the case of a zero-recoil system.

3.1. Modes of Operation

Two modes of operation are possible in a percussion system where recoil is permitted. These modes are termed intermittent percussion and continuous percussion. In the intermittent mode, each blow of the hammer is independent of both the preceding and succeeding blows; while in the continuous mode, a steady oscillation of the hammer and percussor case takes place. In this section, these modes of impact drilling are examined and the conclusion is reached that continuous percussion is the more efficient type of operation. Weight estimates are made for a simplified continuous percussion system.

3.1.1. Intermittent Percussion

Figure F-8 is a schematic diagram of a finite-recoil percussor. The masses of the drill rod assembly, hammer, and drill case are m_d, m_h, and m_c, respectively, and F_o is a constant reaction force acting on the case.

In intermittent percussion, it is assumed that the effects of any particular blow of the percussor completely die out before the next blow occurs. That is, each blow is initiated when the percussor system is at rest. Hence, $\dot{y}_c = \dot{y}_h = 0$.

When the percussor is actuated, a force F_i acts on the hammer, accelerating it toward the drill rod assembly. The reaction to F_i acts against the case, and if $F_i > F_o$, the case will be accelerated in recoil. (If $F_i < F_o$, no recoil will occur, and the system behaves as described in Section 2.)

An exact analysis of the impact and recoil behavior of the percussor illustrated in Figure F-8 requires quantitative knowledge of the variation of the accelerating force F_i. However, if the duration

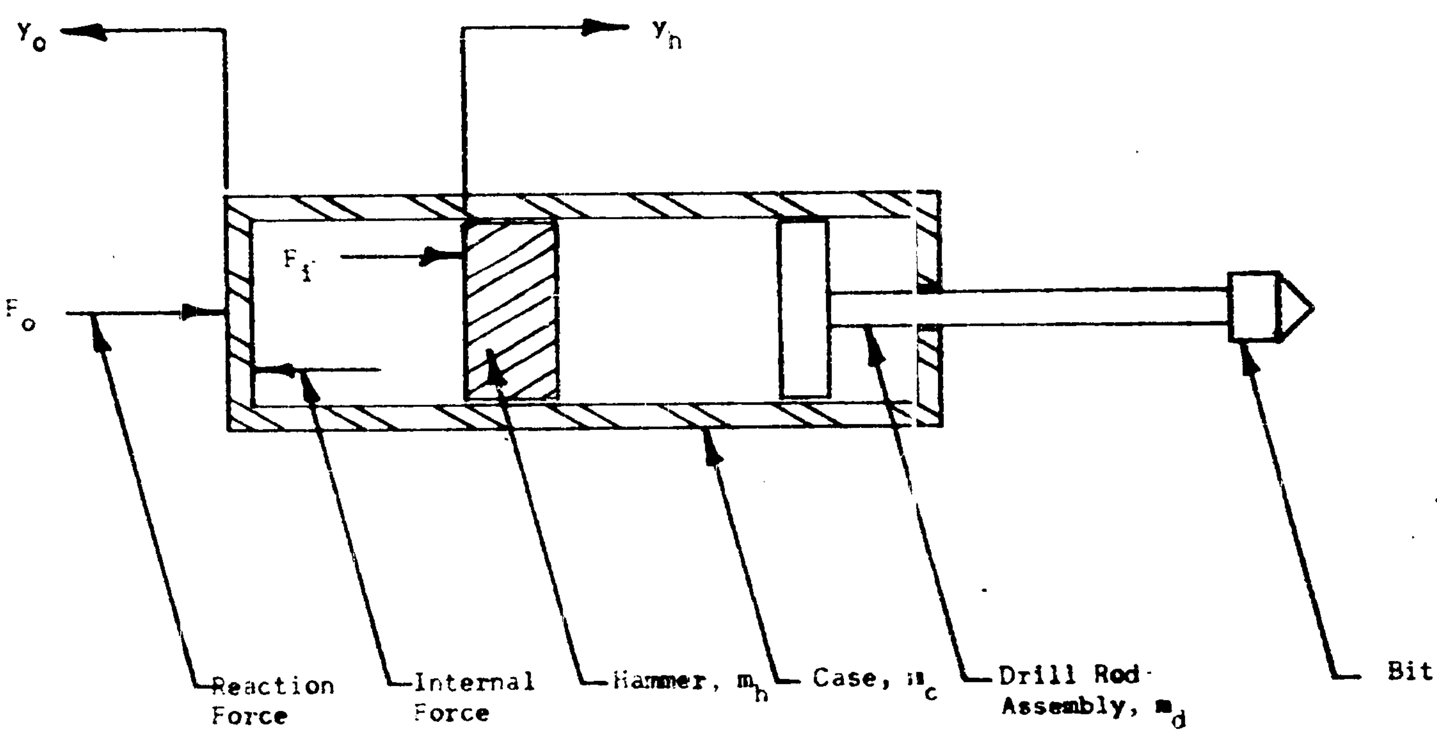

Finite-recoil Percussor

Figure F-8

of F_i is short compared with the time of recoil of the case, a simple analysis, independent of the nature of F_i, is possible.

When forces on the case are summed

$$F_i - F_o = m_c \ddot{y}_c \qquad \text{(F-46)}$$

For the hammer,

$$F_i = m_h \ddot{y}_h \qquad \text{(F-47)}$$

Or, combining Equations (F-46) and (F-47),

$$m_c \ddot{y}_c = m_h \ddot{y}_h - F_o \qquad \text{(F-48)}$$

Equation (F-48) may be integrated with respect to time over the duration T_a of the acceleration m_h. Thus,

$$m_c \dot{y}_c = m_h \dot{y}_h - \int_0^{T_a} F_o \, dt \qquad \text{(F-49)}$$

Assuming that F_o is small compared with F_i, and that T_a is very short, $F_o T_a$ can be neglected in comparison with $m_h \dot{y}_h$. From Equation (F-47), the energy E_b transferred to the hammer mass m_h by F_i is

$$E_b = m_h \dot{y}_h^{\,2}/2 \qquad \text{(F-50)}$$

Equations (F-49) and (F-50) are combined,

$$m_c \dot{y}_c = \sqrt{2E_b \, m_h} \qquad \text{(F-51)}$$

After F_i has acted on the case, imparting to it the momentum given by Equation (F-51), the case will recoil against the reaction force F_o until the velocity $\dot{y}_c$ becomes zero. Thus

$$F_o \, (y_c)_{max} = \frac{1}{2} m_c \dot{y}_c^{\,2} = E_b \cdot \frac{m_h}{m_c} \qquad \text{(F-52)}$$

The recoil distance is therefore

$$(y_c)_{max} = \frac{E_b\, m_h}{F_o\, m_c} \tag{F-53}$$

The time, T_r, for this maximum distance to be reached will now be computed. The acceleration of the case, after $F_i = 0$, is

$$\ddot{y}_c = -\frac{F_o}{m_c} \tag{F-54}$$

$$\dot{y}_c = -\frac{F_o\, t}{m_c} + C_1 \tag{F-55}$$

From Equations (F-49) and (F-51),

$$C_1 = \sqrt{2\, E_b\, m_h}\,/m_c \tag{F-56}$$

Integrating Equation (F-55),

$$(y_c)_{max} = -\frac{F_o}{m_c}\frac{T_r^{\,2}}{2} + \frac{\sqrt{2\, E_b\, m_h}}{m_c} \cdot T_r$$

or,

$$T_r = \frac{\sqrt{2\, E_b\, m_h}}{F_o} \tag{F-57}$$

The criterion for intermittent percussion can be stated in terms of the time between impacts, T_i, and the time of recoil, T_r. For slow percussion,

$$T_i >> T_r. \tag{F-58}$$

The threshold energy for formation of side chips is, for a 3/4" bit diameter,

$$E_b \approx 75 \text{ in lb}$$

Assuming m_h = 2 lbs, m_c = 16 lbs, and F_o = 10 lbs, the recoil distance, from Equation (F-53), is

$$(y_c)_{max} = 1.07 \text{ inches},$$

and from Equation (F-57),

$T_r = 0.088$ seconds.

Figure F-9 shows a plot of the percussor case motion during intermittent percussion.

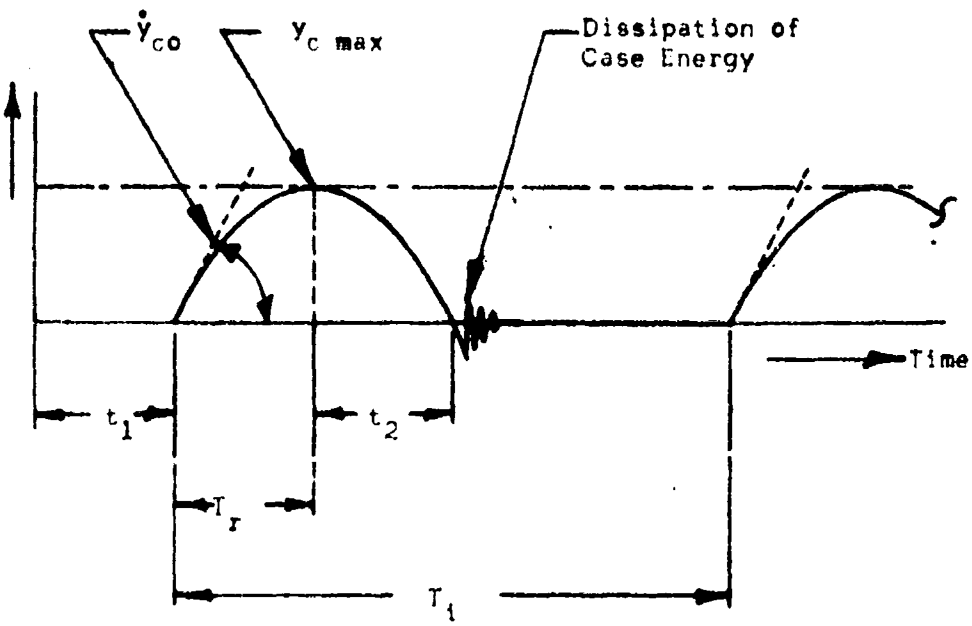

Case Motion During Intermittent Percussion

Figure F-9

At $t = t_1$, the percussor is actuated and a blow takes place, imparting a recoil velocity, $\dot{y}_{co}$, to the case. During time T_r, the case recoils against F_o to a height of $(y_c)_{max}$. As F_o continues to act, the case then accelerates downward and reaches velocity $\dot{y}_{co}$ again when $y_c = 0$. The energy stored in the case as kinetic energy at this time must be dissipated without effectively fracturing additional rock. From Equation (F-49), the energy in the case E_c is related to the energy delivered to the hammer by

$$E_c = E_b \frac{m_h}{m_c} \qquad \text{(F-59)}$$

Typically, for moon drilling, the ratio of m_h to m_c will be of the order of one to eight. Thus a loss of about 20% of the input energy to the

percussor is inherent in the intermittent percussion system. Intermittent percussion will not be considered further here, but attention is now directed toward a continuous percussion drill.

3.1.2. Continuous Percussion

In a continuous percussion system, the blow interval is less than the time required to complete and dissipate the recoil associated with one particular blow. Thus, the recoil behavior after any single blow is influenced by the preceding and succeeding blows, and a steady, cyclic impact and recoil process may occur.

For a continuous percussion process, the average reaction force F_{oa} must supply the average impulse delivered to the rock. When Equation (F-46) is integrated and averaged with respect to time,

$$\left[\int F_i \, dt\right]_{avg} - \left[\int F_o \, dt\right]_{avg} = (m_c \, \dot{y}_c)_{avg} \qquad \text{(F-60)}$$

For steady operation, $(\dot{y}_c)_{avg} = 0$. The average reaction force F_{oa} is defined as

$$F_{oa} = \left[\int F_o dt\right]_{avg} / t \qquad \text{(F-61)}$$

and the momentum of the hammer at impact is

$$m_h \, \dot{y}_h = \left[\int F_i \, dt\right] \text{one blow} \qquad \text{(F-62)}$$

The energy per blow transferred to the rock is therefore related to $\int F_i \, dt$ by

$$\left[\int F_i \, dt\right] \text{one blow} = \sqrt{2 \, E_b \, m_h} \qquad \text{(F-63)}$$

When Equations (F-60), (F-61), and (F-63) are combined,

$$\sqrt{2 \, E_b \, m_h} = F_{oa} \, T_i \qquad \text{(F-64)}$$

where T_i is the time between blows. Let N be the impact rate in blows/second. Then

$$F_{oa} = N \sqrt{2\, E_b\, m_h} \tag{F-65}$$

Equation (F-65) is valid for any variation of F_i with time. If the assumptions are made that the duration of F_i is short compared with the impact interval T_i, and that F_o is constant, the behavior of the case displacement with respect to time is shown in Figure (F-10).

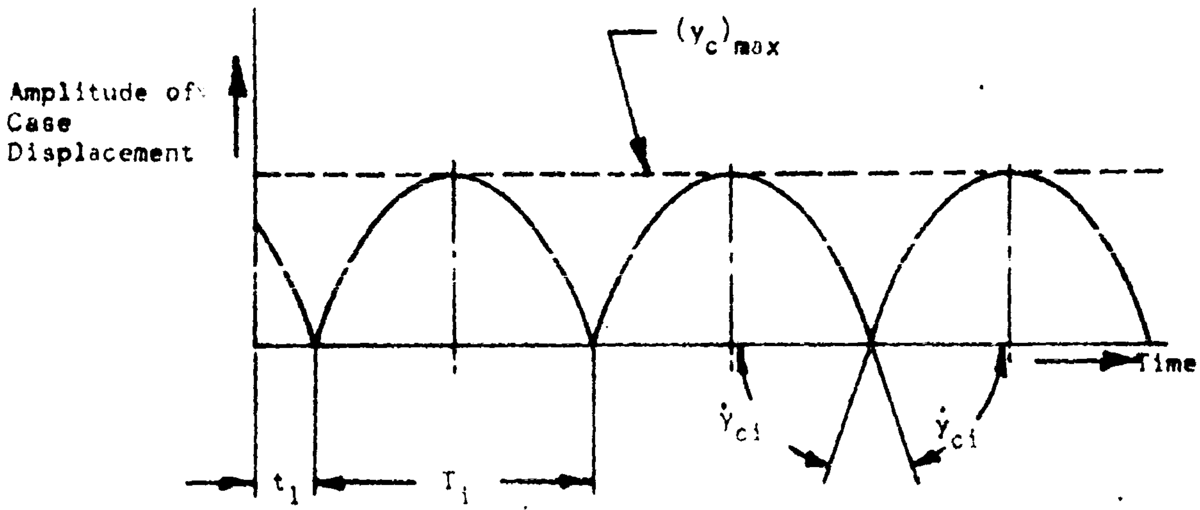

Case Motion During Continuous Percussion

Figure F-10

Each cycle is parabolic in shape and is symmetrical with respect to $(y_c)_{max}$. The blows occur at $y_c = 0$. The velocity of the case just before impact is $-\dot{y}_{ci}$, and just after impact is $+\dot{y}_{ci}$. Thus the momentum change of the case due to the acceleration of the hammer is

$$\Delta \text{ momentum} = 2\, \dot{y}_{ci}\, m_c \tag{F-66}$$

By the reasoning which led to Equation (F-51),

$$m_c\, \dot{y}_{ci} = \frac{1}{2} \sqrt{2\, E_b\, m_h} \tag{F-67}$$

For a constant reaction force F_o, the recoil is therefore,

$$(y_c)_{max} = \frac{1}{2} \frac{E_b m_h}{F_o m_c} \tag{F-68}$$

The time to recoil, or to reach $(y_c)_{max}$ is

$$T_r = T_i/2 = \sqrt{2 E_b m_h} / 2 F_o \tag{F-69}$$

Note that the recoil time given by Equation (F-69) is one half of the recoil time for the intermittent percussor. When T_i is replaced by $1/N$, the reciprocal of the impact rate, Equation (F-69) is identical with Equation (F-65) provided $F_{oa} = F_o$.

In an optimized percussor, no inherent energy loss occurs, since the energy of recoil is not dissipated but is utilized in accelerating the hammer for the next blow. However, it is important to note that this efficient type of operation can only occur if the impact rate and the reaction force are properly matched, as determined by Equation (F-65). Thus, an optimum reaction force exists for any given impact rate, or conversely. Equation (F-65) indicates that any amount of energy per blow can be delivered at any value of reaction force, provided that the impact rate is slow enough. However, according to Equation (F-68), the recoil distance increases, for a given energy per blow, as the reaction force decreases. Thus a minimum reaction force can be established in a continuous percussion system by specification of the allowable recoil distance.

3.2. Finite-Recoil Percussor Configurations

Two types of finite-recoil percussors appear feasible for moon drilling, namely pneumatic and mechanical.

3.2.1. Gas-Operated Percussor

Figure F-11 is a schematic diagram of a gas-actuated continuous percussor. This configuration will permit a hole of about five feet in depth to be drilled by a package which is somewhat less than six feet long. Sheet 3 (at the end of Section III of the main body of the report) shows an artist's conception of an alternative arrangement for the gas-operated percussor. The internal construction of the percussor itself is not shown since it consists of only a gas-driven

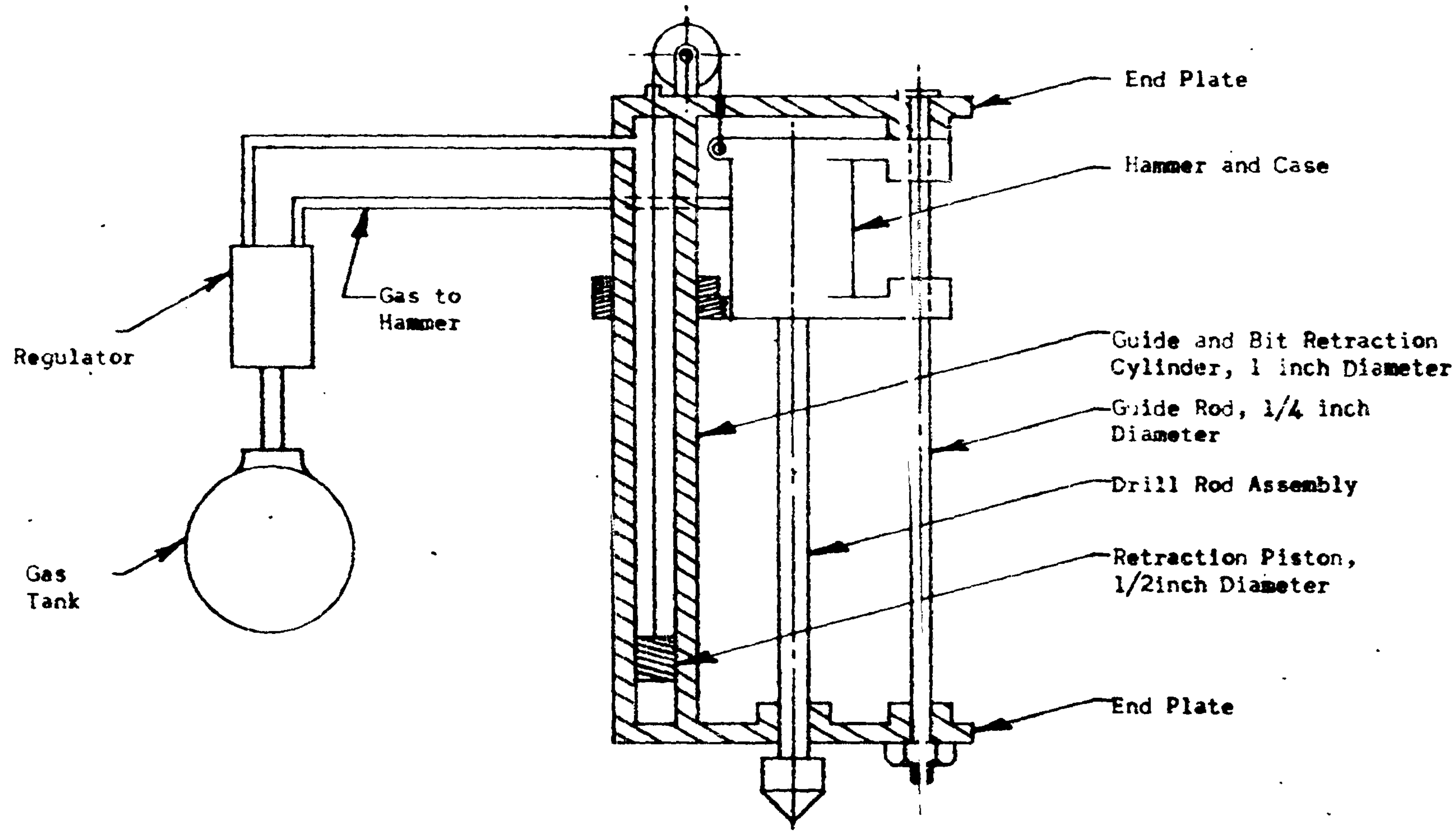

Schematic Diagram of a Finite-Recoil Percussor

Figure F-11

piston-hammer and a sequencing valve which causes continuous oscillation of the piston. From Section 2.1, the weight of the drill-rod assembly is about 5 lbs. For effective transfer of energy from the hammer to the drill rod, the mass of the hammer must not be small compared with the mass of the drill-rod assembly. The hammer mass is taken to be 2 lbs. To minimize recoil, the case mass should be considerably larger than the hammer mass, as shown by Equation (F-68). A mass of 16 lbs is assumed. For formation of side chips and efficient rock drilling, a threshold energy of 100 in-lb/in. is required; thus, for a 3/4 inch diameter bit, $E_b = 75$ in-lb. For a reaction force equal to the moon weight of the case, $F_o = 2.66$ lbs, the recoil distance is, from Equation (F-68),

$$(y_c)_{max} = 0.875 \text{ inches.}$$

From Equation (F-69), the time between impacts must then be

$$T_i = 0.329 \text{ seconds,}$$

or the cyclic rate is

$$N = 1/T_i = 180 \text{ blows per minute.}$$

The weight of the guides is approximately 3 lbs., and that of the end plates, 1 lb.

The weight of this pneumatic hammer assembly and package is shown in Table F-II. Note thatan allowance of 3 pounds is made for miscellaneous components.

Table F-II

Pneumatic Percussor Weights

Hammer Components	Weight (lbs)
Percussor	18
Drill rod and bit	5
Guides and Supports	4
Miscellaneous	3
Total Percussor Assembly Weight	30 lbs

To obtain the total system weight, the source weight must be added to the above percussor assembly weight. Two sources of gas will be considered, namely, stored gas (compressed) and liquid monopropellant.

3.2.1.1. Stored-Gas Source

In Section I -2.3, the weight of a nitrogen source is estimated at 30 pounds when capable of drilling a 3/4 inch hole five feet deep in granite, and assuming an efficiency, η_1, of 50%.

In the stored-gas system, bit rotation would be effected by a ratchet mechanism during the return stroke of the hammer, and chip removal would be obtained by passing part of the percussor exhaust gas through the bit.

Drilling time for a 3/4 inch hole, five feet deep would be about 78 minutes.

$$T = (\text{number of blows}) \times (\text{time/blow})$$

$$\cong 78 \text{ minutes}$$

The total system weight is approximately 60 pounds and the system volume is less than 2.5 cubic feet. An experimental study, reported by Hughes Tool Company in Appendix 1, Bi-weekly Progress Report No. 3 of "Lunar Drill Study" also gives a weight estimate of about 60 pounds for a pneumatic percussor system.

3.2.1.2. Liquid Propellant Source

The pneumatic percussor described in Section 3.2.1. could be powered by a hydrazine hot-gas generator of the type discussed in Section I -3. For the hole size being considered here, the weight of a hydrazine power source is about 5.5 pounds.

Since high-temperature gas cannot be used for chip removal, a chip transport system must be provided for the hydrazine-powered percussor. From Appendix C, allowing 400% more gas for cleaning of chips produced by percussion than is required for cleaning chips produced by diamond drilling, the weight of a chip transport system which must operate for 78 minutes is approximately 2 pounds.

Thus, the total system weight is about 37.5 pounds when hydrazine fuel is employed. There are, however, several problems associated with the use of hot-gas which make the use of a hydrazine gas generator undesirable. These problems are discussed in Section I of this Appendix and in Section III of the main body of this report.

3.2.2. Mechanically-actuated Percussor

Sheet 4 (~~also~~ at the end of Section III of the main body of the report) is an artist's conception of a mechanically-actuated percussor which is driven by an electric motor. The power for the motor is supplied from a zinc-silver storage battery. Although this system is only one of many possible arrangements employing mechanical actuation of the hammer, its weight will be approximately the same, and its efficiency probably somewhat less than any other mechanical system.

As shown by Sheet 4, an electric motor drives a splined shaft continuously through a gear reduction. The hammer mass slides freely on the splined shaft in a vertical direction, but is forced to rotate with the shaft. As the hammer rotates, a follower attached to the hammer moves along a cam surface, thus lifting the hammer against a spring. After about 180 degrees of rotation the hammer has been lifted from its lowest to its highest position. The cam surface then drops off suddenly, allowing the spring to accelerate the mass downwards toward the anvil and drill rod. After another 180 degrees of rotation of the mass, during which time impact and case recoil occur, the cam follower on the hammer again engages with the cam and the hammer starts up the shaft in preparation for the next blow.

The amount of energy required to drill a particular hole in rock with such a percussor will depend in part on the over-all efficiency of the device. The energy losses in this percussor will arise from four main sources:

(a) Electrical and mechanical losses in the drive motor. An efficiency of 90% is assumed here.

(b) Frictional losses in the gearing and in the hammer guides. An efficiency of 75% is assumed.

(c) Energy loss due to intermittent operation of the percussor. It is assumed that mechanical limitations in the cam system prevent the

use of an optimized continuous percussion scheme. Under these conditions, an energy loss occurs which depends on the ratio of the casing mass to the hammer mass. As in the case of a gas-operated percussor (see Section 3.2.1), the hammer mass must be at least 2 pounds to permit efficient transfer of energy from the hammer to a five-foot drill rod. The maximum practical case weight, consistent with system weight limitations, appear to be about 16 pounds. From Equation (F-59), the efficiency of an intermittent percussion system is therefore about 80%.

(d) Frictional losses in the cam. Figure F-8 is a free-body diagram of the cam and follower system. The cam profile is taken to be linear for purposes of estimating the cam efficiency.

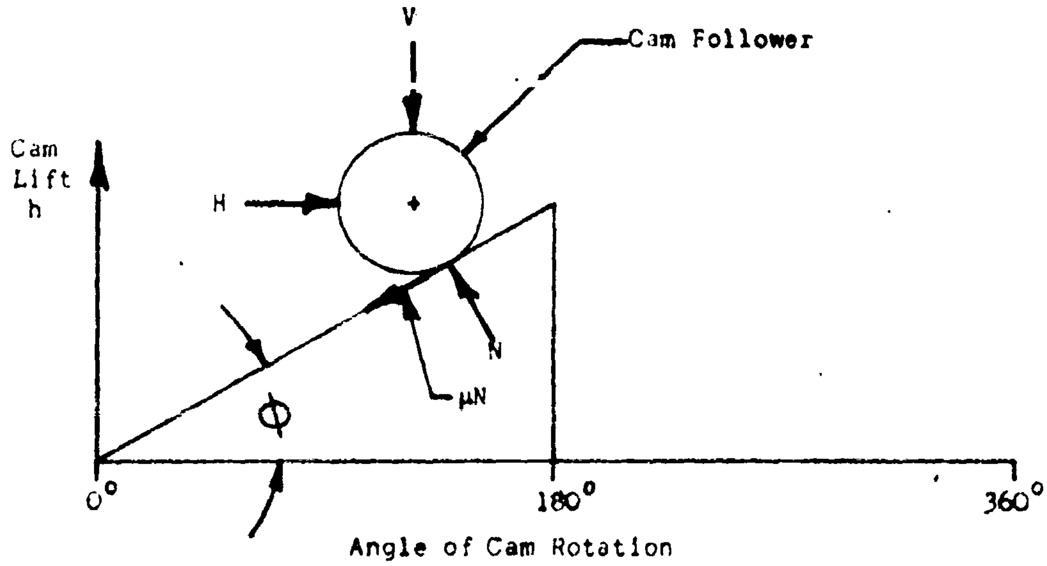

Cam and Follower System

Figure F-8

The forces acting on the cam follower are seen to be a vertical force V from the spring; a horizontal force H from the hammer torque; and a normal force N and tangential force μN from the cam. The quantity μ is the coefficient of friction between the follower and cam, typically 0.15. The slope of the cam is indicated by the angle ϕ. When horizontal and vertical forces are summed,

$$H = \mu N \cos\phi + N \sin\phi \qquad \text{(F-70)}$$

$$V = N \cos\phi - \mu N \sin\phi \qquad \text{(F-71)}$$

The work done by the motor in raising the hammer, neglecting gravity, is

$$dW_m = R_c H \, d\theta \qquad \text{(F-72)}$$

where

W_m = work, in-lb
R_c = cam radius, in
θ = angle of rotation

The work done in compressing the spring is

$$d W_s = R_c V \, d(h) \tan\phi \qquad \text{(F-73)}$$

where

W_s = work done, in-lb
h = compression of spring = rise of cam, in

The efficiency of the cam is, therefore

$$\eta = \frac{d W_s}{d W_m} = \frac{H}{V \tan\phi} \qquad \text{(F-74)}$$

or, when Equations (F-70), (F-71) and (F-74) are combined,

$$\eta = \frac{1-\mu \tan\phi}{1 + \mu \tan\phi} \qquad \text{(F-75)}$$

For $\phi = 45^\circ$ and $\mu = 0.15$, the efficiency is 74%. This cam angle corresponds to a 3 inch cam lift on a 1.85 inch diameter hammer. The spring constant of the accelerating spring must then be 37.5 lbs/inch to deliver a blow of 75 inch-pounds if the effective stroke is 2 inches.

If the cam lift is reduced to 2.5 inches and the effective stroke to 1.5 inches, the cam angle ϕ becomes 39.8 degrees, and the efficiency becomes 74.2%. For $\phi = 50^\circ$, the efficiency drops to 73%. It may be possible to reduce the coefficient of friction somewhat, perhaps to $\mu = 0.1$. However, if this is accomplished, the efficiency rises to only 81.5%.

On the basis of the preceding calculations, a cam angle of about 45° appears to give performance near maximum efficiency. Under these conditions an energy loss of about 25% will be experienced if the coefficient of friction is about 0.15.

The over-all efficiency can now be estimated as the product of the efficiencies determined in (a) through (d) above.

$$\eta_i = 0.90 \times 0.75 \times 0.80 \times 0.75 \approx 0.4 \text{ or } 40\%$$

Using that over-all efficiency, the energy required to drill a five-foot hole of 3/4 inch diameter in granite can be calculated.

$$E = E_o/\eta_i = \frac{\pi D_h^2 \; h \quad \sigma_c}{1.6} = 2.64 \times 10^6 \text{ in-lb}$$

$$= 82.9 \text{ watt-hr}$$

From Section I, the battery weight to supply the above energy is about

$$W_b = 2.5 \text{ lbs}$$

In order to limit recoil and the associated energy loss to about 20%, the case mass of the percussor must be eight times the hammer mass; or since the minimum hammer mass is 2 pounds, the percussor mass must be 16 pounds. Referring to Figure D-24, it is seen that a 0.1 hp motor and gear box for diamond bit drilling weighs less than five pounds. This leaves 11 pounds for additional gear reduction required in the impactor, a spring, spline drive shaft, bearings and housing. Guides must be supplied, which will require an estimated 4 pounds. The drill rod and bit for drilling a five foot hole will weigh about 5 pounds. In addition, a chip transport system is required for chip removal.

Assuming a cyclic rate of 60 blows/minute for the percussor, the time of operation will be

$$T = E_o \; N/E_b = \frac{1.06 \times 10^6 \text{ in-lb}}{75 \text{ in-lb/blow}} \times \frac{h}{3600 \text{ blows}}$$

$$T \cong 4 \text{ hours}$$

From Figure C-12, the weight of a chip transport system for 4 hours operation in a 3/4 inch hole is 1.25 pounds. For percussion drilling, the weight is taken for 400% extra gas, or about 2 pounds.

The component and total weights for the electric percussor can now be listed as in Table F-III.

Table F-III

Electric Percussor Weights

Components	Weight (lbs)
Percussor assembly, including hammer	18
Guides	4
Miscellaneous items	3
Drill rod and bit	5
Chip transport system	2
Battery	2.5
Total System Weight	34.5 lbs

4. Conclusions

In this appendix, three types of energy sources were considered for driving a percussive drill, i.e., compressed gas, liquid-fuel hot-gas, and a storage battery. Of these, the battery source was found to have minimum weight and probably maximum reliability.

Two kinds of percussion mechanisms, gas-actuated and mechanically-actuated, were investigated. These two mechanisms are representative, as far as weight and volume are concerned, of the feasible moon-drill percussors.

Three complete drilling systems were evaluated: a gas-actuated, stored-gas driven system; a gas-actuated hot-gas driven system; and a mechanically-actuated battery and motor-driven system. For drilling a 3/4 inch diameter hole to a depth of five feet in granite, the system weights are:

(a) Pneumatically-actuated, stored-gas source 60 lbs

(b) Pneumatically-actuated, hydrazine source 37.5 lbs

(c) Mechanically-actuated, battery source 34.5 lbs

On the basis of this preliminary feasibility study, three percussion systems have been found to be possible within a weight limitation of 60 pounds. The system which has minimum weight, probably maximum reliability, and which would probably require the least development effort, is the electrical system. However, as discussed in Section III of the main body of this report, this conclusion must be considered tentative until a more thorough study of the percussive and rotary-diamond drilling mechanisms can be made.

HUGHES TOOL COMPANY

LABORATORY REPORT

August 11, 1960

TO: E. M. Galle

cc: F. G. Reeve (2)
T. N. Williamson
G. G. Atkinson
F. A. McCormick
G. R. King
J. G. Zenink
T. G. Stephenson

SUBJECT: Low Bit Weight - High Rotary Speed Drilling Tests On Berea Sandstone, Rush Springs Sandstone And Gray Granite.

REF.: E.M.G.'s IOC, Dated 7-19-60

L.J. 17530-2

Project 40021 FN-64

Job Open

INTRODUCTION

This lab job is a part of the moon drill study. It was requested to determine if satisfactory drilling rates can be obtained on the [illegible] formations using a rolling cutter rock bit and limited bit load. The bit load would be available from part of the weight of the proposed space capsule.

Preliminary tests were made in the Drilling Section using a 1-1/4" 2-cone bit and the microbit drill press. Test results were not considered to be reliable because bit load could not be maintained within the 45-50 pound range as requested by you.

The tests were continued by the Mechanical Testing Section using the high pressure drilling machine.

OBJECT:

The object of this laboratory job is to determine the drilling rate of Berea Sandstone, Rush Springs Sandstone and Gray Granite using a 1-1/4" 2-cone bit, 50 pounds bit load, 570 and 1140 RPM rotary speed and air to carry away the cuttings.

TEST PROCEDURE:

These tests were made on the high pressure drilling machine using a modified setup to permit the use of a low bit load.

A bit load of approximately fifty pounds was obtained by mounting the rock sample in a steel holder weighing 49.2 pounds. Total bit load consisted of the sum of the individual weights of the steel

holder and the rock sample. The rock holder was aligned within the drilling chamber by a rib and groove arrangement and was free to slide as penetration occurred.

One 1-1/4" 2-cone bit was used during the tests on all three formations. The formations were tested in the order of softest to hardest to minimize the effect of bit wear on the results. Air was circulated through the bit for cooling purposes and for removal of cuttings from the hole. Rate of air flow was not determined.

RESULTS:

The results of tests on Berea Sandstone, Rush Springs Sandstone and Gray Granite using 570 and 1140 RPM are listed in Tables I and II, respectively.

The average penetration rates of Berea at 570 and 1140 RPM were 4.72 and 3.75 ft./hr., respectively. Average penetration rates of Rush Springs Sandstone at the same speeds were 0.53 and 0.46 ft./hr. Decreased drilling rates occurred on both types of sandstone when rotary speed was increased from 570 to 1140 RPM.

One interval of depth, .312 inches, was drilled on Gray Granite at a rate of 0.06 ft./hr.

Practically no tooth wear occurred during tests on Berea Sandstone. Approximately .020 inch of diametrical tooth wear occurred during the test on Rush Springs Sandstone. During the 24 minutes required to drill the .312 inch interval of depth in the granite specimen the cone teeth were worn smooth with the cone shell.

Results of preliminary tests by the Drill Rig Section are listed below. The results were not considered to be reliable because of the frictional effect in the loading mechanism.

Bit Load Lbs.	Drilling Rate, Ft./Hr. At Rotary Speeds, RPM, Of:		
	51	325	990
Berea Sandstone			
50	0.31	2.18	1.71
Rush Springs Sandstone			
50	--	--	0.18
125	0.07	0.23	--
Gray Granite			
50	--	--	0.02

ATTACHMENTS:

Table I - Results Of Drilling Tests Using 570 RPM Rotary Speed

Table II - Results Of Drilling Tests Using 1140 RPM Rotary Speed

CONCLUSIONS:

Results of these tests indicate that the harder rock formations such as Rush Springs Sandstone and Gray Granite cannot be drilled satisfactorily with the 1-1/4" 2-cone bit, 50 pounds bit load and either 570 or 1140 RPM rotary speed.

J. G. Stephenson

J. G. STEPHENSON, METALLURGICAL DEPARTMENT, LABORATORY.

JGS:bar

TABLE I

Results Of Drilling Tests Using
570 RPM Rotary Speed

Bit: 1-1/4" 2-Cone
Bit Load: 50 Lbs., Approx.
Circ. Fluid: Air, 90 PSI ([illegible])

Test No.	Core Descr.	Bit Load Lbs.	Interval No.	Interval Depth In.	Interval Time Min.	Drilling Rate Ft./Hr.
1	Berea Sandstone	51.7	1	.454	.500	4.54
			2	.297	.327	4.54
			3	.313	.327	4.79
			4	.281	.327	4.29
			5	.341	.305	5.58
						4.75 Av.
3	Berea Sandstone	51.6	1	.281	.292	4.82
			2	.406	.453	4.48
			3	.344	.353	4.85
			4	.344	.387	4.45
			5	.344	.330	5.20
			6	.312	.362	4.33
			7	.312	.338	4.62
						4.69
5	Rush Springs Sandstone	53.[illegible]	1	.312	2.07	0.76
			2	.312	3.47	0.40
			3	.344	4.11	0.42
						0.53
6	Gray Granite	52.[illegible]	1	.312	24.19	0.06

L.J. 17530-2
8-8-60
J.Q.S.

TABLE II

Results Of Drilling Tests Using 1140 RPM Rotary Speed

Bit: 1-1/4" 2-Cone
Bit Load: 50 Lbs., Approx.
Circ. Fluid: Air, 90 PSI

Test No.	Core Descr.	Bit Load Lbs.	Interval No.	Interval Depth In.	Interval Time Min.	Drilling Rate Ft./Hr.
2	Berea Sandstone	51.6	1	.672	.891	3.77
			2	.468	.670	3.49
			3	.500	.667	3.75
			4	.500	.670	3.73
			5	.500	.721	3.47
						3.64 Av.
4	Berea Sandstone	51.[illegible]	1	.500	.667	3.75
			2	.531	.667	3.99
			3	.500	.667	3.75
			4	.531	.668	3.98
			5	.531	.670	3.97
			6	.375	.503	3.72
						3.86
5	Rush Springs Sandstone	52.1	1	.281	2.83	0.50
			2	.281	3.25	0.43
						0.46

L.J. 17530-2
8-8-60
J.G.S.

G-7

HUGHES TOOL COMPANY

LABORATORY REPORT

August 24, 1960

TO: E. M. Galle

cc: P. G. Reeve (2)
T. N. Williamson (3)
F. A. McCormick
G. R. King
J. G. Eenink
J. G. Stephenson

SUBJECT: Study Of Drilling Performance Of 1-7/8" Core And Full-Hole Type Diamond Bits In Berea Sandstone, Rush Springs Sandstone, And Gray Granite.

REF.: Verbal Requests from E.M.G., 8-5-60, 8-8-60, 8-12-60, 8-15-60.

L.J. 17530-2

Project 40021-64

Job Open

INTRODUCTION:

This report covers one phase of a series of tests run to develop a drill which is to be sent to the moon.

OBJECT:

This phase of the testing was carried on in order to determine the drilling rates of diamond bits at various rotary speeds and different air flows. These tests were carried out with constant weight on the bit. Information was also obtained on the power required to drive the bit and input and output air temperatures to and from the bit.

EQUIPMENT:

All tests in this phase were carried out on the Laboratory high pressure drilling machine. A schematic diagram of the setup used appears as Figure 1 attached to this report. The Rotameter used was a Schutte and Koerting series 18200 with a 4 HCFb tube and a 44-J float. Input air temperature was measured with a mercury thermometer inserted into a tee in the air line. Pressure in the Rotameter was read from a Crosby 0-200 psi test gage with 2 psi scale divisions. Air flow was controlled by an air regulator in the line. Output air temperature was measured with a Copper-Constantan thermocouple referenced to 32°F by an ice-water mixture.

Bits used were manufactured by J. K. Smit & Sons, Inc. of Murray Hill, N.J. Both bits were 1-7/8" (AX size). One of these bits

was a core type, manufacturer's number FX-99. The other bit was a concave-face, full-hole type, manufacturer's number FY-1. These bits were mounted in the high pressure rig by means of a small adapter.

SPECIMENS:

All tests were made on stock specimens made for the high pressure drill rig. Specimen sizes are shown below.

Specimen	Diameter (In.)	Length (In.)
Berea Sandstone	3-1/2	3-1/2
Rush Springs Sandstone	3-1/2	3
Gray Granite	4-1/8	3-1/4

TEST CONDITIONS:

Exact test conditions for each run are shown in Tables 1 and 2 attached to this report.

Rotary speeds were constant at 90, 185, 570, 675, and 1140 rpm. The test loads were 50 and 113 lbs. The exact load on the bit varied by as much as ± 0.23 lb. The average load shown in Tables 1 and 2 was determined by adding the weight of the rock holder to the average weight of the rock as determined by its weight before and after drilling. Air flow varied slightly from one run to another due to fluctuations in the plant air line pressure.

RESULTS:

The results of this phase of the testing are tabulated in Tables 1 and 2 and shown graphically in Figures 2, 3, and 4. The reader is cautioned to observe the scale changes on Figure 2 and between Figure 2 and Figure 3.

Horsepower results taken during the core bit tests (Table 1) are considered unreliable. This was due to the high pressure packings in the drill rig. During tests IV and V, these packings were loosened, but some heating and binding effects were still noted. The packings were removed and replaced by brass bushings with O rings for the full hole bit tests (Table 2) and the results are considered more reliable. The resulting figures are still not completely accurate due to the large scale range of the Watt meter. The horsepower difference in operating the drill rig in the loaded and unloaded conditions was small compared to the horsepower required to operate the rig.

Figures 2 and 3 show that drilling rate is apparently more affected by bit wear than by changes in air circulation.

Bit loads shown in Figures 2 and 3 are nominal. Average actual loads for each test are shown in Tables 1 and 2.

Photographs were taken of the core bit before and after testing in Gray Granite and are included as Figure 5. Figure 6 shows the full-hole bit before and after testing in Berea Sandstone. The full-hole bit would not drill Rush Springs Sandstone at all.

ATTACHMENTS:

Table 1 - Core Bit Data and Results

Table 2 - Full-hole Bit Data and Results

Table 3 - Order of Tests

Figure 1 - Schematic Diagram of Setup Used During Testing

Figure 2 - Core Bit - Drilling Rate versus Rotary Speed

Figure 3 - Full-hole Bit - Drilling Rate versus Rotary Speed

Figure 4 - Full-hole Bit - Average Horsepower versus Rotary Speed

Figure 5 - Core Bit - Before and After Testing in Gray Granite

Figure 6 - Full-hole Bit - Before and After Testing in Berea Sandstone

CONCLUSIONS:

The diamond bits used in these tests dulled rapidly in Berea Sandstone and more rapidly in Rush Springs Sandstone and Gray Granite.

These bits appear to be unsuitable for drilling in the above formations.

E. P. Worden
E. P. WORDEN, METALLURGICAL DEPARTMENT, LABORATORY.

EPW/bsr

Air Temp [illegible]

TABLE 1

CORE BIT DATA AND RESULTS

Test Number	Rock	Rotary Speed (RPM)	Average Load (lb)	Air Flow (cfm)	Air Temp. (°F) Input	Output	Drill Rate (Ft/Hr)	Power (HP)
I-1	Berea	90	49.79	28.9	-	-	2.39	-
-2	Sand-	185	"	29.2	-	-	3.00	-
-3	stone	570	"	29.5	-	-	7.50	-
-4	"	675	"	29.4	-	-	9.92	-
-5	"	1140	"	28.7	-	-	15.62	-
II-1	"	90	50.07	27.6	78	81	1.71	-0.20
-2	"	185	"	28.2	78	81	1.69	-0.18
-3	"	570	"	28.4	78	85	3.76	-0.01
-4	"	675	"	28.0	78	89	4.54	-0.15
-5	"	1140	"	28.0	78	96	7.18	-2.23
III-1	"	90	49.91	22.7	79	82	1.25	-0.26
-2	"	185	"	22.9	79	85	1.88	-0.25
-3	"	570	"	23.2	79	89	5.83	-1.30
-4	"	675	"	23.1	79	91	6.25	-0.44
-5*	"	1140	"	23.0	79	91	7.66	-1.57
IV-1	"	1140	49.90	22.8	79	91	8.25	2.24
-2	"	90	"	15.2	79	85	1.26	0.12
-3	"	185	"	15.1	79	87	1.94	0.11
-4	"	570	"	15.5	79	88	4.52	0.37
-5	"	675	"	15.4	79	91	3.87	0.55
-6	"	1140	"	15.4	79	96	6.63	1.00
V-1	Rush	90	49.83	27.6	78	80	0.089	0.21
-2	Springs	185	"	27.3	78	84	0.130	0.10
-3	Sand-	570	"	27.3	78	99	0.279	-0.05
-4	stone	675	"	27.4	78	106	0.292	-1.17
-5	"	1140	"	27.7	78	108	0.438	-1.24
VI-1	"	90	"	15.4	78	79	0.063	-
-2	"	185	"	15.0	78	82	0.156	-
-3	"	570	"	15.6	78	94	0.219	-
-4	"	675	"	15.1	78	97	0.094	-
-5	"	1140	"	15.0	78	109	0.250	-
-6**	"	675	"	15.1	78	95	0.063	-
VII-1	Gray	90	51.32	28.9	76	75	0.078	-
-2	Granite	185	"	29.2	76	76	0.078	-
-3	"	570	"	29.0	76	83	0.125	-
-4	"	675	"	28.8	76	87	0.140	-
-5	"	1140	"	28.5	76	96	0.094	-

*Core broke during this test, run repeated as Test No. IV-1.
**Run as a check on VI-4.

TABLE 1 (Continued)

CORE BIT DATA AND RESULTS

Test Number	Rock	Rotary Speed (RPM)	Average Load (lb)	Air Flow (cfm)	Air Temp. (°F) Input	Air Temp. (°F) Output	Drill Rate (Ft/Hr)	Power (HP)
VIII-1	Gray	90	51.32	15.3	76	77	0.016	-
-2	Granite	185	"	15.3	76	79	0.000	-
-3	"	570	"	15.2	76	94	0.047	-
-4	"	675	"	15.4	76	102	0.094	-
-5	"	1140	"	15.4	76	116	0.063	-
IX-1	Berea	90	50.08	15.6	76	85	0.250	-
-2	Sand-	185	"	15.3	76	86	0.563	-
-3	stone	570	"	15.4	76	90	0.773	-
-4	"	675	"	15.2	76	91	1.59	-
-5	"	1140	"	15.0	76	96	1.92	-
X-1	"	90	49.74	7.4	76	82	0.313	-
-2	"	185	"	7.4	76	83	0.785	-
-3	"	570	"	7.4	76	88	2.23	-
-4	"	675	"	7.3	76	89	1.83	-
-5	"	1140	"	7.5	76	96	2.11	-
XI-1	"	90	49.81	3.5	76	85	0.219	-
-2	"	185	"	3.5	76	86	0.250	-
-3*	"	570	"	3.9	76	90	0.125	-
-4	"	675	"	3.8	76	94	0.965	-
-5	"	1140	"	3.6	77	98	1.21	-
XII-1	Rush	90	49.98	15.7	77	73	0.000	-
-2	Springs	185	"	16.1	77	72	0.000	-
-3	Sand-	570	"	16.1	78	77 [X]	0.031	-
-4	stone	675	"	15.4	77	79	0.031	-
-5	"	1140	"	15.4	77	85	0.000	-

*Core slipped in holder.

[X] Ice used at reference junction on thermocouple melted.

TABLE 2

FULL-HOLE BIT DATA AND RESULTS

Test Number	Rock	Rotary Speed (RPM)	Average Load (lb)	Air Flow (cfm)	Air Temp. (°F) Input	Output	Drill Rate (Ft/Hr)	Power (HP)
XIII-1	Berea Sand-stone	90	49.68	28.4	74	77	0.156	0.08
-2		185	"	28.3	75	78	0.664	0.15
-3		570	"	28.8	75	80	2.14	0.27
-4	"	1140	"	29.1	75	82	4.00	0.67
XIV-1	"	90	112.88	29.0	75	78	0.125	0.05
-2	"	185	"	28.6	75	80	0.125	0.12
-3	"	570	"	28.4	75	85	1.52	0.33
-4	"	1140	"	28.6	75	87	2.80	0.85
XV-1	"	90	49.77	15.4	76	78	0.000	0.09
-2	"	185	"	15.6	76	79	0.031	0.16
-3	"	570	"	15.6	76	85	0.313	0.37
-4	"	1140	"	15.7	76	101	0.656	0.92
XVI-1	"	90	112.88	15.4	76	83	0.031	0.05
-2	"	185	"	15.4	76	85	0.063	0.18
-3	"	570	"	15.1	76	101	0.250	0.38
-4	"	1140	"	15.2	76	126	1.22	1.06
XVII-1	"	90	49.75	7.6	76	85	0.000	0.03
-2	"	185	"	7.6	76	85	0.000	0.17
-3	"	570	"	7.7	76	93	0.063	0.45
-4	"	1140	"	7.7	76	106	0.688	0.73
XVIII-1	"	90	112.99	7.6	76	87	0.000	-0.04
-2	"	185	"	7.5	76	87	0.000	0.13
-3	"	570	"	7.7	76	90	0.000	0.38
-4	"	1140	"	7.4	76	106	0.125	0.93

TABLE 3

ORDER OF TESTS

I	Core Bit	50 lb. load	Berea Sandstone	28 cfm
II	"	"	"	"
III	"	"	"	23 cfm
IV	"	"	"	15 cfm
V	"	"	Rush Spring Sandstone	28 cfm
VI	"	"	"	15 cfm
VII	"	"	Gray Granite	28 cfm
VIII	"	"	"	15 cfm
IX	"	"	Berea Sandstone	15 cfm
X	"	"	"	7.5 cfm
XI	"	"	"	3.8 cfm
XII	"	"	Rush Springs Sandstone	15 cfm
XIII	Full-hole Bit	"	Berea Sandstone	28 cfm
XIV	"	113 lb. load	"	"
XV	"	50 lb. load	"	15 cfm
XVI	"	113 lb. load	"	"
XVII	"	50 lb. load	"	7.5 cfm
XVIII	"	113 lb. load	"	"

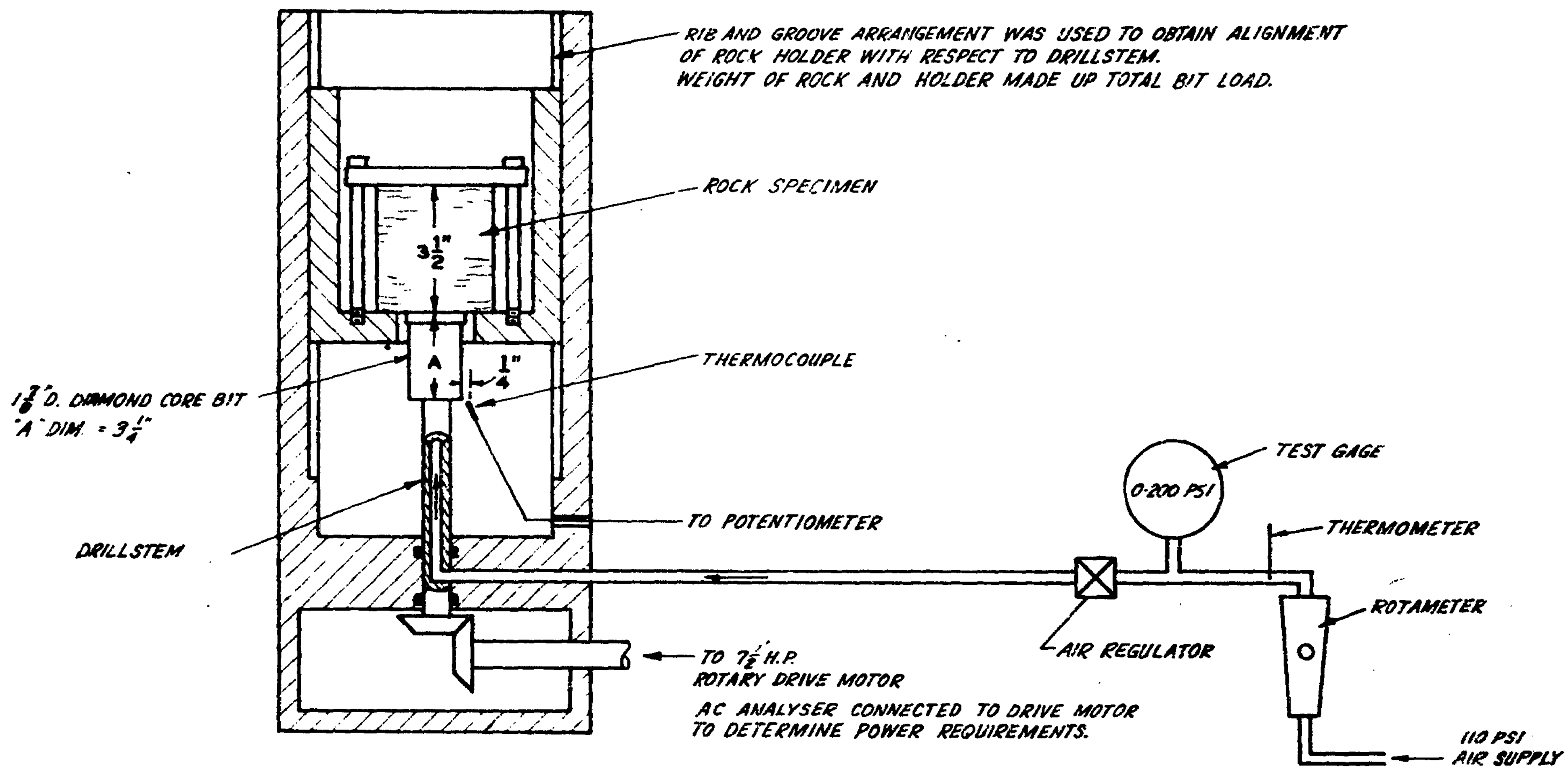

SCHEMATIC SHOWING SETUP DURING TEST WITH DIAMOND CORE BIT.

FIGURE 1

LJ 17530-2

G-15

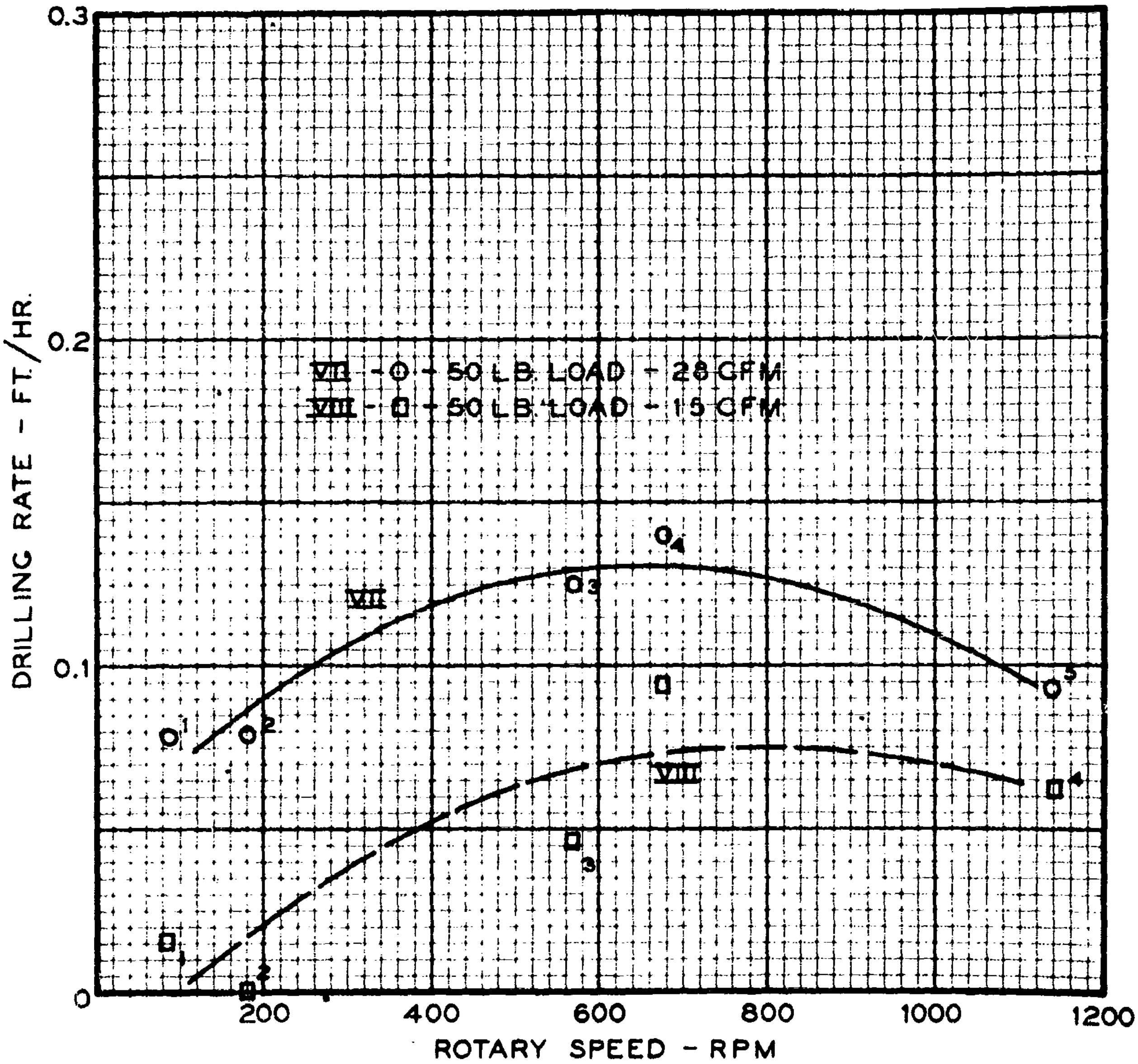

CORE BIT - GRAY GRANITE

FIGURE 2

LJ 17530-2
8-18-60 EPW

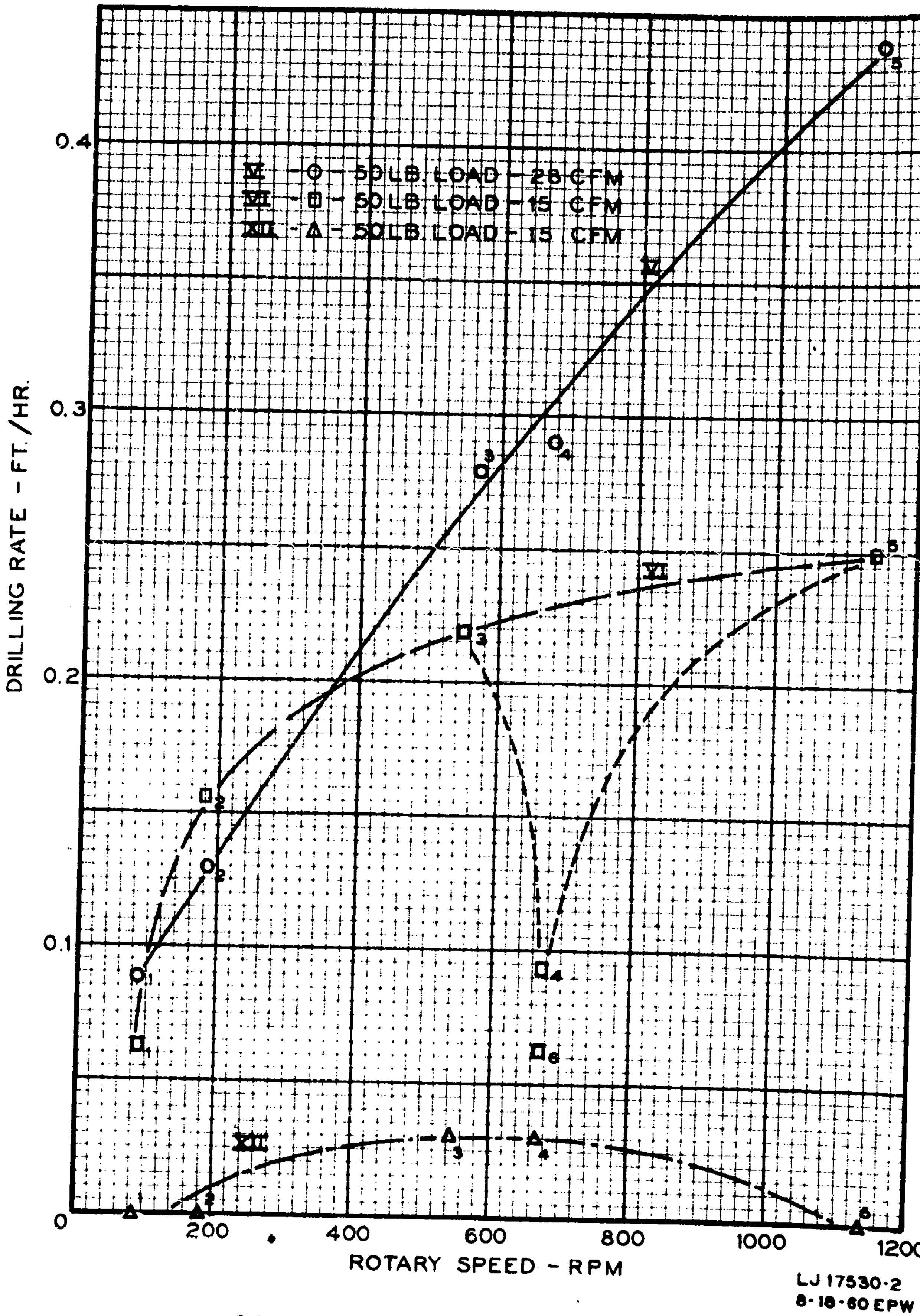

CORE BIT - RUSH SPRINGS SANDSTONE

FIGURE 2A

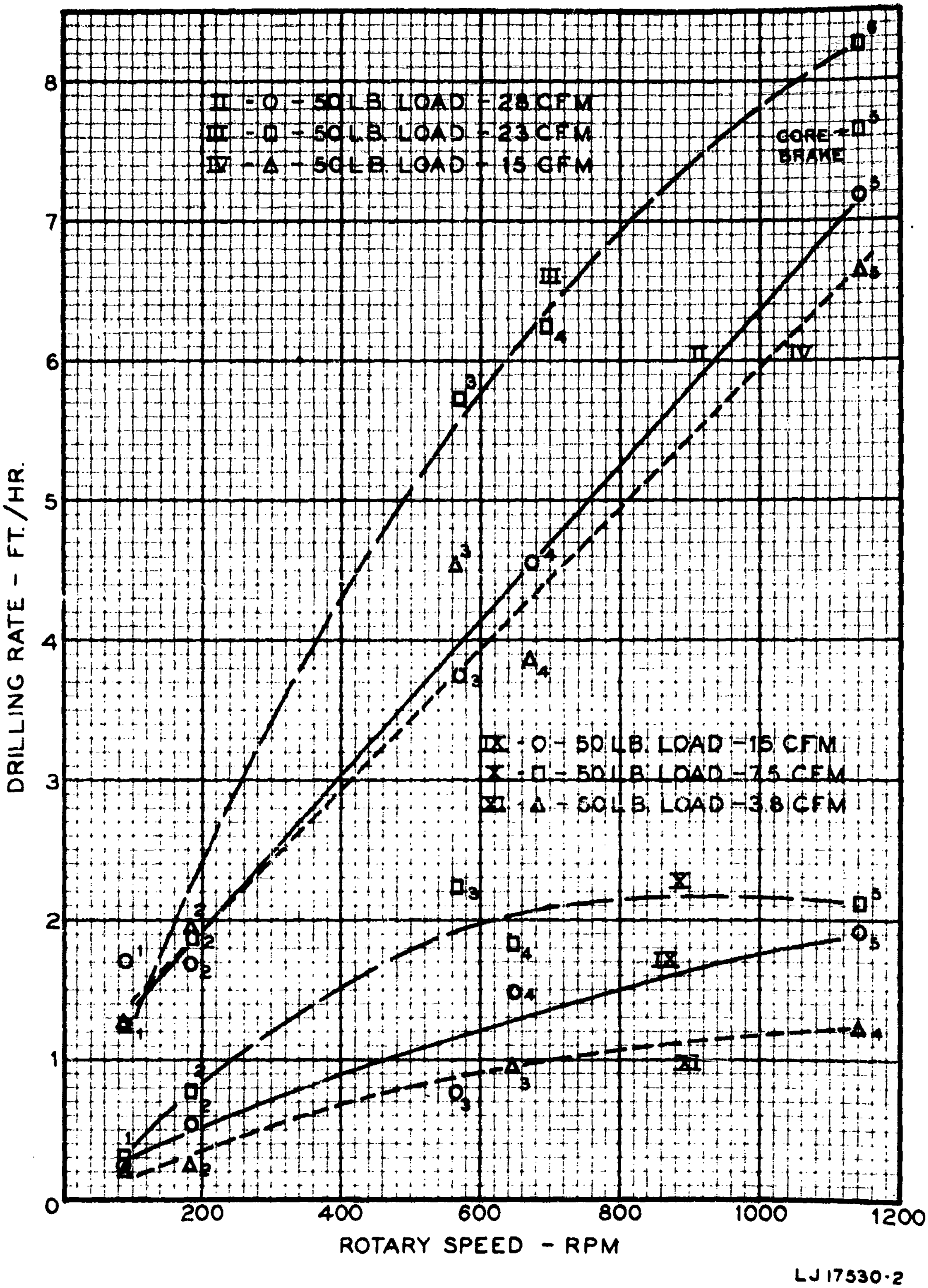

LJ 17530-2
8-18-60 EPW

CORE BIT - BEREA SANDSTONE

FIGURE 2B

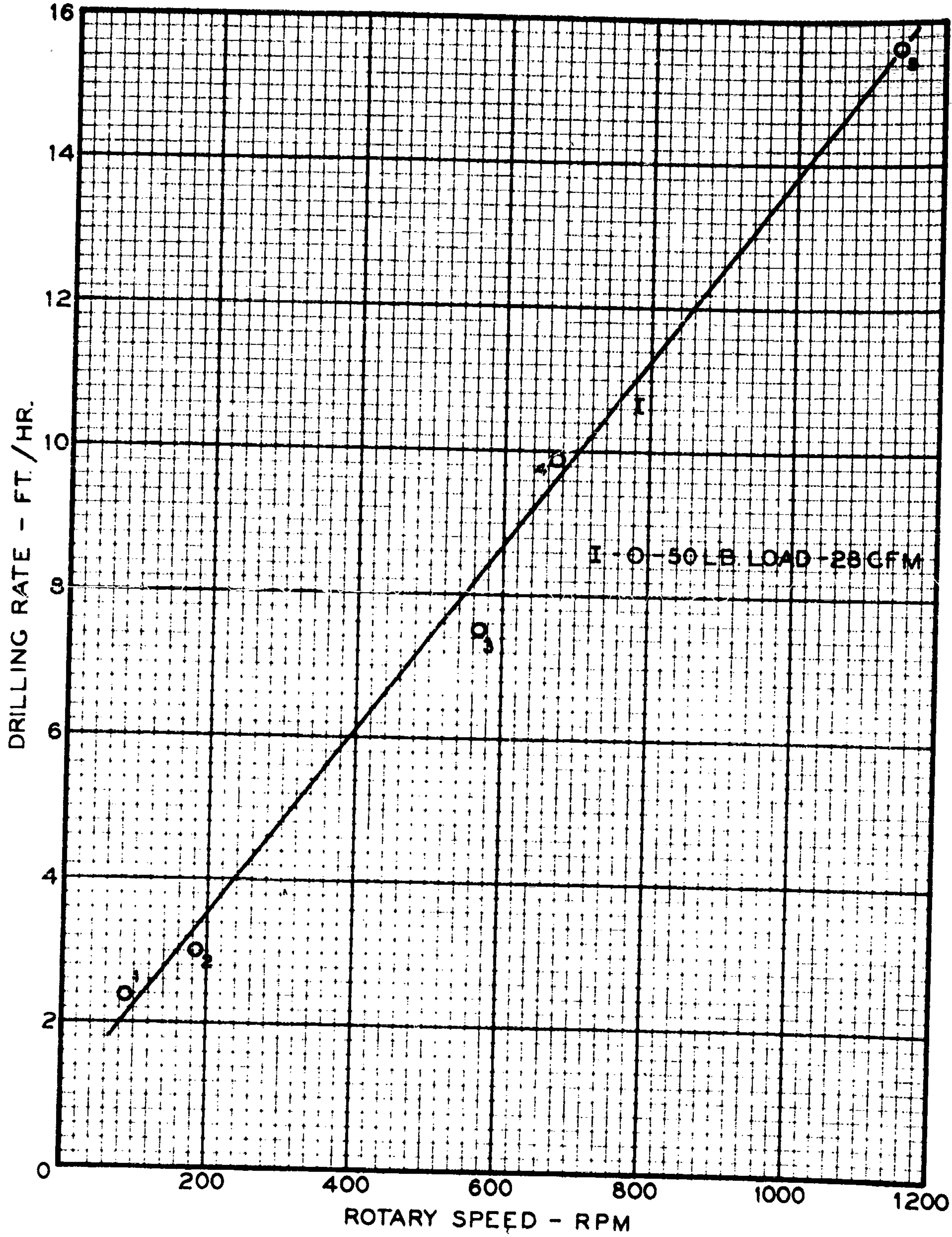

CORE BIT - BEREA SANDSTONE

FIGURE 2C

LJ 17530-2
8-18-60 EPW

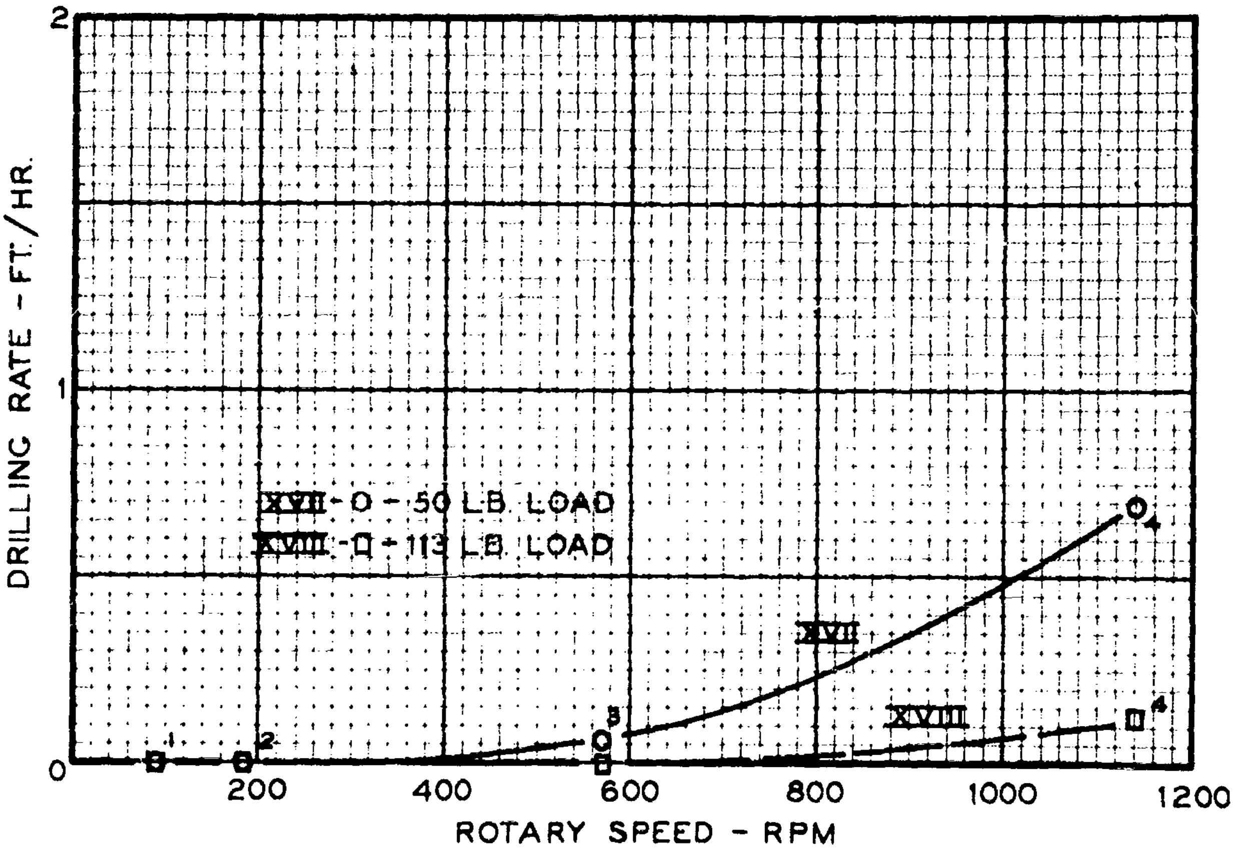

FULL HOLE BIT
BEREA SANDSTONE
7.5 CFM

LJ 17530-2
8-18-60 EPW

FIGURE 3

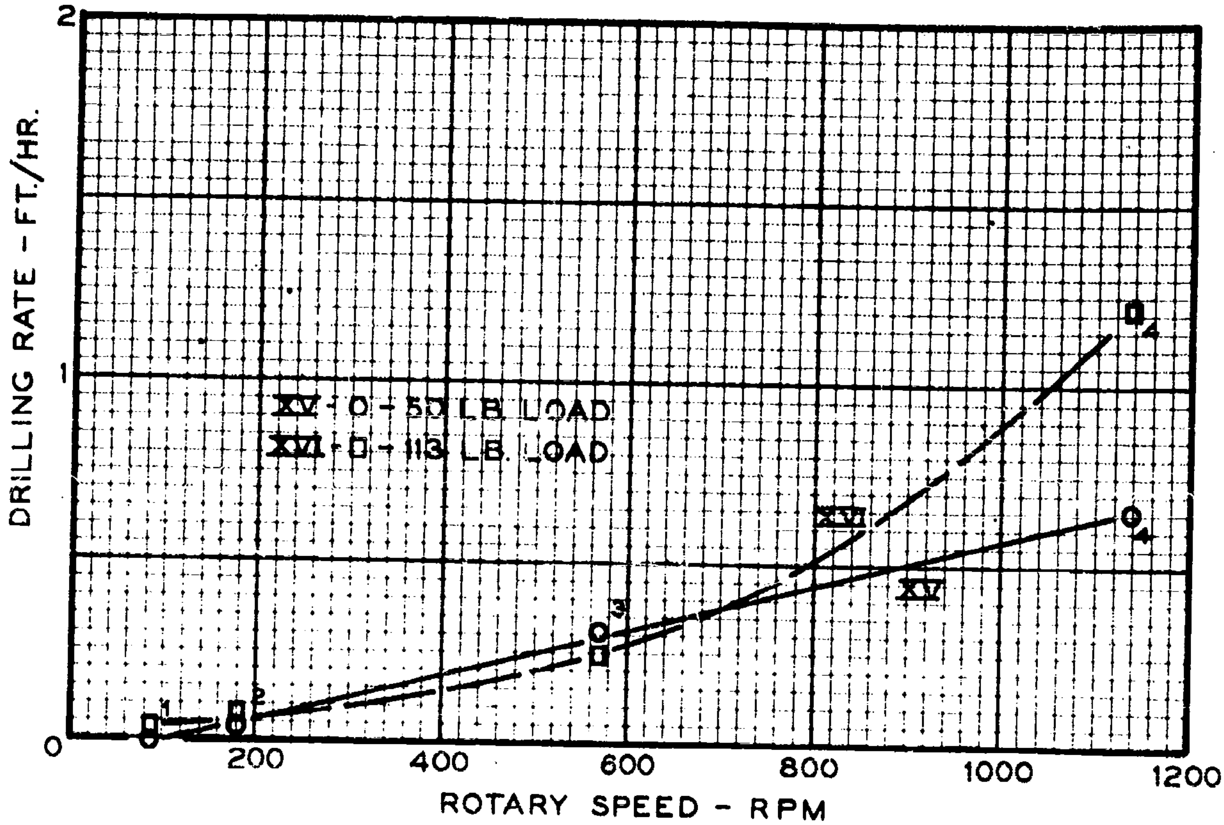

FULL HOLE BIT
BEREA SANDSTONE
15 CFM

LJ 17530-2
8-18-60 EPW

FIGURE 3A

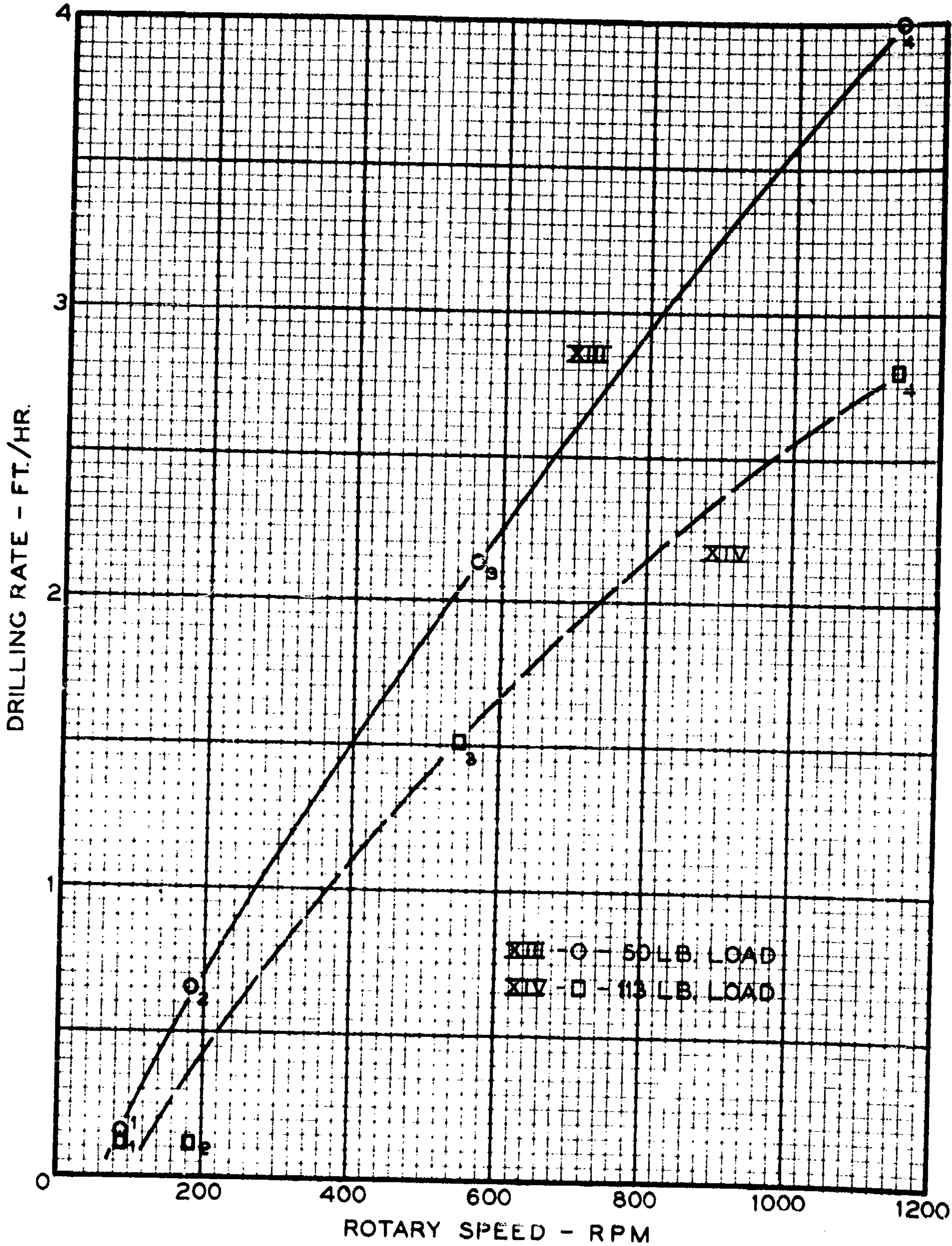

FULL HOLE BIT
BEREA SANDSTONE
28 CFM

FIGURE 3B

LJ 17530-2
8-18-60 EPW

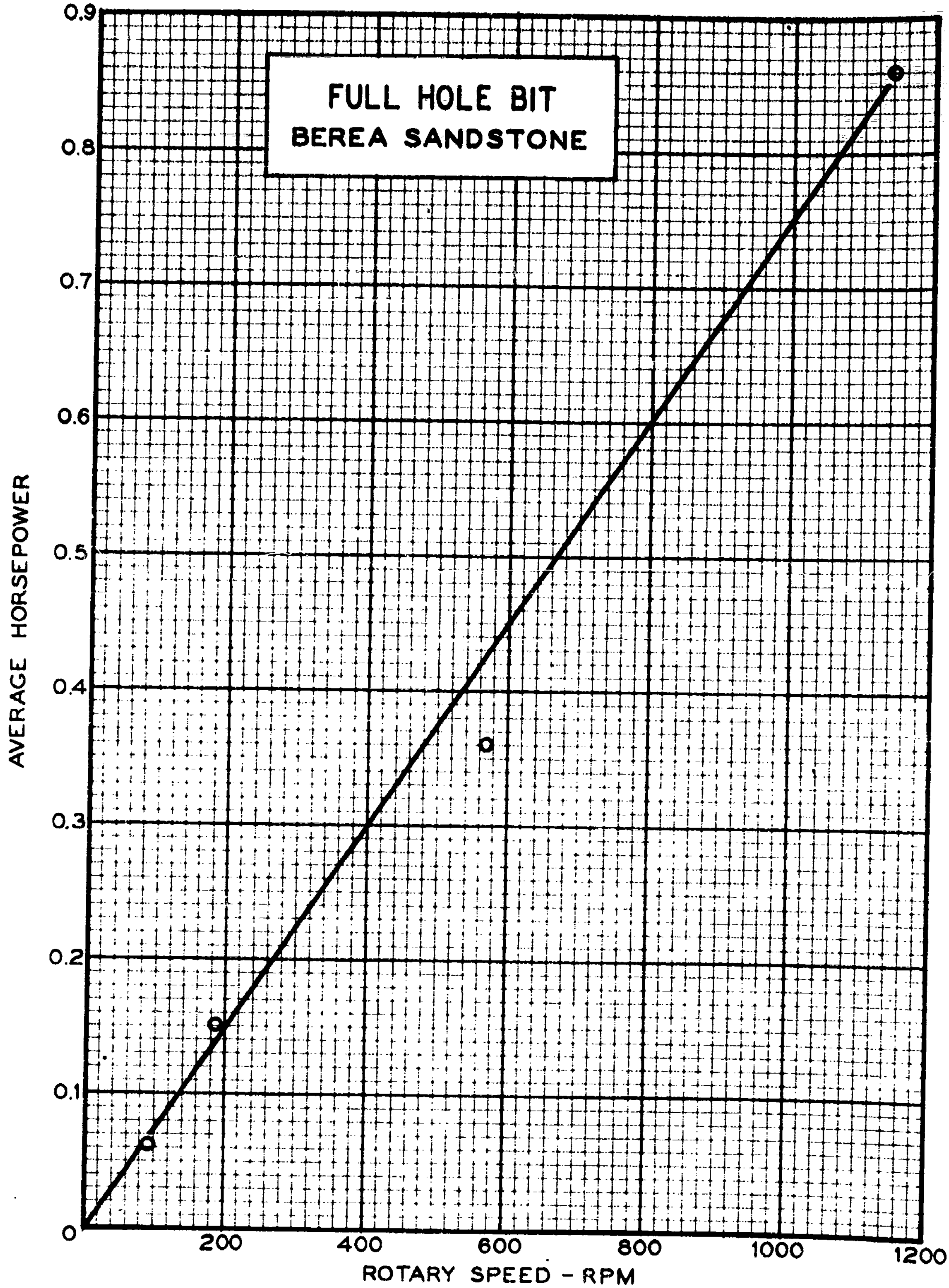

LJ 17530-2
8-18-60 EPW

FIGURE 4

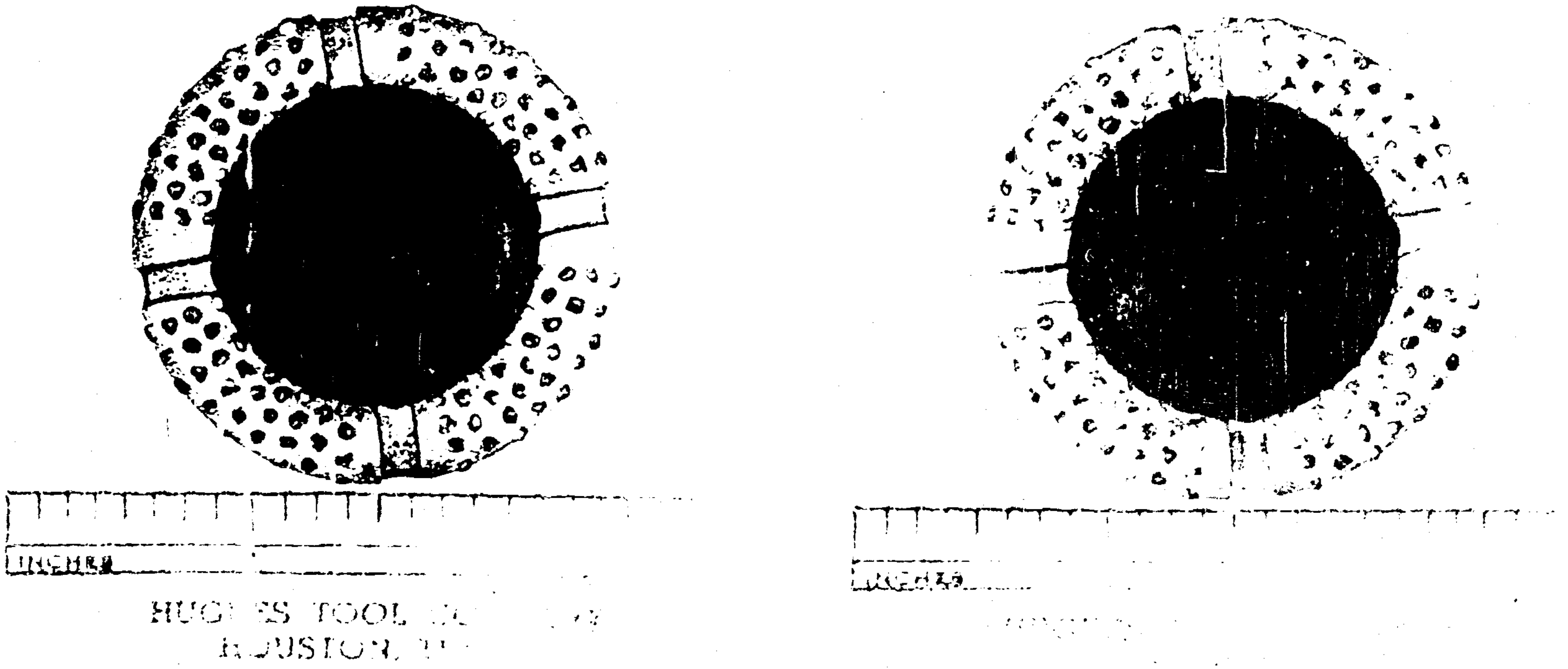

FIGURE 5

6-24

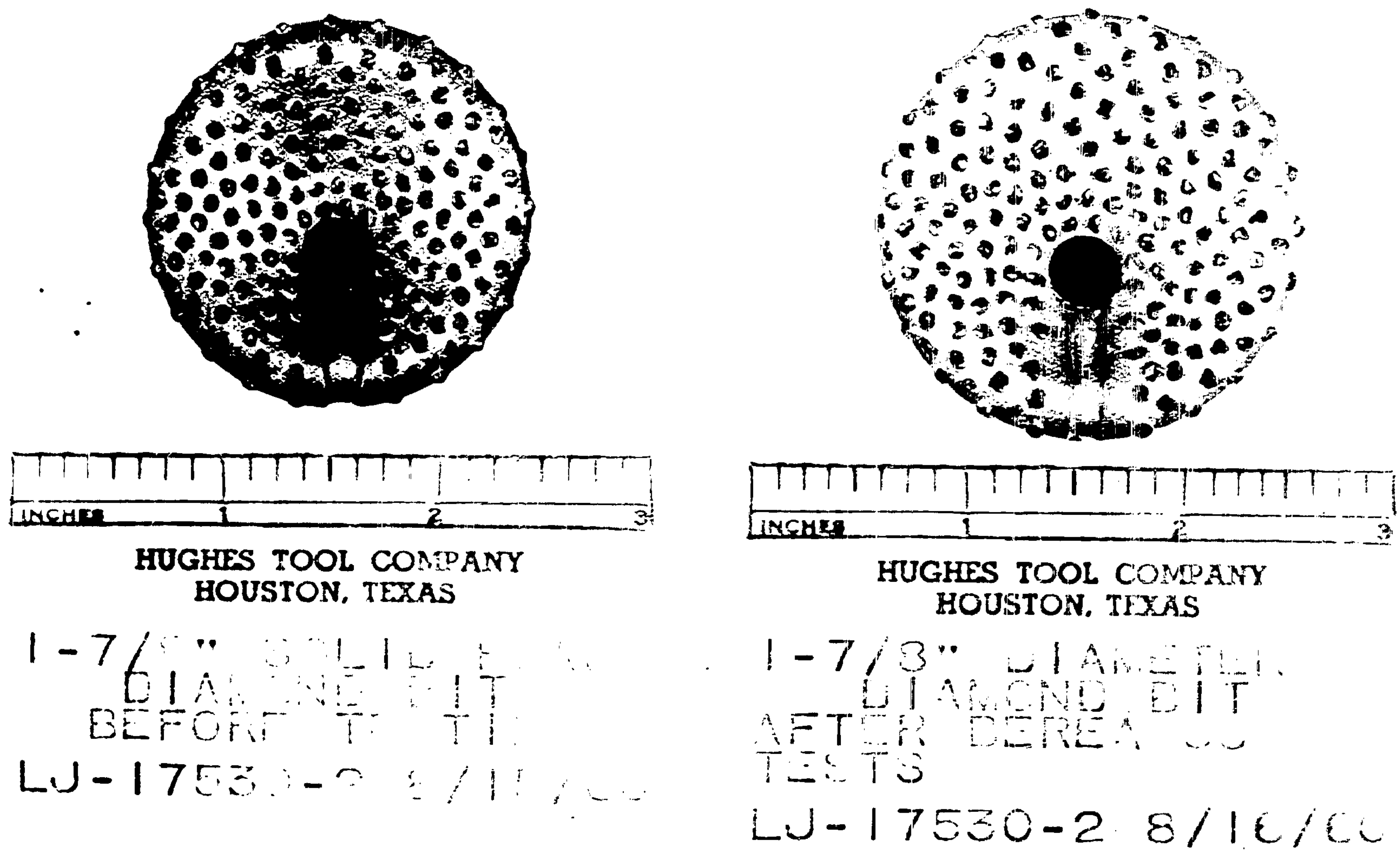

Full-Hole Bit Before and After Testing on Berea Sandstone

G-25

HUGHES TOOL COMPANY

LABORATORY REPORT

August 25, 1960

TO: S. C. Berube

cc: P. G. Reeve (2)
T. N. Williamson (3)
F. A. McCormick
E. M. Galle
G. O. Atkinson
G. R. King
J. G. Fenink
J. G. Stephenson

SUBJECT: Jackhammer Tests On Harris Granite, Rush Springs Sandstone And Berea Sandstone.

REF.: Verbal Request from S. C. Berube, 8-1-60.

L.J. 17530-2

Project 40021 FN-64

Job Open

INTRODUCTION:

This laboratory job is part of the moon drill study. It was set up to investigate the feasibility of drilling a hole to a depth of 8-10 ft. on the moon using a percussor drill driven by a container of compressed gas.

OBJECT:

The object of this laboratory job is to perform drilling tests on Harris Granite, Rush Springs Sandstone and Berea Sandstone to determine:

1. Drilling rate using a percussor drill operated by air and helium.

2. Flow rate of gas used to operate the percussor drill.

PERCUSSOR:

An Ingersoll-Rand J10A jackhammer and three bit sizes were used to perform the drilling tests on this job. The bit sizes were 3/4", 1" and 1-1/4" diameter. All three bits had tungsten carbide insets in the cutting head. The 3/4" and 1" bits were chisel type. The 1-1/4" bit was a cross point. General information on the jackhammer and bits is listed in Table I.

Tests were made to determine jackhammer operating speed, blows per minute, with air and helium. Air flowing through the jackhammer at rates of 10-25 CFM, S.T.P., resulted in speeds of 1980-2280 BPM for the 3/4" bit, 1920-2280 BPM for the 1" bit and 1740-2040 BPM for the 1-1/4" bit.

G-26

Helium flows of 25-50 CFM, S.T.P., resulted in speeds of 1920-2280 BPM for the 3/4" drill. Recordings made during the tests to determine blows per minute indicated that the blows using helium did not occur as uniformly as with air.

Air flow rates resulting from jackhammer operating pressures of 15-58 PSI are shown graphically in Figure 1. Helium flow rates resulting from the same operating pressures were 2.4-2.6 times greater.

FLOW METER:

A Schutte and Koerting #4 HCFB-1/2" SK18210 rotameter was purchased and used to determine gas flow through the jackhammer. Rotameter capacity with S.T.P. gas, 70°F and 14.7 PSIA, is 11.6 CFM.

ROCKS:

Blocks of Harris Granite, Rush Springs Sandstone and Berea Sandstone were used for these tests. All tests on each type of rock were made on a single block of the particular formation, in order to obtain maximum rock uniformity from hole to hole.

RESULTS:

An attempt was made to maintain a constant jackhammer bit load during these tests. Bit load consisted of the weight of the jackhammer and bit plus an estimated force of 10-15 pounds applied by the operator.

Preliminary tests were made with helium and nitrogen to determine if gas flow rate could satisfactorily be determined without the use of a flow meter. Volume rate of flow was determined by relating the decrease in bottle pressure which occurred during a drilling interval to the volume of gas contained in the bottle. Since viscosity and specific weight of nitrogen is practically the same as for air, the plans were to determine nitrogen flow rates under various conditions and assume air flows to be the same under similar conditions. Satisfactory flow rate determinations were not obtained by this procedure. The results of the preliminary tests, 1-14, are listed in Table II.

Results of tests using the 3/4", 1" and 1-1/4" bits are listed in Tables III, IV and V, respectively. Drilling rate, gas flow rate, pounds of gas per inch of hole depth, pounds of gas per cubic inch of rock removed and cubic feet of gas per inch of hole depth are listed in Tables III, IV and V for each test.

Drilling rate as related to jackhammer gas consumption is shown graphically for Harris Granite, Rush Springs Sandstone and Berea Sandstone in Figures 2, 3 and 4, respectively. Jackhammer operating pressure can be related to the curves in Figures 2, 3 and 4 by referring to Figure 1.

G-27

Cubic feet of gas per inch of hole depth is plotted against jackhammer air flow, or operating pressure which is directly related to flow, as an aid to determining the optimum flow related to all three formations tested. Plots for the 3/4", 1" and 1-1/4" bits appear in Figures 5, 6 and 7, respectively.

For example in Figure 1, the optimum jackhammer air flow for the 3/4" bit would be about 18 CFM or more when considering the moon drilling problem from the point of view that the rocks encountered may be similar to Berea, Rush Springs or Harris Granite.

Manufacturers recommended operating pressure for the jackhammer is 80-100 PSI. Due to the setup used during these tests the maximum operating pressure obtained was about 65 PSI.

Two intervals of depth were drilled in Harris Granite using jackhammer operating pressures of 70 and 103 PSI. The rotameter and accessory equipment were removed from the setup in order to obtain operating pressures above 65 PSI. Drilling rate with the 3/4" bit at 70 and 103 PSI was 27.5 and 38.7 ft./hr., respectively.

A request was made to drill Berea Sandstone with the jackhammer using 5 pounds bit load. The jackhammer was suspended in the drilling position by use of springs, a scale and a rope and pulley arrangement. A motion picture was taken of this drilling operation. No data was taken.

ATTACHMENTS:

Table I - General Information On Jackhammer And Bits

Table II - Preliminary Jackhammer Tests

Table III - Results Of Jackhammer Drilling Tests Using A 3/4" Bit

Table IV - Results Of Jackhammer Drilling Tests Using A 1" Bit

Table V - Results Of Jackhammer Drilling Tests Using A 1-1/4" Bit

Figure 1 - Effect Of Operating Pressure On Air Consumption Of J10A Jackhammer

Figure 2 - Effect Of Jackhammer Gas Consumption On Drilling Rate Of Harris Granite

Figure 3 - Effect Of Jackhammer Gas Consumption On Drilling Rate Of Rush Springs Sandstone

Figure 4 - Effect Of Jackhammer Gas Consumption On Drilling Rate Of Berea Sandstone

Figure 5 - Effect Of Jackhammer Gas Flow Rate On Gas Requirements Per Inch Of Hole Depth Using A 3/4" Bit

Figure 6 - Effect Of Jackhammer Gas Flow Rate On Gas Requirements Per Inch Of Hole Depth Using A 1" Bit

Figure 7 - Effect Of Jackhammer Gas Flow Rate On Gas Requirements Per Inch Of Hole Depth Using A 1-1/4" Bit

CONCLUSIONS:

1. Penetration rate varied according to bit size and formation. Increases in bit size were accompanied by decreases in penetration rate and increases in volume of gas required to drill an inch of hole depth. Increases in formation hardness had the same general effect as increases in bit size.

2. From the standpoint of volume rate of flow, air had an advantage over helium as an operating gas for the jackhammer. From the standpoint of operating pressure at the jackhammer, the use of helium resulted in a higher penetration rate than air at the same pressures. Results indicate that air, or perhaps a heavier gas, would be desirable for a moon drilling project of this type.

3. Indications are that a percussor type drilling operation would be feasible for moon drilling application

J. G. Stephenson J. M. Edwards

J. G. STEPHENSON AND J. M. EDWARDS,
METALLURGICAL DEPARTMENT, LABORATORY.

JGS & JME/bsr

TABLE I

GENERAL INFORMATION ON JACKHAMMER AND BITS

		Wgt.	Length (overall)
3/4"	Chisel Steel	1.88#	13-5/8"
1"	Chisel Steel	2.16#	13-7/8"
1-1/4"	Cross Bit With Steel	5.61#	31-3/8"
1-1/4"	Cross Bit Without Steel	0.43#	-

Wgt. of Entire Drill	15.66#	
Wgt. of Handle Assembly (including part #260J10A)	3.22#	
Bore		1.874"
Stroke		2.062"*
Piston Wgt.	1.595#	

*Approx. effective stroke 1.812".

G-30

TABLE II

PRELIMINARY JACKHAMMER DRILLING TESTS

Test No.	Type of Rock	Nominal Bit Size	Gas	Drilling Rate Ft/Hr	Gas Flow Ft^3/Min*	Lbs Gas Per In Of Depth	Lbs Gas Per In^3 Of Rock	Ft^3 Gas Per In Of Depth
1	Harris Granite	3/4"	Air	28.8	-	-	-	-
2			Helium	37.6	57.3	.079	.156	7.6
3			Nitrogen	20.1	25.9	.486	.962	6.9
4			Helium	32.2	70.8	.112	.238	6.7
5			Nitrogen	9.2	13.6	.537	1.06	7.4
6			Helium	15.4	29.4	.099	.196	9.6
7			Nitrogen	12.3	17.5	.513	1.01	7.1
8			Helium	20.3	39.1	.100	.198	9.6
9			Air	24.6	-	-	-	-
10			Air	22.3	-	-	-	-
11			Air	17.4	-	-	-	-
12			Helium	26.7	37.1	072	.143	7.0
13			Nitrogen	14.4	17.2	430	.852	5.9

*Gas Flow at 14.7 PSIG & 70°F

L.J. 17530-2

TABLE III

RESULTS OF JACKHAMMER DRILLING TESTS USING A 3/4" BIT

Test No.	Type Of Rock	Gas	Drilling Rate Ft/Hr	Gas Flow 70°F 14.7 PSIA CFM	Lbs Gas Per In Of Depth	Lbs Gas Per In^3 Of Rock Removed	Ft^3 Gas Per In Of Depth
14	Harris Granite	Air	5.2	10.1	.68	1.33	9.7
15			9.0	12.0	.48	.95	6.6
16			13.6	13.7	.35	.69	5.0
17			17.4	15.7	.32	.63	4.5
18			21.6	17.3	.28	.55	4.0
19			18.2	18.2	.35	.69	5.0
20			24.7	18.2	.26	.51	3.0
44(1)			25.8	17.2	.36	.41	5.1
58	Rush Springs Sand-stone	Air	24.6	15.8	.22	.41	3.22
59			27.7	19.2	.24	.45	3.47
60			34.9	22.4	.22	.41	3.20
61			37.5	25.1	.23	.43	3.34
62			40.6	25.6	.22	.41	3.16
38	Berea Sand-stone	Air	32.8	10.2	.109	.215	1.56
39			47.5	12.1	.089	.175	1.27
40			50.6	13.8	.094	.185	1.35
41			69.4	15.9	.080	.158	1.14
42			80.5	17.5	.075	.148	1.08
43			91.6	18.8	.071	.140	1.02
32	Harris Granite	Helium	10.4	24.8	.119	.233	11.9
33			14.4	29.7	.103	.202	10.3
34			19.1	34.0	.089	.174	8.9
35			22.5	38.5	.085	.166	8.5
36			27.8	44.2	.079	.155	7.9
37			29.7	49.8	.084	.165	8.4

(1) Tungsten carbide inset was relieved by grinding away some of the surrounding steel.

TABLE IV

RESULTS OF JACKHAMMER DRILLING TESTS USING A 1" BIT

Test No.	Type of Rock	Gas	Drilling Rate Ft/Hr	Gas Flow 70°F 14.7 PSIA CFM	Lbs Gas Per In Of Depth	Lbs Gas Per In^3 Of Rock Removed	Ft^3 Gas Per In Of Depth
21	Harris Granite	Air	4.2	10.3	.85	.95	12.2
22			6.1	12.0	.69	.78	9.6
23			6.6	13.9	.74	.84	10.5
24			10.1	15.7	.55	.62	7.8
25			9.4	17.1	.64	.72	9.1
26			8.9	18.2	.71	.80	10.2
45(1)			17.0	17.2	.36	.41	5.1
63	Rush Springs Sand-stone	Air	10.7	15.8	.52	.58	7.39
64			13.4	19.1	.49	.54	7.12
65			15.3	22.3	.51	.57	7.27
66			19.4	25.4	.46	.51	6.55
46	Berea Sand-stone	Air	20.9	10.2	.171	.197	2.44
47			30.2	12.1	.140	.161	2.00
48			36.2	13.8	.133	.158	1.90
49			46.3	15.6	.118	.136	1.69
50			54.2	17.6	.113	.130	1.62
51			62.7	18.6	.104	.120	1.49

(1) Tungsten carbide inset was relieved by grinding away some of the surrounding steel.

G-33

TABLE V

RESULTS OF JACKHAMMER DRILLING TESTS USING A 1-1/4" BIT

Test No.	Type of Rock	Gas	Drilling rate Ft/Hr	Gas Flow 70°F 14.7 PSIA CFM	Lbs Gas Per In Of Depth	Lbs Gas Per In3 Of Rock Removed	Ft^3 Gas Per In Of Depth
27	Harris Granite	Air	1.4	10.3	2.59	1.84	37.8
28			1.4	12.0	3.00	2.14	42.8
29			.9	13.7	5.12	3.64	73.0
30			1.2	15.5	4.64	3.30	66.3
31			1.4	16.4	4.10	2.85	57.1
67	Rush Springs Sand-stone	Air	3.13	16.6	1.86	1.33	26.6
68			2.82	20.0	2.49	1.78	35.6
69			4.75	24.0	1.77	1.26	25.2
70			5.94	25.8	1.53	1.09	21.8
52	Berea Sand-stone	Air	11.1	10.5	.332	.231	4.75
53			8.1	12.3	.238	.116	3.40
54			15.6	14.1	.316	.210	4.52
55			13.5	15.8	.409	.284	5.83
56			18.6	17.5	.330	.230	4.72
57			19.4	18.5	.334	.232	4.77

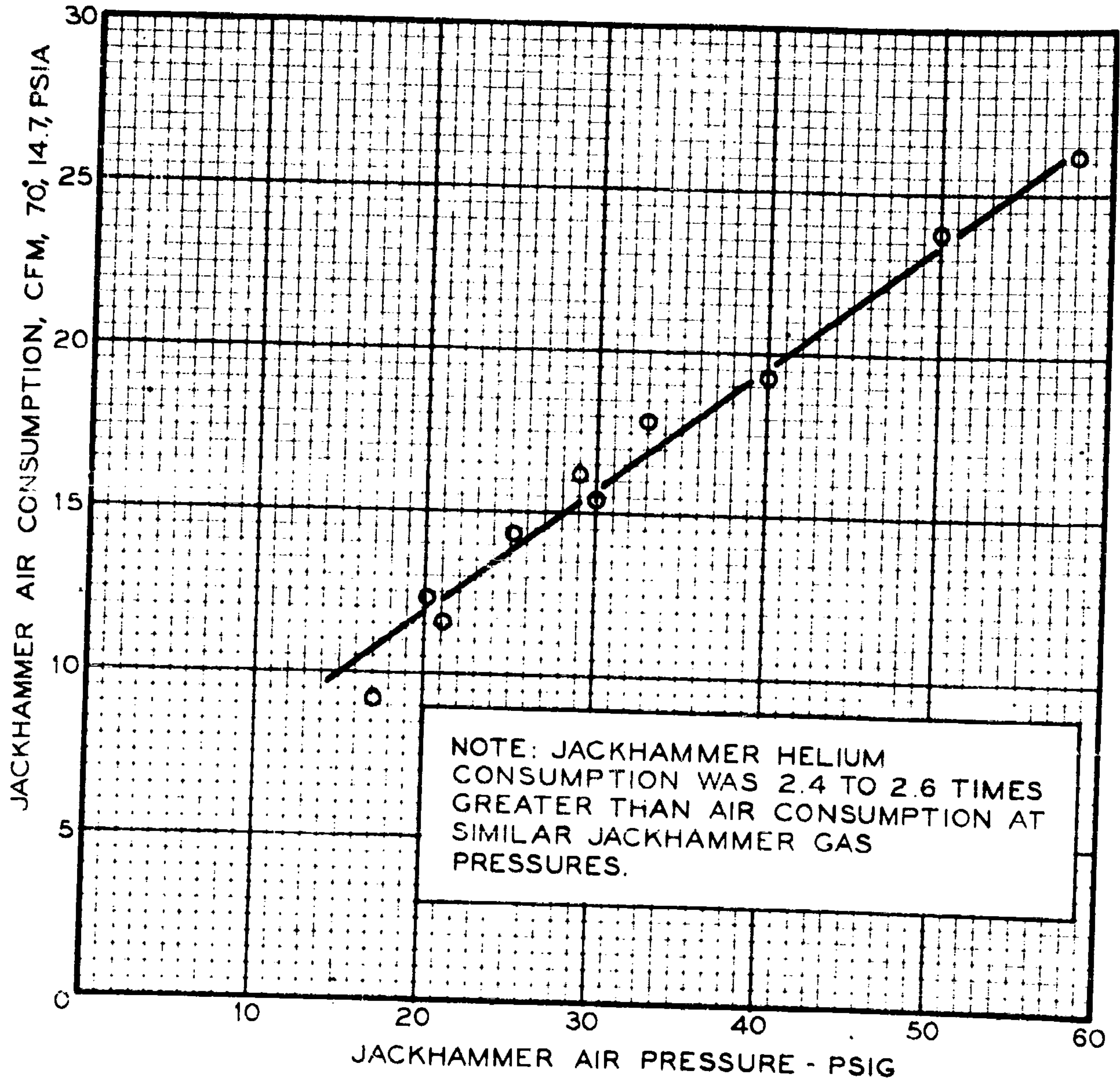

EFFECT OF OPERATING PRESSURE
ON AIR CONSUMPTION
OF J 10 A JACKHAMMER

FIGURE 1

LJ 17530-2
8-19-60 JME

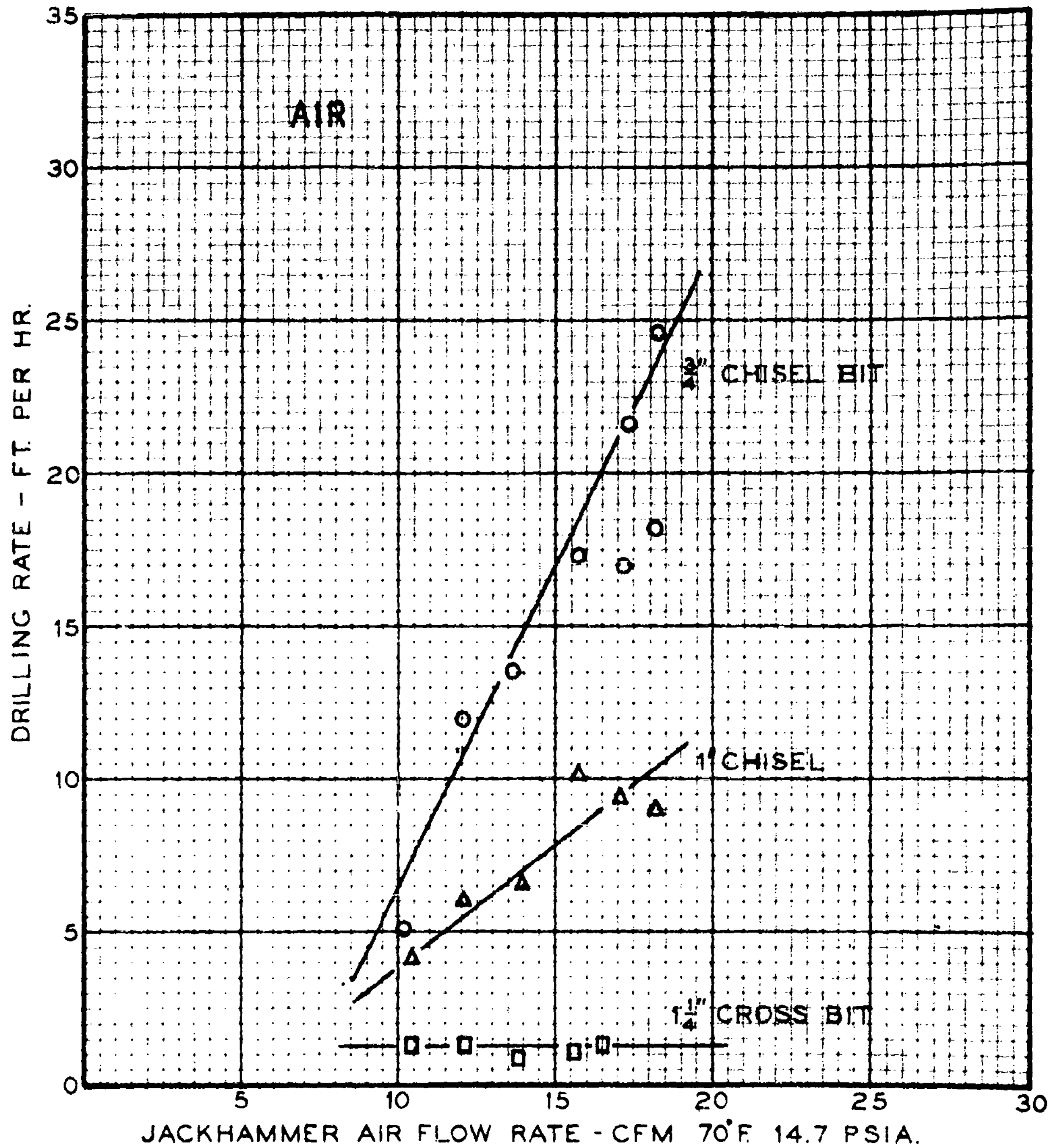

EFFECT OF JACKHAMMER
GAS CONSUMPTION ON DRILLING
OF HARRIS GRANITE

FIGURE 2

LJ 17530-2
8-23-60 JGS

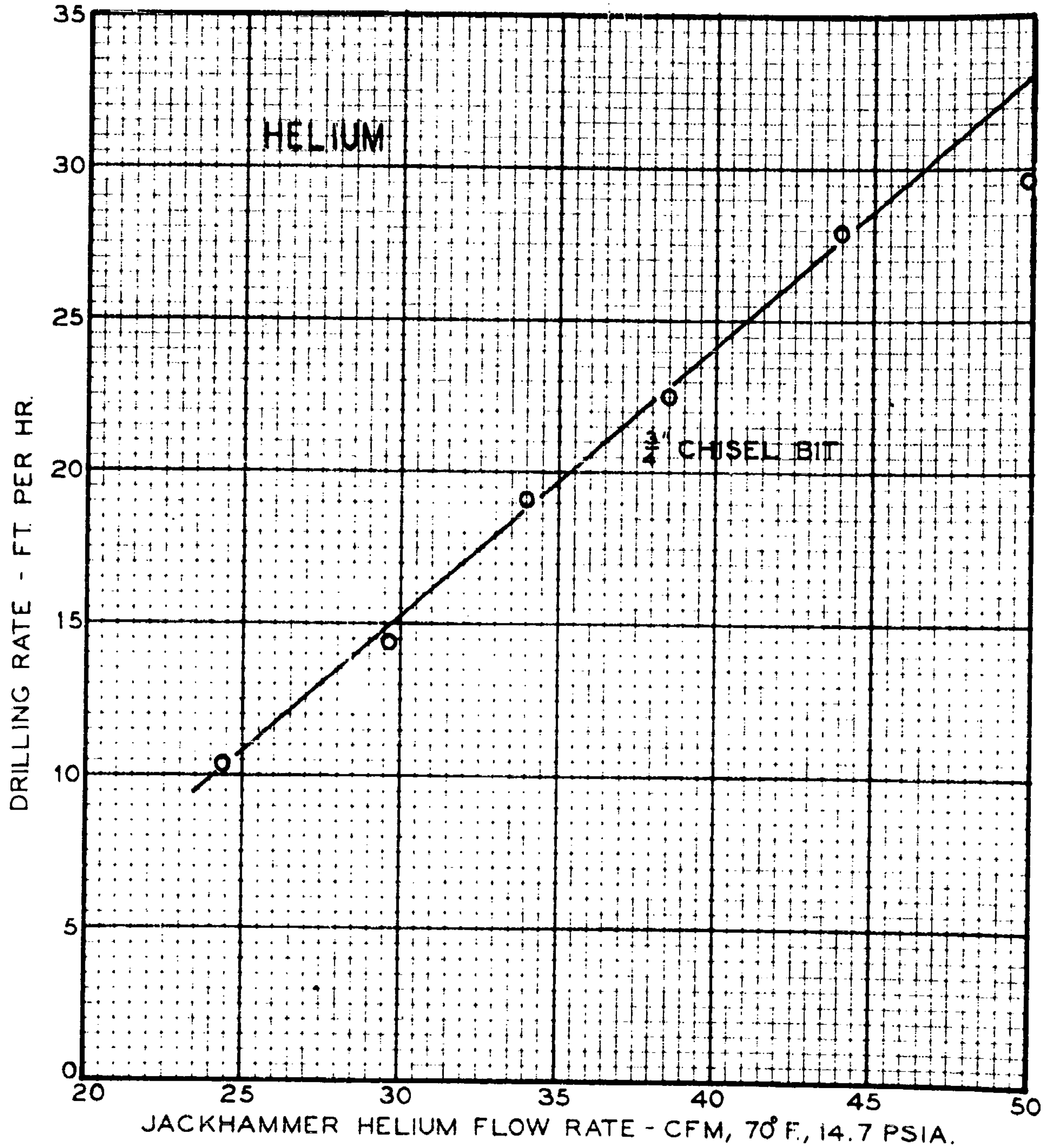

EFFECT OF JACKHAMMER
GAS CONSUMPTION ON DRILLING
OF HARRIS GRANITE

FIGURE 2A

LJ 1753-2
8-23-60 JGS

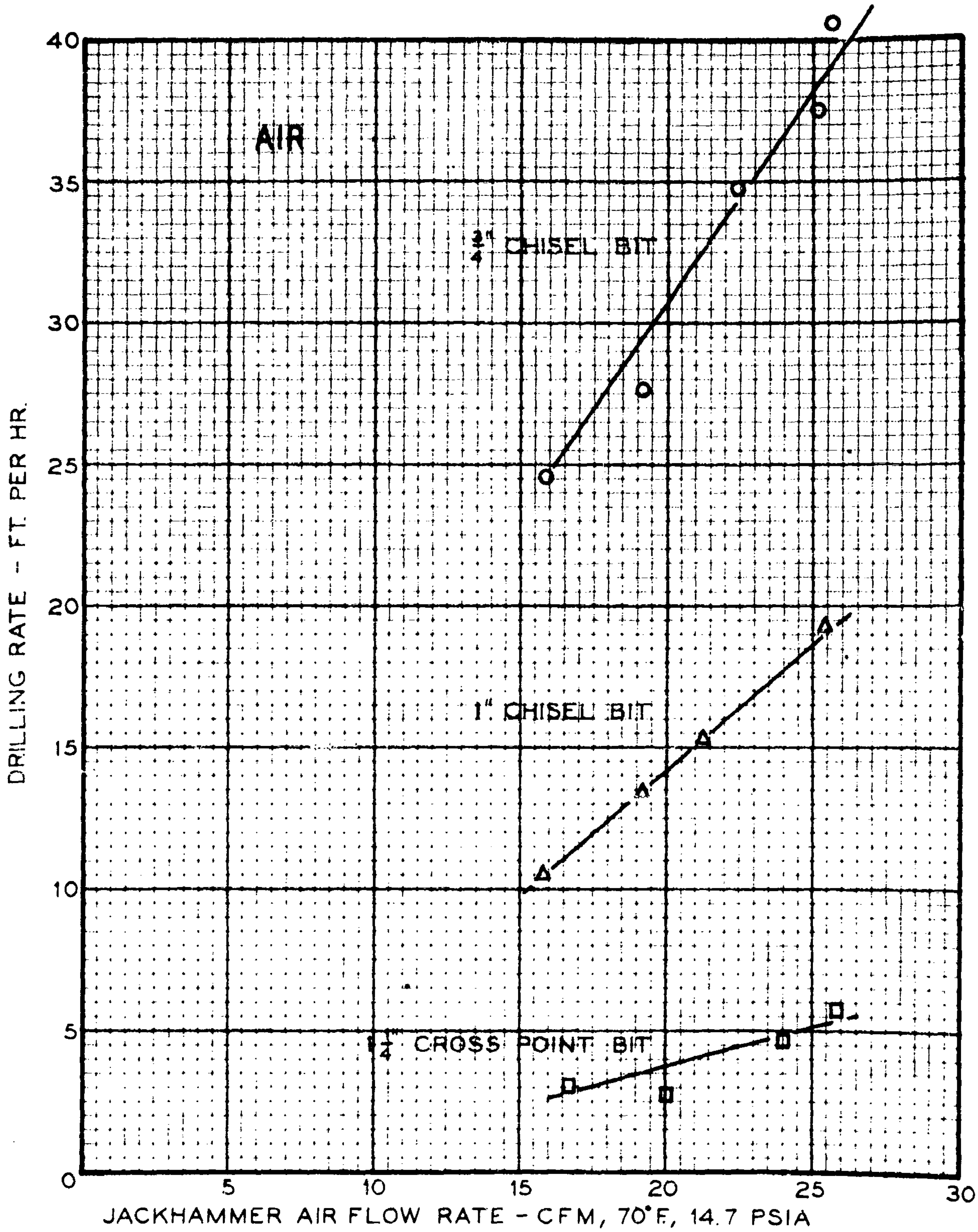

EFFECT OF JACKHAMMER GAS CONSUMPTION ON DRILLING RATE OF RUSH SPRINGS SANDSTONE

FIGURE 3

LJ17530-2
8-23-60 JGS

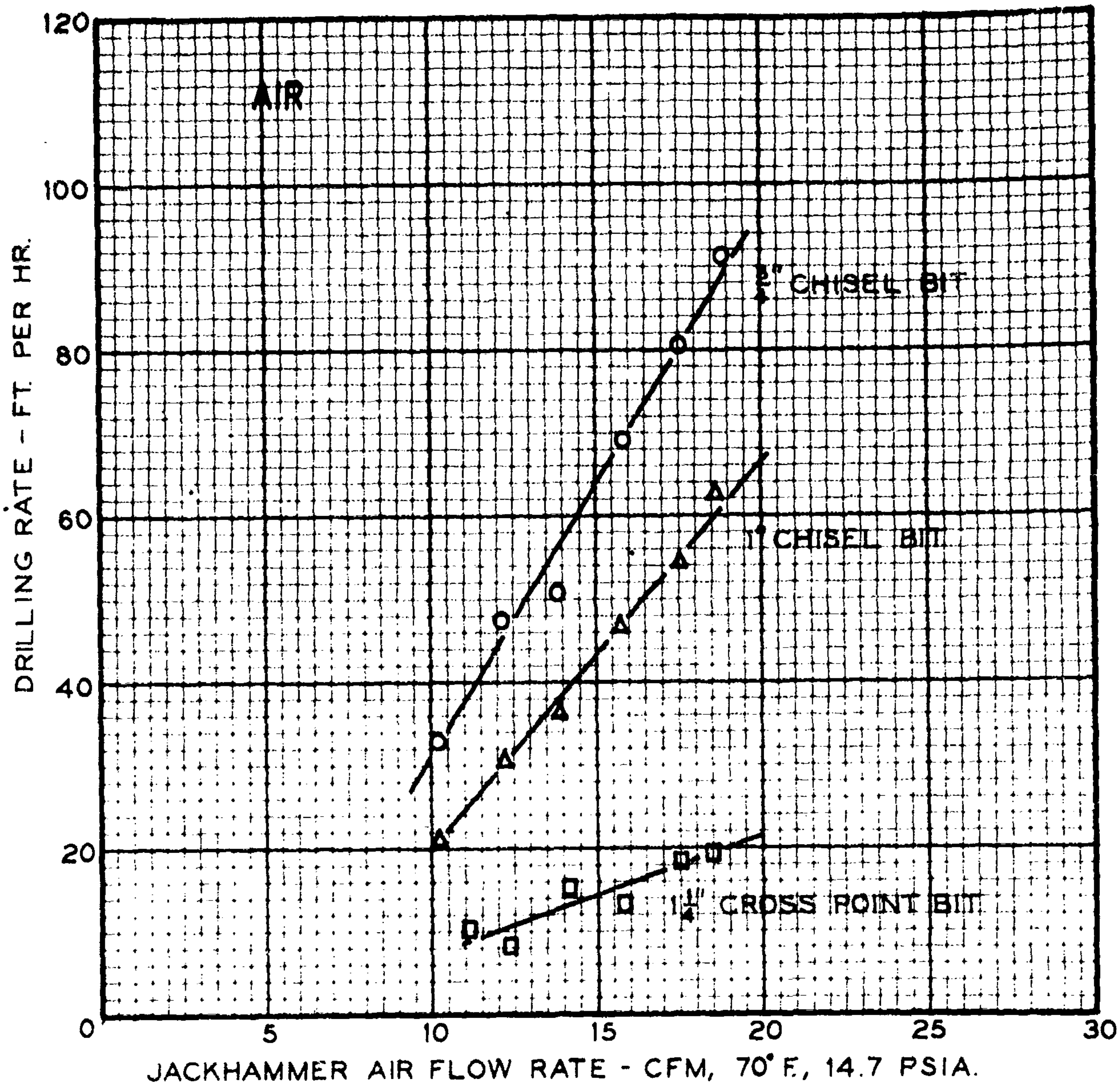

EFFECT OF JACKHAMMER GAS CONSUMPTION ON DRILLING RATE OF BEREA SANDSTONE.

LJ 17530-2
8-23-60 JGS

FIGURE 4

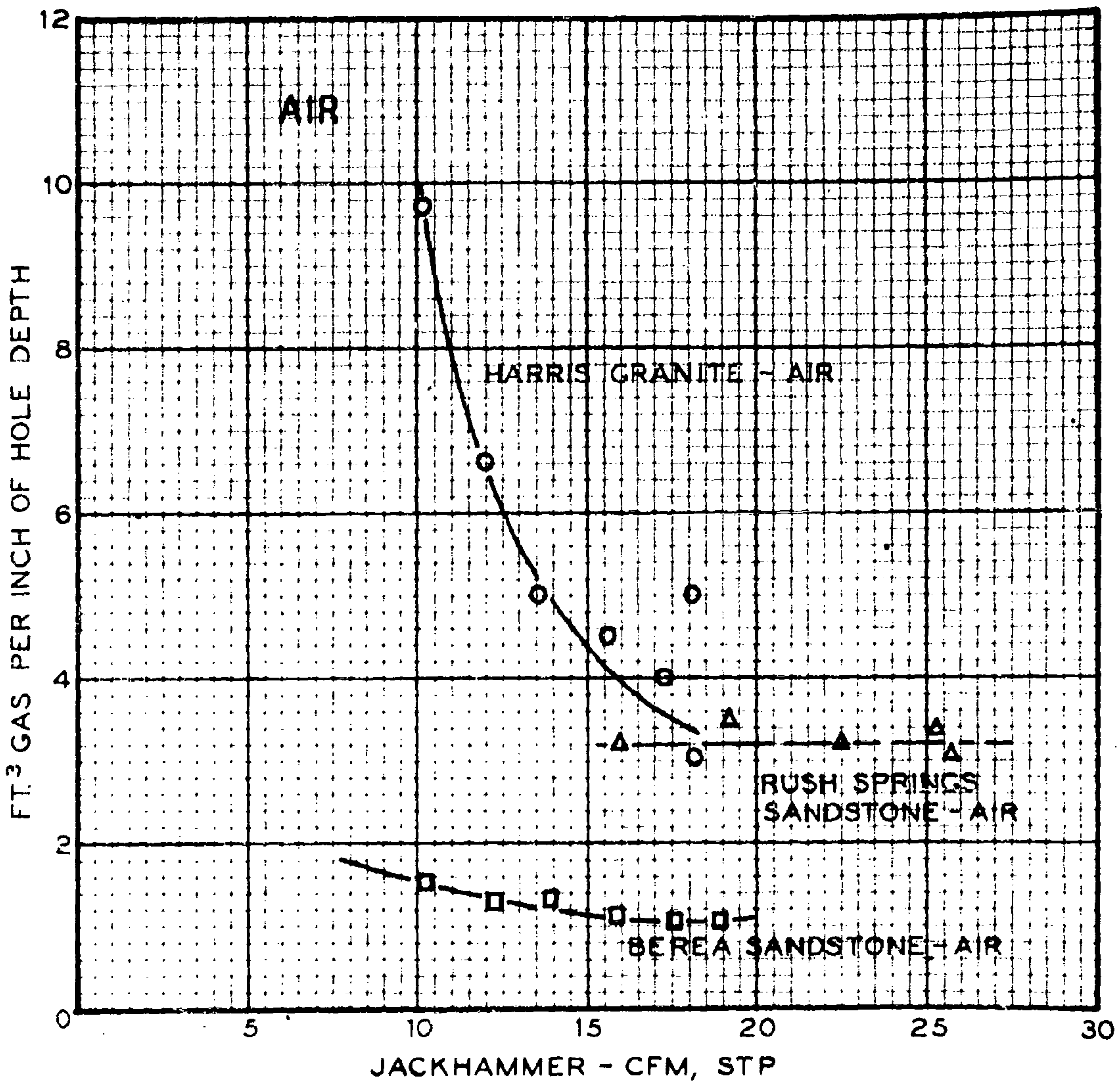

EFFECT OF JACKHAMMER GAS FLOW RATE ON GAS REQUIREMENTS PER INCH OF HOLE DEPTH USING A $\frac{3}{4}''$ BIT.

FIGURE 5

LJ 17530-2
8-23-60 EPN

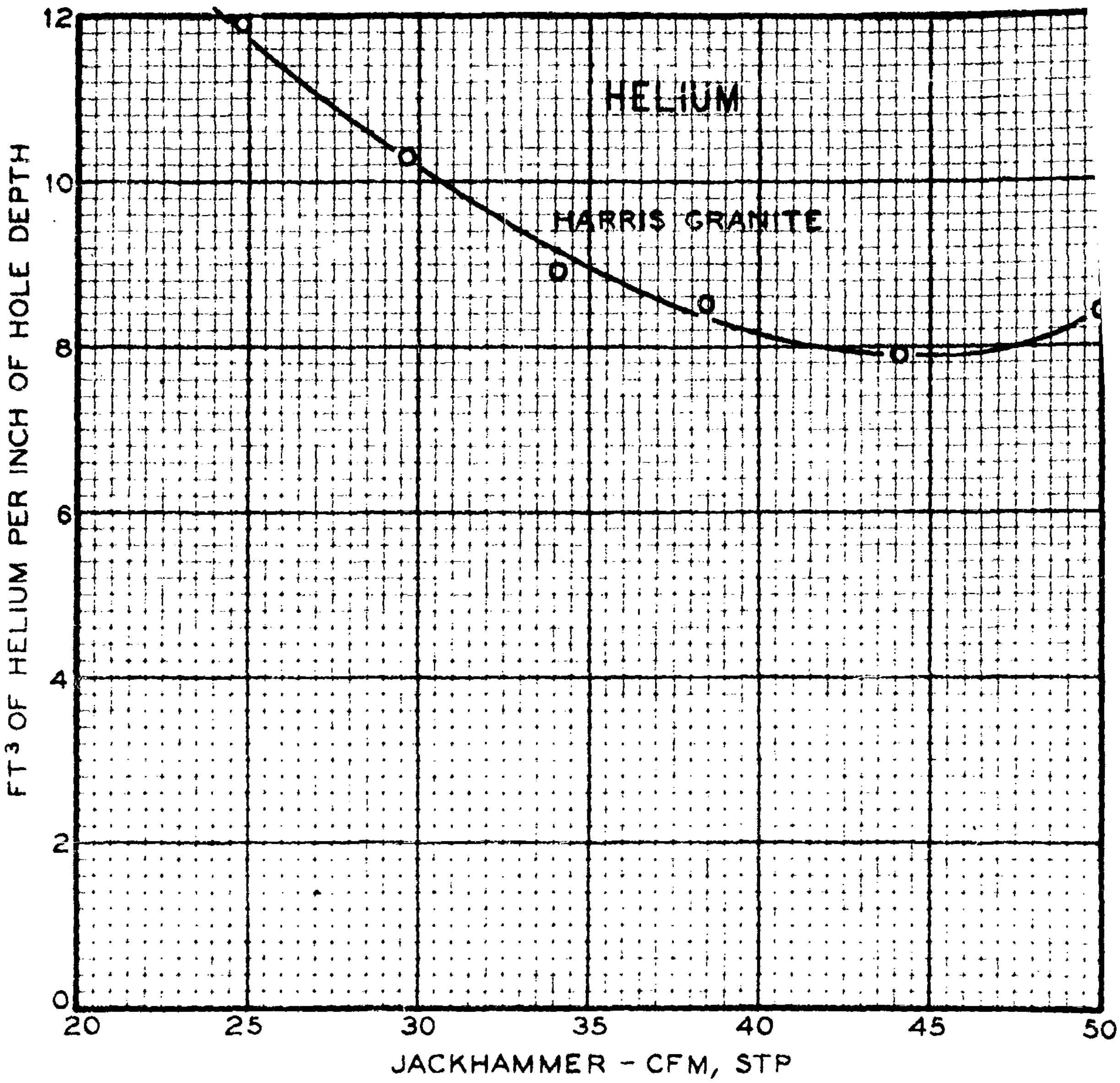

EFFECT OF JACKHAMMER GAS FLOW RATE ON GAS REQUIREMENTS PER INCH OF HOLE DEPTH USING A $\frac{3}{4}$" BIT.

FIGURE 5A

LJ 17530-2
8-23-60 EPN

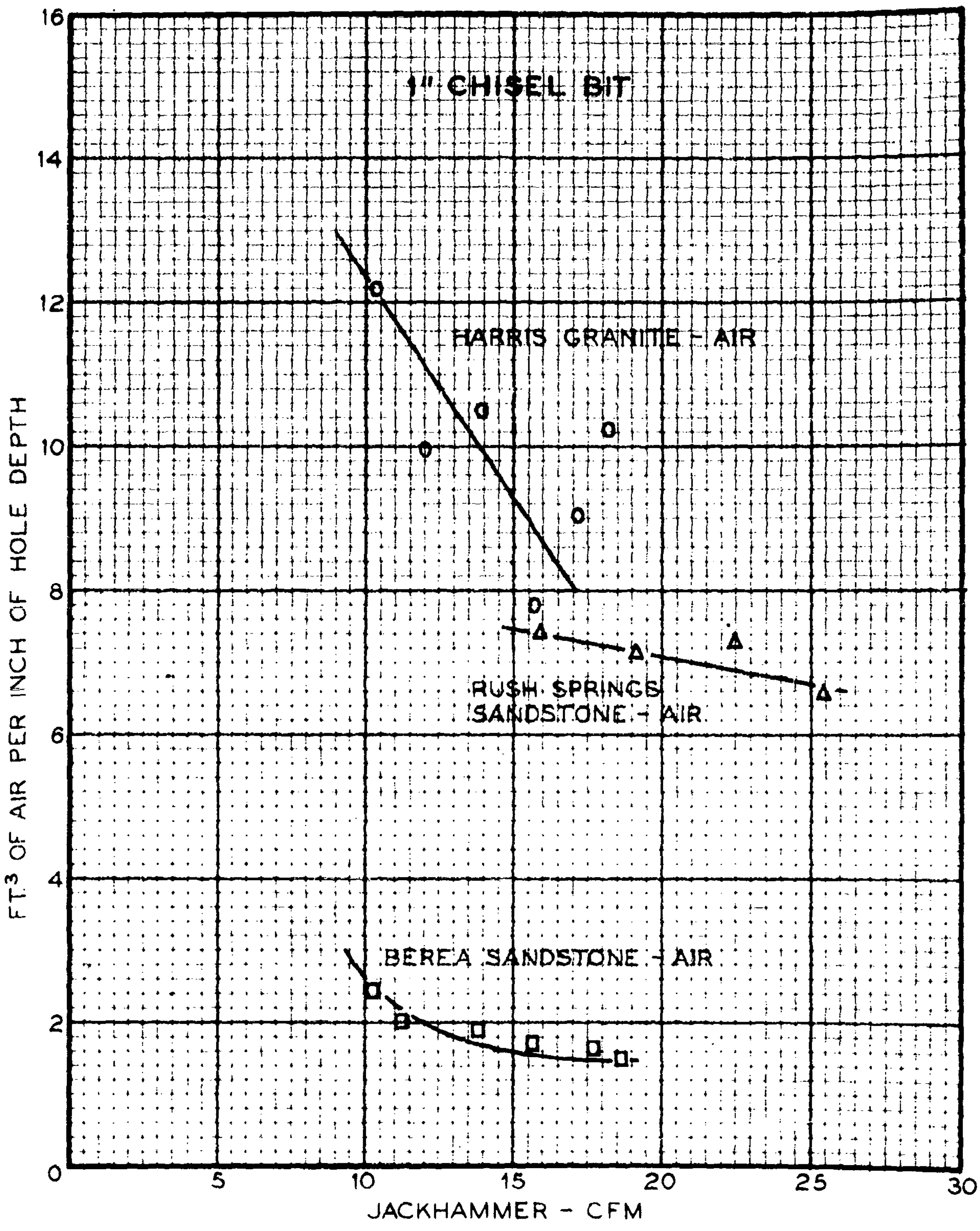

EFFECT OF JACKHAMMER GAS FLOW RATE ON GAS REQUIREMENTS PER INCH OF HOLE DEPTH USING A 1" BIT.

L J. 17530-2
8-23-60 RAH

FIGURE 6

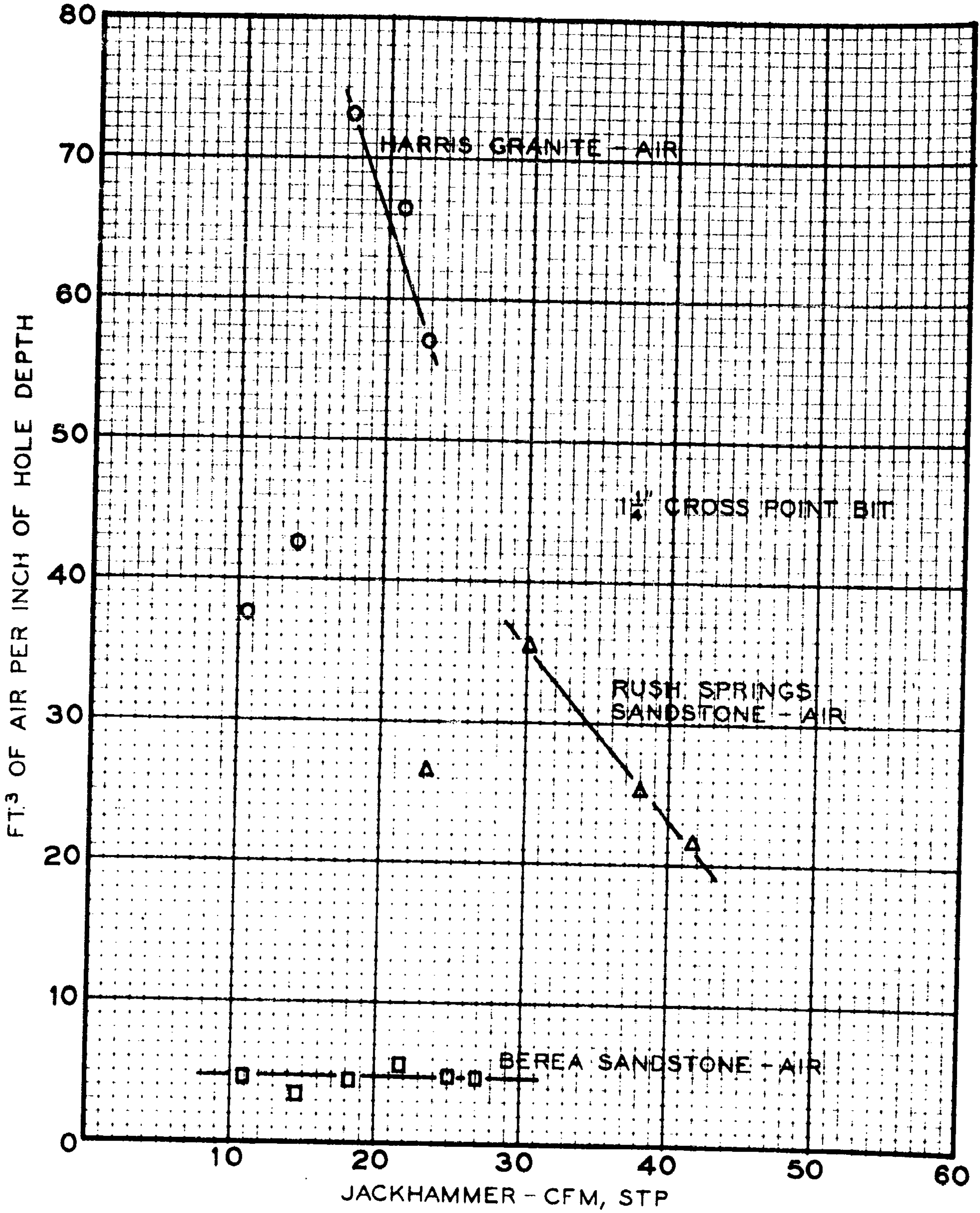

EFFECT OF JACKHAMMER GAS FLOW RATE ON GAS REQUIREMENTS PER INCH OF HOLE DEPTH USING A $1\frac{1}{4}''$ BIT.

FIGURE 7

LJ 17530-2
8-24-60 RAH

HUGHES TOOL COMPANY

LABORATORY REPORT

September 6, 1960

TO: G. O. Atkinson

cc: P. G. Reeve (2)
T. N. Williamson (3)
F. A. McCormick
G. R. King
J. G. Eenink
J. G. Stephenson

SUBJECT: Study Of Drilling Performance Of Sonic Drill On Rush Spring Sandstone And Harris Granite Using Different Bits.

REF.: Verbal Request from G.O.A. 8-22-60

L.J. 17530-2

Project 40021 - 64

Job Open

INTRODUCTION:

This report covers one phase of a series of tests run to develop a drill which is to be sent to the moon.

OBJECT:

This phase of testing was carried on in order to evaluate the performance of a Stanley "Sonic" drill in Rush Springs Sandstone and Harris Granite. Four different types of bits were used in these tests.

EQUIPMENT:

The drill used in this phase of testing was a "Sonic" model 404 manufactured by Stanley Electric Tools, Division of The Stanley Works, New Britain, Conn. This drill is rated to 1/2" to 4" diameter bits. The no load RPM is 900. This drill is rated to draw 12 amperes of current at a potential of 115 volts. The drill vibrates at approximately 21,000 impacts per minute. Four different bits were used in these tests. The first bit tested was a drag type bit which was supplied with the drill. This bit has a 2" O.D. and a 1-3/8" I.D. This bit has eight tungsten-carbide inserts mounted on the cutting edge (see Figure 1). Two of the bits used were the same 1-7/8" diamond bits which were tested in a previous phase of this job. One of these was a full-hole type and the other a coring type. The last bit tested was a 1-1/4" two cone soft-formation rotary bit. This is the same bit that is normally used on the high pressure drilling machine. The last three of these bits were attached to the drill by means of a special adaptor. A swivel on this adaptor permitted air to be circulated through the bit.

Power consumption was measured by means of a wattmeter preamplifier in the Sanborn recorder. This device was connected to the power supply line through a 25 ampere 50 mv shunt.

SPECIMENS:

These tests were run on Harris Granite #1 and Rush Springs Sandstone #69.

TEST CONDITIONS:

The drag bit was run with 50 and 100 lbs. of load. The two cone bit was given a 50 lb. load and the diamond bits were loaded at 100 lb. These are nominal loads; the exact loads used on each bit are shown in Table I. Loads were obtained by hanging steel weights on the handles of the drill. The rotary speed of the drill was 900 RPM under no load conditions and 830 RPM under loaded conditions. The drill was guided and kept from turning by hand, but no extra force was applied. A small starter hole was drilled before any test data was taken from each hole. Air was supplied for bit cooling and hole cleaning purposes during all tests except those in which the drag bit was used. Hole cleaning with the drag bit is carried out by the action of a spiral notch machined on the core barrel. Air, when used, was supplied by the Lab. air system and measured by means of a Rotameter.

RESULTS:

The exact results of each run made are tabulated in Table I. Test number 1 was discarded since it was run on a piece of Rush Springs Sandstone different from the one used in other tests on this job. The same Rush Springs specimen that had been used for the jackhammer tests was used for the remaining "Sonic" drill tests. Power consumption figures are accurate to ±50 watts since 1 mm on the recorder tape represented 125 watts of power. Total power consumption, as recorded, varied by as much as 200 watts during some tests. In these cases an approximate average for the run was taken as the test result. Somewhat erratic drilling rates were noted in tests 2 through 9. These runs were repeated as tests 22 through 29 after the other tests had been run. In tests 22 through 29, the runs were made in pairs with the first run of each pair (22, 24, 26, and 28) run in a new hole, while the second run of each pair was run in the same hole as the previous run. A study of the results shows a decrease in drilling rate with an increase in hole depth. This is attributed to two factors, (1) the poor cleaning action of the drag bit and core barrel, and (2) the difficulty in maintaining a straight hole. It was found that when the hole becomes slightly crooked, the core barrel has a strong tendency to bind. As previously mentioned, the diamond bits used in these tests were the same ones used in a previous phase of this same job. Before the present tests were begun, these bits would not drill Rush Springs Sandstone by normal rotary drilling. The vibrating action of the "Sonic" drill seems to have enabled these bits to drill again. This same action,

G-45

however, caused excessive diamond wear in just a few inches of drilling. (See Figure 3). Penetration rates did not differ appreciably from one bit to another, but the drag bit did appear to be slightly faster. Wear was very hard on the diamond bits especially when they were used on the Harris Granite. Wear was moderate on the 2-cone bit with some cone interference noted. Very little apparent wear was noted on the drag bit even after drilling on the Granite. Figures 1, 2, 3 and 4 show the condition of the bits at the end of the tests.

ATTACHMENTS:

Table I - Summary Of Results

Figure 1 - Drag Bit - After Testing

Figure 2 - Diamond Core Bit - After Testing

Figure 3 - Diamond Full-Hole Bit - After Testing

Figure 4 - Two Cone Bit - After Testing

CONCLUSIONS:

The "Sonic" drill operates most effectively with the drag type core bit which was supplied with the drill. A better method of cuttings removal would help the performance of this bit. The primary drawback in the use of this bit is the necessity of maintaining an absolutely straight hole. Moderate to severe wear when drilling Harris Granite make the other three bits tested inadvisable for use with this drill. In all cases drilling rates achieved with this drill are relatively slow. This type of drill is satisfactory in any case where rate of penetration is not a critical factor.

E. P. Worden

E. P. WORDEN, METALLURGICAL DEPARTMENT, LABORATORY.

EPW/bsr

TABLE I

SUMMARY OF RESULTS

Test Number	Bit Type	Rock Type	Load (Lb)	Drilling Rate (Ft/Hr)	Air Flow (CFM)	Total Power (Watts)	Power** For Drilling
2	Drag	Rush Springs Sandstone	48.4	3.20	-	875	275
3	"	"	"	2.03	-	810	210
4	"	"	"	1.56	-	810	210
5	"	"	"	1.25	-	810	210
6	"	"	98.4	1.56	-	1090	490
7	"	"	"	3.44	-	1000	400
8	"	"	"	3.44	-	1120	520
9	"	"	"	2.42	-	1120	520
10	Diamond Core	"	103.7	2.50	29.2	940	340
11	"	"	"	2.42	28.5	875	275
12	Diamond Full-Hole	"	104.5	1.80	26.5	875	275
13	"	"	"	1.88	26.6	1000	400
14	Two Cone	"	52.8	1.88	27.6	800	200
15	"	"	"	2.34	27.5	800	200
16	"	Harris Granite	"	0.27	27.6	750	150
17	Diamond Full-Hole	"	104.5	0.70	28.2	1000	400
18	"	"	"	0.39	28.2	1000	400
19	Diamond Core	"	103.7	0.63	29.0	1000	400
20	Drag	"	48.4	0.31	-	725	125
21	"	"	98.4	0.63	-	1000	400
22	"	Rush Springs Sandstone	48.4	1.95	-	-	-
23	"	"	"	1.17	-	-	-
24	"	"	"	1.88	-	-	-
25	"	"	"	1.33	-	-	-
26	"	"	98.4	2.34	-	-	-
27	"	"	"	1.64	-	-	-
28	"	"	"	2.03*	-	-	-
29	"	"	"	1.09	-	-	-

*Core broke out during or at the end of this test.
**No load power consumption = 600 Watt.

L.J. 17530-2

G-47

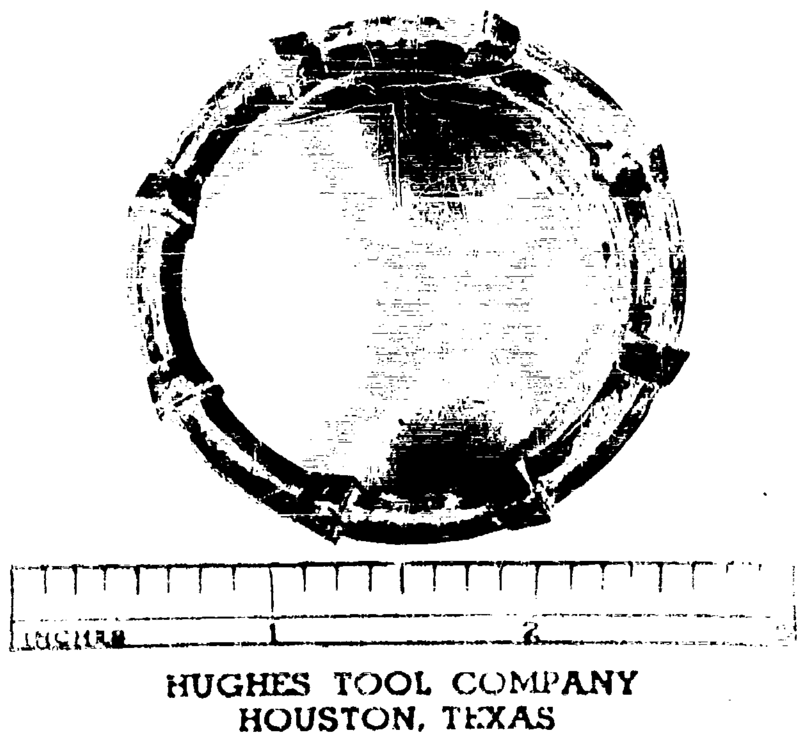

Drag bit after testing. This bit was new at the start of this series of tests.

FIGURE 1

L.J. 17530

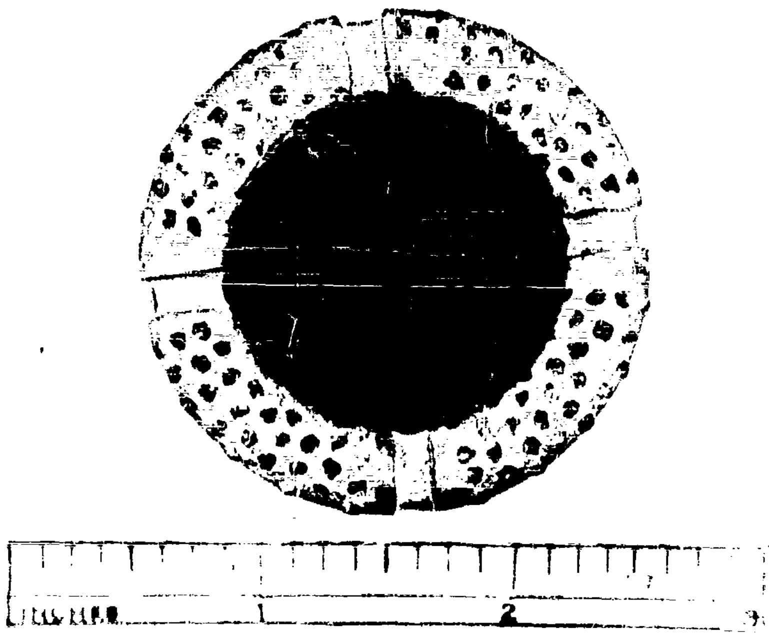

Diamond core bit after testing. This bit was used previously in this L.J. series. For condition of bit at start of testing see report L.J. 17530-2 dated 8-24-1960, Figure 5.

FIGURE 2

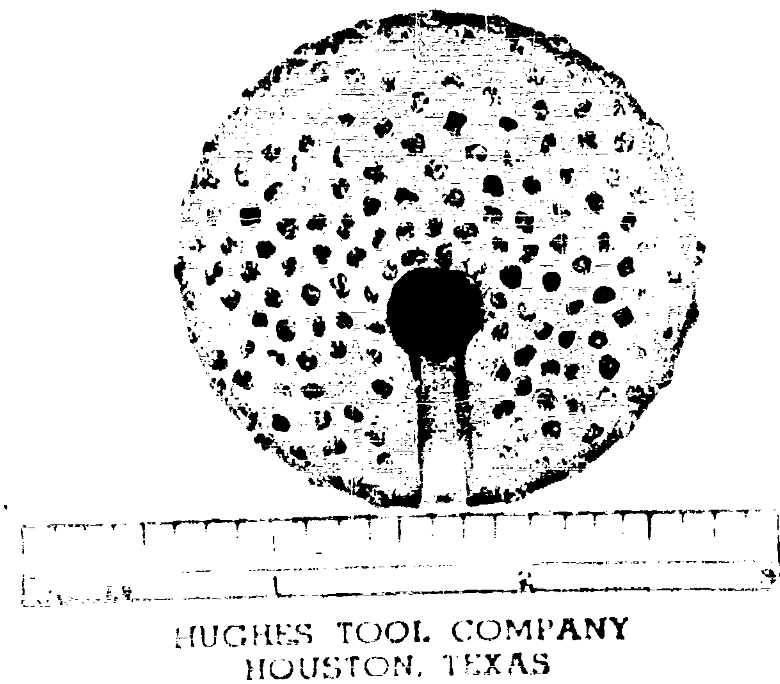

Diamond full hole bit after testing.
This bit was used previously in this
L.J. series. For condition of bit at
start of present tests see report L.J.
17530-2 dated 8-24-1960, Figure 6.

FIGURE 3

6-50

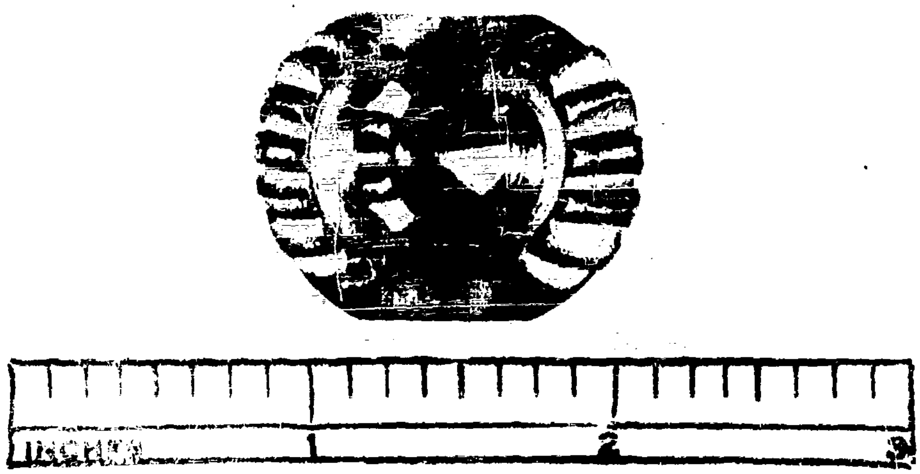

HUGHES TOOL COMPANY
HOUSTON, TEXAS

Two cone bit after testing.
This bit was new at start of
this series of tests.

FIGURE 4

I.J. 17530-2

G-51

HUGHES TOOL COMPANY

LABORATORY REPORT

October 5, 1960

TO: G. O. Atkinson

cc: P. G. Reeve (2)
T. N. Williamson (12)
F. A. McCormick
G. R. King
J. G. Eenink
J. G. Stephenson

SUBJECT: Low Bit Load, High Rotary Speed Drilling Tests On Gabbro.

REF.: Request from G.O.A., 9-8-60.

L.J. 17530-2

Project 40021 - 64

Job Open

INTRODUCTION:

This job is one of a series set up to develop a moon drilling machine. Previous tests were made on Berea Sandstone, Rush Springs Sandstone, Gray Granite and Harris Granite. These formations may or may not be similar to the type formation that will be encountered on the moon but they do represent a rather wide range of drillability.

A sample of Gabbro, 1 ft. x 1 ft. x 4 ft., was received from the Jet Propulsion Laboratory, California Institute of Technology, for this series of tests.

OBJECT:

The object of this job is to make drilling tests on a sample of Gabbro from the Jet Propulsion Laboratories using the:

1. Ingersoll-Rand J 10 A jackhammer and a 3/4" D. chisel bit.

2. High pressure drilling machine and an EX full hole diamond bit, a 1-1/4" 2-cone bit and a 3/4" D. Ruska diamond core bit.

EQUIPMENT:

The drilling equipment and general test procedure used during this series of tests were the same as that used on previous moon drilling jobs performed by this section.

The EX full hole diamond bit furnished for these tests contained a smaller size of diamond particles than the full hole diamond bit previously tested.

A 3/4" D. diamond core bit of the type used in conjunction with the Laboratory permeameter was used during these tests also. The 3/4" D. core bit was made by Ruska Instruments Company for the preparation of rock samples for permeability determinations. The cutting head of the bit consisted of a diamond impregnated ring brazed onto the core barrel. The diamond particle size in the 3/4" bit was very small in comparison to the particles in the EX bit mentioned above.

TEST CONDITIONS:

J 10 A Jackhammer:

Bit size:	3/4" D. chisel point
Operating gas:	air
Gas flow rate:	15, 20, 25 and 30 CFM, approximately, (70°F, 14.7 PSIA)
Bit load:	Minimum amount of manually applied load required to hold the drill in the hole, 10-15 pounds estimated.

High pressure drilling machine with EX diamond bit:

Rotary speed:	1140 RPM
Bit load:	60 lbs.
Circulating fluid:	air
Circulating rate:	30 CFM, approximately, (70°F, 14.7 PSIA)

Test conditions used with the 1-1/4" 2-cone bit and the 3/4" D. diamond core bit were essentially the same as those used with the EX diamond bit except that a bit load of 33 pounds was used during part of the tests with the 3/4" D. core bit. A bit load of 33 pounds was the lowest value of bit load obtainable using the existing core holders.

RESULTS:

The results of tests on Gabbro using the jackhammer are listed in Table I. Drilling rates are shown in Figure 1 at the various flow rates used. Drilling rate appears to increase linearly with increases in air flow rate within the range tested.

The results of tests using the EX diamond bit are listed in Table II. Drilling rates were very low and bit dulling occurred quickly. After drilling a depth of 1-19/32" in the Gabbro the diamonds were worn flat and the bit was considered worn out.

Two intervals of depth were drilled in the Gabbro using a 1-1/4" 2-cone bit. Interval number one was drilled using a set of hard formation cones and resulted in a drilling rate of 0.01 ft/hr. On the following interval the hard formation cones were replaced with

a set of standard cones which resulted in a drilling rate of 0.04 ft/hr. The result of this test is listed in Table III.

The results of tests using the 3/4" D. core bit are listed in Table IV. Tests were made on Rush Springs Sandstone, Berea Sandstone, Gray Granite and Gabbro.

Photographs of the EX diamond bit were taken prior to its use in a drilling test and after becoming worn to the extent that it was no longer usable. The photographs are shown in Figures 2 and 3. Also shown in Figure 3 with the worn EX bit are the set of hard formation cones and the 3/4" D. core bit used during the tests.

The horsepower determinations listed in Tables II, III and IV are approximate. The analyser used in the horsepower determination was not sensitive enough to accurately indicate the small difference between the loaded and unloaded conditions of the bit.

ATTACHMENTS:

Table I - Results Of Jackhammer Tests On Gabbro

Table II - Results Of Drilling Tests On Gabbro Using An EX Full Hole Diamond Bit

Table III - Results Of Drilling Tests Using A 1-1/4" 2-Cone Bit

Table IV - Results Of Drilling Tests With A 3/4" D. Ruska Diamond Core Bit

Figure 1 - Effect Of Jackhammer Air Consumption On Drilling Rate Of Gabbro

Figure 2 - View Of Cutting Head Of EX Diamond Bit Showing Sharpness Of Diamonds Before Testing

Figure 3 - EX Diamond Bit, 3/4" Diamond Bit, and 1-1/4" Hard Formation Cones After Testing

CONCLUSIONS:

1. The EX full hole diamond bit penetrated the Gabbro at an unsatisfactory rate and became dull after drilling to a depth of 1-19/32".

2. The 3/4" core bit produced unsatisfactory drilling rates also. Dulling did not appear to be a problem but the rate of wear on the cutting head was excessive during tests on Gray Granite and Gabbro.

G-54

3. Drilling rates resulting from tests on Gabbro with a 1-1/4" 2-cone bit were extremely low.

4. Drilling rates produced by the Ingersoll-Rand J 10 A Jackhammer varied from 8.2 to 38.3 ft/hr at air flow rates of 13.3 to 28.4 CFM.

J. G. Stephenson
J. G. STEPHENSON
METALLURGICAL ENGINEERING DEPARTMENT, LABORATORY.

JGS/bsr

TABLE I

Results Of Jackhammer Tests On Gabbro

Bit: 3/4" Chisel Steel
Jackhammer: Ingersoll-Rand J 10 A
Operating Gas: Air

Test & Hole No.	Drilling Rate (1) Ft/Hr	Air Flow Rate Cor. To STP. (2) CFM	Air Pres. Recorded At Jack-Hammer	Lbs. Gas Per Inch Of Hole Depth	Ft^3 Gas Per Inch Of Hole Depth (2)
1	38.3	28.4	54	0.28	3.69
2	--(3)	27.7	55	--	--
3	33.8	27.7	54	0.30	3.95
4	23.9	22.6	46	0.36	4.74
5	26.0	23.0	46	0.33	4.40
6	17.4	18.4	35	0.39	5.27
7	18.4	18.2	35	0.37	4.95
8	8.3	13.3	24	0.60	8.00
9	8.2	13.3	24	0.60	8.05
10	71.0	--	105	--	--
11	62.0	--(4)	102	--	--

(1) Each drilling rate was obtained by drilling to a hole to a depth of approx. 5 inches.

(2) STP - 70°F, 14.7 PSIA.

(3) Time was not recorded for this hole.

(4) Two holes were drilled with large I.D. hose and without the flow measuring equipment.

L.J. 17530-2
9-19-60
J.G.S.

TABLE II

Results Of Drilling Tests On Gabbro Using An EX Full Hole Diamond Bit

Bit Wt: 60 Lbs.
Rotary Speed: 1140 RPM

Test & Core No.	Interval No.	Air Flow CFM STP.*	Av. Rotary Drive H.P.		Depth Drilled In.	Drilling Rate Ft/Hr
			Loaded	Idyling		
1	1**	29.4	--	--	5/16	1.37
	2	29.4	3.7	--	19/64	0.61
	3	29.4	3.7	3.3	17/64	***
	4	29.4	3.3	3.3	7/32	0.26
	5	29.4	3.2	3.0	13/64	0.15
2	1**	21.0	3.7	--	1/4	0.09
	2	21.6	3.3	--	3/64	0.01

*Air flow rates were corrected to 70°F, 14.7 PSIA.

**Interval drilled to set concave bit face to rock.

***Interval time was not recorded.

L.J. 17530-2
9-27-60
J.G.S.

TABLE III

Results Of Drilling Tests Using A 1-1/4" 2-Cone Bit

Formation: Gabbro
Bit Load: 60 Lbs.
Rotary Speed: 1140 RPM
Circulating Fluid: Air

Test No.	Interval No.	Air Flow CFM STP.*	Av. Rotary Drive H.P.		Depth Drilled In.	Drilling Rate Ft/Hr
			Loaded	Idyling		
Hard Formation Cones						
6	1	29.4	3.7	2.7	1/32	0.01
Standard Cones						
6	2	29.4	3.2	2.7	5/64	0.04

*Air flow rates were corrected to 70°F, 14.7 PSIA.

L.J. 17530-2
9-27-60
J.G.S.

TABLE IV

Results Of Drilling Tests With A 3/4" D. Ruska Diamond Core Bit

Bit Load: 60 Lbs.
Rotary Speed: 1140 RPM

Av. Motor H.P. (60 Lbs. Load): 3.4
Av. Motor H.P. (33 Lbs. Load): 3.1
Motor H.P. (No Load): 2.7

Test No.	Formation	Interval No.	Air Flow CFM STP*	Depth Drilled In.	Drilling Rate Ft/Hr	Bit Longi-Tudinal Wear In.
3	Rush Springs Sandstone	1	29.4	1-1/2	0.73	0.006
4	Berea Sandstone	1	29.4	1-7/16	0.92	0.007
5	Gray Granite	1	29.4	1-9/32	0.21	0.021
7**	Gabbro	1 2 3	29.4 29.4 28.1	9/64 5/32 1-3/64	0.14 0.16 0.17	-- -- .021
8**	Gabbro	1	28.1	31/32	0.16	.021

*Air Flow rates were corrected to 70°F, 14.7 PSIA.

**Bit load -- 33 Lbs.

L.J. 17530-2
9-27-60
J.G.S.

G-59

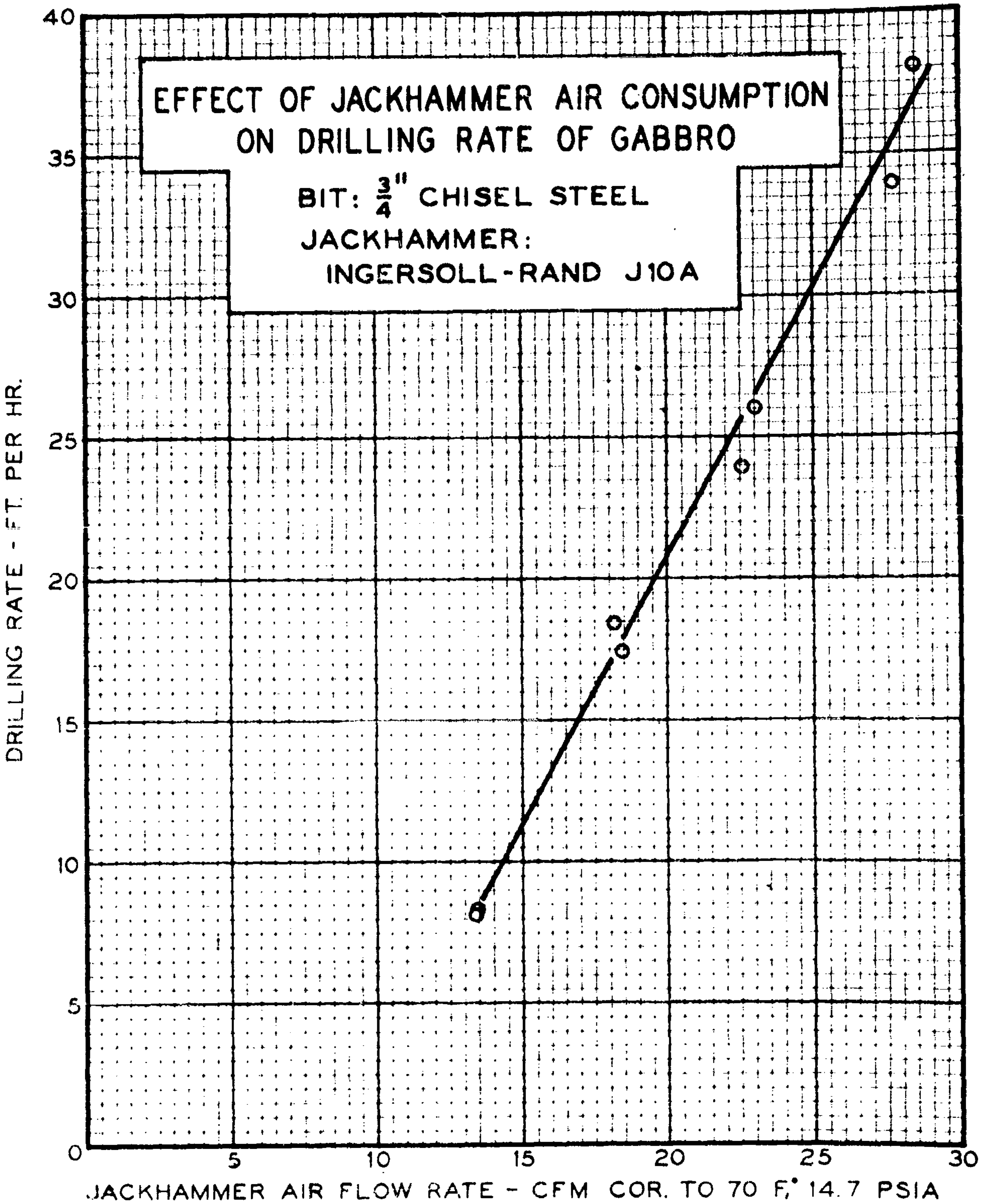

LJ 17530-2
9-9-60 JGS

FIGURE 1

G-60

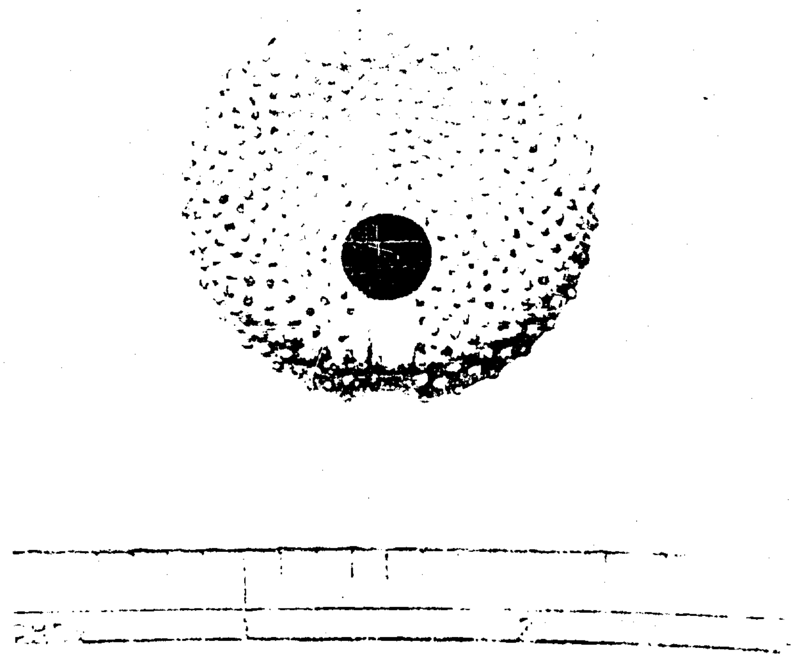

HUGHES TOOL COMPANY
HOUSTON, TEXAS

Bit Dia. - 1-7/16", Approx.
Mfg. - J. K. Smit Co.

View Of Cutting Head Of EX Diamond Bit Showing
Sharpness Of Diamonds Before Testing

FIGURE 2

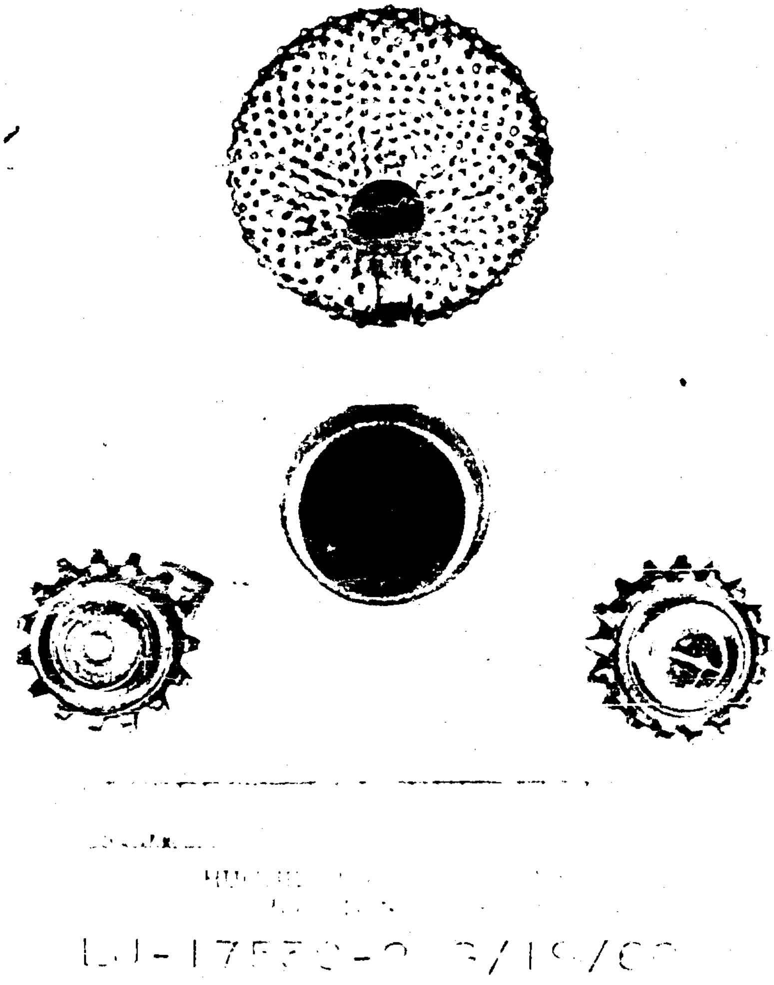

EX Diamond Bit, 3/4" Diamond Bit And 1-1/4" Hard Formation Cones After Testing

FIGURE 3

L.J. 17530-2
9-27-60
J.G.S.

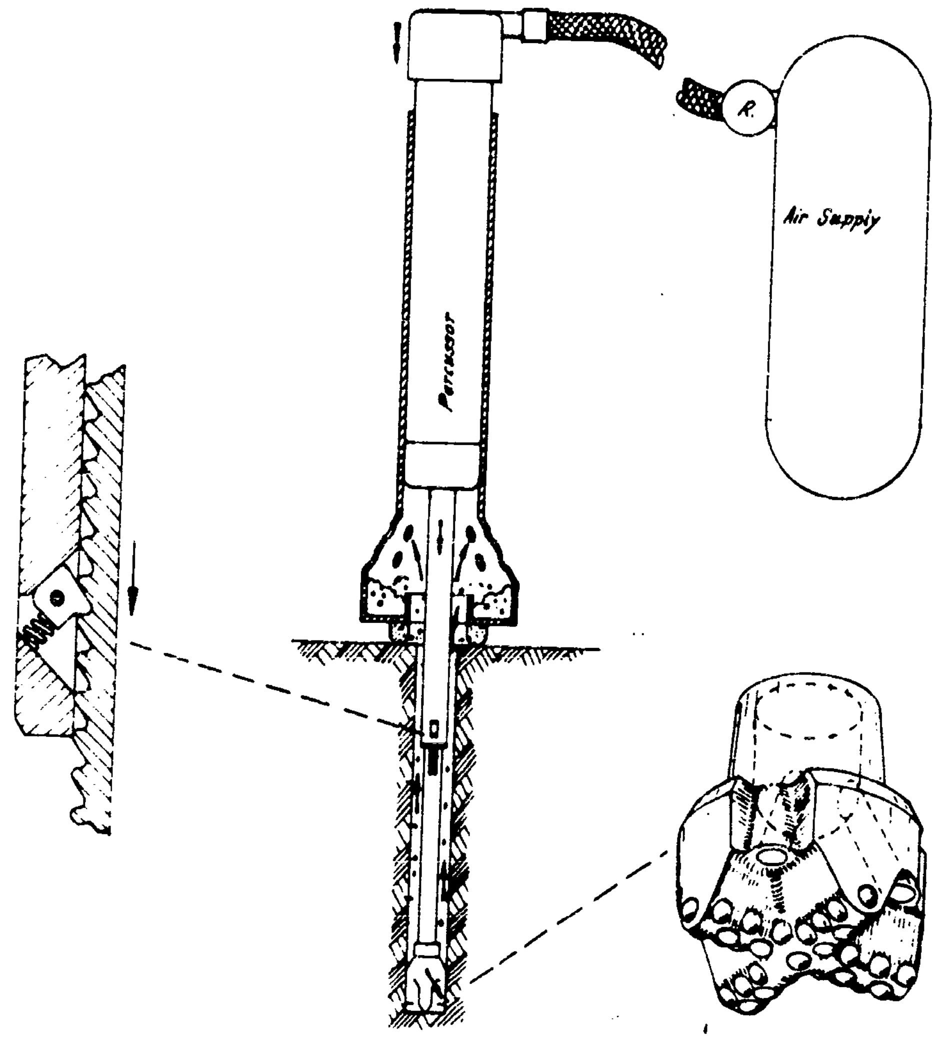

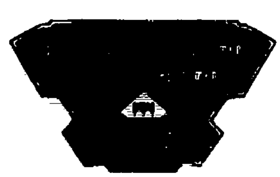

Atkinson & Berube 7-20-60

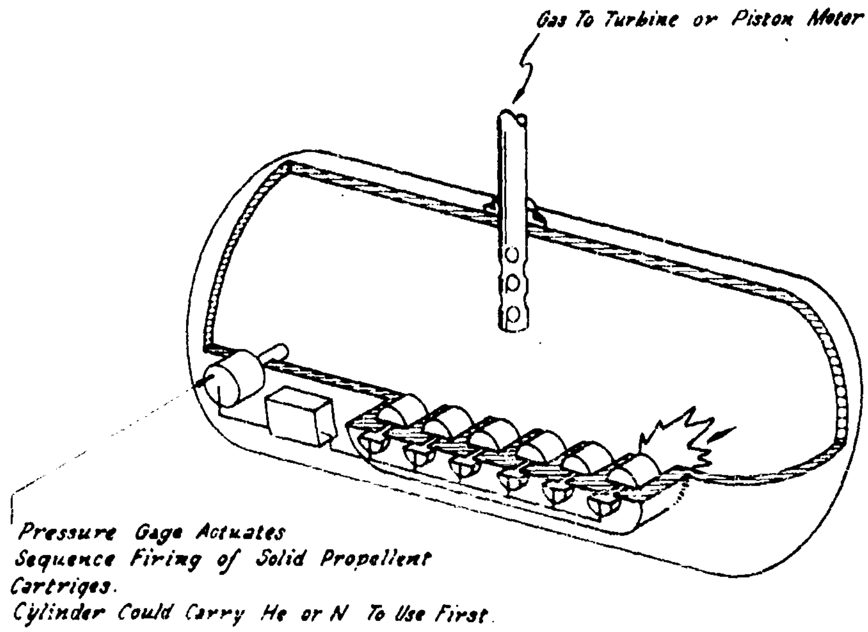

GAS GENERATOR

Wirz 7-20-60

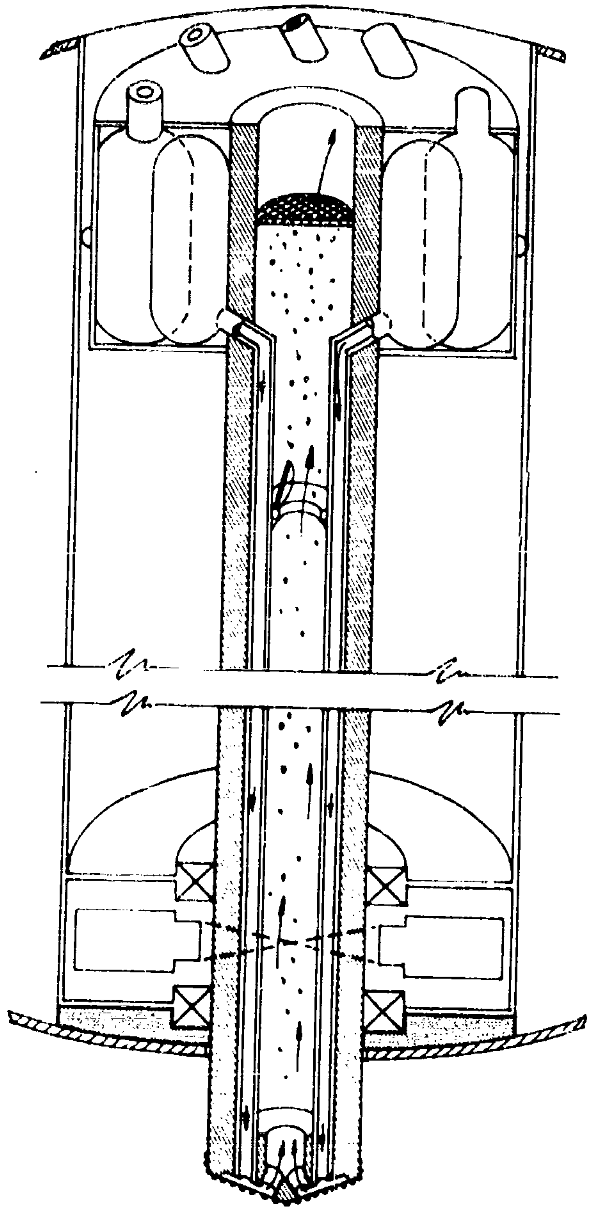

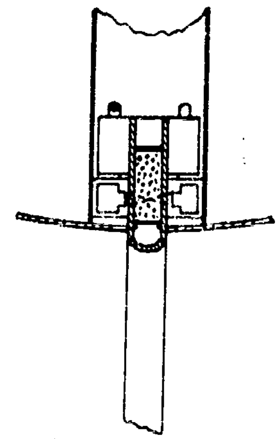

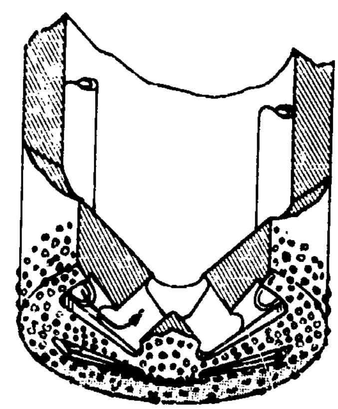

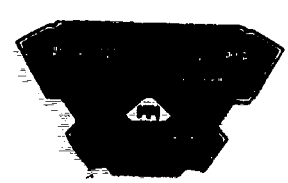

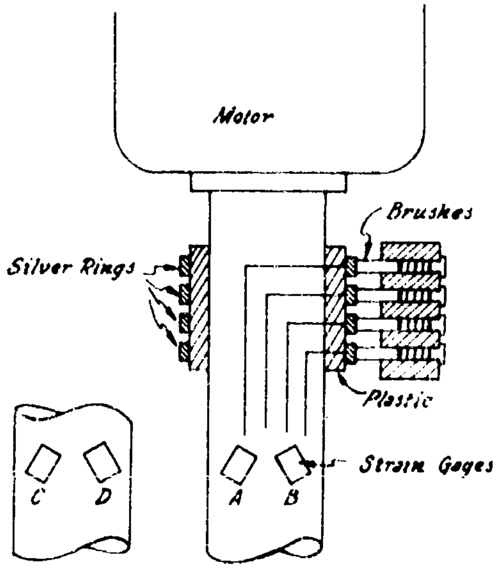

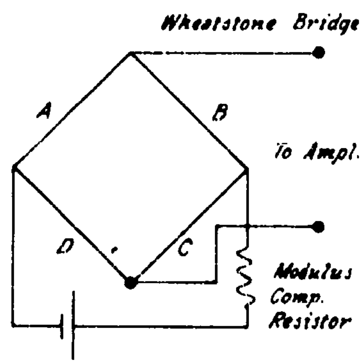

TORQUE MEASURING DEVICE

Eenick 7 25 60

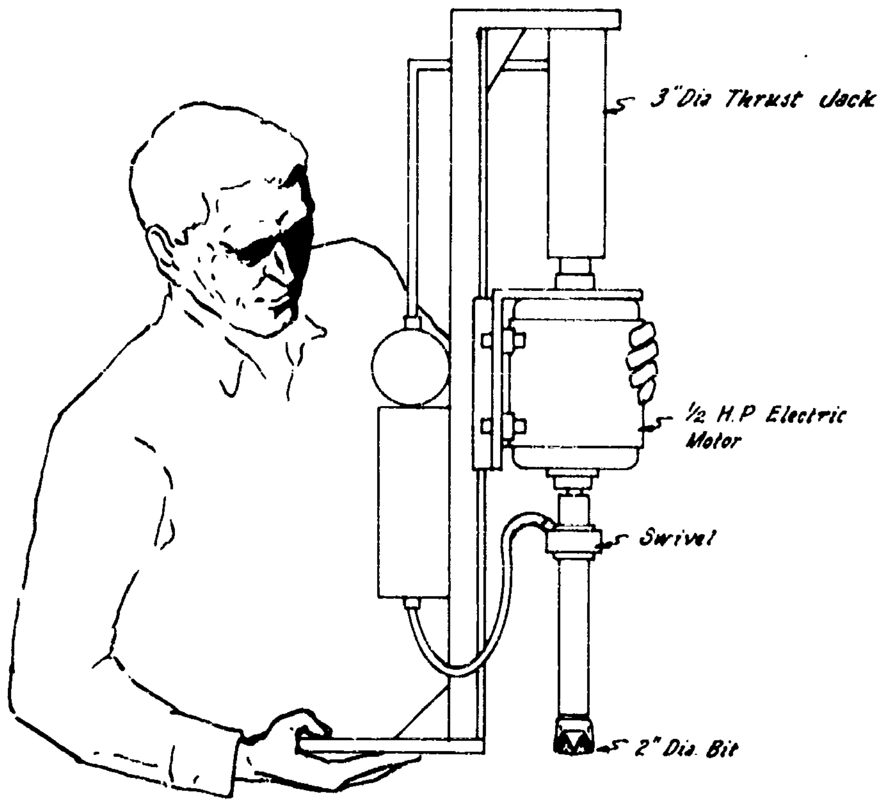

EQUIPMENT SIZE COMPARISON

Myers 7-24-60

H-7

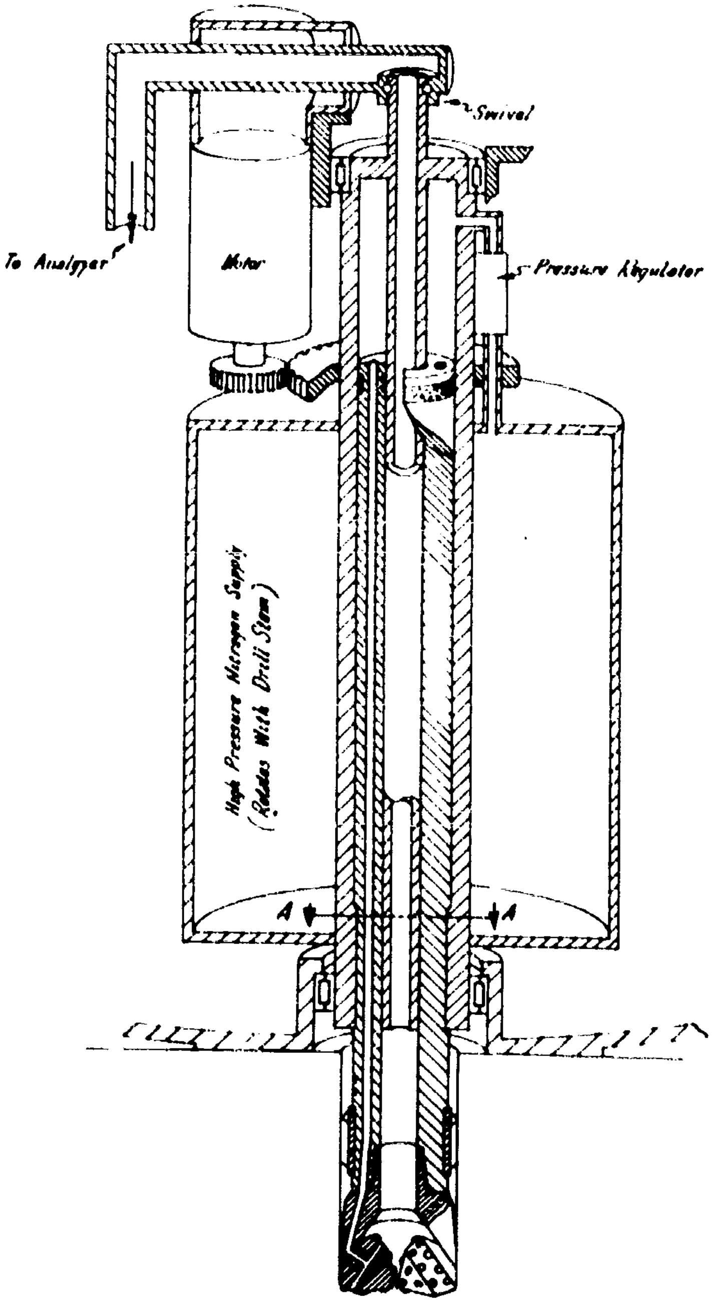

Low Strength Drill for Very Unconsolidated Formation

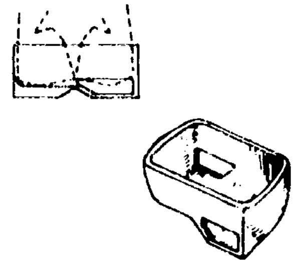

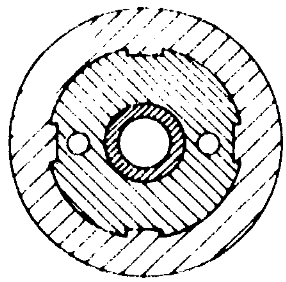

"A A"

Edward M. Salle

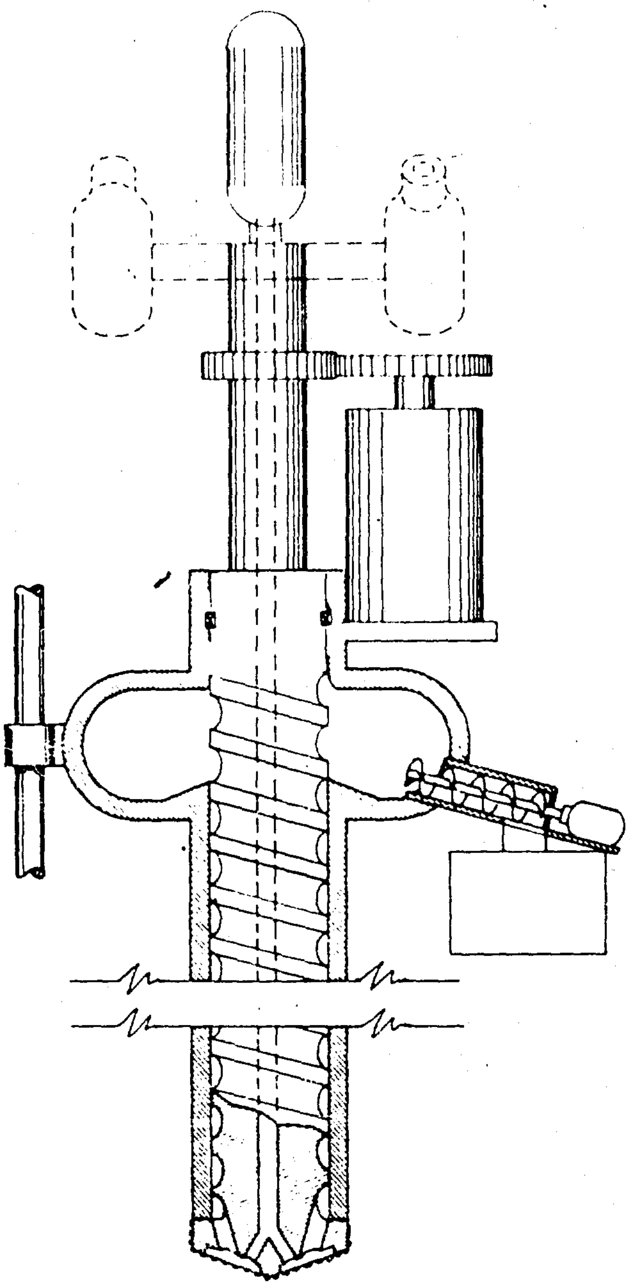

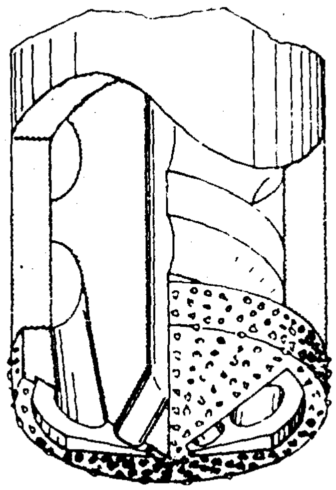

Special Applications Department
Engineering Department

H-9

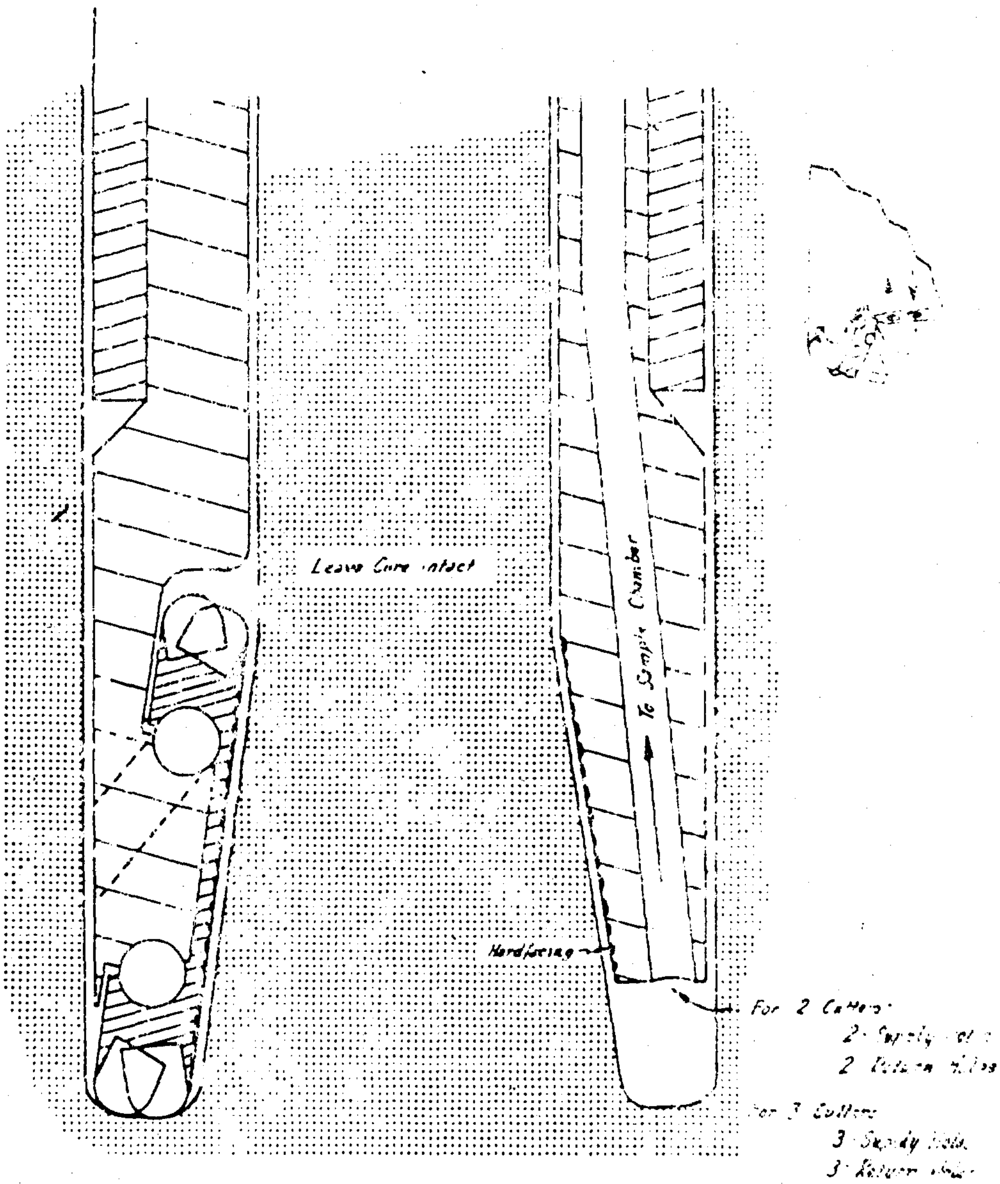

J.D. Mudlo 7-8-60

Best Available Copy